Natural and Induced Nitrate Attenuation Processes in Pétrola Basin (Albacete, Spain)

Raúl Carrey Labarta

UNIVERSITAT DE BARCELONA

Facultat de Geologia

Departament de Cristal·lografia, Mineralogia i Dipòsits Minerals

NATURAL AND INDUCED NITRATE ATTENUATION PROCESSES IN PÉTROLA BASIN (ALBACETE, SPAIN)

Thesis presented by

Raúl Carrey Labarta

to obtain the degree of Doctor in Earth Sciences

Work conducted in the "Mineralogia Aplicada i Medi Ambient" research group (MAiMA) under the supervision of

Dr. Albert Soler i Gil

Departament de Cristal·lografia, Mineralogia i Dipòsits Minerals, Universitat de Barcelona.

Dra. Neus Otero Pérez

Departament de Cristal·lografia, Mineralogia i Dipòsits Minerals, Universitat de Barcelona.

Barcelona, March 2014

Universitat de Barcelona

maima

This thesis has been funded by the Universitat de Barcelona with an APIF (Ajut de personal investigador en formació) grant. This work was financed by PEIC11-0135-8842 and PAC08-0187-6481 (ANNA: Atenuación natural del nitrato en aguas subterráneas) from the Castilla La Mancha Government. The projects CICYT-CGL2008-06373-CO3-01 (PAIS: Ground water pollution from agricultural and industrial sources: Contaminant fate, natural and induced attenuation, and vulnerability"), CICYT-CGL2011-29975-C04-01, CICYT-CGL2011-29975-C04-02 (Atenuación natural e inducida de la contaminación de origen agrícola e industrial en aguas subterráneas), and TRACE PET2008-0034 ("Aplicación de técnicas isotópicas para la cuantificación y seguimiento de procesos de desnitrificación de acuíferos") from the Spanish Government. The 2009SGR 103 project from the Catalan Government, and the MARSOL FP7-ENV-2013-WATER-INNO-DEMO from European Union.

Llegados a este punto, toca dar las gracias a todas aquellas personas que por activa o por pasiva, han contribuido en la elaboración de este trabajo.

En primer lugar, a mis directores el Dr. Albert Soler y la Dra. Neus Otero por darme la oportunidad de realizar esta tesis así como por su dedicación, apoyo, paciencia y lo más importante, su amistad. Un agradecimiento especial para el Dr. Juan José Gómez-Alday y el Dr. Carlos Ayora por su trabajo, comentarios y ayuda para la realización de esta tesis. De igual manera, muchas gracias a Georgina Vidal y Paula Rodríguez que han colaborado activamente en una parte importante de este trabajo.

Al Dr. Pascal Boeckx por su hospitalidad y colaboración durante la estancia realizada en la Universidad de Gante así como a todas las personas del grupo ISOFYS que me ayudaron, especialmente a Dries, Jan, Katia y Saskia.

Agradecer a Merçe su ayuda y trabajo en el laboratorio, también gracias a Laia por su ayuda en la realización de los análisis biológicos. Un especial agradecimiento a los Centres Científics i Tecnològics de la Universidad de Barcelona, especialmente a los responsables de las unidades de Medi Ambient, y Cromatografía de gasos Rosa Maria Marimon y Pilar Teixidor, así como a todos los técnicos que han colaborado en los análisis realizados durante esta tesis: Eva, Jaume, Laia, Joaquim, Toni, Pili y Lourdes. También dar las gracias a los estudiantes fin de carrera David, Daniel y Carles por su trabajo durante la realización de los experimentos.

Al personal administrativo de la Facultad de Geología en especial a Mª. Carmen Rebellón por su ayuda con todos los trámites para la correcta finalización de esta tesis. También agradecer al Dr. Carles Martín Closas por su paciencia y trabajo para la gestión de la comisión de seguimiento.

A todos las personas del departamento de Cristalografía, Mineralogía y Depósitos Minerales de la Universidad de Barcelona.

Muchas gracias los compañeros y amigos del grupo MAiMA (maimones) y alrededores: Angels, Massimo, Jordi, Roger, Marta, Pablo, Carme, Clara, Manuela, Albert F., Joan, Mónica, Cristina D.,

Ango-Lito, Diana y Alba y también a todos aquellos investigadores que han realizado estancias de en el grupo, Daniele, Martina, Adriana, Merchan, Genevieve y Takahiro. Durante este tiempo hemos compartido grandes historias y anécdotas; como olvidar las llamadas al Sr. León, las "Firas de Molins", el 50 cumpleaños de Albert, aquel concierto de Roger en las Borges Blancas, el "open your mind, que no pasa nada", las noches "locas" en el Átame, las cenas en general (con jamón y paté de Georgina en particular) los chotis típicos de brasil, la ventilación de la cámara anaerobia, la SEM de Salamanca, las meriendas de fruta "*made in Merchan*", el combo Helado-Negroni-Montelo, la famosa grabación del "celebrities" y un largo etc.

También quería agradecer a todos mis amigos Zaragoza, a las cuales veo mucho menos de lo que a mí me gustaría, en especial a Dani y Jesús. Gracias también a todos mis amigos y compañeros de la Universidad de Zaragoza con los que disfrute muchos cafés, cervezas y alguna clase que otra.

A mis padres, José Manuel y Lucia así como a mis hermanos Juan y Daniel.

Y por último, a Cristina que ha estado todo este tiempo a mi lado haciendo que merezca la pena todo este esfuerzo, muchas gracias.

Abstract

One of the main problems of diffused groundwater contamination is produced by nitrate (NO_3^-). NO_3^- pollution is linked with fertilizer application, manure management and wastewater. Many areas of Spain have NO_3^- concentration over the human consumption (0.8 mM NO_3^-) established by the Directive 98/83/CE. Endorheic basins located in semiarid or arid regions constitute one of the most vulnerable environments to NO_3^- pollution. The Pétrola basin (Central Spain) is an outstanding example of these endorheic systems. Understanding the processes that affect NO_3^- concentration in these endorheic systems is essential in order to improve water resources management. Among the different processes of the nitrogen cycle, denitrification is considered one of the most significant NO_3^- attenuation processes. Nitrate concentration in surface and groundwater from Pétrola basin ranged from $<1.6x10^{-3}$ mM to 2.5 mM. The observed variation in NO_3^- concentration could be linked with natural attenuation. In this basin two different sediments are able to produce denitrification: 1) the organic and sulphide-rich sediment from the Utrillas Facies (Lower Cretaceous) and 2) the bottom lake sediment. In this context, laboratory experiments can provide useful information to understand the natural attenuation mechanisms and the global attenuation potential of the different sediments present in the Pétrola basin. Laboratory experiments coupled with field data can be applied to improve the understanding of the nitrogen cycle in Pétrola basin.

The results obtained in the column experiment using Utrillas Facies showed that this sediment was able to remove NO_3^- contamination from groundwater (0.8 mM) under specific flow conditions. During the experiment, two different stages were observed. Stage I started at the beginning of the experiment up to day 21. An important increase in DOC was observed during this stage pointing out that NO_3^- attenuation could be promoted by heterotrophic denitrification. However, during this stage an important leaching from the sediment was observed, masking any chemical (SO_4^{2-} concentration) or isotopic ($\delta^{34}S_{SO4}$ and $^{18}O_{SO4}$) variation produced by autotrophic denitrification. Therefore, the role of pyrite in NO_3^- attenuation could not be neither discarded nor confirmed for this stage. The Stage 2 started at day 21 and lasted until the end of the experiment (day 332). During this stage NO_3^- concentration in the outflow changed when flow rate was modified reaching complete NO_3^- and NO_2^- attenuation whit a flow rate of 15 mL/d. Coupled with complete NO_3^- and NO_2^- removal, DOC increased in the outflow. In addition, SO_4^{2-} concentration and $\delta^{34}S_{SO4}$ and $\delta^{18}O_{SO4}$ remained unchanged, pointing out that

denitrification was produced using organic matter as electron donor. The nitrogen reduction rates (NRR) calculated during different flow-rate periods ranged from $1.0x10^{-2}$ mmol N d^{-1} L^{-1} (Stage I) to $3.1x10^{-2}$ mmol N d^{-1} L^{-1} (Stage II). The isotopic fractionations obtained were −11.6‰ and −15.7‰ for εN and −12.1‰ and −13.8‰ for εO during denitrification produced in Stage I and II respectively. The observed NO_3^- attenuation from water samples collected in the field ranged from 0% to 60%.

In the column experiment performed using the bottom lake sediment, results showed complete NO_3^- attenuation in the outflow after 7 days, and remained below input water NO_3^- concentration after 288 days. During the first days of the experiment dissimilatory nitrate reduction to ammonium (DNRA) was observed. This reaction was favored by the high C/N ratio and high salinity at the early stages. After 10 days, denitrification became in the main NO_3^- attenuation reaction. Sulphate reduction could not be confirmed neither discarder during the experiment since chemical and isotopic variations were masked by sulphate leaching from the sediment. The average NRR reduction rate obtained was 1.25 mmol N d^{-1} L^{-1} and remained constant despite several changes in flow rate. The NRR of bottom lake sediment was two orders of magnitude higher than the obtained for the Utrillas Facies. The calculated amount of organic carbon (C_{org}) mobilized during the experiment was about 18% of solid organic matter from the sediment (SOM =0.5 mol Kg^{-1}). Differences in the reactivity of C_{org} could be related with the sediment age. The isotopic fractionations obtained were −14.7‰ and −14.5‰ for N and O respectively. These values were similar to the ones obtained for the Utrillas Facies.

The hydrogeological field study showed that groundwater flow in Pétrola basin could be considered as the result of two main flow components: 1) regional groundwater flow, from perimeter areas to the lake, and 2) density driven flow from surface lake water towards the underlying aquifer. Results showed that NO_3^- contamination was linked with agricultural activities developed in the area. The isotopic signatures of dissolved nitrate suggested that the main nitrate source was the use of synthetic fertilizers (slightly volatilized). The isotopic study performed in 2010 showed that nitrate attenuation ranged from 0 to 60%. The attenuation was negligible in the perimeter area of the basin, whereas close to the lake the mean attenuation was 20%, reaching maximum values of 60%. However, some samples with high denitrification showed NO_3^- content of 0.77 mM close to the threshold for human water supply. Chemical and isotopic data from field samples were affected by other processes such as gypsum dissolution or calcite precipitation that could mask the concentration and isotopic composition of the different by-products of denitrification reactions. Higher DOC concentration in those samples with higher

nitrate attenuation suggested that organic matter was acting as the main electron donor. These results were in agreement with the laboratory experiment using Utrillas Facies, where the attenuation was linked to organic matter oxidation and the complete attenuation only was reached under low flow rate. With regards to the attenuation in the aquifer-lake area, results from piezometers located inside the lake showed NO_3^- concentration below detection limit down to 37 m depth (below ground surface). However, the influence of density driven down flow was restricted to the saltwater-freshwater interface (down to 12 m-14m). The absence of NO_3^- in the deepest part of the aquifer was attributed to groundwater regional flow with longer residence times, since tritium data in these samples indicated that infiltration was prior to 1950.

To enhance the heterotrophic denitrification in the Pétrola basin, a biostimulation treatment was proposed. The biostimulation involved periodically injecting glucose to act as an electron donor to promote complete NO_3^- removal. The C/N ratios tested were nearly stoichiometric to prevent the generation of undesirable compounds, such as NO_2^- or H_2S. Complete NO_3^- reduction was achieved after 13 days, along with transient NO_2^- accumulation that was observed until day 27. In addition to NO_3^- attenuation, the glucose injection repressed the DNRA, reducing NH_4^+ concentration in the outflow. Changes in the C/N ratio during the experiment reduced the amount of glucose discharged from the system. However, despite these changes, NO_3^- attenuation continued because secondary carbon sources (DOC in input water and/or biomass) were present during the experiment and accounted for approximately 30% of the total attenuated NO_3^-. Isotopic characterisation of the SO_4^{2-} proved that the SO_4^{2-} reduction did not occur, even though carbon excess and low redox conditions were present. This is attributed to the lack of time for SO_4^{2-} reduction to occur inside the column. The N and O isotopic fractionation obtained during the induced attenuation were -8.8‰ and -8.0‰ respectively; these values were lower (in absolute values) than the isotopic fractionation in natural denitrification. This variation was caused by differences in the organic carbon source. Overall, periodically injecting glucose might be a feasible method to remove NO_3^- from groundwater; a pilot-scale test should be performed to verify its applicability during long-term treatments at field-scale.

1. Introduction 1
1.1 N-cycle reactions 2
1.1.1 Nitrification 2
1.1.2 Denitrification 4
1.1.3 Dissimilatory nitrate reduction to ammonium (DNRA) 5
1.1.4 Anaerobic ammonium oxidation 5
1.2 Induced Nitrate Remediation/Attenuation 6
1.3 Kinetic of denitrification 7

2. Rationale 7

3. Study area 8

4. General goals 10

5. Methodology 12
5.1 Field survey 12
5.2 Experimental design 12

6. Results and discussion 13
6.1 Natural attenuation: Utrillas Facies 13
6.2 Natural attenuation: Bottom lake sediments 16
6.3 Chemical and isotopic characterization of Pétrola basin 19
6.4 Induced nitrate attenuation 22

7. General conclusions 25

8. Thesis outline 27

References 28

Appendix A 38
Appendix A.1 39
Abstract 41
1. Introduction 41
2. Methods 42
2.1 Experimental set-up 42
2.2 Analytical methods 43
3. Results 44
4. Discussion 45
4.1 Identifying the electron donor for the denitrification reaction 45
4.2 Denitrification rate 47
4.3 Fractionation of N and O 48
5. Conclusions 50
References 50

Appendix A.2 51
Abstract 53
1. Introduction 54
2. Methodology 58
2.1 Flow-through experiment 58
2.2 Batch experiments 59
2.3 Sediment and water description 59
2.4 Analytical methods 60

2.5 Isotopic analyses 60
2.6 Biogeochemical model construction 61
3. Results 63
3.1 FTR results 63
3.2 Batch experiment results 68
3.3 Isotopic results 68
4. Discussion 69
4.1 NO_3^- attenuation processes 69
4.2 NO_2^- accumulation 70
4.3 Sulfate reduction reaction 71
4.4 Biogeochemical model and natural attenuation potential 71
4.5 N and O isotopic fractionation 74
5. Conclusions 76
References 77

Appendix A.3 83
Abstract 85
1. Introduction 86
2. The study area 89
3. Methods 90
3.1 Field survey 90
3.2 Chemical analyses 92
3.3 Isotopic analyses 92
3.4 Electrical Resistivity Tomography (ERT) 93
4. Hydrogeology of the Pétrola basin 95
5. Results 96
5.1 Hydrochemistry of Zones 1 and 2 97
5.2 Hydrochemistry of Zone 3 97
5.3 Stable isotope results 98
5.4 Tritium concentrations 99
6. Discussion 99
6.1 Nitrification and denitrification in Zones 1 and 2 99
6.2 Identifying the electron donor for denitrification 102
6.3 Nitrate reduction in Zone 3 106
7. Conclusions 108
References 109

Appendix A.4 115
Abstract 117
1. Introduction 117
2. Methodology 118
2.1 Experimental set-up 119
2.2 Carbon source and C/N ratio during the biostimulation experiment 119
2.3 Analytical methods 119
2.3.1 Chemical analyses 119
2.3.2 Isotopic analyses 119
2.3.3 Microbial analyses 119
3. Results 119
3.1 Outflow water before biostimulation 119
3.2 Outflow water during biostimulation 119
3.2.1Redox potential and pH evolution 119
3.2.2 Chemical data 120
3.2.3 Isotopic results 120

3.3 C-$C_6H_{12}O_6$ concentration 120
3.4 MPN results 120
4. Discussion 122
4.1 NH_4^+ generation before biostimulation 122
4.2 Denitrification enhanced by biostimulation 122
4.3 Organic carbon balance 123
4.4 Fractionation of N and O 123
5. Conclusions 124
References 125

Appendix B 127

1. Water Sampling and preservation 129
1.1 Field samples 129
1.2 Laboratory experiment samples 129
2. Chemical analyses 130
2.1 Anion analyses 130
2.2 Cation analyses 130
2.3 Organic carbon analyses 131
2.4 Dissolve inorganic carbon analyses 131
3. Isotopic analyses 131
3.1 $\delta^{15}N$ and $\delta^{18}O$ of dissolved NO_3^- 133
3.2 $\delta^{34}S$ and $\delta^{18}O$ of dissolved SO_4^{2-} 134
3.3 $\delta^{13}C$ of dissolved inorganic carbon 135
4. Microbial analyses 135
5. Set-up of new isotopic methods 136
5.1 $\delta^{15}N$-NH_4^+ analyses by diffusion method 136
5.2 $\delta^{15}N$ and $\delta^{18}O$ analyses by cadmium method 137
5.2.1 Cadmium preparation 137
5.2.2 Conversion of NO_3^- to NO_2^- 137
5.2.3 Conversion of NO_2^- to N_2O 138
References 138

Appendix C 141

Appendix C.1 143
Appendix C.2 149
Appendix C.3 161
Appendix C.4 177

1. Introduction

In the last decades nitrate pollution has become a major threat to groundwater quality. Presence of nitrate (NO_3^-) in water can cause serious health problems in both humans and domestic animals, and environmental impacts. High NO_3^- ingestion can cause methemoglobinemia in infants and young children (Comly et al., 1945; Magee and Barnes, 1956) and also can promote cancer in humans (Volkmer et al., 2005; Ward et al., 2005). Moreover, NO_3^- impacts the environment, contributing to the eutrophication of surface water bodies (Rivett et al., 2008; Vitousek et al., 1997). The natural NO_3^- content in water is moderate; however, anthropogenic activities increase the NO_3^- concentration, reducing water quality. Frequently, the sources for the NO_3^- pollution in groundwater are linked to the extensive use of synthetic and organic fertilisers, inappropriate placement of animal waste, and spills from septic system effluents. The European Groundwater Directive (EC 2006) considers NO_3^- as one of the most important contaminants that could prevent the achievement of the goals of the Water Framework Directive (EC 2000). The NO_3^- concentration threshold established by Directive 98/83/CE for human water supplies is 0.81 mM (50 mg/L NO_3^-, or 11 mg/L N-NO_3^-).

In order to improve characterization and water resources management in nitrate polluted or nitrate vulnerable areas, it is necessary to understand the different processes that affect nitrogen compounds in the environment. The most important processes found in hydrogeological systems affecting nitrogen compounds are nitrification, denitrification (including nitrifier denitrification), dissimilatory nitrate reduction to ammonia (DNRA or ammonification) and anaerobic ammonium oxidation (Anammox). As NO_3^- is a key compound for these processes (Fig. 1), it is very important to know the reactions pathways and the conditions for these reactions to take place. Depending on the biological pathway, a different chemical signature of groundwater can be produced, which can help, for instance to identify whether denitrification is promoted by autotrophic or heterotrophic bacteria. However, when chemical data are not conclusive, multi-isotopic studies are an effective tool to identify and describe these processes (Aravena and Robertson, 1998; Mariotti et al., 1988; Pauwels et al., 2000; Vitoria et al., 2008; Wassenaar, 1995; among others). Stable isotopes are usually measured as the ratio between the less abundant isotope(s) and the most abundant one, e.g. ^{15}N against ^{14}N. Ratios are usually established with respect to international standards using the delta notation (Eq. 1).

$\delta^{15}N = [(R_{sample} - R_{std}) / R_{std}] \times 1000$ (1)

where $R = {}^{15}N/{}^{14}N$ in the sample (sa) and the standard (std)

Changes in the isotopic composition or fractionation produced by biological processes such as denitrification or DNRA used to be expressed as a Rayleigh distillation process (ε) (Eq. 2 and 3 in the case of NO_3^- fractionation) (Mariotti et al., 1988). Fractionation is useful to distinguish between microbial/chemical/biological reactions from other processes such as dilution, which can also affect to nitrogen compounds concentration but without changing the isotopic value (Clark and Fritz, 1997; Kendall et al., 2007).

$\delta^{15}N_{residual} = \delta^{15}N_{initial} + \varepsilon \ln ([NO_3^-]_{residual} / [NO_3^-]_{initial})$ (2)

$\delta^{18}O_{residual} = \delta^{18}O_{initial} + \varepsilon \ln ([NO_3^-]_{residual} / [NO_3^-]_{initial})$ (3)

1.1 Main N-cycle reactions

Most important N-cycle reactions in groundwater and the intermediate steps of oxidation and reduction processes are represented in Figure 1.

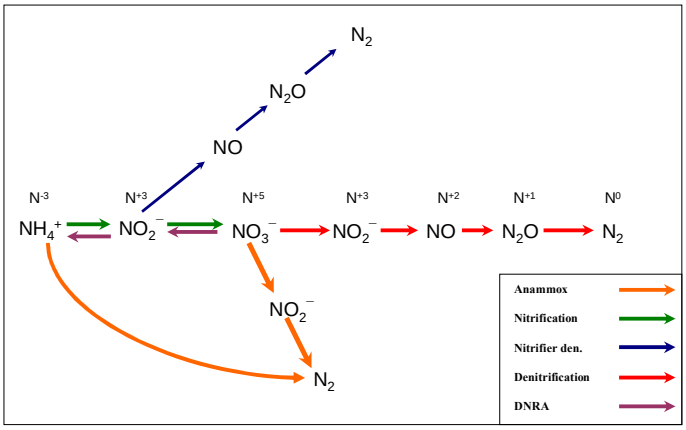

Figure 1. Schematic representation of the soil microbial pathways affecting N compounds.

1.1.1 Nitrification

Nitrification is one of the most important processes that produce the increase of NO_3^- concentration in groundwater. Nitrification is the oxidation of NH_4^+ compounds to NO_3^- under aerobic conditions by nitrifying bacteria. Main sources of NH_4^+ in soil are: 1) NH_4^+ formed by the mineralization

of organic-N in soils, 2) the application of synthetic fertilizer and 3) NH_4^+ from animal or sewage waste, formed by the hydrolysis of urea to NH_3, that is subsequent converted to NH_4^+ (Eq 4 and 5) (Table 1) (Heaton, 1986).

$$CO(NH_2)_2 + 2H_2O \rightarrow 2NH_3 + H_2CO_3 + H^+ \quad (4)$$

$$2NH_3 + 2H_2O \leftrightarrow 2NH_4^+ + 2OH^- \quad (5)$$

NH_4^+ oxidation (Eq. 6 and 7, Table 1 Fig. 1) is mainly produced under aerobic conditions in the non saturated zone, but it can also take place under saturated conditions (Choi et al., 2003).

$$2NH_4^+ + 3O_2 \rightarrow 2NO_2^- + H_2O + 4H^+ \quad (6)$$

$$2NO_2^- + O_2 \rightarrow 2NO_3^- \quad (7)$$

Nitrification produces the consumption of NH_4^+ and the increase of NO_3^- in groundwater. Isotopically, during this reaction the $\delta^{15}N$ of the residual NH_4^+ increases whereas the $\delta^{15}N$ of the generated NO_3^- is depleted with respect to the $\delta^{15}N$ of NH_4^+. However, as Heaton (1986) pointed out, during nitrification processes NH_4^+ is completely nitrified and no isotopic fractionation is observed. Nevertheless, the isotopic composition of $\delta^{15}N\text{-}NH_4^+$ can be affected by volatilization of NH_3 when animal or sewage waste is stored for long periods of time, or during their application on the surface of the soil. Volatilization tends to increase the $\delta^{15}N$ of residual NH_3 and therefore the generated NH_4^+ will have a higher value of $^{15}N\text{-}NH_4^+$ (Högberg, 1997). With regards to ^{18}O, during nitrification the $\delta^{18}O_{NO3}$ is mainly derived from water and atmospheric oxygen and the resulting $\delta^{18}O_{NO3}$ can be calculated following Equation 8 defined by Anderson and Hooper (1983).

$$\delta^{18}O_{NO3} = 1/3\ \delta^{18}O_{O2} + 2/3\ \delta^{18}O_{H2O} \quad (8)$$

This equation can be applied when NH_4^+ is abundant and nitrification rates are high. It also assumes negligible isotope fractionation effects during water and atmospheric O_2 ($O_{2(atm)}$) incorporation (Mayer et al., 2001). It is also supposed that the $\delta^{18}O$ of O_2 used by the microorganisms is that of $O_{2(atm)}$. In this case, two-thirds of the oxygen atoms of NO_3^- produced are derived from water, whereas one-third is incorporated from atmospheric oxygen ($\delta^{18}O_{atm}$= +23.5‰; Lane and Dole, (1954)). Thus the calculated $\delta^{18}O_{NO3}$ will depend of the isotopic composition of the regional or local water.

One of the most important applications of isotopes is source identification of groundwater NO_3^- (Wassenaar et al., 1995, Kendall et al., 1997). The isotopic composition of $^{15}N\text{-}NO_3^-$ formed via nitrification will depend on the $^{15}N\text{-}NH_4^+$ that is controlled by the source of the NH_4^+ (i.e. manure or ammonium fertilizer). However there are overlaps in the $^{15}N\text{-}NO_3^-$ from different sources such as between NO_3^- fertilizer and ammonium fertilizer (Xue et al., 2009 and references therein). Nonetheless, plotting $\delta^{15}N_{NO3}$ vs. $\delta^{18}O_{NO3}$ has shown to be useful to identify the source of groundwater NO_3^- to a certain extent (Aravena and Robertson 1998; Mayer et al., 2002; Vitòria et al., 2004; Kendall et al., 2007; among others).

1.1.2 Denitrification

Among the different biological pathways, denitrification is considered the main reaction that irreversibly eliminates dissolved NO_3^- from groundwater (Aravena and Robertson 1998). In natural systems, denitrification leads to nitrate elimination through conversion into harmless N_2 (Knowles 1982) but is limited by the availability of electron donors. Denitrification is a redox reaction driven by autotrophic or heterotrophic bacteria that reduce NO_3^- to nitrogen gas (N_2) under anaerobic conditions. Autotrophic bacteria promote denitrification using reduced sulphur compounds such as Fe^{2+} bearing minerals (i.e. Fe^{2+}-sulphides and Fe^{2+}-silicates) whereas heterotrophic bacteria use organic matter as the electron donors for NO_3^- reduction. In both cases, denitrification occurs through a number of sequential reactions. NO_3^- is initially converted to nitrite (NO_2^-), which is in fact a more serious health hazard than NO_3^- (De Beer et al., 1997). The maximum allowed NO_2^- concentration in drinking water is 0.01 mM (Directive 98/83/CE). The next reaction transforms NO_2^- into nitric oxide gas (NO), and NO is subsequently converted into nitrous oxide gas (N_2O); both gaseous species are greenhouse gases. Finally, N_2O is transformed into N_2. The chain of reactions can, however, discontinue at each step depending on biological and kinetic factors. Usually, this reaction sequence is presented as a single reaction (Eqs. 9 and 10).

$$5CH_2O + 4NO_3^- + 4H^+ \rightarrow 2N_2 + 5CO_2 + 7H_2O \quad (9)$$

$$5FeS_2 + 15NO_3^- + 5H_2O \rightarrow 10SO_4^{2-} + 7.5N_2 + 5FeOOH + 5H^+ \quad (10)$$

During denitrification reaction, the $\delta^{15}N$ and $\delta^{18}O$ of the residual nitrate increase as nitrate concentration decreases with a $\varepsilon N/\varepsilon O$ ratio that ranges from 0.9 (Otero et al., 2009) to 2.1 (Böttcher et al., 1990). Likewise, the isotopic composition of the reaction by-products (HCO_3^- and SO_4^{2-}) may be used to identify the metabolic processes involved in natural or induced denitrification scenarios (Aravena and

Robertson, 1998; Hosono et al., 2013; Kendall et al., 2007; Otero et al., 2009; Rodríguez-Escales et al., 2014; Vidal-Gavilan et al., 2013)(Aravena and Robertson, 1998; Hosono et al., 2013; Kendall et al., 2007; Otero et al., 2009; Rodríguez-Escales et al., 2014; Vidal-Gavilan et al., 2013).

Another kind of denitrification is the nitrifier denitrification, which is usually considered separately in the nitrogen cycle (Fig 1). This reaction is produced by ammonia-oxidizing bacteria that reduce NO_2^- produced during nitrification (or denitrification) to N_2 (Ritchie et al., 1972, Poth et al., 1985). This process is considered one of the main production pathways of $N_2O_{(g)}$ in soils (Wunderlin et al., 2013; Zhu et al., 2013).

1.1.3 DNRA

DNRA is an anaerobic reduction reaction enacted by fermentative bacteria that reduce NO_3^- to NO_2^- before the final reduction to NH_4^+ (Korom, 1992). The global DNRA reaction is commonly represented by Equation 11.

$$2H^+ + NO_3^- + 2CH_2O \rightarrow NH_4^+ + 2CO_2 + H_2O \qquad (11)$$

This reaction occurs under similar conditions as denitrification, however, is less observed in practice. The main factors affecting the development of every reaction are the biomass in the system that is finally controlled by the organic matter type and availability (Nijburg et al., 1998). DNRA has been reported mainly when the electron acceptor (NO_3^-) is limited (Burgin and Hamilton, 2007; Lind et al., 2013). Despite DNRA is rarely observed, some authors have found DNRA in groundwater systems (Bulger et al., 1989; Smith et al., 1991). Nizzoli et al. (2010) found a shift from denitrification to DNRA in hypolimnetic sediments due to an increase in both, organic carbon and the reducing conditions. Isotopically, DNRA will produce an enrichment in $\delta^{15}N$ and $\delta^{18}O$ of the residual NO_3^- whereas the $\delta^{15}N\text{-}NH_4^+$ is strongly depleted (McCready et al., 1983; Lehmann et al., 2004).

1.1.4 Anammox

Anammox reaction was discovered by Mulder et al., (1995) in a wastewater treatment experiment. The reaction occurs under anaerobic conditions driven by autotrophic bacteria where NH_4^+ is oxidized using NO_2^- and NO_3^- as electron donors Eq. 12, 13 and 14 (Van de Graaf et al., 1995 and 1996).

$$3NO_3^- + 2NH_4^+ \rightarrow 3NO_2^- + N_2 + 3H_2O + 2H^+ \quad (12)$$

$$NH_4^+ + 1.3NO_2^- \rightarrow N_2 + 2H_2O + 0.3NO_3^- \quad (13)$$

Anammox is a very important process in marine environments where about 50% of N is removed through this reaction (Dalsgaard et al., 2005; Nicholls and Trimmer, 2009; Thamdrup and Dalsgaard, 2002). In addition, Anammox has been described in lake systems (Schubert et al., 2006) and in some groundwater systems (Clark et al., 2008; Meyer et al., 2005). During Anammox reaction, the ^{15}N becomes heavier in the residual molecules of NO_3^-, NO_2^- and NH_4^+ as concentration decreases; likewise, the isotopic composition of ^{18}O increases in the unreacted NO_3^- and NO_2^-.

1.2 Induced nitrate attenuation

The human supply threshold of NO_3^- is exceeded by many aquifers worldwide because NO_3^- is highly mobile in groundwater and often persists in aquifers where the concentration of dissolved oxygen is over 0.06 mM and/or there are few electron donors, such as labile organic carbon, sulphides and/or Fe(II)-bearing minerals (Korom, 1992). As a consequence, there are many areas where NO_3^- cannot be naturally removed in the environment. In this context, Europe has proposed actions to reduce NO_3^- pollution (Directive 91/976/ECC). For instance, preventing pollution at the source involves improving farming practices (Aarts et al., 2001; Flessa et al., 2002; Moreau et al., 2012) and/or the conceptual management framework (Almasri, 2007). Furthermore, different remedial strategies have been proposed to remove NO_3^- from groundwater, such as membrane technologies, permeable reactive barriers, ion exchange, hydrogenotrophic denitrification (Haugen et al., 2002; Pintar et al., 2001; Schmidt and Clark, 2012; Soares et al., 2011; Xia et al., 2010), or microbial desalination-denitrification (Zhang and Angelidaki, 2013). Of the different strategies, one of the most efficient treatments for removing NO_3^- involves enhanced biological denitrification within the aquifer using biodenitrification technologies (Khan and Spalding, 2004; Tartakovsky B. et al., 2002; Vidal-Gavilan et al., 2013, among others).

In natural systems, denitrification is predominantly restricted by the availability of electron donors (Knowles, 1982), In this sense, different field- and lab-scale treatments have been tested to remove NO_3^- from both ground- and wastewaters by adding an external electron donor to promote heterotrophic or autotrophic denitrification with significant success (Borden et al., 2011; Istok et al., 2004; Leverenz et al., 2010; Tartakovsky et al., 2002; Torrentó et al., 2010; Vidal-Gavilan et al., 2013). In the case of the induction of

heterotrophic denitrification biostimulation, frequently tested electron donors included alcohols, such as ethanol or methanol, sugars, such as glucose or sucrose, or other organic compounds, such as acetic acid, glycerol or lactic acid (Aesoy et al., 1998; Akunna et al., 1993; Fernández-Nava et al., 2010; Ge et al., 2012; Gómez et al., 2000; Lee and Welander, 1996; Martin et al., 2009; Osaka et al., 2008; Peng et al., 2007; Vidal-Gavilan et al., 2013; among others). Complex organic compounds, such as pine bark, compost or sawdust have also been investigated (Schipper and Vojvodic, 2000; Trois et al., 2010). In the case of autotrophic denitrification, some compounds such as pyrite have been evaluated to enhance nitrate attenuation at field and lab scale (Torrentó et al., 2010). Multi-isotopic characterisation is an important tool to identify and describe induced denitrification reactions and can be used to quantify the attenuation performed at field-scale (Vidal-Gavilan et al., 2013, Barford et al., 1999, Delwiche & Steyn, 1970, Torrentó et al., 2011).

1.3 Kinetics of nitrate attenuation

Useful information about nitrate attenuation reactions can be obtained through the kinetic studies that can be applied to model the reactive transport in aquifers. This type of models can be helpful to understand the behavior of the system under different conditions, describing the chemical distribution of species in water along time. Most of the kinetic studies of denitrification were focused on induced attenuation, adding an external organic or inorganic substrate ((Dinçer and Kargi, 2000; Koenig and Liu, 2001; Nielsen et al., 1996) or a specific bacteria strain (Joshi et al., 2007). Kinetic studies can be based on batch experiments (Joshi et al., 2007; Vasiliadou et al., 2008) and/or continuous systems (Andre et al., 2011; Fu et al., 2009; Mathioudakis and Aivasidis, 2009; Roychoudhury and Viollier, 1998). Commonly, Monod kinetic equation has been utilized to describe biological redox reactions, however, this equation must be considered purely descriptive and should not be used to predict transformation rates outside the range of concentration performed in the experiments (Bekins et al., 1998). Despite this limitation, Monod equations have been applied to biodegradation models (Van Cappellen and Wang, 1996; Koenig and Liu, 2001; Hunter et al., 1998 and references therein).

2. Rationale

Many areas of Spain have been declared as vulnerable to NO_3^- pollution according to European directive (EC, 1991), and most of these zones have NO_3^- concentration over the threshold level

established by Directive 98/83/CE for human water supply. One of the most vulnerable environments to nitrate pollution are the systems without drainage to large water bodies such as endorheic basins located in semiarid or arid regions because these closed systems have low precipitation and high evaporation rates. Endorheic basins are very frequent in the central part of Spain. Among the endorheic systems from Central Spain, Pétrola basin, located in the SE of Spain, in the Castilla-La Mancha Region, is an excellent example. Pétrola basin covers 43 km^2 with a saline lake located near the SW edge of the basin. This area, vulnerable to nitrate pollution, has been declared both a highly-modified superficial water body and a nature reserve (Spanish Decree 102/2005, September 13th). Despite the use of fertilizers is restricted and under the authorities supervision (Order 2011/7/2 CMA), nitrate pollution has been observed in the region and is linked to farming activities producing an estimated input of NO_3^- in the lake about 3.76 t/year (Cortijo et al., 2012). Furthermore, there is an additional NO_3^- input from the municipal wastewaters, which are spilled directly to the lake. These NO_3^- sources enhance eutrophication processes and produce harmful algal blooms in the Pétrola Lake.

3. Study area

Geology of the Pétrola basin is formed mainly by Mesozoic materials (Fig. 2). The bottom of the sequence is formed by oolitic carbonate Jurassic rocks with porosity related to the fracture network. The base of the Lower Cretaceous unit corresponds to the Weald Facies and consists on lutite sediments, overlayed by sands and sandy-conglomerate sediments with intergranular porosity, which reaches the Barremian time. Aptian carbonates overlay Barremian terrigenous deposits. Albian deposits (Utrillas Facies) consist on siliciclastic sands, sandy-conglomerates and reddish to dark grey clay to lutite sediments. The Utrillas Facies materials are interstratified by grey-to-black lutitic and sandy sediments with high contents in organic matter and sulphides. These deposits show noticeable lateral changes in thickness and different oxidation states throughout the Pétrola basin with an average thickness of about 7m.

Hydrogeologically, the basin is formed by two unconnected aquifers. A confined aquifer formed by highly permeable oolitic Jurassic carbonates. The overlaying lutitic Weald Facies forms the confining layer. The second aquifer is composed of siliciclastic sands, conglomerates and lutites (Utrillas Facies, Albian). Groundwater flow in the system converges on the Pétrola Lake. The lake is connected to the

aquifer and the saline system can be considered as a terminal discharge zone. However, the difference between salty surface water from lake and fresh-groundwater can produce a density-driven flow from surface lake water towards underlying aquifer (Zimmerman et al., 2006).

NO_3^- concentration in surface and ground-water in the basin for the period 2008-2010 ranged from <0.1 to 154.7mg/L. The observed variation in NO_3^- concentration can be linked with natural attenuation processes. However, some limitations can mask the whole rate of these processes at field-scale. The inaccessibility to sampling points in a flow line, mixing processes and the variation in the solutes load make difficult the identification of attenuation processes. In addition, the role of different electron donors and their capacity to promote denitrification at calculated from field data can also be affected by these processes. In this context, laboratory experiments can provide useful information to understand the role of both, the different sediments from the basin that are able to produce denitrification and the different electron donors present in the sediments. As a result, laboratory coupled with field data can be therefore used to improve understanding of the nitrogen cycle of Pétrola basin.

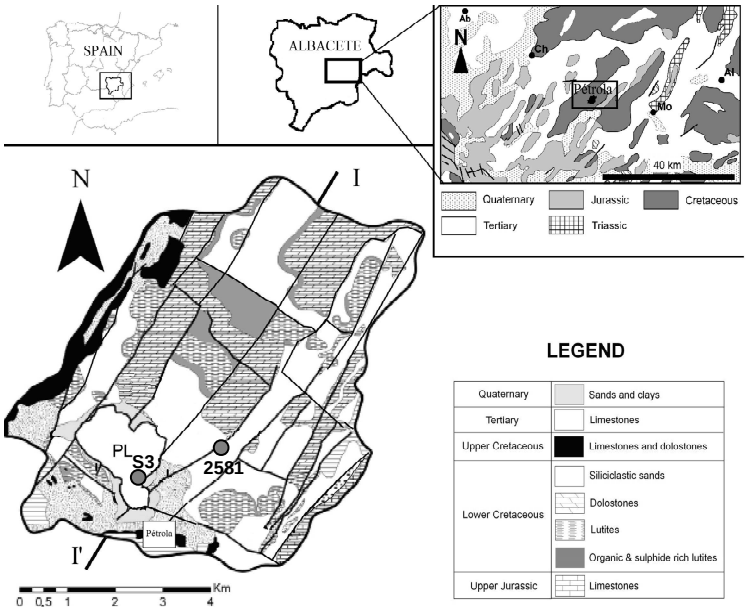

Figure 2. Location and regional geology (modified from Baena-Pérez and Jerez-Mir, 1982) and simplified geological map of the Pétrola Lake endorheic basin. Ab: Albacete, Ch: Chinchilla de Montearagón, Mo : Montealegre del Castillo, AL : Almansa, masl: meters above sea level.

In this context, in this thesis innovative laboratory experiments coupled with field survey were performed in order to understant the key factors affecting nitrogen cycle in the Pétrola Basin. The work

developed represents a step forward in the knowledge of natural and induced nitrate attenuation using isotopic tracers ($\delta^{15}N\text{-}NO_3^-$, $\delta^{18}O\text{-}NO_3^-$, $\delta^{34}S\text{-}SO_4^{2-}$, $\delta^{18}O\text{-}SO_4^{2-}$, $\delta^{13}C\text{-}HCO_3^-$).

4. General goals

The general goal of this thesis is to improve the knowledge on natural and induced nitrate attenuation using isotopic tracers ($\delta^{15}N\text{-}NO_3$, $\delta^{18}O\text{-}NO_3$, $\delta^{34}S\text{-}SO_4$, $\delta^{18}O\text{-}SO_4$, $\delta^{13}C\text{-}HCO_3$). The aim is to understand the key factors affecting nitrogen cycle in Pétrola Basin by means of both laboratory and field scale studies.

The first main objective is to assess the natural attenuation mechanisms present in the Pétrola basin. To achieve this goal laboratory-scale (flow-through experiments) with different sediments of the basin were performed to determine their global natural attenuation potential. The specific goals are:

- To study the availability and the role of the different electron donors in the Utrillas Facies and bottom lake sediments from Pétrola basin to promote denitrification.

- Calculate the denitrification rates of both sediments and to relate it with different flow rates used during the experiments.

- Characterize the possible generation of toxic compounds such as NH_4^+ and/or NO_2^-, as well as other redox processes such as the sulphate reduction. Identify the factors that control their production during the experiments.

- Obtain the fractionation factors (εN and εO) during denitrification produced by Utrillas Facies and bottom lake sediment in order to quantify the denitrification degree at field scale.

The second main goal of the thesis is to characterize natural attenuation processes of NO_3^- in Pétrola basin at field scale and to understand the key factors affecting nitrogen cycle. The specific goals are:

- To study the hidrogeological system of the Pétrola basin focusing on the aquifer-lake relationships in order to confirm the occurrence of denisity down-flow from the hypersaline lake to the underlying groundwater.

- Identify the source of NO_3^- and understand the factors controlling NO_3^- distribution in the Pétrola basin, focusing in the surroundings of the hypersaline lake and its connection to the regional-scale groundwater system.

- Describe the NO_3^- attenuation processes in Pétrola basin with the integration of laboratory and field data to confirm the role of the different electrons donors present in the basin.

- Calculate the capacity of the density driven flow to transport the dissolved organic carbon from lake sediments into deep anoxic aquifer zones for enhancing denitrification processes.

Finally the third main goal of the thesis is to asses the feasibility of induced attenuation methods (biostimulation) to allow to reduce the contamination where natural nitrate attenuation was not observed or was insuficient. The specific goals are:

- Evaluate the viability of periodically injecting glucose to promote denitrification in groundwater from Pétrola basin using C/N ratios close to stoichiometric value of heterotrophic denitrification reaction.

- Achieve complete NO_3^- elimination while preventing the generation of undesirable compounds and processes, such as NO_2^- or sulphate reduction

- Obtain the isotopic fractionation factor (ε) for N and O during the induced denitrification reaction to evaluate the efficiency of future field tests.

5. Methodology

The description of the analytical methods employed in this thesis, are detailed in the appendix B.

5.1 Field survey

A total of 252 samples from 20 control points (springs, streams and agricultural wells) where analysed between April 2008 and December 2010. Twelve sampling points were selected for assessing denitrification in the saline lake-aquifer system. Eight of them (2554, 2564, 2571, 2581, 2602, 2640, 2641, 2642) were selected for evaluating denitrification processes based on their accessibility, location in the hydrogeological context, hydrogeochemical parameters, and the dominant land use (irrigation crops). Additionally, four PVC piezometers (2623, 2624, 2625, 2626) were installed during 2008 close to the lake in order to measure vertical profiles of hydrogeochemical parameters at different depths. The piezometers were 5 cm in inner diameter and were installed to depths ranging from 12.1 m (2626) to 37.9 m (2623).

5.2 Experimental design

The experiments consisted of flow-through glass columns (40 cm in length and 9 cm in diameter) filled with sediments from the Pétrola basin (Fig. 3). Two different sediments were studied: 1) the organic and sulphide-rich material from Utrillas sediments and 2) the bottom lake sediment. In September 2008 four piezometers (S1 to S4) were drilled close to the SE edge of the lake. The sediment was sampled in one of these piezometers (S3) (Fig. 2). During the drilling, the core was sampled at various depths (a) 1.5 – 2.0 m, (b) 5.30 – 5.45 m, (c) 9.00 – 9.60 m, and (d) 15.30 – 15.45 m. The core was then isolated from the atmosphere with polypropylene and immediately frozen in the field with solid CO_2 to preserve it at -30ºC. X-ray powder diffraction (XRD) analyses from the fine size (<40 μm) fraction of the sediments were performed. Measured total organic carbon was 0.4% for Utrillas Facies and 1.2% for the bottom lake sediment. The sulphur percentage was 2% in the Utrillas Facies, mainly as disseminated pyrite, whereas in bottom lake sediments sulphur was 4%, in this case as sulphate forms such as gypsum and magnesite. The water used in the experiment was sampled at well 2581 (Fig. 2) with average NO_3^- concentration of 0.81 mM (50 mg/L).

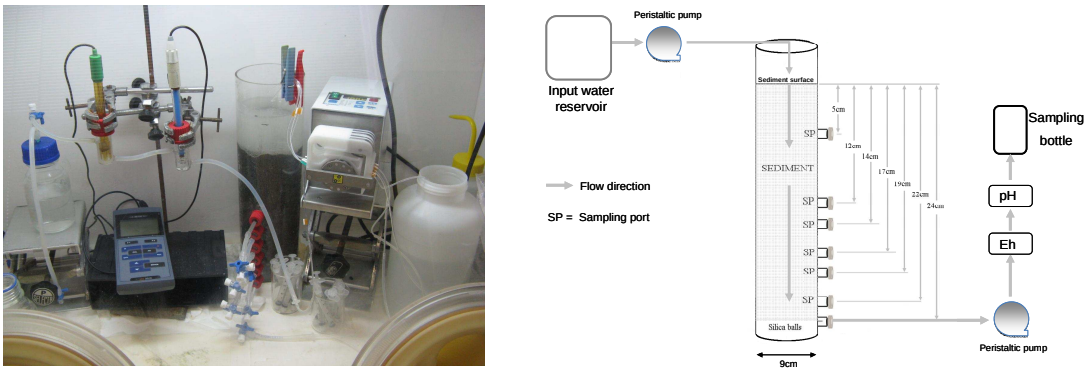

Figure 3. Set-up of the flow-through experiments. Flow rate in the experiment was controlled by a peristaltic pump. Arrows indicate the flow direction in the flow-through experiment.

6. Results and discussion

6.1 Natural attenuation: Utrillas Facies

The results obtained in column experiment showed that Utrillas Facies sediments were able to remove NO_3^- contamination from groundwater (0.8 mM) under specific flow conditions. In addition, the role of the different electron donors present in this sediment was also evaluated. During the experiment, two different stages were observed.

Stage I started at the beginning of the experiment up to day 21. Denitrification was observed at the beginning coupled with an increase NO_2^- in the outflow (Fig. 4). The important NO_2^- accumulation observed was related with the initial growth of denitrifiers and the induction of nitrite reductase (Abell et al., 2009). An important increase in DOC was observed during this stage pointing out that NO_3^- attenuation could be promoted by heterotrophic denitrification. However, during this stage an important leaching from the sediment was observed, masking any chemical (SO_4^{2-} concentration) or isotopic ($\delta^{34}S$-SO_4^{2-} and ^{18}O-SO_4^{2-}) variation produced by autotrophic denitrification. Therefore, the role of pyrite in the NO_3^- attenuation could not be discarder neither confirmed for this period. The denitrification rate ($NO_3^- + NO_2^- \rightarrow N_2$) calculated for this period was 10 µmol N d^{-1} L^{-1}.

The Stage 2 started at day 21 until the end of the experiment, with a flow rate of 0.1 mL/min. The outflow NO_3^- concentration was similar to the input water, whereas NO_2^- concentration remained constant around 0.04 mM. After a flow rate change down to 0.05 mL/min, NO_3^- in the outflow decreased

down to 0.48 mM and NO_2^- increased to values around 0.15 mM. At day 96, when the flow rate was again reduced to 0.01 mL/min, NO_3^- and NO_2^- were below detection limit ($3x10^{-3}$ and $4x10^{-3}$ mM respectively) in the outflow water. Coupled with complete NO_3^- and NO_2^- removal, DOC increased in the outflow up to 0.75 mM (Fig. 4). In addition, during Stage II, SO_4^{2-} concentration, $\delta^{34}S\text{-}SO_4^{2-}$ and $\delta^{18}O\text{-}SO_4^{2-}$ did not varied in the outflow water compared to the input water, pointing out that denitrification was produced using organic matter as electron donor. The degree of attenuation during this stage showed to be controlled by changes in flow rate. After 215 days, NO_3^- concentration in the outflow showed an increasing trend towards values close to the input water due to organic carbon depletion. The higher denitrification rate during this stage was 31 µmol N d^{-1} L^{-1}.

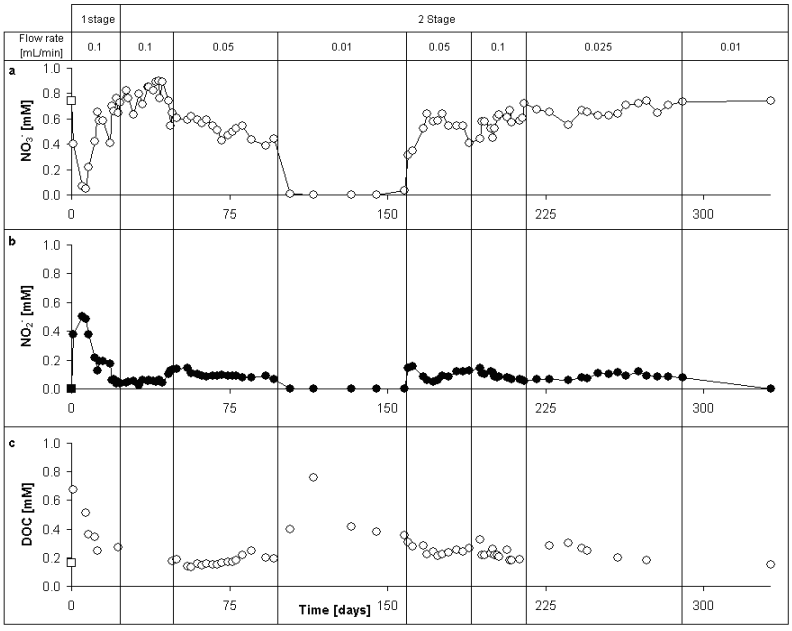

Figure 4. Nitrate, NO_2^- and DOC concentration over time showing flow rates and denitrification stages. Square points represent input water concentration.

The isotopic fractionation of N and O from the residual NO_3^- was calculated. The obtained values were −11.6‰ and −15.7‰ for εN and −12.1‰ and −13.8‰ for εO during attenuation produced in stages I and II respectively (Fig. 5).

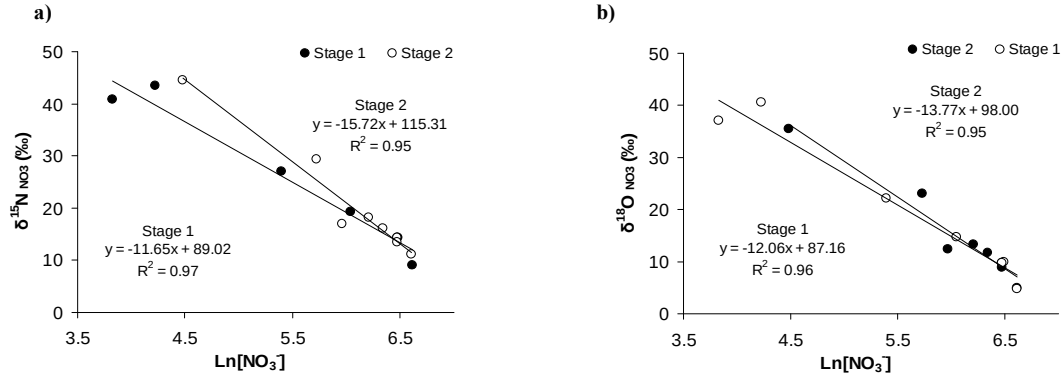

Figure 5. (a) $\delta^{15}N$ vs. $\ln[NO_3^-]$ for both stages of denitrification. Slopes correspond to the isotopic fractionation value of ^{15}N. (b) $\delta^{18}O$ vs. $\ln[NO_3^-]$ for both stages. Slope corresponds to the isotopic fraction of ^{18}O

With the fractionation values obtained in this experiment, the percentage of denitrification at the field scale was calculated using:

$$DEN\ (\%) = [1 - e^{(\delta residual - \delta initial/\varepsilon)}] \times 100 \qquad (14)$$

The observed NO_3^- attenuation from water samples collected in the field ranged from 0% to 60% with an average attenuation of 20%. The percentage was calculated using both εN and εO for the two stages (Fig. 6). Slight differences were observed in the attenuation depending on the fractionation factor used. This can be explained to the different processes affecting the changes in $\delta^{15}N$ and $\delta^{18}O$ during nitrification reactions such as volatilization occurring in the field. Overall, the isotopic study of the field samples has showed that denitrification is taking place in the basin but it cannot completely remove NO_3^- from groundwater.

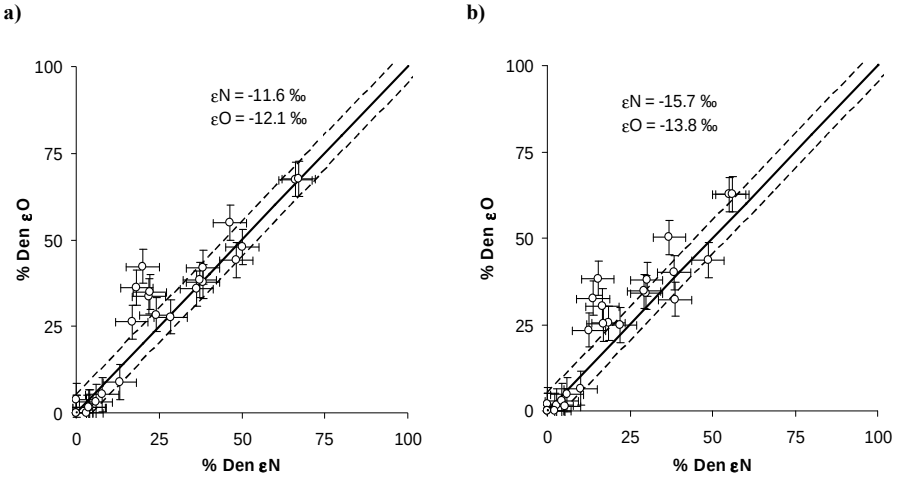

Figure 6. Comparison of the percentage of NO_3^- attenuation using the different fractionation values obtained in the column experiment. (a) Percentage obtained using fractionation values of the first stage. (b) Percentage obtained using fractionation values of the second stage. The solid lines indicate the 1:1 ratio and the dashed lines represent variation of 5%. Error bars of samples are 5%, in agreement with the standard deviation of isotopic analyses.

6.2 Natural attenuation: Bottom lake sediments

In the column experiment performed using bottom lake sediment results showed complete NO_3^- attenuation in the outflow water after 7 days. Nitrate attenuation in the outflow was observed during 288 days. Coupled with NO_3^- attenuation, a very important increase in the salinity of the outflow water was observed produced by the dissolution of the salty minerals present in the sediment. During the first days of the experiment NH_4^+ and NO_2^- concentration increased up to 0.88 mM and 0.52 mM respectively. The increase of NH_4^+ was related with dissimilatory nitrate reduction to ammonium (DNRA) favored by high C/N ratio and salinity at early stages. Hence, the NO_2^- accumulated was produced by uncompleted DNRA reaction. After 10 days NH_4^+ concentration decreased pointing out the repression of DNRA, and denitrification became in the main NO_3^- attenuation reaction. These results were similar to other studies performed in lakes where DNRA had a limited extent (e.g., Mengis et al., 1997; Lehmann et al., 2003). Sulphate reduction could be promoted due to the low redox observed when NO_3^- was completely consumed (<150 mV). However, the possible variation of SO_4^{2-} concentration was masked by both leaching and gypsum dissolution of the sediment that increased SO_4^{2-} content in the outflow water. In addition, the leaching masked variations in the isotopic composition of dissolved SO_4^{2-} in the outflow water. Therefore, sulphate reduction could not be confirmed neither discarder during the experiment. However at field scale the migration of dissolved organic C coupled with the reducing environment could promote sulphate reduction.

Using Phreeqc-2d a biogeochemical model was developed to determine the organic carbon transfer from solid sediment to water, and to model organic matter oxidation consumed to reduce $N\text{-}NO_x^-$ (NO_3^- + NO_2^-) from input water. Data from different vertical profiles of the column experiment under different flow rate were employed to validate the proposed model. Equations for nitrate reduction and organic transfer were Equation 15, and 16.

$$r_1 = \mu_{\max} \cdot [C]_t \cdot \left(\frac{[N]_t}{K_s + [N]_t} \right) \qquad (15)$$

$$r_2 = Q \cdot r_1 \qquad (16)$$

where [C] is the concentration of the soluble electron donor (mmol L^{-1}) (DOC), [N] is the concentration of the electron acceptor ($N\text{-}NO_x^-$, mmol L^{-1}); μ_{max} is the maximum specific growth rate (h^{-1}); K_s is the half saturation constant of $N\text{-}NO_x^-$ (mmol L^{-1}) and Q is the stoichiometric relationship between the electron

acceptor and the electron donor; in the case of heterotrophic denitrification, Q is 0.8 (Knowles, 1982)

The immobilized organic carbon can be attached to the aquifer matrix and/or to the biofilms. From there, particulate organic matter will be successively solubilized and subsequently oxidized during denitrification (Janning et al., 1998). Solubilization, i.e., mass transfer process, is assumed to be a rate-limited process where the rate can also depend on the solubility of the dissolved organic compounds. We have modeled this processes it following the instructions of Greskowiak et al. (2005), who slightly modified model from Kinzelbach et al. (1991), as Eq. 17:

$$r_{DOC,sol} = C_{SOM}\beta\frac{C_{sat} - C_{DOC}}{C_{sat}} \qquad (17)$$

where r is a mass transfer rate (mmol L^{-1} h^{-1}), C_{sat} is the saturation concentration (mmol L^{-1}), C_{DOC} is the soluble organic carbon (mmol L^{-1}), C_{SOM} is the solid organic carbon in the sediment normalized to the mass of water in the reactor (mol Kg^{-1}) and β is the maximum transfer rate (h^{-1}).

The calibrated parameters used to reproduce the model are listed in Table 1. Figure 7 shows how the model fits well with experimental data (each figure is related to a different flow velocities). The calculated denitrification parameters (μ_{max} and $K_{sat,nit}$) were in the same range as other similar natural attenuation experiences, and were also similar to other enhanced denitrification studies at lab-scale.

Table 1. Estimated values of different parameters used in this work

Parameter	Unit	Value
μ_{max}	[h^{-1}]	0.04
$K_{sat,nit}$	[mmol/L]	5 x 10^{-2}
C_{sat}	[mmol/L]	4.65
β	[h^{-1}]	1.78 x 10^{-3}

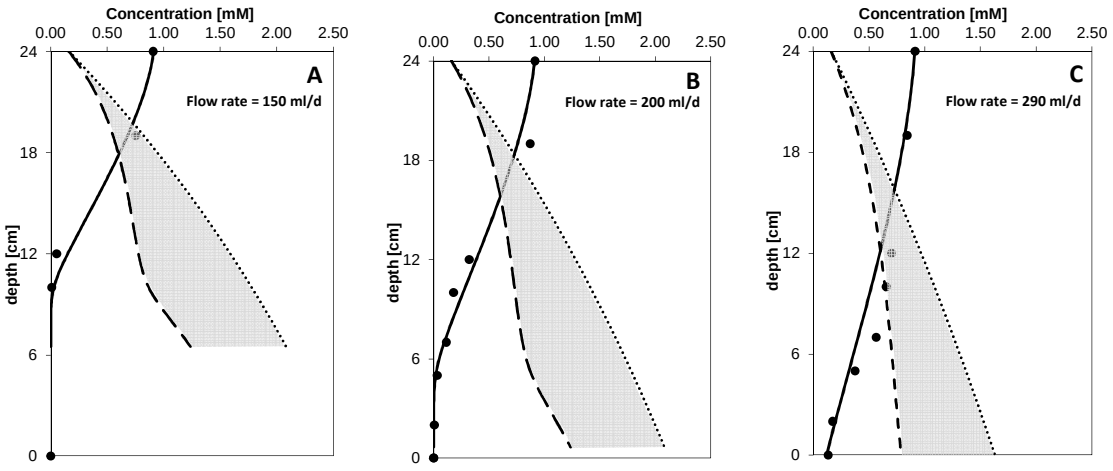

Figure 7. Modeling results (lines) versus experimental data (circles). Solid line represents nitrate concentration; dashed line represents organic carbon degraded; dotted line represents organic carbon transfer to liquid from solid phase without degradation and grey surface represents the organic carbon consumed due to denitrification.

The results from the kinetic model showed that the attenuation rate was similar for every period despite the different flow-rate. The average nitrogen reduction rate obtained was 1.25 mmol N d^{-1} L^{-1}. This value was in the range of bibliographic data from other brackish environments such as hypersaline lakes or estuaries (Laverman et al., 2012). In addition the nitrogen reduction rate obtained for lake sediment from Pétrola was two orders of magnitude higher than the obtained using the sediment of the Utrillas Facies.

The amount of organic carbon mobilized during the experiment calculated from the model and validated with measured DOC in the outflow. The total amount of reactive organic carbon mobilized from the sediment was 53.5 mmol. The amount of organic carbon consumed to reduce NO_3^- to N_2 was 28.8 mmol. This amount represented about 18% of solid organic carbon presented in the sediment (1.2%). This result was considerably higher than the Utrillas Facies results were only 2% of the solid organic carbon (0.4%) was degraded. The remarkable differences in denitrification rate and the carbon availability could be linked to different reactivity of organic carbon sources.

The isotopic fractionation values obtained were ‒14.7‰ and ‒14.5‰ for N and O respectively (Fig. 8). These values were similar to those obtained using the Utrillas Facies sediment. Some authors observed that fractionation values were lower as denitrification rate increased (Mariotti et al., 1988), whereas other authors observed that more negative values of fractionation were associated with higher rates of kinetic denitrification (Korom et al., 2012). Our results showed that despite denitrification rates

using bottom lake sediments were two orders of magnitude higher than using sediment of the Utrillas Facies, the isotopic fractionation was similar for both sediments. Therefore, isotopic fractionation of $\delta^{15}N$ and $\delta^{18}O$ during denitrification cannot be only explained by variation in reaction rate and other factors can also affect to it such as bacteria community or environment conditions.

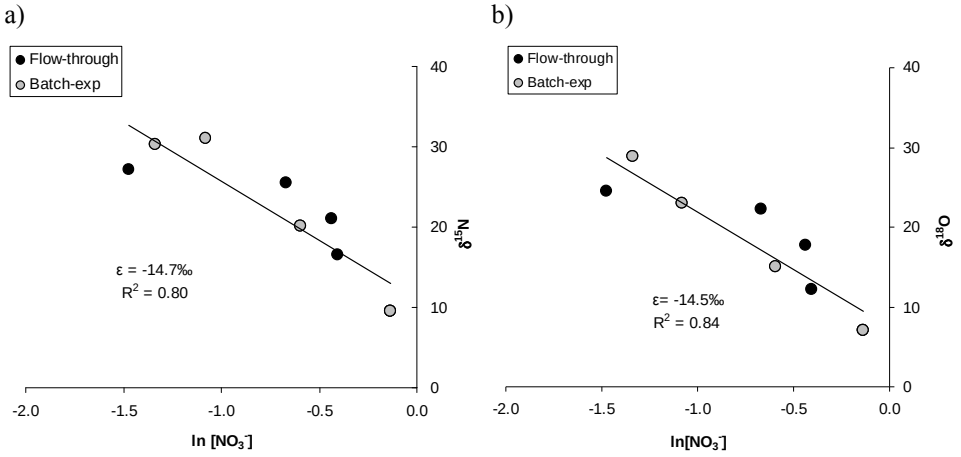

Figure 8. (a) Plot of $\delta^{15}N$ vs $\ln[NO_3^-]$ values. Slopes correspond to the isotopic fractionation value of ^{15}N. (b) Plot of $\delta^{18}O$ vs $\ln[NO_3^-]$ values. Slope corresponds to the isotopic fractionation of ^{18}O.

6.3 Chemical and multi-isotopic characterization of Pétrola basin

According to its hydrological dynamics the study area has been divided in three different zones (Fig. 9). Zone 1 corresponds with the recharge area of the upper aquifer in the North whereas Zone 2 is located nearby the lake following the groundwater flow direction from Zone 1. Therefore, Zones 1 and 2 will be discussed together in order to understand the chemical and isotopic evolution of groundwater in Pétrola basin. In other hand, Zone 3 represented the zone of density-driven groundwater flow located under the lake and showing the down-flow from the lake to the underlying aquifer as was observed in the Electrical Resistivity Tomography (ERT) survey performed in the lake.

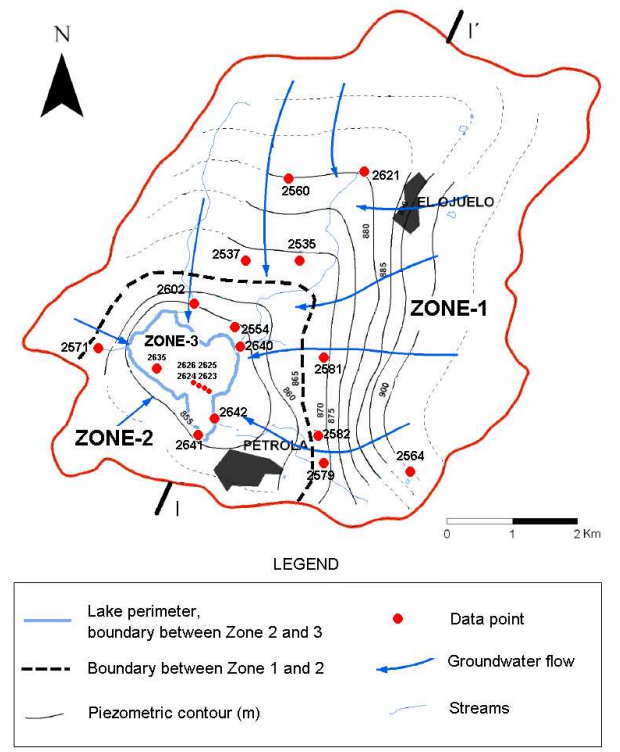

Figure 9. Map showing the distribution of piezometric surface (masl) of Cretaceous aquifer (2003) and sampling locations.

A field survey was performed in the Pétrola basin during 2008-2010 in order to determine the distribution of NO_3^- contamination. The integration of the experimental results with the field data were used to depict the attenuation processes acting in the basin. The NO_3^- concentration increased in Zone 1 following the groundwater flow. Higher NO_3^- values were located at the Center and South-West of the basin in agreement with agricultural activities developed in the area. The isotopic composition of $\delta^{15}N_{NO3}$ and $\delta^{18}O_{NO3}$ indicated that the origin of NO_3^- was derived from synthetic fertilizers slightly volatilized. With regards Zone 2, samples nearby the lake showed a slightly decrease in NO_3^- concentration coupled with an increase in isotopic composition of $\delta^{15}N_{NO3}$ and $\delta^{18}O_{NO3}$. This increase in the isotopic composition pointed out the presence of denitrification in Pétrola basin. The % of NO_3^- attenuation in Zone 1 reached a maximum of 10% whereas Zone 2 showed a higher denitrification percentage, between 10% and 60% (Fig. 10). However, samples in with higher denitrification showed an average NO_3^- concentration of 44.8 mg/L, close to the human water supply threshold.

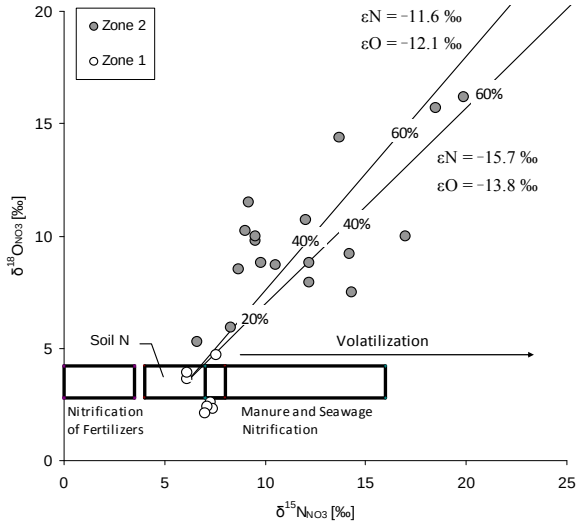

Figure 10. $\delta^{15}N_{NO3}$ vs $\delta^{18}O_{NO3}$ of field samples together with the isotopic composition of the main nitrate sources (Vitoria et al 2004). Line shows the % of attenuation calculated with isotopic fractionation obtained in the column experiment.

Interpretation of chemical and isotopic data from field surveys had an added difficulty, since samples were also affected by other processes (no only denitrification) such as dissolution of gypsum or precipitation of calcite. These reactions affected the concentration and isotopic composition of the different by-products of denitrification reactions (SO_4^{2-} and HCO_3^-) complicating their interpretation. Only DOC in some samples showed a similar trend than the observed in the experiments, with higher DOC concentration in samples with higher attenuation, suggesting that organic matter was acting as the main electron donor, in agreement with the experiment performed with the sediment from the Utrillas Facies. The observed denitrification at field scale showed an important spatial variability linked to the variation of the amount and reactivity of labile organic matter as well as NO_3^- supply.

The Zone 3 involves both, surface lake water and the mixing area of contaminated groundwater with density flow from lake. In both systems the NO_3^- contents were below the detection limit. In surface water, NO_3^- was mainly consumed promoting the development of the algal blooms observed in the lake that produce the eutrophication of the lake. Under the lake, the hydrogeologic model suggested that saline lake water (with no NO_3^-) is mixed with fresh-groundwater (contaminated by NO_3^-). However, NO_3^- concentration measured in the piezometers under the lake during the year 2010 was below the detection limit. The experiment performed with bottom lake sediment indicated that this sediment was playing an important role as source of electron donors that could promote denitrification in the underlying groundwater. However, ERT results indicated that the saltwater-freshwater interface extents down to 12-16m. The density driven downflow therefore could not explain the absence of NO_3^- measured in the

deepest piezometers. An alternative explanation is that the deepest piezometers are groundwater with longer residence time and absence of NO_3^-. It was supported by the analyses of Tritium in deepest piezometers (2624, 2625 and 2626) that showed values close to the detection limit (~0.8 TU), suggesting waters infiltrating before 1950. Since in the Castilla-La Mancha Region, the surface of irrigation crops began to be noticeable at the beginning of the 80´s of the past century (Calera and Martín, 2005), the absence of NO_3^- in the deepest part of the aquifer under the lake is related to regional groundwater flow with longer residence time and it was not linked to denitrification. Therefore, tritium data confirmed that the role of DOC transported by the density-driven downflow would be restricted to the freshwater-saltwater interface in the upper part of the aquifer (down to 12 m below ground surface), in agreement with ERT results. Consequently, the geometry of the density downflow plays an important role in denitrification under the lake.

6.4 Induced attenuation experiment

To enhance the heterotrophic denitrification in the Pétrola basin, a biostimulation treatment was proposed. The present work sought to design an efficient strategy for inducing biostimulation. The biostimulation consisted on the periodical injection of glucose in a flow-through system. Three different C/N ratios were tested along experiment. From the beginning of the experiment to day 39 the C/N ratio was 1.6. Nitrate concentration displayed several increase-decrease cycles until day 18. Coupled with NO_3^- attenuation, NO_2^- was accumulated in the outflow up to day 27. From that day on, NO_3^- was completely removed and NO_2^- was not detected. Changes performed in the C/N ratio to lower values of 1.25 and 1.12 did not further affect the denitrification efficacy, and complete NO_3^- attenuation lasted until day 125 without NO_2^- accumulation (Fig. 11).

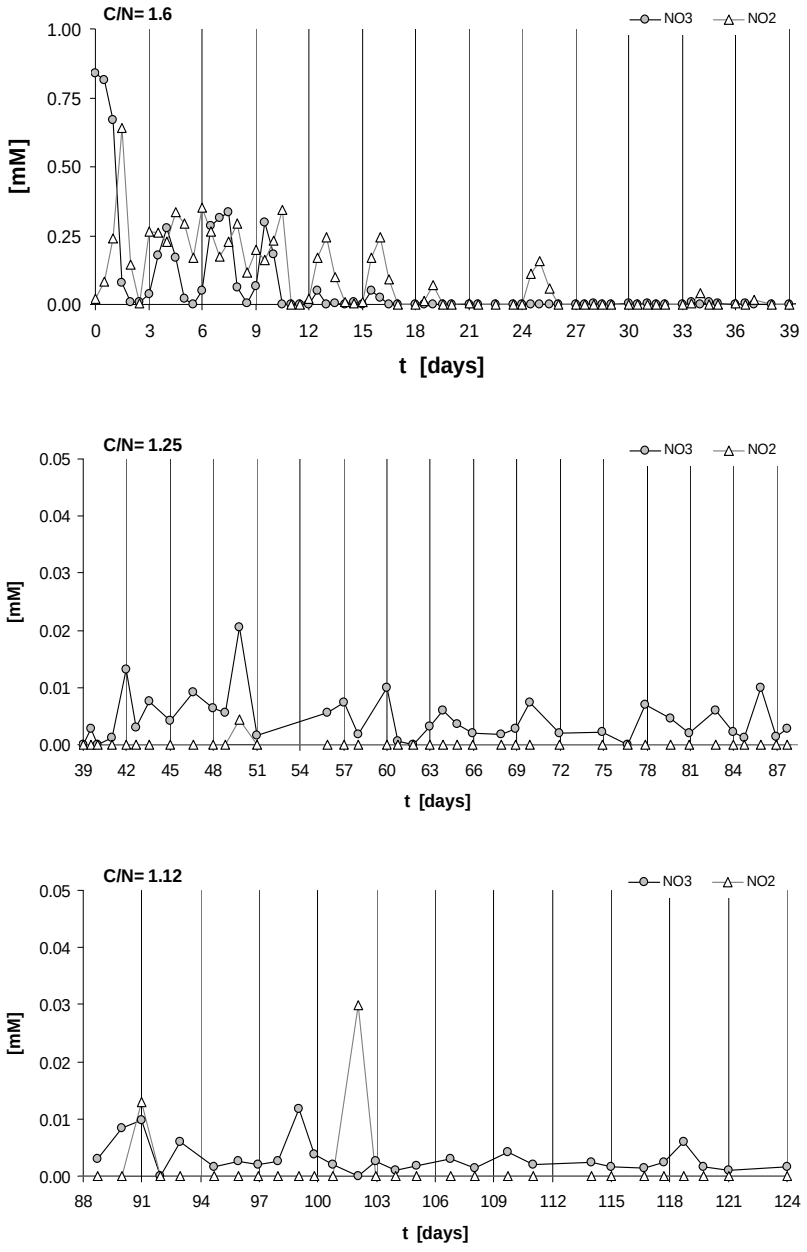

Figure 11. NO_3^- and NO_2^- evolution during the experiment. (a) Stage I C/N = 1.6. (b) Stage II C/N = 1.25. (c) Stage III C/N =1.12. *Note that the graph (a) has a different y-axis scale. Vertical lines represent the glucose injections.

The NO_2^- accumulation was produced because bacteria preferentially use NO_3^- at the beginning of denitrification when NO_3^- and NO_2^- are available, accumulating NO_2^-. In addition, samples with detectable NO_2^- concentrations had a pH ranging from 8.4 to 8.7; these values are within the range that inhibits the NO_2^- reduction (between 8.5 and 9.0) (Glass and Silverstein, 1998) (Fig. 12).

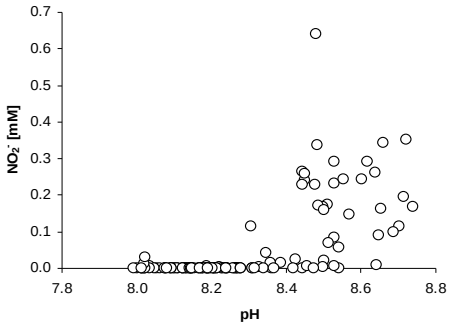

Figure 12. NO_2^- accumulation vs. pH. NO_2^- was usually detected on samples with pH > 8.4.

Glucose was detected in the outflow samples during all the experiment despite the C/N injected was stoichiometric or lower and complete NO_3^- attenuation was achieved. The results indicated that a supplementary C source was necessary to promote the observed NO_3^- attenuation for every injection. This secondary source might include the DOC of the input water with a concentration up to 0.21 mM or the C from the biomass growing inside the reactor. The amount of extra C needed to achieve the complete NO_3^- attenuation in the outflow ranged between 20 and 35%.

The presence of glucose in the outflow water might suggest the possible development of sulphate reduction processes. In addition, the Eh values were below reported values able to promote SO_4^{2-} reduction (<-150 mV) (Connell and Patrick Jr. 1968). Therefore, once NO_3^- was completely removed, the glucose excess could promote SO_4^{2-} reduction. However, the isotopic composition of $\delta^{34}S_{SO4}$ and $\delta^{18}O_{SO4}$ was constant indicating that SO_4^{2-} reduction was most likely not occurring. It is hypothesized that once NO_3^- was completely consumed, the residence time of water inside the reactor was too short to promote sulphate reduction. Although in the present work the SO_4^{2-} reduction was not observed, an excess of available glucose is undesirable because this reaction could occur during field-tests**.**

The isotopic fractionation of the N and O of the biostimulation experiment was 8.8‰ for εN and 8.0‰ for εO (Fig. 13). These values were lower than those obtained for the Utrillas Facies and bottom lake sediments. These variations in the denitrification rate might be related to the specific C source used for biostimulation being different than the C-natural sources present in the sediment, affecting the evolution of the microbial populations and, consequently, the denitrification kinetics (Song and Tobias, 2011)(Song and Tobias, 2011). The isotopic fractionation can be applied in a future pilot-test assay in order to quantify the efficiency of the induced degradation.

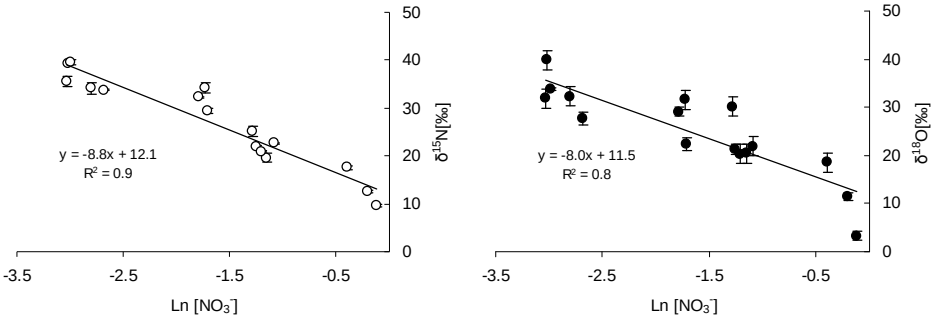

Figure 13. $\delta^{15}N$ and $\delta^{18}O$ of NO_3^- against the natural logarithm of NO_3^- concentration [mM]. Slopes of the regression lines represent the isotopic fractionation factor for N and O. Error bars represent the standard deviation of the replicates.

7. General conclusions

The study of Cretaceous Utrillas Facies and bottom lake sediments in laboratory experiments combining multi-isotopic techniques and chemical data showed that natural attenuation produced by both materials was mainly linked with the oxidation of the organic matter. In the case of Utrillas Facies, isotopic values of $\delta^{34}S_{SO4}$ and $\delta^{18}O_{SO4}$ throughout the most important denitrification stage, ruled out pyrite as electron donor. Bottom lake sediments showed higher potential to remove NO_3^- than the Utrillas Facies. Important differences between both sediments were observed in the amount of reactive organic carbon, and in the nitrogen reduction rate. The reactive organic carbon from Utrillas Facies was 1.7mmol C that corresponds to 2% of the total organic carbon present in the sediment (0.4%) with a maximum nitrogen reduction rate of $3.1x10^{-2}$ mmol N d^{-1} L^{-1}. With regards lake sediments, reactive organic carbon was 53.0 mmol that represents 18% of the total organic carbon of the sediment (1.2%). The nitrogen reduction rate of lake sediment obtained from the biogeochemical model was 1.25 mmol N d^{-1} L^{-1}. These differences were linked to the variation in the reactivity of the different organic carbon sources. Despite the remarkable differences, similar isotopic fractionation of N and O during denitrification for the Utrillas Facies and the bottom lake sediment were observed. The Utrillas Facies displayed values of −11.6‰ and −15.7‰ for εN and −12.1‰ and −13.8‰ for εO whereas denitrification produced by the bottom lake sediments showed εN of −14.7‰ and εO of −14.5‰. Furthermore the εN/εO ratios for both sediments were analogous, with values of 0.96 and 1.14 for the Utrillas Facies and 1.01 for the bottom lake sediment.

The hydrogeological study showed that groundwater flow in the Pétrola basin can be considered as the result of two main flow components: a regional groundwater flow, from the recharge areas (Zone 1) to the discharge ones located near the lake (Zone 2) and the density driven flow from surface water from the lake towards the underlying aquifer (Zone 3). Hydro-chemical and isotopic results suggested that NO_3^- in the basin is derived from synthetic fertilizers slightly volatilized. Isotopic results from the field showed that denitrification was taking place in the basin although it was restricted to the surrounding area (Zone 2) and under the lake (Zone 3). In addition, the using the isotopic fractionations obtained in the laboratory experiments, the percentage of NO_3^- attenuation was calculated. NO_3^- removed ranged from 0% to 60% with an average percentage of 20%. The degree of denitrification observed at field scale showed an important spatial variability related with the amount, availability and reactivity of labile organic matter as well as spatial variation of NO_3^- supply. The observed denitrification in Cretaceous aquifer in the basin is likely to be produced by organic carbon oxidation of the Utrillas Facies sediment since dissolved SO_4^{2-} distribution could be explained by gypsum dissolution. However, in specific wells, sulphide minerals could not be discarded as a potential electron donor. Attenuation processes by heterotrophic denitrification reactions were more likely to occur in zones of the saline lake-aquifer system. Density downflow from surface water effectively transported the DOC to aquifer zones under reducing conditions; however, its influence decreased with depth becoming negligible in the deepest part of the aquifer.

As consequence of the incomplete NO_3^- attenuation observed in groundwater of Pétrola basin a biostimulation treatment was proposed. Periodically injecting an organic carbon source might be a suitable method to remove NO_3^- from groundwater during long-term treatments. The induced attenuation experiment showed that the injection of glucose enhanced denitrification over other processes such as DNRA. Remarkable presence of NO_2^- was produced during the first days due to enzymatic repression of nitrite reductase as well as the pH conditions of the system. Complete NO_3^- attenuation without NO_2^- accumulation was reached after 27 days. Changes in C/N ratio to stoichiometric or lower ratio did not further affect the achieved complete NO_3^- attenuation because secondary carbon sources were available in the system (DOC in the input water and/or biofilms). The isotopic fractionation values of N and O during induced denitrification were ‒8.8‰ and ‒8.0‰ respectively, lower (in absolute values) than natural denitrification fractionation of both the Utrillas Facies sediment and the bottom lake sediment.

Overall, the elaboration of this thesis has improved the knowledge of the NO_3^- attenuation processes that are taking place in the endorheic systems of the central part of Spain. Focusing on an excellent example of this kind of basins, the exhaustive laboratory work based on flow-trough experiments has showed the role and the potential to produce nitrate attenuation from different sediments. Combination of chemical and isotopic data from these experiments with field data is a robust method to depict and evaluate the processes and key factors controlling the reactions of these hydro-geological systems.

More research is needed to understand the temporal distribution and degree of denitrification in Pétrola basin. In addition, exhaustive field data analyses of $\delta^{34}S$ and $\delta^{18}O$ from dissolved SO_4^{2-} and solid (sulphides and evaporate) samples coupled with their spatial distribution are needed to depict the role of sulphide oxidation in denitrification. The identification of sulphate reduction or methanogenesis processes in the lake can be another fact to take into account in future works. All this information can used to develop hydrogeological and reactive transport models that can be applied to similar environments of Castilla-La Mancha region. Finally, the application of bioremediation treatment in specific wells affected by NO_3^- pollution should be tested in a pilot-scale field test following the treatment strategy used in the flow-through experiment.

8. Thesis outline

This thesis is composed of 2 published papers and 2 manuscripts that are currently in prepararion for publication or under review by international peer-reviewed journals.

Two of the papers deals the potential of denitrification with Utrillas Facies and Bottom lake sediments from Pétrola basin in order to know the intrisic potential of these materials to promote denitrification. The first paper, published in Appliend Geochemistry, was focused on the Utrillas Facies and discusse the role of the different electron donors present in this material (pyrite and organic matter) for NO_3^- attenuation. The second paper (under review) is focused on role of the bottom lake sediment as carbon source to promote denitrification and include the kinetic study of the NO_3^- attenuation reaction to quantify the reaction rate.

The third paper is focused on the characterization of the natural NO_3^- attenuation occurring in groundwater of the Pétrola basin by means of a multi-isotopic approach integrated with hydrochemistry data. The main objetives of this part are: i) to describe the hydrogeological system and the relationship between groundwater system and the saline lake; ii) idenitfy and characterize the denitrification processes ocurring in the Pétrola basin; iii) determine the role of the different electron donors present in the basin and to study its spatial and temporal distribution. Results from previous papers were used in order to understand the chemical and isotopic distribution at field.

Last paper discusses the potential of denitrification with glucose as bioremediation strategy of NO_3^- contaminated groundwater of Pétrola basin. The experiment is performed to evaluate the viability of a biostimulation treatment consisting on periodical injections of glucose to promote complete NO_3^- attenuation. Different C/N ratios were tested to achieve complete NO_3^- elimination while preventing the generation of undesirable compounds, such as NO_2^- or H_2S. Isotopic and chemical analyses were used to monitor the efficacy of stimulated denitrification. The impact of the biostimulation in the indigenous microbial community was also evaluated.

Appendix A includes the published papers and the manuscrpits under review. Appendix B encompasses a short description of the main laboratory methods and protocols used in the experimental work of the thesis. Appendix C includes the bulk dataset of experimental results and field survey presented in papers.

References

Aarts, H.F.M., Conijn, J.G., Corré, W.J., 2001. Nitrogen fluxes in the plant component of the “De Marke” farming system, related to groundwater nitrate content. Netherlands J. Agric. Sci. 49, 153–162.

Abell, J., Laverman, A.M., Cappellen, P., 2009. Bioavailability of organic matter in a freshwater estuarine sediment: long-term degradation experiments with and without nitrate supply. Biogeochem. 94, 13–28.

Aesoy, A., Odegaard, H., Bach, K., Pujol, R., Hamon, M., 1998. Denitrification in a packed bed biofilm reactor (Biofor) - Experiments with different carbon sources. Water Res. 32, 1463–1470.

Akunna, J.C., Bizeau, C., Moletta, R., 1993. Nitrate and Nitrite Reductions with Anaerobic Sludge Using Various Carbon Sources: Glucose, Acetic Acid, Lactic Acid and Methanol. Water Res. 27, 1303–1312.

Almasri, M.N., 2007. Nitrate contamination of groundwater: A conceptual management framework. Environ. Impact Assess. Rev. 27, 220–242.

Andersson, K.K., y Hooper, A.B., 1983. O_2 and H_2O are each the source of one O in NO_2 produced from NH_3 by Nitrosomonas: ^{15}N-NMR evidence. FEBS Lett. 164, 236-240.

Andre, L., Pauwels, H., Dictor, M.C., Parmentier, M., Azaroual, M., 2011. Experiments and numerical modelling of microbially-catalysed denitrification reactions. Chem. Geol. 287, 171–181.

Aravena, R., Robertson, W.D., 1998. Use of multiple isotope tracers to evaluate denitrification in ground water: Study of nitrate from a large-flux septic system plume. Ground Water 36, 975–982.

Baena-Pérez, J., Jerez-Mir, L., 1982. (IGME) Síntesis para un ensayo paleogeográfico entre la Meseta y la Zona Bética (s:srt). Col. Informe. Madrid, pp 256.

Barford, C.C., Montoya, J.P., Altabet, M. A., Mitchell, R., 1999. Steady-state nitrogen isotope effects of N_2 and N_2O production in *Paracoccus denitrificans*. Appl. Environ. Microbiol. 65, 989–994.

Bekins, B.A., Warren, E., Godsy, E.M., 1998. A Comparison of zero-order, first-order, and Monod biotransfromation models. Ground Water 36, 261–268.

Borden, A.K., Brusseau, M.L., Carroll, K.C., McMillan, A., Akyol, N.H., Berkompas, J., Miao, Z., Jordan, F., Tick, G., Waugh, W.J., Glenn, E.P., 2011. Ethanol addition for enhancing denitrification at the uranium mill tailing site in Monument Valley, AZ. Water, Air, Soil Pollut. 223, 755–763.

Böttcher, J., Strebel, O.L., Voerkelus, S., Schmidt, H.L., 1990. Using isotope fractionation of nitrate-nitrogen and nitrate-oxygen for evaluation of microbial denitrification in sandy aquifer. J. Hydro. 144, 413–424.

Bulger, P.R., Kehew, A.E., Nelson, R.A., 1989. Dissimilatory nitrate reduction in a waste-water contaminated aquifer. Ground Water 27, 664–671.

Burgin, A.J., Hamilton, S.K., 2007. Have we overemphasized the role of denitrification in aquatic ecosystems? A review of nitrate removal pathways. Front. Ecol. Environ. 5, 89–96.

Calera, A., Martín, F., 2005. Uso de la teledetección en el seguimiento de los cultivos de regadío. In Martín F, López P, Calera A. (eds), Agua y Agronomía. Mundi-Prensa, Madrid.

Choi, W.J., Ro, H.M., 2003. Differences in isotopic fractionation of nitrogen in water-saturated and unsaturated soils. Soil Biol. Biochem. 35, 483-486.

Clark, I.D., Fritz, P., 1997. Environmental isotopes in hydrogeology. Lewis Publishers, New York.

Clark, I., Timlin, R., Bourbonnais, A., Jones, K., Lafleur, D., Wickens, K., 2008. Origin and fate of industrial ammonium in anoxic ground water ^{15}N evidence for anaerobic oxidation (Anammox). Ground Water Monit. Remediat. 73–82.

Comly, H.H., 1945. Cyanosis in infants caused by nitrates in well water. J. Am. Med. Assoc. 129. 112-116.

Connell, W.E., Patrick Jr., W.H., 1968. Sulfate reduction in soil: Effects of redox potential and pH. Sci. 159, 86–87.

Cortijo, A., Carrey, R., Gómez-Alday, J.J., Otero, N., Soler, A., Sanz, D., Castaño, S., Recio, C., Carnicero, A., Ayora, C., Gómez-Sánchez, E., 2011. Aportes de nitrato a la laguna de Pétrola (SE, Albacete). Impacto de la agricultura y de los vertidos de agua residuales. In: Congreso Ibérico sobre las aguas subterráneas (AIH-GE).

Dalsgaard, T., Thamdrup, B., Canfield, D.E., 2005. Anaerobic ammonium oxidation (anammox) in the marine environment. Res. Microbiol. 156, 457–464.

De Beer, D., Schramm, A., Santegoeds, C.M., Kuhl, M., 1997. A nitrite microsensor for profiling environmental biofilms. Appl. Environ. Microbiol. 63, 973–977.

Delwiche, C.C., Steyn, P.L., 1970. Nitrogen isotope fractionation in soils and microbial reactions. Environ. Sci. Technol. 4, 929–935.

Dinçer, A., Kargi, F., 2000. Kinetics of sequential nitrification and denitrification processes. Enzyme Microb. Technol. 27, 37–42.

EEC, 1991. Council Directive 91/676/EEC, of 12 December 1991, concerning the protection of waters against pollution caused by nitrates from agricultural sources [online]. Off. J. Eur. Comm. L 375, 1–8 (Brussels). Available from: <http://www.europa.eu.int/eur-lex> (31.12.1991)

EC, 1998. Council Directive 98/83/EC, of 3 November 1998, on the quality of water intended for human consumption [online]. Off. J. Eur. Comm. L 330, 32–54 (Brussels). Available from: <http://www.europa.eu.int/eur-lex> (5.12.1998).

EC, 2000. Council Directive 2000/60/EC, of 23 October 2000, establishing a frame- work fro Community action inthe field of water policy [online].Off. J. Eur. Comm. L 327, 1–73 (Brussels). Available from: <http://www.europa.eu.int/eur-lex> (22.12.2000).

EC, 2006. Council Directive 2006/118/EC, of 12December 2006, on the protection of groundwater against pollution and deterioration [online]. Off. J. Eur. Comm. L 372, 19–31 (Brussels). Available from: <http://www.europa.eu.int/eur-lex> (27.12.2006)

Fernández-Nava, Y., Marañón, E., Soons, J., Castrillón, L., 2010. Denitrification of high nitrate concentration wastewater using alternative carbon sources. J. Hazard. Mater. 173, 682–688.

Flessa, H., Ruser, R., Dörsch, P., Kamp, T., Jimenez, M.A., Munch, J.C., Beese, F., 2002. Integrated evaluation of greenhouse gas emissions (CO_2, CH_4, N_2O) from two farming systems in southern Germany. Agric. Ecosyst. Environ. 91, 175–189.

Fu, Z., Yang, F., An, Y., Xue, Y., 2009. Bioresource Technology Characteristics of nitrite and nitrate in situ denitrification in landfill bioreactors. Bioresour. Technol. 100, 3015–3021.

Ge, S., Peng, Y., Wang, S., Lu, C., Cao, X., Zhu, Y., 2012. Nitrite accumulation under constant temperature in anoxic denitrification process: The effects of carbon sources and COD/NO_3-N. Bioresour. Technol. 114, 137–143.

Glass, C., Silverstein, J.A., 1998. Denitrification kinetics of high nitrate concentration water: pH effect on inhibition and nitrite accumulation. Water Res. 32, 831–839.

Gómez, M.A., González-López, J., Hontoria-García, E., 2000. Influence of carbon source on nitrate removal of contaminated groundwater in a denitrifying submerged filter. J. Hazard. Mater. 80, 69–80.

Greskowiak, J., Prommer, H., Vanderzalm, J., Pavelic, P., Dillon, P., 2005. Modeling of carbon cycling and biogeochemical changes during injection and recovery of reclaimed water at Bolivar, South Australia. Water Resour. Res., 41(10): W10418.

Haugen, K.S., Semmens, M.J., Novak, P.J., 2002. A novel in situ technology for the treatment of nitrate contaminated groundwater. Water Res. 36, 3497–506.

Heaton, T., 1986. Isotopic studies of nitrogen pollution in the hydrosphere and atmosphere: a review. Chem. Geol. 59, 87–102.

Högberg, P., 1997. Tansley Review No. 95─ ^{15}N natural abundance in soil–plant systems. New Phytologist 137, 179–203.

Hosono, T., Tokunaga, T., Kagabu, M., Nakata, H., Orishikida, T., Lin, I.T., Shimada, J., 2013. The use of $\delta^{15}N$ and $\delta^{18}O$ tracers with an understanding of groundwater flow dynamics for evaluating the origins and attenuation mechanisms of nitrate pollution. Water Res. 47, 2661–2675.

Hunter, K., Wang, Y., Van Cappellen, P., 1998. Kinetic modeling of microbially-driven redox chemistry of subsurface environments: coupling transport, microbial metabolism and geochemistry. J. Hydrol. 209, 53–80.

Istok, J.D., Senko, J.M., Krumholz, L.R., Watson, D., Bogle, M.A., Peacock, A., Chang, Y.J., White, D.C., 2004. In situ bioreduction of technetium and uranium in a nitrate-contaminated aquifer. Environ. Sci. Technol. 38, 468–475.

Janning, K.F., Le Tallez, X., Harremoës, P., 1998. Hydrolysis of organic wastewater particles in laboratory scale and pilot scale biofilm reactors under anoxic and aerobic conditions. Water Sci. Technol. 38(8–9).

Joshi, K., Binnal, P., Srinikethan, G., 2007. Denitrification: Mass transfer and kinetic studies. In: Proceedings of the World Congress on Engineering and Computer Sicence (Lecture Notes) 188–193.

Kendall, C., Elliott, E.M., Wankel, S.D., 1997. Tracing anthropogenic inputs of nitrogen to ecosystems. Stable Isot. Ecol. Environ. Sci. 61, 375–449.

Kendall, C., Elliott, E.M., Wankel, S.D., 2007. Tracing antropogenic inputs of nitrogen to ecosystems, in: Michener, R.H., Lajtha, K. (Eds.), Stable Isotopes in Ecology and Environmental Science. Blackwell Publishing, pp. 375–450.

Khan, I.A., Spalding, R.F., 2004. Enhanced in situ denitrification for a municipal well. Water Res. 38, 3382–3388.

Killingstad, M.W., Widdowson, M.A., Smith, R.L., 2002. Modeling enhanced in situ denitrification in groundwater. J. Environ. Eng., 128: 14.

Knowles, R., 1982. Denitrification. Microbiol. Rev. 46, 43–70.

Koenig, A., Liu, L.H., 2001. Kinetic model of autotrophic denitrification in sulphur packed-bed reactors. Water Res. 35, 1969–1978.

Korom, S.F., 1992. Natural denitrification in the saturated zone: A review. Water Resour. Res. 28, 1657–1668.

Korom, S.F., Schuh, W.M., Tesfay, T., Spencer, E.J., 2012. Aquifer denitrification and in situ mesocosms: Modeling electron donor contributions and measuring rates. J. Hydrol. 432-433, 112–126.

Lane G., Dole M., 1956. Fractionation of oxygen isotopes during respiration. Sci. 123, 74–576.

Laverman, A.M., Pallud, C., Abell, J., Cappellen, P. Van, 2012. Comparative survey of potential nitrate and sulfate reduction rates in aquatic sediments. Geochim. Cosmochim. Acta 77, 474–488.

Lee, N.M., Welander, T., 1996. The effect of different carbon sources on respiratory denitrification in biological wastewater treatment. J. Ferment. Bioeng. 82, 277–285.

Lehmann, M.F., Reichert, P., Bernasconi, S.M., Barbieri, A., McKenzie, J. a., 2003. Modelling nitrogen and oxygen isotope fractionation during denitrification in a lacustrine redox-transition zone. Geochim. Cosmochim. Acta 67, 2529–2542.

Lehmann, M.F., Sigman, D.M., Berelson, W.M., 2004. Coupling the $^{15}N/^{14}N$ and $^{18}O/^{16}O$ of nitrate as a constraint on benthic nitrogen cycling. Mar. Chem. 88, 1–20.

Leverenz, H.L., Haunschild, K., Hopes, G., Tchobanoglous, G., Darby, J.L., 2010. Anoxic treatment wetlands for denitrification. Ecol. Eng. 36, 1544–1551.

Lind, L.P.D., Audet, J., Tonderski, K., Hoffmann, C.C., 2013. Nitrate removal capacity and nitrous oxide production in soil profiles of nitrogen loaded riparian wetlands inferred by laboratory microcosms. Soil Biol. Biochem. 60, 156–164.

Magee, P.N., Barnes, J.M., 1956. The production of malignant primary hepatic tumours in the rat by feeding dimethylnitrosamine. Br. J. Cancer 10, 114–122.

Mariotti, A., Landreau, A., Simon, B., 1988. ^{15}N isotope biogeochemistry and natural denitrification process in groundwater: Application to the chalk aquifer of northern France. Geochim. Cosmochim. Acta 52, 1869–1878.

Martin, D., Salminen, J.M., Niemi, R.M., Heiskanen, I.M., Valve, M.J., Hellstén, P.P., Nystén, T.H., 2009. Acetate and ethanol as potential enhancers of low temperature denitrification in soil contaminated by fur farms: a pilot-scale study. J. Hazard. Mater. 163, 1230–1238.

Mathioudakis, V.L., Aivasidis, A., 2009. Heterotrophic denitrification kinetics in a pressurized sewer biofilm reactor. Desalination 248, 696–704.

Mayer, B., Bollwerk, S.M., Mansfeldt, T., Hütter, B., Veizer, J., 2001. The oxygen isotope composition of nitrate generated by nitrification in acid forest floors. Geochim. Cosmochim. Acta 65, 2743–2756.

Mayer, B., Boyer, E.W., Goodale, C., Jaworski, N.A., Van Breemen, N., Howarth, R.W., Seitzinger, S., Billen, G., Lajtha, K., Nadelhoffer, K., Van Dam, D., Hetling, L.J., Nosal, M., Paustian, K., 2002.

Sources of nitrate in rivers draining sixteen watersheds in the northeastern US: Isotopic constraints. Biogeochem. 57, 171–197.

McCready, R.G.L., Gould,W.D., Barendregt, R.W., 1983. Nitrogen isotope fractionation during the reduction of NO_3^- to NH_4^+ by *Desulfovibrio* sp. Can. J. Microbiol. 29, 231–234.

Mengis M., Gachter R., Wehrli B., and Bernasconi S. (1997) Nitrogen elimination in two deep eutrophic lakes. Limnol. Oceanogr. 42(7), 1530–1543.

Meyer, R.L., Rigaard-Petersen, N., Allen, D.E., 2005. Correlation between anammox activity and microscale distribution of nitrite in subtrophical mangrove sediment. Appl. Environ. Microbiol. 71, 6142–6149.

Moreau, P., Ruiz, L., Mabon, F., Raimbault, T., Durand, P., Delaby, L., Devienne, S., Vertès, F., 2012. Reconciling technical, economic and environmental efficiency of farming systems in vulnerable areas. Agric. Ecosyst. Environ. 147, 89–99.

Mulder, A., Van de Graaf A.A., Robertson L.A., Kuenen J.G., 1995. Anaerobic ammonium oxidation discovered in a de- nitrifying fluidized bed reactor. Microbiol. Ecol. 16, 177–183.

Nicholls, J., Trimmer, M., 2009. Widespread occurrence of the anammox reaction in estuarine sediments. Aquat. Microb. Ecol. 55, 105–113.

Nielsen, P.E.R.H., Bjerg, P.L., Christensen, T.H., 1996. Determined first-order degradation rate constants of specific organic compounds in an aerobic aquifer. Environ. Sci. Technol. 30, 31–37.

Nijburg, J.W., Gerards, S., Laanbroek, H.J., 1998. Competition for nitrate and glucose between *Pseudomonas fluorescens* and *Bacillus licheniformis* under continuous or fluctuating anoxic conditions. Microbiol. Ecol. 26, 345–356.

Nizzoli, D., Carraro, E., Nigro, V., Viaroli, P., 2010. Effect of organic enrichment and thermal regime on denitrification and dissimilatory nitrate reduction to ammonium (DNRA) in hypolimnetic sediments of two lowland lakes. Water Res. 44, 2715–2724.

Osaka, T., Shirotani, K., Yoshie, S., Tsuneda, S., 2008. Effects of carbon source on denitrification efficiency and microbial community structure in a saline wastewater treatment process. Water Res. 42, 3709–3718.

Otero, N., Torrentó, C., Soler, A., Menció, A., Mas-Pla, J., 2009. Monitoring groundwater nitrate attenuation in a regional system coupling hydrogeology with multi-isotopic methods: The case of Plana de Vic (Osona, Spain). Agric. Ecosyst. Environ. 133, 103–113.

Pauwels, H., Foucher, J.C., Kloppmann, W., 2000. Denitrification and mixing in a schist aquifer: influence on water chemistry and isotopes. Chem. Geol. 168, 307–324.

Peng, Y.Z., Ma, Y., Wang, S.Y., 2007. Denitrification potential enhancement by addition of external carbon sources in a pre-denitrification process. J. Environ. Sci. 19, 284–289.

Pintar, A., Batista, J., Levec, J., 2001. Integrated ion exchange / catalytic process for efficient removal of nitrates from drinking water. Chem. Eng. Sci. 56, 1551–1559.

Poth M., Focht D.D., 1985. Nitrogen-15 kinetic analysis of nitrous oxide production by *Nitrosomonas europaea*: An examination of nitrifier denitrification. Appl. Environ. Microbiol 49 (5), 1134–1141.

Ritchie, G.A., Nicholas D. J. D., 1972. Identification of the source of nitrous oxide produced by oxidative and reductive processes in *Nitrosomonas europaea*. Biochem. J. 126, 1181–1191.

Rivett, M.O., Buss, S.R., Morgan, P., Smith, J.W.N., Bemment, C.D., 2008. Nitrate attenuation in groundwater: a review of biogeochemical controlling processes. Water Res. 42, 4215–4232.

Rodríguez-Escales, P., Van Breukelen, B.M., Vidal-Gavilan, G., Soler, A., Folch, A., 2014. Integrated modeling of biogeochemical reactions and associated isotope fractionations at batch scale: A tool to monitor enhanced biodenitrification applications. Chem. Geol. 365, 20–29.

Roychoudhury, A., Viollier, E., 1998. A plug flow-through reactor for studying biogeochemical reactions in undisturbed aquatic sediments. Appl. Geochem. 13, 269–280.

Schipper, L.A., Vojvodic, M., 2000. Nitrate removal from groundwater and denitrification rates in a porous treatment wall amended with sawdust. Ecol. Eng. 14, 269–278.

Schmidt, C.A., Clark, M.W., 2012. Efficacy of a denitrification wall to treat continuously high nitrate loads. Ecol. Eng. 42, 203–211.

Schubert, C.J., Durisch-kaiser, E., Wehrli, B., Thamdrup, B., Lam, P., Kuypers, M.M., 2006. Brief report Anaerobic ammonium oxidation in a tropical freshwater system (Lake Tanganyika). Environ. Microbiol. 8 (10), 1857–1863.

Smith, R.L., Howes, B.L., Duff, J.H., 1991. Denitrification in nitrate-contaminated groundwater: Occurrence in steep vertical geochemical gradients. Geochim. Cosmochim. Acta 55, 1815–1825.

Soares, O.S.G.P., Órfão, J.J.M., Pereira, M.F.R., 2011. Nitrate reduction in water catalysed by Pd–Cu on different supports. Desalination 279, 367–374.

Song, B., Tobias, C.R., 2011. Molecular and stable isotope methods to detect and measure anaerobic ammonium oxidation (anammox) in aquatic ecosystems. Methods Enzymol. 496, 63–89.

Tartakovsky, B., Millette, D., Delisle, S., Guiot, S.R., 2002. Ethanol-stimulated bioremediation of nitrate-contaminated ground water. Ground Water Monit. Remediat. 22, 78–87.

Thamdrup, B., Dalsgaard, T., 2002. Production of N_2 through anaerobic ammonium oxidation coupled to nitrate reduction in marine sediments. Appl. Environ. Microbiol. 68, 1312–1318.

Torrentó, C., Cama, J., Urmeneta, J., Otero, N., Soler, A., 2010. Denitrification of groundwater with pyrite and Thiobacillus denitrificans. Chem. Geol. 278, 80–91.

Torrentó, C., Urmeneta, J., Otero, N., Soler, A., Viñas, M., Cama, J., 2011. Enhanced denitrification in groundwater and sediments from a nitrate-contaminated aquifer after addition of pyrite. Chem. Geol. 287, 90–101.

Toyoda, S., Mutobe, H., Yamagishi, H., Yoshida, N., Tanji, Y., 2005. Fractionation of N_2O isotopomers during production by denitrifier. Soil Biol. Biochem. 37, 1535–1545.

Trois, C., Pisano, G., Oxarango, L., 2010. Alternative solutions for the biodenitrification of landfill leachates using pine bark and compost. J. Hazard. Mater. 178, 1100–1105.

Van Cappellen, P., Wang, Y. 1996. Cycling of Irion and manganeses in surface sediment.pdf. Am. J. Sci. 296, 197–243.

Van de Graaf, A.A., Mulder, A., de Bruijn, P., Jetten, M., Robertson, L., Kuenen, J., 1995. Anaerobic oxidation of ammonium is a biologically mediated process. Appl. Environ. Microbiol. 61, 1246–1251.

Van de Graaf, A.A., De Bruijn, P., Robertson, L.A., Jetten, M.S.M., Kuenen, J.G., 1996. Autotrophic growth of anaerobic ammo- nium-oxidizing microorganisms in a fluidized bed reactor. Microbiol. UK 142, 2187–2196.

Vasiliadou, I.A., Tziotzios, G., Vayenas, D.V., 2008. A kinetic study of combined aerobic biological phenol and nitrate removal in batch suspended growth cultures. Int. Biodeterior. Biodegrad. 61, 261–271.

Vidal-Gavilan, G., Folch, A., Otero, N., Solanas, A.M., Soler, A., 2013. Isotope characterization of an in situ biodenitrification pilot-test in a fractured aquifer. Appl. Geochem. 32, 153–163.

Vitòria, L., Otero, N., Soler, A., Canals, A., 2004. Fertilizer characterization: Isotopic data (N, S, O, C, and Sr). Environ. Sci. Technol. 38, 3254–3262.

Vitoria, L., Soler, A., Canals, A., Otero, N., 2008. Environmental isotopes (N, S, C, O, D) to determine natural attenuation processes in nitrate contaminated waters: Example of Osona (NE Spain). Appl. Geochem. 23, 3597–3611.

Vitousek, P.M., Aber, J.D., Howarth, R.W., Likens, G.E., Pamela, A., Schindler, D.W., Schlesinger, W.H., Tilman, D.G., 1997. Human alteration of the global nitrogen cycle: Sources and consequences. Ecol. Appl. 7, 737–750.

Volkmer, B.G., Ernst, B., Simon, J., Kuefer, R., Bartsch, G., Bach, D., Gschwend, J.E., 2005. Influence of nitrate levels in drinking water on urological malignancies: a community-based cohort study. BJU Int. 95, 972–976.

Ward, M.H., deKok, T.M., Levallois, P., Brender, J., Gulis, G., Nolan, B.T., VanDerslice, J., 2005. Workgroup Report: Drinking-Water Nitrate and Health—Recent Findings and Research Needs. Environ. Health Perspect. 113, 1607–1614.

Wassenaar, L.I., 1995. Evaluation of the origin and fate of nitrate in the abbotsford aquifer using the isotopes of ^{15}N and ^{18}O in NO_3^-. Appl. Geochem. 10, 391–405.

Wunderlin, P., Lehmann, M.F., Siegrist, H., Tuzson, B., Joss, A., Emmenegger, L., Mohn, J., 2013. Isotope signatures of N_2O in a mixed microbial population system: constraints on N_2O producing pathways in wastewater treatment. Environ. Sci. Technol. 47, 1339–1348.

Xia, S., Zhong, F., Zhang, Y., Li, H., Yang, X., 2010. Bio-reduction of nitrate from groundwater using a hydrogen-based membrane biofilm reactor. J. Environ. Sci. 22, 257–262.

Xue, D., Botte, J., De Baets, B., Accoe, F., Nestler, A., Taylor, P., Van Cleemput, O., Berglund, M., Boeckx, P., 2009. Present limitations and future prospects of stable isotope methods for nitrate source identification in surface- and groundwater. Water Res. 43, 1159–1170.

Zhang, Y., Angelidaki, I., 2013. A new method for in situ nitrate removal from groundwater using submerged microbial desalination-denitrification cell (SMDDC). Water Res. 47, 1827–1836.

Zhu, X., Burger, M., Doane, T.A., Horwath, W.R., 2013. Ammonia oxidation pathways and nitrifier denitrification are significant sources of N_2O and NO under low oxygen availability. PNAS, 110 (16), 6328-6333.

Zimmermann, S., Bauer, P., Held, R., Kinzelbach, W., Walther, J.H., 2006. Salt transport on islands in the Okavango Delta: Numerical investigations. Adv. Water Resour. 29 11–29.

Appendix A:

A-1	The role of Lower Cretaceous sediments in groundwater nitrate attenuation in central Spain: Column experiments
A-2	Nitrate attenuation potential of hypersaline lake sediments in central Spain: Flow-through and batch experiments
A-3	Denitrification processes in a hypersaline lake-aquifer system (Pétrola basin, central Spain)
A-4	Induced nitrate attenuation by glucose in groundwater: Flow-through experiment

Appendix A-1:

The role of Lower Cretaceous sediments in groundwater nitrate attenuation in central Spain: Column experiments

R. Carrey, N. Otero, A. Soler, J.J. Gómez-Alday, C. Ayora

2013

Applied Geochemistry 32, 142-152

(Supporting information of this paper is available in Appendix C-1)

THE ROLE OF LOWER CRETACEOUS SEDIMENTS IN GROUNDWATER NITRATE ATTENUATION IN CENTRAL SPAIN: COLUMN EXPERIMENTS

Carrey, R. (1), Otero, N. (1), Soler, A. (1), Gómez-Alday, J. J. (2), Ayora, C. (3)

(1) Grup de Mineralogia Aplicada i Medi Ambient, Dept. De Cristal·lografia, Mineralogia i Dipòsits Minerals, Facultat de Geologia. Universitat de Barcelona. C/ Martí i Franques s/n, 08028 Barcelona, Spain. raulcarrey@ub.edu, notero@ub.edu, albertsoler@ub.edu

(2) Hydrogeology Group. Institute for Regional Development (IRD). University of Castilla-La Mancha (UCLM). Campus Universitario, s/n. 02071. Albacete. Spain. JuanJose.Gomez@uclm.es

(3) Institute of Environmental Assessment and Water Research, IDAEA- CSIC, C/Jordi Girona, 18, 08028 Barcelona, Spain. caigeo@idaea.csic.es

Abstract

Endorheic basins located in semiarid or arid regions constitute one of the most vulnerable and exposed environments to nitrate pollution. The Pétrola basin (Central Spain) is an outstanding example of this endorheic system. Several constraints have been observed that impede a correct picture of the denitrification pathway and degree at the field scale. To better understand the key factors controlling nitrate attenuation, a five-stage column experiment was performed using organic and pyrite rich sediments from the Utrillas Facies (Lower Cretaceous) as possible electron donor source to promote denitrification. A chemical and multi-isotopic characterization ($\delta^{15}N_{NO3}$, $\delta^{18}O_{NO3}$, $\delta^{13}C_{DIC}$, $\delta^{34}S_{SO4}$, $\delta^{18}O_{SO4}$) of the outflow of the column experiment showed that nitrate attenuation was driven by organic matter. The total amount of organic carbon consumed during denitrification was 2% of the total organic carbon present in the sediment. Both the degree and rate of denitrification were related to flow rate variations. Lower flow rates favored bacterial growth at the beginning of the experiment producing an increase of complete denitrification rate (CDR). When NO_3^- reduction was higher than 15%, CDR remained constant (around 30 μmol L^{-1} d^{-1}) under different flow rates. In the last stage, flow rate had no effect on output NO_3^- concentration because the organic carbon supply was limited and had become the main kinetic factor of denitrification. Isotopic fractionation (ε) of $^{15}N\text{-}NO_3^-$ and $^{18}O\text{-}NO_3^-$ between reaction products and remaining reactants were calculated using representative column samples. The results for the two attenuation stages observed were -11.6‰ and -15.7‰ for εN, and -12.1‰ and -13.8‰ for εO. Most of the field samples showed a percentage of attenuation ranging from 0 to 60% of nitrate removal.

1. Introduction

In the last decades nitrate pollution has become a major threat to groundwater quality. Nitrate pollution can cause serious health problems in both humans and domestic animals, and contributes to the eutrophication of surface water bodies (Rivett et al., 2008; Vitousek et al., 1997). High nitrate ingestion can cause methemoglobinemia in infants and young children (Comly et al., 1945; Magee and Barnes, 1956) and also nitrogen compounds can promote cancer in humans (Volkmer et al., 2005). Nitrate

pollution is linked to the intensive use of synthetic and organic fertilizers, as well as livestock and septic system effluents. The European Groundwater Directive (EC 2006) considers nitrate as one of the most important contaminants that could prevent the achievement of the goals of the Water Framework Directive (EC 2000). Many areas of Spain have been declared vulnerable to nitrate pollution according to European directive (ECC, 1991), with nitrate concentration over the threshold level established by Directive 98/83/CE for human water supply (50 mg/L). One of the most vulnerable environments to nitrate pollution are the systems without drainage to large water bodies such as endorheic basins located in semiarid or arid regions because these closed systems have low precipitation and high evaporation rates.

In order to improve characterization and water resources management for these areas exposed to nitrate pollution, it is necessary to understand the processes that affect nitrate concentration in the hydrogeologic system. Denitrification is an effective process that irreversibly eliminates nitrate from groundwater. In natural systems, denitrification leads to nitrate elimination through conversion into harmless N_2 (Knowles 1982) but is limited by the availability of electron donors. The denitrification reaction has several intermediate steps. Nitrate (NO_3^-) is first converted to nitrite (NO_2^-), which is in fact a more serious health hazard than nitrate (De Beer et al., 1997). The next intermediate step of denitrification converts NO_2^- to N_xO (g), which are greenhouse gases, and finally if the reaction is complete, to harmless N_2 (g). The chain of reactions can, however, discontinue at each step depending on biological and kinetic factors.

Denitrification takes place under anaerobic conditions where bacteria use nitrate as an oxidant for different compounds such as organic matter, sulphides and Fe^{2+}-bearing minerals. There are two different denitrification reactions driven by different bacteria. Heterotrophic bacteria use nitrate to oxidize organic matter (Eq. 1) and autotrophic bacteria use nitrate to oxidize reduced sulfur compounds as pyrite (Eq. 2).

$$5CH_2O + 4NO_3^- + 4H^{+1} \rightarrow 2N_2 + 5CO_2 + 7H_2O \qquad (1)$$

$$5FeS_2 + 15NO_3^- + 5H_2O \rightarrow 10SO_4^{2-} + 7.5N_2 + 5FeOOH + 5H^+ \qquad (2)$$

Reaction 1 generates CO_2 which implies an increase in dissolved inorganic carbon (DIC), whereas reaction 2 produces an increase in sulphate concentration as nitrate decreases. Therefore, depending on the denitrification pathway a different chemical signature of groundwater will be produced, which can help to identify whether denitrification is promoted by autotrophic or heterotrophic bacteria. However, when chemical data are not conclusive, multi-isotopic studies are an effective tool to identify and describe denitrification processes (Aravena and Robertson, 1998; Mariotti et al., 1988; Pauwels et al., 2000; Vitòria et al., 2008; Wassenaar et al., 1995; among others). Stable isotopes of the gases are usually measured as the ratio between the minor isotope and the major isotope, e.g. ^{15}N against ^{14}N. Ratios are almost always established with respect to international standards using the delta notation (Eq. 3).

$$\delta^{15}N = [(R_{sample} - R_{std}) / R_{std}] \times 1000 \qquad (3)$$

Where R = $^{15}N/^{14}N$

In denitrification processes, the $\delta^{15}N$ and $\delta^{18}O$ of the residual nitrate increases as nitrate concentration decreases. This change in the isotopic composition, or fractionation (ε) (Eq. 4), is useful to distinguish between denitrification and other processes such as dilution, which can also decrease nitrate concentration but without changing the isotopic value (Clark and Fritz, 1997; Kendall et al., 2007).

$$\varepsilon_{product/reactant} = (R_{product} / R_{reactant} - 1) * 10^3 \text{ (‰)} \qquad (4)$$

During denitrification processes, the εN/εO ratio ranges from 0.9 (Otero et al., 2009) to 2.1 (Böttcher et al., 1990). Likewise, the isotopic analyses of the solutes involved ($\delta^{34}S_{SO4}$, $\delta^{18}O_{SO4}$ and $\delta^{13}C_{DIC}$) are also a useful method to study denitrification reactions.

Endorheic basins are very frequent in the central part of Spain. Nitrate pollution in the region is linked to farming activities and wastewaters. Among these endorheic systems from Central Spain, Pétrola basin, located in the SE of Spain, in the Castilla-La Mancha Region, is an excellent example (Fig. 1). This area, vulnerable to nitrate pollution, has been declared both a highly-modified superficial water body and a nature reserve (Spanish Decree 102/2005, September 13th). The study area covers 43 km^2 with a saline lake located near the SW edge of the basin. This basin is located in the South-East of Spain in the Castilla-La Mancha Region. The climate of the study area is continental and semiarid. Mean annual precipitation is usually below 400 mm and mainly falls during the spring and autumn. Mean temperature oscillates from 4.9 ºC (January) to 24.2 ºC (July).

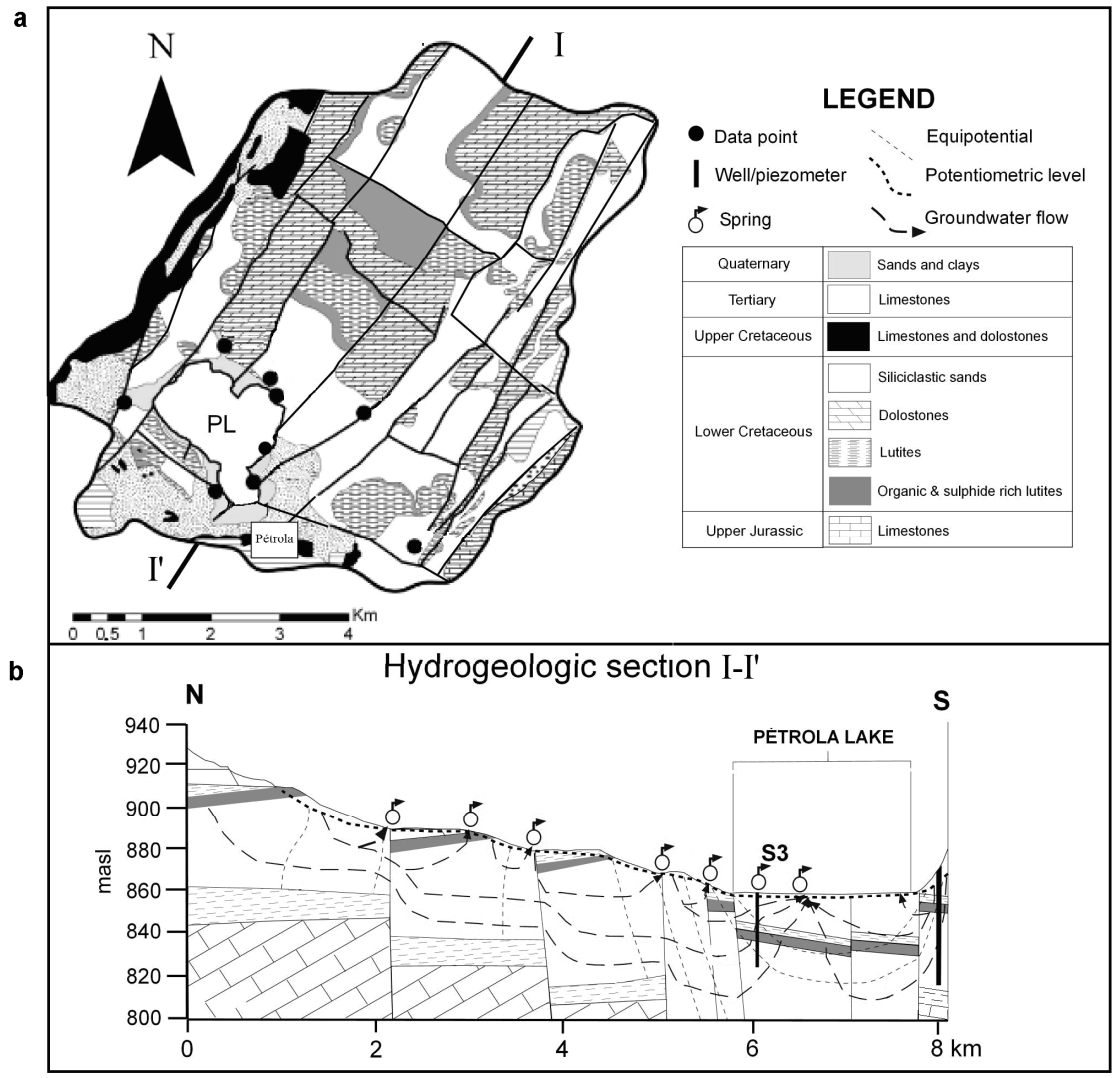

Figure 1. a) Simplified geological map of the Pétrola Lake endorheic basin with sampling point locations. b) Hydrostratigraphic cross section. masl: meters above sea level.

The geology of the area is mostly formed by Mesozoic materials affected by faulting and minor folding. The main aquifer, made up of Cretaceous sedimentary material, is known as the Utrillas Facies (Fig. 1). This facies is mainly composed of siliciclastic sands and conglomerates. Grey-to-black sandy-to-lutitic sediments with high content of organic matter and pyrite can be found interestratified in the Utrillas Facies. The average thickness of this unit is about 7 m (Gómez-Alday et al., 2004). Groundwater flow in the system converges to the Pétrola Lake. Springs and small streams drain the aquifer which is confined by organic and sulphide rich terrigenous deposits in the saline lake area where flowing wells are observable. During 2010, groundwater NO_3^- in the basin varied from 13.7 to 70.2 mg/L. Higher NO_3^- values were observed at the SW edge of the basin, coinciding with agricultural activities carried out in the area.

Denitrification at the field scale can occur in the upflowing groundwater at the expense of the organic matter and pyrite of the Utrillas Facies where anoxic conditions were observed in the groundwater. However several constraints have been observed that hinder a full and complete visualization of the

reaction pathway at the field scale. For example, inaccessibility to representative points located in a flow line, mixing processes and variations in solute loads complicate the evaluation of the potential electron donor source and its capacity to promote denitrification at the field scale. Moreover, the degree of denitrification calculated with field data is also affected by these limitations. In this context, laboratory experiments have proven to be a useful tool to evaluate the denitrification potential of the black-grey sediments of the Utrillas Facies and to identify the role of different electron donors involved in denitrification (Grischek et al., 1998; Torrentó et al., 2010; Laverman et al., 2012; Abell et al., 2009).

The Utrillas Facies is of interest due to its regional extent and the common presence of interestratified organic matter and pyrite rich sediments. The experiment reported here consisted of a flow-through/column system with chemical and isotopic characterization of the solutes involved in the reactions. The aim of the experiment was to study the availability and the role of the different electron donors in the sediment and to relate denitrification rate with flow rate. Finally, the fractionation factors (εN and εO) from dissolved NO_3^- in denitrification processes were determined at the laboratory scale, in an attempt to estimate the natural attenuation at field scale.

2. Methods

2.1 Experimental set-up

The experiment consisted of a flow-through glass column (30 cm in length and 9 cm in diameter) filled with organic and sulphide-rich material from Utrillas sediments (Fig. 2). In September 2008 four piezometers (S1 to S4) were drilled close to the SE edge of the lake. The sediment was sampled at well S3 (Fig. 1). During the drilling, the core was sampled at various depths (a) 5.30 – 5.45 m, (b) 9.00 – 9.60 m, and (c) 15.30 – 15.45 m. The core was isolated from the atmosphere with polypropylene and immediately frozen in the field with solid CO_2 to preserve it at -30ºC. To fill the column, sediments from the three depths were mixed. X-ray powder diffraction (XRD) analysis from the fine size (<40 μm) fraction obtained from the sediment mixture indicated that the most abundant minerals were quartz, orthoclase, clay minerals (illite and kaolinite) and pyrite. The total amount (%) of nitrogen, carbon, sulphur and hydrogen in the sediment was also determined by Elemental Analysis (EA 1108 CHNS-O Carlo Erba Instruments). Measured total organic carbon was around 0.4%, implying a total weight of carbon of 2.4 g in the experiment. The percentage of sulphur was higher (up to 2%) indicating an abundance of pyrite. The water used in the experiment was sampled at well 2581.

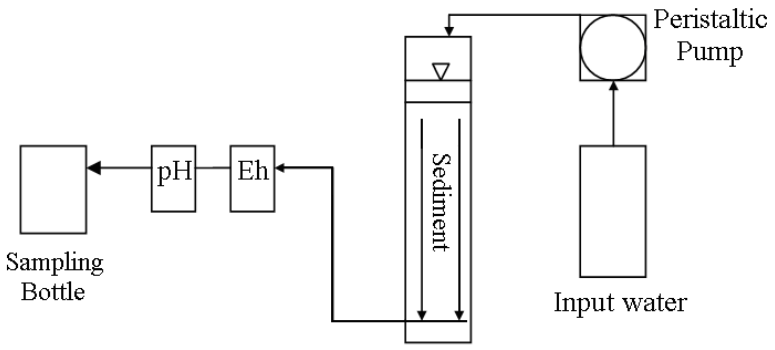

Figure 2. Set-up of the column experiment. Sediment was obtained in piezometer S3 near Pétrola Lake. Water was sampled in well 2581; nitrate concentration was 46.1 mg/L. Flow rate in the experiment was controlled by a peristaltic pump.

The experiment was set up and carried out in an anaerobic chamber with an Ar atmosphere to avoid the presence of O_2. The glass column was filled with 600 g of organic and sulphide-rich sediment (200 g from each sampled depth) mixed with 1200 g of clean silica sand (1-2 mm) Panreac® to increase the permeability. The bottom of the column was filled with silica balls (2 mm ∅) to avoid sediment clogging of the outlet. Prior to filling the column, the input water was bubbled with Ar to remove dissolved O_2. The column was filled up with water leaving a 5 cm free nappe over the sediment to avoid the occurrence of preferential flow pathways. The total volume of water was 0.5 L and the porosity of the filling was approximately 0.35-0.40. Four different flow rates were used during the experiment: 0.1, 0.05, 0.025 and 0.01 mL/min (peristaltic pumps Gilson Minipuls3 of 2 channels and Micropump Reglo Digital 4 channels ISMATEC). Eh and pH were measured every hour at the outlet of the column. The experiment lasted for 12 months.

2.2 Analytical methods

During the experiment, 96 samples were collected over 12 months. Chemical analyses were performed for each sample and isotopic data were compiled on a subset of samples considered representative with respect to nitrate concentration. Samples were filtered through a 0.45 µm Millipore® filter. NH_4^+ was analysed by spectrophotometry (ALPKEM, Flow Solution IV). Major anions (NO_3^-, SO_4^{2-}, Cl^-, and NO_2^-) were analysed by high performance liquid chromatography (HPLC) using a WATERS 515 HPLC pump with IC-PAC Anions columns and WESCAN and UV/VIS KONTRON detectors; dissolve organic carbon (DOC) was measured by organic matter combustion (TOC 500 SHIMADZU). For major cations analysis, samples were filtered through a 0.2 µm Millipore® filter and acidified with 1% HNO_3^-. Ca^{2+}, Na^+, K^+, and Mg^{2+} were determined by inductively coupled plasma-optical emission spectrometry (ICP-OES, Perkin-Elmer Optima 3200 RL). Periodically, from every other sample a volume of 25 mL was extracted through the column outlet to measure the dissolved inorganic carbon (DIC) by titration (METROHM 702 SM Titrino).

The isotopic characterization included $\delta^{34}S$ and $\delta^{18}O$ of SO_4^{2-}, $\delta^{15}N$ and $\delta^{18}O$ of NO_3^- and $\delta^{13}C$ of DIC. For the $\delta^{34}S$ and $\delta^{18}O$ determination, dissolved SO_4^{2-} was precipitated as $BaSO_4$ by adding $BaCl_2$, after acidifying the sample with HCl and boiling it to prevent $BaCO_3$ precipitation, following standard methods (e.g. Dogramaci el al., 2001). For the $\delta^{13}C_{DIC}$ determination, unfiltered samples were treated with NaOH-$BaCl_2$ solution to precipitate $BaCO_3$. $\delta^{34}S$ and $\delta^{13}C$ were analysed in a Carlo Erba Elemental Analyzer (EA) coupled in continuous flow to a Finnigan Delta C IRMS. $\delta^{18}O$ was analyzed in duplicate with a ThermoQuest TC/EA (high temperature conversion elemental analyzer) unit with a Finnigan Matt Delta C IRMS. $\delta^{15}N$ and $\delta^{18}O$ from dissolved NO_3^- were analysed by the bacterial denitrifier method of Sigman et al. (2001) and Casciotti et al. (2002). Isotope ratios were calculated using both international and internal laboratory standards. Notation was expressed in terms of delta (δ) per mil relative to the international standards (V-SMOW for $\delta^{18}O$, Atmospheric N_2 for $\delta^{15}N$, V-CDT for $\delta^{34}S$ and V-PDB for $\delta^{13}C$). Precision of the analyses calculated from the reproducibility of standards interspersed in the analytical batches was ±0.3‰ for $\delta^{15}N$, ±0.2‰ for $\delta^{34}S$, ±0.5‰ for $\delta^{18}O$ of SO_4^{2-} and NO_3^-, and ±0.2‰ for $\delta^{13}C$. Isotopic analyses were prepared at the Mineralogia Aplicada i Medi Ambient research laboratory and analyzed at the Serveis Científico-Tècnics of the Universitat de Barcelona, except for the isotopic composition of dissolved nitrate which was analyzed at the Woods Hole Oceanographic Institution (Massachusetts, USA).

3. Results

Complete chemical and isotopic data of the column experiment are available as supporting information. The evolution of NO_3^- concentration throughout the studied period is shown in Figure 3a. Two NO_3^- attenuation stages were detected. The first stage (from day 0 to 21), had an approximate flow rate of 0.1 mL/min, and a mean residence time of 3 days. During this stage, NO_3^- dropped quickly to reach values of 0.03 mM after 5 days. Thereafter, NO_3^- concentration rose gradually reaching its initial values after 20 days, and higher values than the initial ones (up to 0.8 mM) after 40 days. The decrease in NO_3^- output was coupled with a significant increase of NO_2^- which reached values of 0.43 mM and then diminished to values close to 0.04 mM, but never reached the input values (below the detection limit) (Fig. 3b). At the beginning of the experiment the flow was not constant, resulting in irregular residence times that could explain the observed high and low peaks in NO_3^- concentration, with lower NO_3^- content in those samples with higher residence time (e.g. sample at day 18 had 0.41 mM of NO_3^- with 6 days of residence time) and higher NO_3^- content in those samples with lower residence time (e.g. sample at day 21 had 0.76 mM of NO_3^- with 3 days of residence time). On day 46, the pump was replaced resulting in both a constant flow rate and a regular residence time. On day 48, the flow rate was modified from 0.1 to 0.05 mL/min, increasing the residence time up to 6 days. Following this first flow rate change, NO_3^- content decreased abruptly, from 0.8 mM to 0.64 mM. After this initial drop, NO_3^- concentration decreased gradually to values below 0.48 mM. This NO_3^- decrease period coincided with a moderate increase of NO_2^-, from an initial range between 0.04 and 0.06 mM to values between 0.08 and 0.14 mM (Fig. 3a, b). On day 96, the flow rate was lowered again down to 0.01 mL/min resulting in a residence time up to 12 days, and both NO_3^- and NO_2^- concentrations dropped down to values below the detection limit. On day 158, the flow

rate was increased to 0.05 mL/min, and NO_3^- increased up to 0.48 - 0.64 mM. Thereafter, NO_3^- content rose gradually to the initial value and was not affected by further flow rate changes (0.1, 0.025 and 0.01 mL/min).

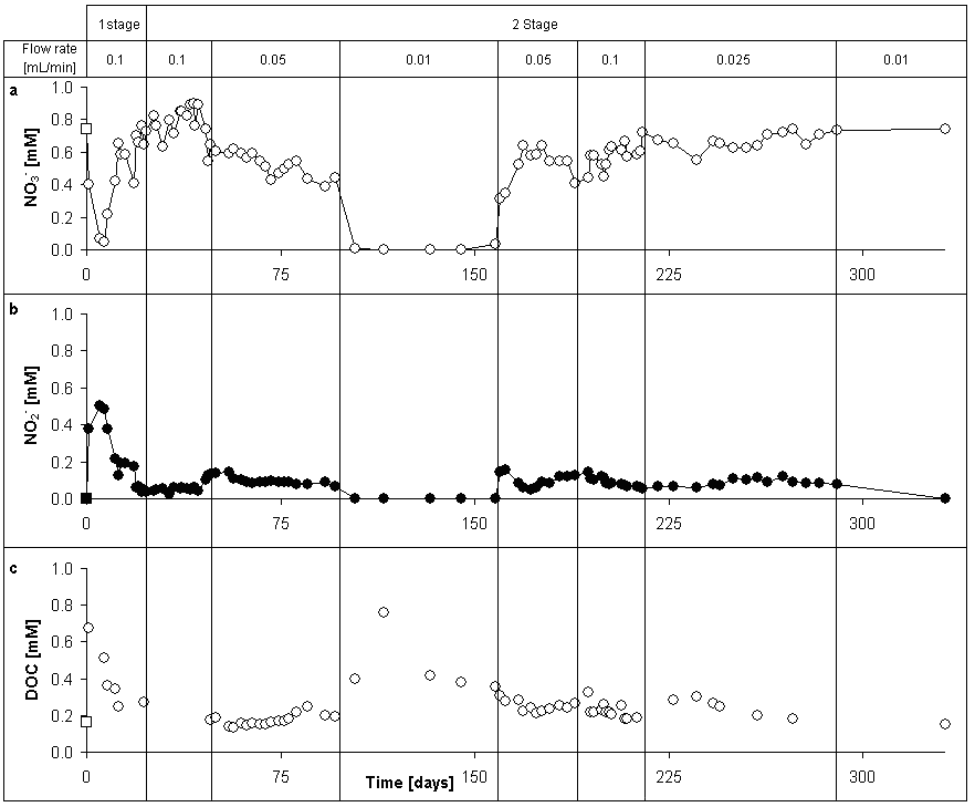

Figure 3. Nitrate, nitrite and DOC concentration over time showing flow rates and denitrification stages. Square points represent inflow concentration.

During the first NO_3^- reduction stage (from day 0 to 21, Fig. 3a), the isotopic composition of dissolved NO_3^- showed an increase from +9.0‰ to +43.4‰ for $\delta^{15}N$, and from +4.8‰ to +40.6‰ for $\delta^{18}O$ (Fig. 4). The observed increase in δ values coincided with a NO_3^- decrease from 0.76 to 0.03 mM. Furthermore $\delta^{15}N$ showed a linear relationship with $\delta^{18}O$, with a slope of 1.04 (Fig. 4). Similarly the isotopic composition of NO_3^- during the second attenuation stage (from day 22 to 332) showed an increase of $\delta^{15}N$ and $\delta^{18}O$ as NO_3^- content decreased. $\delta^{15}N$ varied from +11.2‰ to +44.5‰ and $\delta^{18}O$ ranged from +4.9‰ to +35.5‰. $\delta^{15}N$ showed a similar linear relationship with $\delta^{18}O$ and the slope was 0.88 (Fig.4). These values confirmed the fact that NO_3^- attenuation during both stages was caused by denitrification.

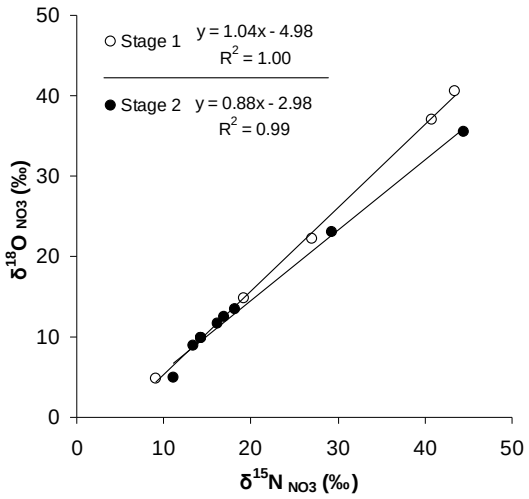

Figure 4. $\delta^{15}N$ vs $\delta^{18}O$ for first and second denitrification stages with a slope of 1.04 and 0.88, respectively. Both slopes are typical of denitrification processes.

The experiment began with an increase of one order of magnitude of Cl^-, SO_4^{2-}, K^+, Na^+ and Mg^{2+} concentrations (Fig. 5). The observed increase in major ions was linked to the displacement of the initial saline porewater and the leaching of the sediment. After 20 days, Mg^{2+} and SO_4^{2-} concentrations decreased gradually down to values close to the inflow levels. Cl^- , Na^+ and K^+ did not recover to the input-water concentration. Higher concentration in those samples with higher residence time indicated a continuous leaching of the sediment. Finally, Ca^{2+} and DIC concentrations showed a constant decrease throughout the experiment. Measured Ca^{2+} showed a slight increase at the beginning (first sample had 3.49 mM) with respect to the input water (inflow water 3.03 mM). After that, Ca^{2+} content tended to decrease with output concentrations between 1.58 and 0.89 mM (Fig. 5b). DIC content in the output samples was lower than the initial input value (6.28 mM), ranging from 2.14 to 6.12 mM (Fig. 6). After 20 days DIC values reached a constant concentration, around 2.46 mM. The output samples had $\delta^{13}C_{DIC}$ values from -8.9‰ to -23.2 ‰ (Fig. 6). Dissolved organic carbon (DOC) concentration varied from an initial value of 0.07 to 0.31 mM during the first 21 days, with a sharp increase in the first sample but a rapid decrease to the initial values of the input water (Fig. 3c). After 21 days, DOC content remained between 0.06 and 0.12 mM. When flow rate was changed to 0.01 mL/min, however, DOC increased to values between 0.16 and 0.75 mM (Fig. 3c). After 160 days, DOC concentration showed values ranging from 0.08 to 0.15 Mm again.

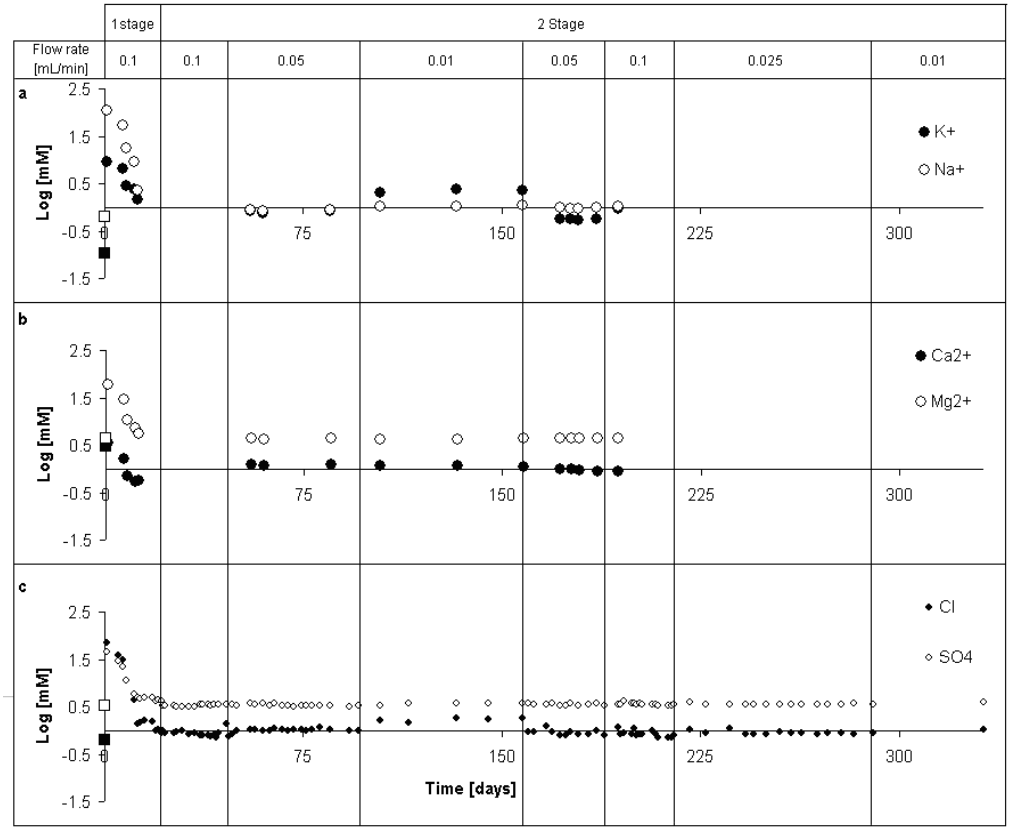

Figure 5. Logarithmic of major ion outflow concentrations during the flow-through experiment showing flow rates and denitrification stages. Square points represent the inflow concentration.

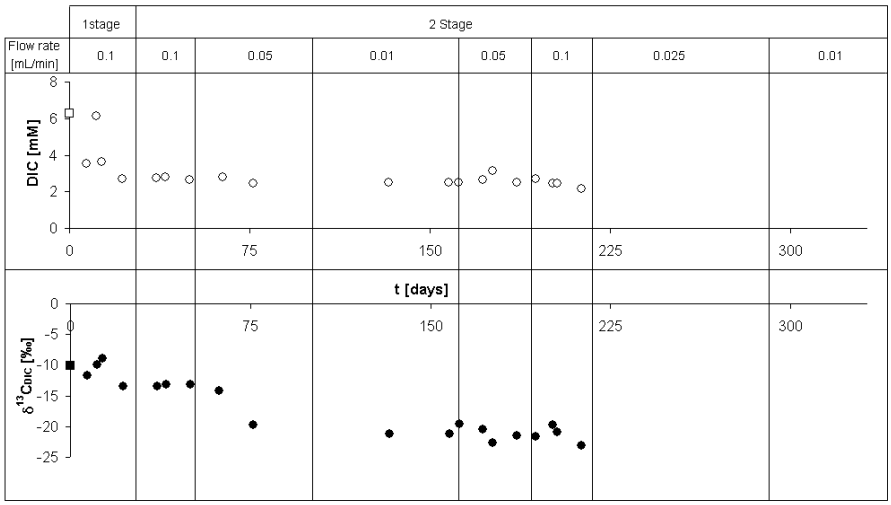

Figure 6. DIC and $\delta^{13}C_{DIC}$ evolution during the flow-through experiment showing flow rates and denitrification stages. Square points represent inflow concentration.

4. Discussion

4.1 Identifying the electron donor for the denitrification reaction

The variation in isotopic composition of N and O of dissolved NO_3^- of the output water indicated that NO_3^- attenuation was caused by denitrification in both stages. The role of the potential different electron

donors in the aquifer material was evaluated and quantified by means of the chemical and isotopic characterization of the outflow water. However, any chemical and isotopic variation associated with denitrification produced at the beginning of the experiment was masked by the release of pore water and the leaching of sediment. Because this process increased the major ion concentration by about one order of magnitude, the discussion of the electron donors will focus on the second stage.

Denitrification produced by sulphide oxidation should result in an increase in SO_4^{2-} concentration coupled with NO_3^- removal following reaction 2. Moreover, there should be an isotopic variation in S and O of the SO_4^{2-} molecule towards values derived from pyrite oxidation. Values of $\delta^{34}S_{SO4}$ and $\delta^{18}O_{SO4}$ should match with a mixing between the isotopic composition of SO_4^{2-} from the input water and the isotopic composition of SO_4^{2-} from sulphide oxidation. During the second stage of the experiment, SO_4^{2-} contents from outflow water ranged from 3.25 to 3.95 mM. However the observed variation in SO_4^{2-} concentration was not related with the observed trends in NO_3^- concentration. The slight differences in SO_4^{2-} concentration could have been caused by sediment leaching, since higher SO_4^{2-} values matched up with higher residence times, similarly to the observed variations for Cl^-, K^+ and Na^+ concentrations. Moreover, the isotopic composition of dissolved SO_4^{2-} also indicated that denitrification was not responsible for the SO_4^{2-} concentration increase. The mean value of $\delta^{34}S$ in the organic and sulphide-rich sediment was -22.5‰, whereas SO_4^{2-} from the input water had an isotopic composition of -16.8‰ for $\delta^{34}S$ and +5.3‰ for $\delta^{18}O$. The fact that throughout the second stage the isotopic composition of SO_4^{2-} in the output water showed constant values of -16.9‰ for $\delta^{34}S_{SO4}$ and +5.5‰ for $\delta^{18}O_{SO4}$ (Fig. 7), equal to the input water dissolved SO_4^{2-} confirms that pyrite oxidation plays an insignificant role in SO_4^{2-} variation, and, subsequently, in NO_3^- attenuation.

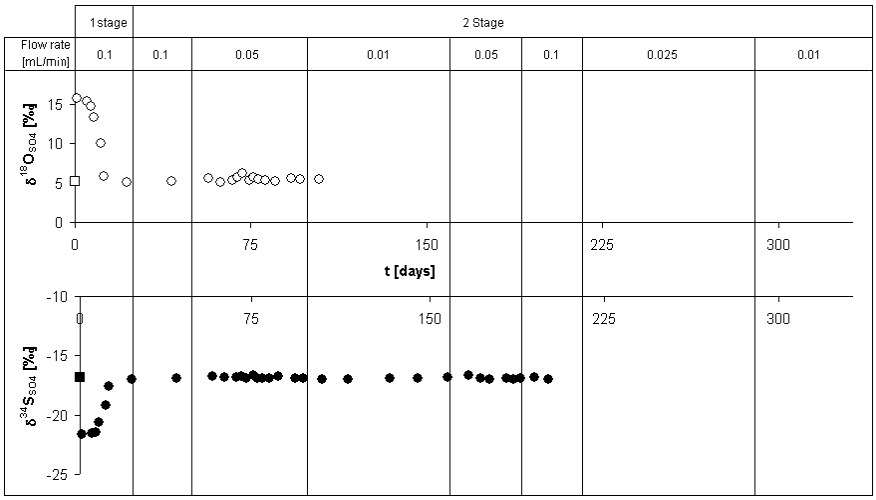

Figure 7. $\delta^{34}S_{SO4}$ and $\delta^{18}O_{SO4}$ evolution during the flow-through experiment showing flow rates and denitrification stages. Square points represent inflow concentration.

With regard to reaction (1), DIC values in the output samples showed a constant concentration of approximately 2.5 mM, and $\delta^{13}C_{DIC}$ values ranged from -13.2‰ to -23.2‰ (Fig 7). During this period calcium carbonate (aragonite) precipitation was observed in the free nappe of the column. Groundwater

used in the experiment was previously bubbled with Ar to remove O_2 (g) inside the Ar chamber. This process also removed dissolved CO_2 (g), producing calcium carbonate precipitation. Because aragonite predominates over calcite as the stable $CaCO_3$ mineral for high Mg concentrations in solution (Morse and Malkenzie, 1990), a parallel experiment was carried out in order to asses the effect of aragonite precipitation in the concentration and $\delta^{13}C$ of the DIC in the input water. Every 5 days, over a period of 30 days, the input water placed in the anaerobic chamber was analyzed and the results showed that aragonite precipitation actually hindered the possible variations in DIC concentration linked with denitrification. Moreover, aragonite precipitation also modified the $\delta^{13}C_{DIC}$ of the input water, which showed a decrease from its initial value of -10.1 to -24.6‰ after 30 days in the anaerobic chamber (data not shown). As a result, we discarded the use of $\delta^{13}C$ to trace the role of organic matter oxidation in the column experiment.

As an alternative indicator of the organic matter role in denitrification, during the period with complete NO_3^- elimination (between days 100 and 150) an increase in DOC concentration was observed when the flow rate was changed from 0.05 to 0.01 mL/min (Fig 3). DOC concentration varied from 0.2 mM (t_r= 6 days) to 0.4 mM (t_r= 12 days). Sample Col-41, with t_r=21 days, showed the highest DOC concentration up to 0.7 mM. The total amount of DOC released from the column during the experiment (calculated subtracting input water DOC from output water DOC) was 1.5 mmol. Organic compounds degraded from the sediment increased as flow rate decreased. The reactive organic fraction was mobilized due to increased residence times promoting heterotrophic denitrification. After 225 days, the DOC concentration tended to gradually decrease despite increasing residence time. This latter decrease in the DOC concentration could be caused by depletion of the degradable carbon source in the sediment. Results indicated that denitrification was limited by the availability of the organic carbon substrate. The measured total organic carbon concentration in the sediment (0.4%) only provides a rough indicator of electron donor availability due to the compositional variation and accessibility of organic matter (Laverman et al., 2012). The reactive organic carbon was calculated from the amount of carbon consumed in denitrification. Total NO_3^- reduced to N_2 throughout the experiment was 1.7 mmol. Following equation (1) the C-CH_2O consumed was 2.2 mmol. Moreover 1.4 mmol of NO_3^- was reduced to NO_2^- (uncompleted denitrification). The molar N:C ratio for this intermediate reaction of denitrification is 2:1, hence, the C-CH_2O consumed by this reaction was 0.7 mmol and the total reactive C-CH_2O in the sediment was 2.9 mmol. This mass of consumed C-CH_2O is 2% of the total C available in the sediment. Degradable organic carbon was calculated adding the total reactive C-CH_2O and the DOC released from the column. Degradable organic carbon was 4.6 mmol, which corresponded to about a 3% of total C in the sediment. In a similar flow-through experiment Abell et al. (2009) found that only a small fraction of total organic matter is degraded on experimental time scales. Furthermore, these authors found that only between 4 - 6% of total organic carbon was consumed by nitrate reduction. The lower reactivity of C-CH_2O observed in the Utrillas sediment can be caused by the aged organic matter that has shown to be of lower reactivity than fresh organic matter (Kristensen et al., 2000). Despite the lower reactivity observed in the Utrillas sediment, this material had the potential to remove NO_3^-. In fact, assuming a constant C-

CH_2O fraction and 7 m thickness of the organic-rich sediment from Utrillas Facies, this sediment has the potential to remove 100 mg/L of NO_3^- from a groundwater flux of 5 $m^3/m^2/yr$ over a period of 6 years.

4.2 Denitrification rate

As shown in the previous section, two denitrification stages were identified, with different kinetic behaviour. During the experiment, NO_2^- appeared as an intermediate product of the denitrification reaction. The accumulation rate of NO_2^- throughout the experiment was calculated in order to determine the complete denitrification rate ($NO_3^- \rightarrow N_2$). Zero-order nitrate attenuation rate and zero-order nitrite accumulation rate (μmol L^{-1} d^{-1}) were calculated according to the following equations:

$$R_{NO3} = q\,(C_{NO3}^{i} - C_{NO3}^{o}) / Vs \qquad (5)$$

$$A_{NO2} = q\,C_{NO2}^{o} / Vs \qquad (6)$$

where R_{NO3} is the nitrate reduction rate, A_{NO2} is the nitrite accumulation rate, q is the flow rate (L/d), C_{NO3}^{i} and C_{NO3}^{o} are the input and output nitrate concentration, respectively (μmol/L), C_{NO2}^{o} is the output nitrite concentration (μmol/L) and Vs is the sediment volume inside the column (L). The difference between R_{NO3} and A_{NO2} is the complete denitrification rate (CDR) that represents the velocity of nitrate transformation to N_2. The main factors that determine CDR are: pH, temperature and microbial population, the latter controlled by the abundance and availability of nitrate and organic and inorganic substrates (Hunter et al., 1998). Temperature and pH remained constant throughout the entire experiment. However changes in flow rate had an impact on nitrate and organic carbon loads.

Reported values of R_{NO3} and A_{NO2} corresponded to the average of each constant flow period. The first stage was less notable with regard to the amount of NO_3^- eliminated and the time period involved. The average R_{NO3} was 101 μmol L^{-1} d^{-1} but the reduction only lasted 21 days. On the other hand, significant A_{NO2} of 91 μmol L^{-1} d^{-1} was observed during this stage, but only about 10% of NO_3^- was reduced to N_2. A higher production of NO_2^- is generally observed when a system is perturbed (Martin et al., 2009), as occurred at the start of the experiment. Higher denitrification and nitrite accumulation rates have been observed in column and batch experiments and reflect the initial growth of denitrifiers and the induction of nitrite reductasa (Abell et al., 2009).

.

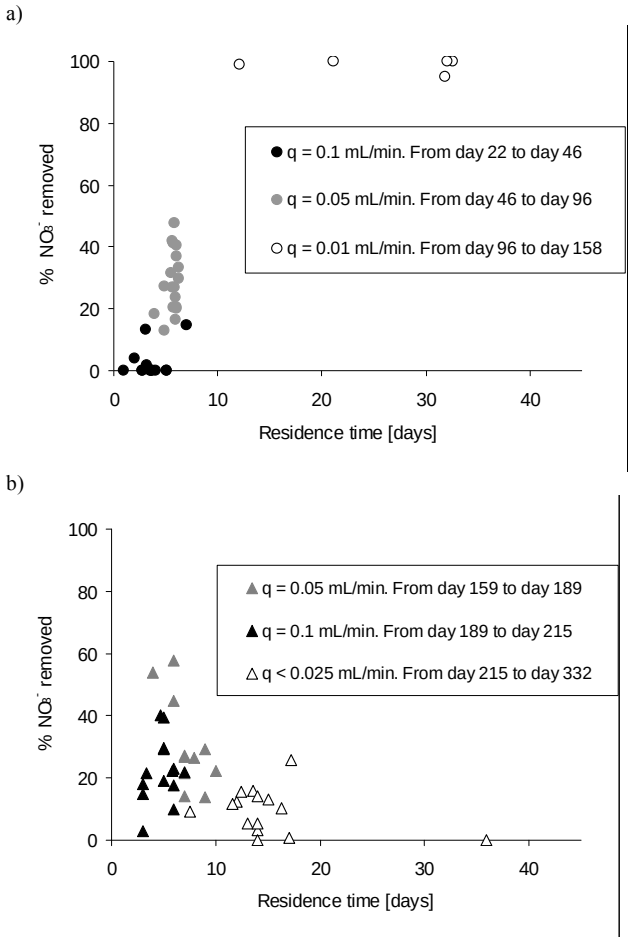

Figure 8. a) % of nitrate attenuation vs. residence time between day 21 and day 158. b) % nitrate attenuation from day 158 to the end of the experiment (day 332) showing a gradual decrease in denitrification % up to the last sample where it reaches 0%. In these plots nitrite was not taken into account.

The second stage of our experiment began on day 22 (Fig. 3). The degree of attenuation during this second stage was linked to flow rate variation and, therefore, to the residence time (t_r) (Fig. 8a). At an early stage (from day 22 to day 46), with a flow rate of 0.1 mL/min NO_3^-, attenuation was not higher than 15%. Denitrification was taking place but to a limited extent, with a R_{NO3} of 26 µmol L^{-1} d^{-1}. During this period, however, A_{NO2} measured was 25 µmol L^{-1} d^{-1}, which means that only 5% of the NO_3^- reduced was completely converted to N_2. From day 46 to day 96, with a flow rate of 0.05 mL/min, the NO_3^- removed increased from 15% to 50% with an average value of 30% (Fig. 8a). R_{NO3} was 54 µmol L^{-1} d^{-1} with a gradual increase over time, whereas A_{NO2} was constant with a value of 22 µmol L^{-1} d^{-1}. CDR increased from negligible to 32 µmol L^{-1} d^{-1}. The rise in CDR may have been related to an increase in biomass concentration favored by longer residence time.

Between days 97 and 158, flow rate was decreased to 0.01 mL/min (t_r up to 12 days); NO_3^- was completely removed to N_2 with average R_{NO3} of 31 µmol L^{-1} d^{-1} and with no NO_2^- accumulation. CDR was equal to that of the previous period with 0.05mL/min showing that flow rate variation had an effect on yield amount of denitrification but not on the kinetics of the reaction. Similar results were obtained in the next periods. From day 158 to day 189, with flow rate of 0.05, average NO_3^- attenuation was 35%

with R_{NO3} and A_{NO2} of 53 mmol L^{-1} d^{-1} and 22 mmol L^{-1} d^{-1}. Whereas from day 189 to day 215, with flow rate of 0.1 mL/min, average NO_3^- attenuation was about 20% (Fig 8b) and R_{NO3} and A_{NO2} of 54 mmol L^{-1} d^{-1} and 25 mmol L^{-1} d^{-1}. The CDR of these periods (31-29 μmol L^{-1} d^{-1}) remained the same as the previous periods. Therefore, variation of flow rate had an effect on both the kinetics of the reaction at early stages and in the percentage of NO_3^- removed when steady state were reached. After day 215, nitrate reduction ranged from 0 to 15% regardless of residence time (from 8 to 36 days) (Fig. 8b) and R_{NO3} and A_{NO2} decreased despite flow rate changes. In this case decreasing flow rate had no effect on the percentage of nitrate removed, nor on the kinetics of the reaction. Exhaustion of organic carbon in the sediment controlled the kinetics of the reaction during the last periods of the experiment.

Denitrification rates obtained in the present study were one or two orders of magnitude lower than those measured in flow-through experiments for fresh sediments from lakes, rivers, estuaries and marine coastal areas (Laverman et al., 2012). Zero-order denitrification rates obtained in field studies using NO_3^- gradient range from <0.05 to 45 μmol L^{-1} d^{-1} (Green et al., 2008), similar to the CDR values measured in the present study (up to 31 μmol L^{-1} d^{-1}). However, experimental and field rates show significant differences. These differences are attributed to the variability of the field conditions such as nitrate load changes, heterogeneous media or groundwater mixing. Temperature also has an important effect on denitrification rate, with increasing rates as temperature increases. Rivett et al., (2008) report that the effects of temperature cause the denitrification rate double for every 10ºC increase in temperature following the Arrhenius rate law, and that the observed increase in denitrification rate, from 10 to 25ºC, for different soils can vary from 1.7 to 23 times. The present experiment was performed at room temperature ranging from 20 to 25ºC while the usual groundwater temperature in the studied basin is 15 to 19ºC. Therefore, denitrification rates expected in the field may be slightly lower than values obtained in our experiment.

4.3 Fractionation of N and O

In order to properly assess the rate of denitrification at the field scale, fractionation (ε) must first be estimated in laboratory experiments. Whereas dilution can sometimes conceal the denitrification process, fractionation allows us to quantify the biodegradation rate regardless of an existing dilution process. Denitrification can be expressed as a Rayleigh distillation process (Eqs. 7 and 8) (Aravena & Robertson, 1998; Mariotti et al., 1988)

$$\delta^{15}N_{residual} = \delta^{15}N_{initial} + \varepsilon \ln f \quad (7)$$

$$\delta^{18}O_{residual} = \delta^{18}O_{initial} + \varepsilon \ln f \quad (8)$$

where f is the residual NO_3^- concentration divided by the initial NO_3^- and ε is the fractionation factor (defined above). In this study, fractionation was calculated for each denitrification stage. ε was obtained using a linear regression between ln[NO_3^-] and both $\delta^{15}N$ and $\delta^{18}O$ (Fig. 9a, b). A plot of $\delta^{15}N$ or $\delta^{18}O$ versus ln[NO_3^-] should show a linear correlation if denitrification occurs (Kendall et al., 2007). The

studied samples showed a good correlation of these parameters for both stages (Stage 1 r^2>0.96; Stage 2 r^2=0.95). Fractionation values calculated for the first stage were -11.6‰ ±2‰ for εN and -12.1‰ ±2‰ for εO. During the second stage fractionation values were -15.7‰ ±2‰ for εN and -13.8‰ ±2‰ for εO.

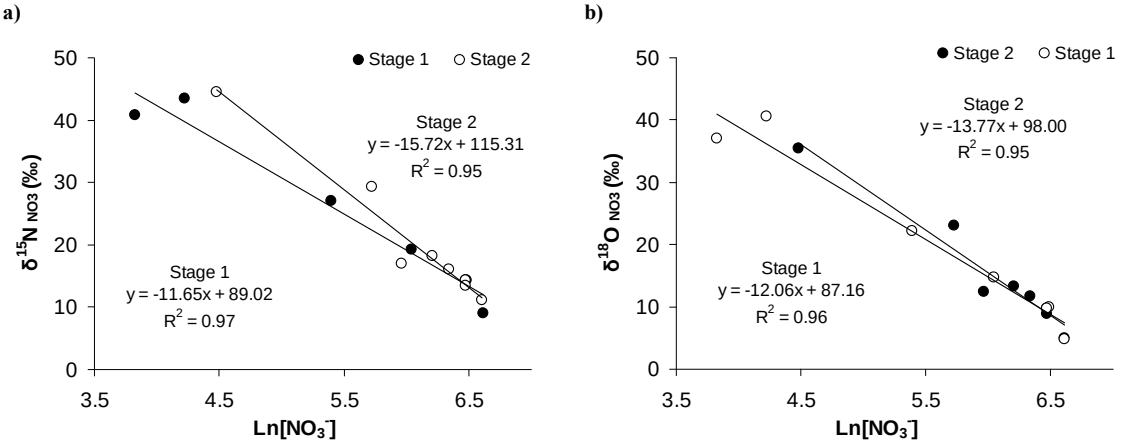

Figure 9. a) $\delta^{15}N$ vs $ln[NO_3^-]$ for both stages of denitrification. Slopes correspond to the isotopic fractionation value of ^{15}N. b) $\delta^{18}O$ vs $ln[NO_3^-]$ for both stages. Slope corresponds to the isotopic fractionation of ^{18}O.

The ε values obtained in this experiment were compared with those obtained in other experiments or field studies based on heterotrophic or autotrophic denitrification. To our knowledge there are only two similar column experiments dealing with natural denitrification process using flow-through experiments and isotopic characterization reported in the literature: Grischek et al. (1998) and Tsushima et al. (2006). Whereas Grischek et al. used alluvial aquifer material and obtained a εN value of -14.6‰, Tsushima et al. calculated εN using sediment from a riparian aquifer and obtained a value of -34.1‰. Results of the present experiment (-11.6‰ and -15.7‰) were close to the values reported by Grischek et al. (1998). Other εN values in the literature have been obtained by induced attenuation batch experiments and field studies. Isotopic characterization of different heterotrophic denitrifying strains and/or different electron donors has been carried out in the last decades by Bardford et al. (1999), Delwiche and Steyn (1970) and Wellman et al. (1968). Values obtained in these studies varied from -13.4‰ to -30.0‰. Field studies of denitrification report values of εN that range from -4‰ to -30‰ (Pauwels et al., 2000; Vogel et al., 1981). The εN values calculated in the present study fall within the range of previous field studies and are comparable with the lower absolute values obtained during induced denitrification batch experiments (-13.4‰), although fractionation calculated for the first denitrification stage (-11.6‰) was slightly lower in absolute values.

As for εO values, to our knowledge there are no published data of εO values obtained in flow-through column experiments of natural denitrification. Only a few publications report εO during heterotrophic denitrification in batch experiments. Toyoda et al. (2005) reported εO of two heterotrophic denitrifying cultures that converted NO_3^- to N_2O and the εO values obtained ranged from -3‰ to +32‰ showing inverse fractionation produced by ^{16}O loss during reduction of NO_3^- to nitrous oxide (Casciotti et al., 2002; Toyoda et al., 2005). Torrentó et al. (2010, 2011) also reported εO, but during induced autotrophic denitrification. Whereas the fractionation values reported by Torrentó et al. ranged from -13.5‰ to -

20.4‰ for εO, the εO calculated in the present study ranged from -12.1‰ to -13.8‰, similar (though slightly lower in absolute values) to the values obtained by induced autotrophic denitrification. Compared with field data, fractionation values obtained in the present study fall within the range of -2‰ to -18‰ for εO (Otero et al., 2009; Mengis et al., 1999).

Torrentó et al. (2010, 2011) obtained an εN/εO ratio of between 1.13 and 1.3 in batch experiments with pure culture, higher than the ratio obtained in the present experiment for the first denitrification stage where εN/εO = 0.96±0.04, but comparable to those values obtained during the second stage where εN/εO = 1.14±0.04. Our εN/εO values fall within ratios from *in situ* studies of denitrification in groundwater which range from 0.9 to 2.3 (see Otero et al., 2009 and references therein).

Gómez-Alday et al. (2011) performed a field survey during 2010. These authors identified the nitrification of slightly volatilized ammonium fertilizers as the main source of NO_3^- in the basin. Furthermore, a positive correlation (r^2= 0.65) between $\delta^{15}N_{NO3}$ and $\delta^{18}O_{NO3}$ was observed, indicating that denitrification processes can be taking place (Fig 10).

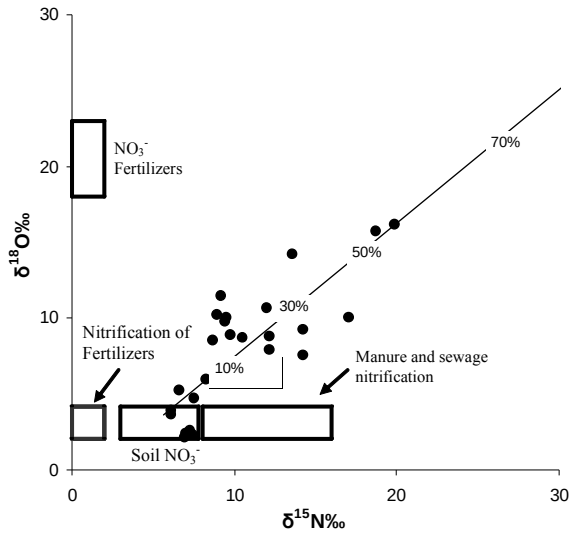

Figure 10. $\delta^{15}N_{NO3}$ vs $\delta^{18}O_{NO3}$ of field samples together with the isotopic composition of the main nitrate sources (Vitoria et al 2004). Line shows the % of attenuation calculated with isotopic fractionation obtained in the column experiment.

With the fractionation value obtained in the laboratory, the percentage of denitrification at the field scale can be calculated using both εN and εO by Equation 9.

$$DEN\ (\%) = [1 - e^{(\delta residual - \delta initial/\varepsilon)}] \times 100 \qquad (9)$$

Calculated nitrate attenuation % from water samples collected in the field, using fractionation values from the second stage of our experiments, varied from 0% to 60% (Fig. 10). Average denitrification in the water samples was 20% ± 5%. Slight differences were observed in the percentage of attenuation depending on the fractionation factor used. When considering εO values, the nitrate attenuation percentage was slightly higher than using εN values. The variability in the percentage in most of the

samples was within the range of the standard deviation of the isotopic data (±5%) (Fig. 11). However, some samples showed higher differences in the percentage of attenuation (up to 15%). This variation can be related to the different processes affecting the changes in $^{15}N/^{14}N$ and $^{18}O/^{16}O$ ratio during nitrification reactions such as volatilization occurring in field. Overall, denitrification is taking place in the basin but it cannot remove NO_3^- completely from the groundwater. The degree of attenuation estimated using laboratory-derived enrichment factors is in general underestimated with respect to the extent of denitrification estimated *in situ* (Mariotti et al., 1988)A more detailed field sampling survey is needed to know the real extent of denitrification at the field scale and field denitrification rates.

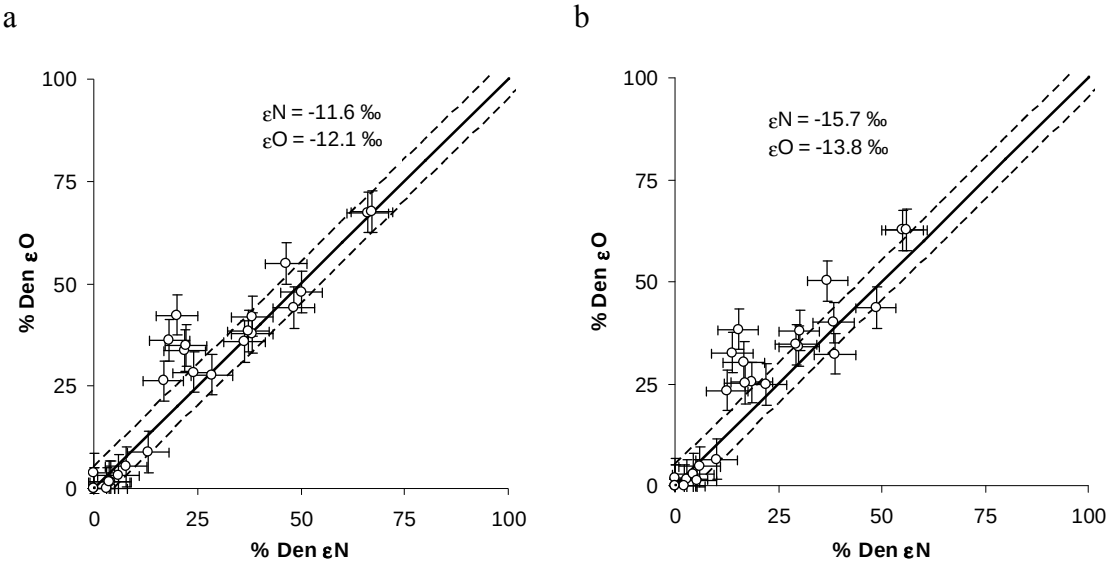

Figure 11. Comparison of the percentage of nitrate attenuation using the different fractionation values obtained in the column experiment. a) Percentage obtained from fractionation values of the first stage. b) Percentage obtained from fractionation values of the second stage. The solid lines indicate the ratio 1:1 and dashed lines represent variation of ±5%. Error bars of samples are the 5%, in agreement with the standard deviation of isotopic analyses.

5. Conclusions

Flow-through column experiments are a useful method to address the role of the different electron donors that promote denitrification, to quantify the attenuation rates and to obtain fractionation factors of denitrification. Our column experiment showed that the sediments from the Cretaceous Utrillas Facies can attenuate NO_3^- pollution. Constant isotopic values of $\delta^{34}S_{SO4}$ and $\delta^{18}O_{SO4}$ throughout the denitrification stage ruled out pyrite as an electron donor. However, due to aragonite precipitation in the experimental column, DIC concentration and $\delta^{13}C_{DIC}$ values could not be used to prove unambiguously that denitrification was driven by organic matter oxidation. Nevertheless, an increase in $C\text{-}CH_2O$ concentration during complete NO_3^- attenuation was in agreement with heterotrophic denitrification. Total NO_3^- removed during the experiment was 3.1 mmoL. The stoichiometric $C\text{-}CH_2O$ necessary to remove this amount of NO_3^- is 2.9 mmol which corresponds to 2% of the total C present in the sediment. The degree and rate of denitrification were related to flow rate variations. Lower flow rates favored bacterial growth at the beginning of the experiment which in turn produced an increase of complete denitrification rate (CDR). When NO_3^- reduction was higher than 15%, CDR remained constant at around 30 μmol L^{-1} d^{-1} under different flow rates. In the last stage, flow rate had no effect on output NO_3^-

concentration because organic carbon supply was limited and became the limiting factor of denitrification. Finally, an isotopic fractionation of NO_3^- was calculated for both $^{15}N\text{-}NO_3^-$ and $^{18}O\text{-}NO_3^-$. The first stage had a εN of -12.1‰ and a εO of -11.6‰ whereas the second stage had a εN of -15.7‰ and a εO of -13.8‰ with a εN/εO ratio of 0.96 and 1.14, respectively. Using the calculated isotopic fractionation the percentage of natural attenuation due to denitrification in the field samples of Pétrola basin can be estimated to be from 0 to 60%. Thus, the results from a column experiment have revealed very useful information to characterize the natural denitrification processes taking place in a regional aquifer basin.

Acknowledgments

This work was financed by PAC08-0187-6481 from the Castilla-La Mancha CGL Government Projects CICYT-CGL2008-06373-CO3-01, CICYT-CGL2011-29975-CO4-01, CICYT-CGL2011-29975-C042 and TRACE PET2008-0034 from the Spanish Government, and Project 2009SGR 103 from the Catalan Government. We would like to thank the Centres Científics i Tecnològics of the Universitat de Barcelona for the analysis and Frances Luttikhuizen for her linguistic comments on the final draft.

References

Abell, J., Laverman, A. M., & Cappellen, P. 2009. Bioavailability of organic matter in a freshwater estuarine sediment: long-term degradation experiments with and without nitrate supply. Biogeochemistry 94, 13-28.

Aravena, R., Robertson, W.D., 1998. Use of multiple isotope tracers to evaluate denitrification in ground water: study of nitrate from a large-flux septic system plume. Ground Water 36, 975-981

Bardford, C., Montoya, J., Altabet, M., Mitchell, R., 1999. Steady-state nitrogen isotope effects of N_2 and N_2O production in Paracoccus denitrificans. Appl. Environ. Microbiol. 65, 989-994.

Böttcher, J., Strebel, O.L., Voerkelus, S., Schmidt, H.L., 1990. Using isotope fractionation of nitrate-nitrogen and nitrate-oxygen for evaluation of microbial denitrification in sandy aquifer. Journal of Hydrology 144. 413-424

Casciotti, K.L., Sigman, D.M., Galanter Hastings, M., Böhlke, J.K., Hilkert, A., 2002. Measurement of the oxygen isotopic composition of nitrate in seawater and freshwater using the denitrifier method. Anal. Chem. 74. 4905-4912.

Clark, I.D., Fritz, P., 1997. Environmental Isotopes in Hydrogeology. Lewis Publishers, New York.

Comly, H.H., 1945. Cyanosis in infants caused by nitrates in well water. J. Am. Med. Assoc. 129. 112-116

De Beer, D., Schramm, A., Santegoeds, C., Küh M., 1997. A nitrite microsensor for profiling environmental biofilms. Appl. Environ. Microbiol. 63, 973-977.

Delwiche, C., Steyn, P., 1970. Nitrogen isotope fractionation in soils and microbial reactions. Environ. Sci. Technol 4, 929-935.

Dogramaci, S.S., Herczeg, A.L., Schiff, S.L., Bone, Y., 2001. Controls on $\delta^{34}S$ and $\delta^{18}O$ of dissolved SO_4 in aquifers of the Murray Basin, Australia and their use as indicators of flow processes. Appl. Geochem. 16, 475-488

EC, 2000. Council Directive 2000/60/EC, of 23 October 2000, establishing a frame- work fro Community action inthe field of water policy.Off. J. Eur. Comm. L 327, 1–73 (Brussels).

EC, 2006. Council Directive 2006/118/EC, of 12December 2006, on the protection of groundwater against pollution and deterioration. Off. J. Eur. Comm. L 372, 19–31 (Brussels).

Gómez-Alday, J.J., Castaño, S., Sanz, D., 2004. Geological origin of pollutants (sulphate) in the Pétrola Lagoon groundwater (Albacete, Spain). Preliminary results. Geogaceta 35, 167-171.

Gómez Alday, J.J., Carrey, R., Otero, N., Soler, A., Ayora C., Sanz, D., Castaño, S., Recio, C., Carnicero, A., 2011. Denitrification assessmeent in a high vulnerable area to nitrate pollution (Pétrola lake endorheic basin, SE Albacete, Spain. 9th International Symposium on Applied Isotope Geochemistry, pp 72

Green, C.T., Puckett, L.J., Böhlke, J.K., Bekins, B.A, Phillips, S.P., Kauffman, L.J., Denver, J.M., 2005. Limited occurrence of denitrification in four shallow aquifers in agricultural areas of the United States. J. Environ. Qual. 37, 994-1009.

Grischek, T., Hiscock, K.M., Metschies, T., Dennis, P.F., Nestler, W., 1998. Factors affecting denitrification during infiltration of river water into a sand and gravel aquifer in saxony, Germany. Water Res. 32, 450-460.

Hunter, K., & Wang, Y., 1998. Kinetic modeling of microbially-driven redox chemistry of subsurface environments: coupling transport, microbial metabolism and geochemistry. Journal of Hydrology, 209, 53-80.

Kendall, C., Elliott, E.M., Wankel, S.D., 2007. Tracing anthropogenic inputs of nitrogen to ecosystems, Chapter 12, in: R.H. Michener and K. Lajtha (Eds.), Stable Isotope in Ecology and Environmental Science. 2nd edition Blackwell publishing, 375-449

Knowles, R., 1982. Denitrifification. Microbiol. Rev. 42, 43-70.

Kristensen, E., 2000. Organic matter diagenesis at the oxic / anoxic interface in coastal marine sediments, with emphasis on the role of burrowing animals, Hydrobiologia 426, 1-24.

Laverman, A.M., Pallud, C., Abell J., Van Cappellen, P., 2012. Comparative survey of potential nitrate and sulfate reduction rates in aquatic sediments. Geochimica et Cosmochimica Acta 77, 474-488.

Magee, P.N., Barnes, J.M., 1956. The production of malignant primary hepatic tumourus in the rat by feeding dimethylnitrosamine. Br. J. Cancer 10, 114-122.

Mariotti, A., Landreau, A., Simon, B., 1988. ^{15}N isotope biogeochemistry and natural denitrification process in groundwater application to the chalk aquifer of northern France. Geochim. Cosmochim. Acta 52, 1869-1878.

Martin, D., Salminen, J.M., Niemi, R.M., Heiskanen, I.M., Valve, M.J., Hellstén, P.P., & Nystén, T.H., 2009. Acetate and ethanol as potential enhancers of low temperature denitrification in soil contaminated by fur farms: a pilot-scale study. J. Hazard. Mater. 163, 1230-1238.

Mengis, M., Schiff, S.L., Harris, M., English, M.C., Aravena, R., Elgood, R.J., MacLean, A., 1999. Multiple geochemical and isotopic approaches for assessing ground water NO_3^- elimination in a riparian zone. Ground Water 37, 448-457.

Morse, J.W., Mackenzie, F.T., 1990. Geochemistry of sedimentary carbonates. Developments in Sedimentology 48, 1-707.

Otero, N., Torrentó, C., Soler, A., Menció, A., Mas-Pla, J., 2009. Monitoring groundwater nitrate attenuation in a regional system coupling hydrogeology with multi-isotopic methods: The case of Plana de Vic (Osona, Spain). Agriculture, Ecosystems and Environment 133, 103-113.

Pauwels, H., Foucher, J.C., Kloppmann, W., 2000. Denitrification and mixing in a schist aquifer: influence on water chemistry isotopes. Chem. Geol. 168, 307-324

Rivett, M.O., Buss, S.R., Morgan, P., Smith, J.W.N., Bemment, C.D., 2008. Nitrate attenuation in groundwater: a review of biogeochemical controlling processes. Water. Res. 42, 4215-4232.

Sigman, D.M., Casciotti, K.L., Andreani, M., Bardford, C., Galanter, M., Böhlke, J.K., 2001. A bacterial method for the nitrogen isotopic analysis of nitrate in seawater and freshwater. Anal. Chem. 73, 4145-4153.

Torrentó, C., Cama, J., Urmeneta, J., Otero, N., Soler, A., 2010. Autotrophic denitrification with pyrite: implications for bioremediation of nitrate contaminated groundwater. Chem. Geol. 278, 80-91.

Torrentó, C., Urmeneta, J., Otero, N., Soler, A., Viñas, M., Cama, J., 2011. Enhanced denitrification in groundwater and sediments from a nitrate-contaminated aquifer after addition of pyrite. Chem. Geol., 287, 90-101.

Toyoda, S., Mutobe, H., Yamagishi, H., Yoshida, N., Tanji, Y., 2005. Fractionation of N_2O isotopomers during production by denitrifier. Soil Biol. Biochem. 37, 1535-1545.

Tsushima, K., Ueda, S., Ohno, H., Ogura, T.K., Watanabe, K., 2006. Nitrate decrease with isotopic fractionation in riverside sediment column during infiltration experiment. Water, Air, Soil Pollut. 174, 47-61.

Vitòria, L., Grandia, F., Soler, A., 2004. Evolution of the chemical (NH_4) and isotopic (^{15}N-NH_4) composition of pig manure stored in an experimental pit. In: IAEA (Eds.), Isotope Hydrology and Integrated Water Resources Management. Conference & Symposium Papers, Vienna, pp. 260–261.

Vitòria, L., Soler, A., Canals, A., Otero, N., 2008. Environmental isotopes (N, S, C, O, D) to determine natural attenuation processes in nitrate contaminated waters: example of Osona (NE Spain). Appl Geochem. 23, 3597-3611.

Vitousek, P.M., Aber, J.D., Howarth, R.W., Likens, G.E., Matson, P.a., Shindler, D.W., Schelesinger, W.H., Tilman, D.G., 1997. Human alteration of the global nitrogen cycle: source and consequence. Ecol. Appl. 7 (3), 737-750.

Vogel, J.C., Talma, A.S., Heaton, T.H.E., 1981. Gaseous nitrogen as evidence for denitrification in groundwater. J. Hydrol. 50, 191-200.

Volkmer, B., Ernst, B., Simon, J., Kuefer, R., Bartsch, G., Bach, D., Gschwend, J., 2005. Influence of nitrate levels in drinking water on urological malignancies: a community- based cohort study. Bju. International 95, 972-976.

Wassenaar, L.I., 1995. Evaluation of the origin and fate of nitrate in Abbostsford Aquifer using the isotopes of ^{15}N and ^{18}O in NO_3^-. Appl. Geochem. 10, 391-405.

Wellman, R.P., Cook, F.D., Krouse, H.R., 1968. Nitrogen-15: Microbiological alteration of abundance. Science 161, 269-270.

Appendix A-2

Nitrate attenuation potential of hypersaline lake sediments in central Spain: Flow-through and batch experiments

R. Carrey, P. Rodríguez-Escales, N. Otero, C. Ayora, A. Soler, J.J. Gómez-Alday,

2014

Submitted to Journal of Contaminant Hydrology

(Supporting information of this paper is available in Appendix C-2)

Nitrate attenuation potential of hypersaline lake sediments in central Spain: Flow-through and batch experiments

R. Carrey[(1)], P. Rodríguez-Escales[(2)], N. Otero[(1)], C. Ayora[(3)], A. Soler[(1)], J.J. Gómez-Alday[(4)]

1 Grup de Mineralogia Aplicada i Medi Ambient, Facultat de Geologia, Universitat de Barcelona, C/ Martí i Franquès s/n, 08028, Barcelona, Spain; e-mail: raulcarrey@ub.edu, notero@ub.edu, albertsoler@ub.edu

2 Grup d'Hidrologia Subterrània (GHS), Departamentd'Enginyeria del Terreny, Cartogràfica i Geofísica, Universitat Politècnica de Catalunya-BarcelonaTech, JordiGirona 1-3, Mòdul D-2, 08034 Barcelona, Spain; e-mail: prescales@gmail.com

3 Grup d'Hidrologia Subterrània (GHS), Instituto de Diagnóstico Ambiental y Estudios del Agua, IDAEA- CSIC, C/Jordi Girona, 18, 08028 Barcelona, Spain; e-mail: cayora1@gmail.com

4 Hydrogeology Group. Institute for Regional Development (IRD). University of Castilla-La Mancha (UCLM) Campus Universitario de Albacete 02071 Albacete, Spain; e-mail: JuanJose.Gomez@uclm.es

Abstract

Complex lacustrine systems, such as hypersaline lakes located in endorheic basins, are exposed to nitrate (NO_3^-) pollution. An excellent example of these lakes is the hypersaline lake located in the Pétrola basin (central Spain), where the lake acts as a sink for NO_3^- from agricultural activities and from sewage from the surrounding area. Because density-driven downflow across the bottom sediment has been observed in hypersaline lakes, the lake sediments can promote different biological pathways affecting the nitrogen cycle in the underlying groundwater. To better understand the role of the organic carbon (C_{org}) deposited in the bottom sediment in promoting denitrification, a four-stage flow-through experiment (FTR) and 9 batch experiments using lake bottom sediment were performed. The chemical, multi-isotopic and kinetic characterization of the outflow and the vertical profiles of the reactor showed that the intrinsic NO_3^- attenuation potential of the lake bottom sediment was able to remove 95% of the NO_3^- input over 295 days under different flow conditions. At the beginning of the FTR experiment, some dissimilatory nitrate reduction to ammonium was produced, favored by the high C/N ratio and salinity. Sulfate reduction could be neither confirmed nor rejected during the experiments because the sediment leaching masked the chemical and isotopic signatures of this reaction. The kinetic model simulates the dissolution of solid C_{org} into the aquifer and its subsequent oxidation due to denitrification, as observed in

the vertical profiles of FTR. The average nitrogen reduction rate (NRR) obtained from the model was 1.25 mmol d^{-1} Kg^{-1} and was independent of the flow rate employed. The amount of reactive C_{org} from the bottom sediment consumed during denitrification was 28.8 mmol, representing approximately 10% of the total C_{org} of the sediment (1.2%). The isotopic fractionations (ε of $^{15}N\text{-}NO_3^-$ and $^{18}O\text{-}NO_3^-$) between the reaction products and the remaining reactants were calculated using batch and vertical profile samples. The results were -14.7‰ for εN and -14.5‰ for εO. To the authors' knowledge, these are the first isotopic fractionations of denitrification related exclusively to hypersaline lake sediment.

1. Introduction

Human activities have modified the global nitrogen cycle through the input of substantial amounts of nitrate (NO_3^-) into the hydrological system. This anthropogenic NO_3^- has led to the degradation of water resources. Because freshwater demand for drinking and agricultural purposes has increased in recent decades, NO_3^- pollution of surface and groundwater is considered one of the most important water quality issues worldwide (Nolan, 2001; Puckett et al., 2011). NO_3^- contamination originates either from diffuse (non-point) sources, linked to the intensive use of synthetic and organic fertilizers and livestock, or point sources, such as septic system effluents. High NO_3^- ingestion impacts human health, promoting cancer and producing methahemoglobinemia in infants (Comly, 1945; Magee and Barnes 1956; Ward et al., 2005). Furthermore, an increase of NO_3^- in surface water can produce an increase in primary production and therefore anoxic conditions, promoting the eutrophication of surface water bodies (Rivett et al., 2008; Vitousek et al., 1997). As a consequence, the European Directive 98/83/CE established a NO_3^- concentration threshold level for human water supplies of 0.80 mM.

Lakes and wetlands have a recognized attenuation potential in removing excess dissolved NO_3^- from water (Harrison et al., 2009; Schubert et al., 2006; Seitzinger et al., 2006). Among the biological pathways used, denitrification is the main reaction in removing dissolved nitrogen compounds from lake systems (Piña-Ochoa and Álvarez-Cobelas, 2006; Wetzel, 2001). Denitrification is a redox reaction that occurs during microbial metabolism under anaerobic conditions, where NO_3^- is reduced to N_2 through several intermediate steps ($NO_3^- \rightarrow NO_2^- \rightarrow NO \rightarrow N_2O \rightarrow N_2$) (Knowles, 1982; Mariotti et al., 1988). Denitrification can be produced by both heterotrophic and/or autotrophic bacteria that use organic or inorganic compounds, respectively, as electron donors (Aravena and Robertson, 1998; Dendooven et al.,

2010, 2009; Kendall et al., 2007; Otero et al., 2009; Pauwels et al., 2000). If optimal conditions do not exist (e.g., an inadequate supply of organic carbon (C_{org}) or the presence of oxygen), intermediate nitrite (NO_2^-) can temporarily accumulate, which is even more harmful than NO_3^- (De Beer et al., 1997). Further reactions that can affect NO_3^- levels are the dissimilatory nitrate reduction to ammonium (DNRA) and anaerobic ammonium oxidation (Anammox). The DNRA reaction is promoted by fermentative bacteria that transform NO_3^- to NH_4^+. In contrast with denitrification, DNRA does not remove nitrogen from the ecosystem (Bulger et al., 1989; Nizzoli et al., 2010; Schmidt et al., 2011; Smith et al., 1991). The Anammox reaction consists of the oxidation of NH_4^+ using NO_3^- and NO_2^- as electron acceptors, producing N_2. Studies have shown that Anammox can be restricted in the presence of denitrification reactions due to the lower biological growth rate of Anammox bacteria compared with denitrifying bacteria (Jetten and Strous, 2007; Kraft et al., 2011). In addition, complete NO_3^- removal from groundwater can occur when electron donors are still available. Under these conditions, other redox reactions, such as sulfate reduction, can occur, decreasing the water quality.

Different approaches have been useful in identifying the key processes that enable the natural attenuation of NO_3^- in lakes. Investigating the isotopic composition of the different by-products of the reactions can further elucidate these reactions (Aravena and Robertson, 1998; Clark et al., 2008; Lehmann et al., 2003; Mariotti et al., 1988; Schmidt et al., 2011; Vitoria et al., 2008; among others). Stable isotopes are usually measured as the ratio between the heavier isotope and the lighter isotope, e.g., ^{15}N against ^{14}N. Ratios are established with respect to international standards using the delta notation (Eq. 1):

$$\delta^{15}N = [(R_{sa} - R_{std}) / R_{std}] \times 1000 \qquad (1)$$

where $R = {}^{15}N/{}^{14}N$ in the sample (sa) and in the standard (std). During denitrification and DNRA, the $\delta^{15}N$ and $\delta^{18}O$ of the residual NO_3^- increase as the NO_3^- concentration decreases. This change in the isotopic composition or fractionation (ε) is useful in distinguishing between biological reactions and other processes, such as dilution, which can also decrease the NO_3^- concentration but do not change the isotopic value (Clark and Fritz, 1997; Kendall et al., 2007). The isotopic fractionation (ε) is defined as follows (Eq. 2):

$$\varepsilon_{product/reactant} = (R_{product} / R_{reactant} - 1) * 10^3 \text{ (‰)} \qquad (2)$$

During denitrification processes, the εN/εO ratio ranges from 0.9 (Otero et al., 2009) to 2.1 (Böttcher et al., 1990). Differences in the isotopic fractionation and in the εN/εO ratio reflect the variety of environmental conditions. However, to our knowledge, the isotopic fractionation during NO_3^- attenuation produced by hypersaline lake sediments have not been reported to date.

Furthermore, the rates of attenuation reactions can be evaluated through biogeochemical models. These models permit the quantitative analysis of the interactions among reaction processes (Steefel et al., 2005) and provide a framework to improve the characterization and monitoring of denitrification. The majority of the kinetic studies of NO_3^- attenuation processes have focused on attenuation induced by adding an external organic or inorganic substrate (Nielsen et al., 1996; Dinçer and Kargi, 2000; Koenig and Liu, 2001) or a specific bacteria strain (Joshi et al., 2007). Kinetic studies can be based on batch experiments (Joshi et al., 2007; Vasiliadou et al., 2008; Rodríguez-Escales et al., 2014) and/or flow-through systems (Roychoudhury and Viollier, 1998; Fu et al., 2009; Mathioudakis and Aivasidis, 2009; Andre et al., 2011).

In lakes, denitrification can occur in the benthic environment (Nizzoli et al., 2010), when water flows through lake bottom sediments, or by NO_3^- diffusion into the lake sediment (Lehmann et al., 2003). These sediments are an important source of electron donors because freshly deposited C_{org} can be easily degraded by denitrifying bacteria (Seitzinger, 1988). Several authors have shown that the attenuation produced in sediment is more important than that in benthic environments (Lehmann et al., 2004; Woszczyk et al., 2011). Other reactions that can affect NO_3^-, including DNRA and Anammox, have been observed in lakes under similar anaerobic conditions to denitrification (Laverman et al., 2007; Nizzoli et al., 2010). In complex lacustrine systems such as hypersaline lakes located in endorheic basins, these different biological pathways can affect the nitrogen cycle. An important surface area of the region of La Mancha in central Spain is composed of endorheic basins draining to hypersaline lakes. These lakes serve as a sink for N compounds from agriculture and sewage waters (Brinson et al., 1995). An excellent example of this type of lake is located in the Pétrola basin (Fig. 1).

The increase in the NO_3^- levels in Pétrola lake has promoted the growth of harmful algal blooms, which have led to the eutrophication of the lake. Biological production increases the amount of organic matter deposited in Pétrola Lake, which can be an important source of electron donors to promote different redox reactions. In addition, in hypersaline lakes, a density-driven flow has been observed,

produced by the instability of the saline boundary layer, which promotes a vertical downflow across the lake bottom sediment (Zimmermann et al., 2006). However, the rates and pathways of the microbial reactions occurring in lake bottom sediments and the capacity of the C_{org} in the sediment to be mobilized to the underlying groundwater are poorly understood. In this context, the present study attempts to elucidate the NO_3^- attenuation processes in the bottom sediments of Pétrola Lake and to investigate the generation of undesirable compounds, such as NO_2^- or H_2S. The study is based on chemical and multi-isotopic data from laboratory experiments. In addition, a biogeochemical model was developed to obtain the kinetic constants of the NO_3^- attenuation reaction and the reactive carbon solubilization. As a secondary goal of this study, the isotopic fractionation produced during denitrification by the lake bottom sediment was calculated.

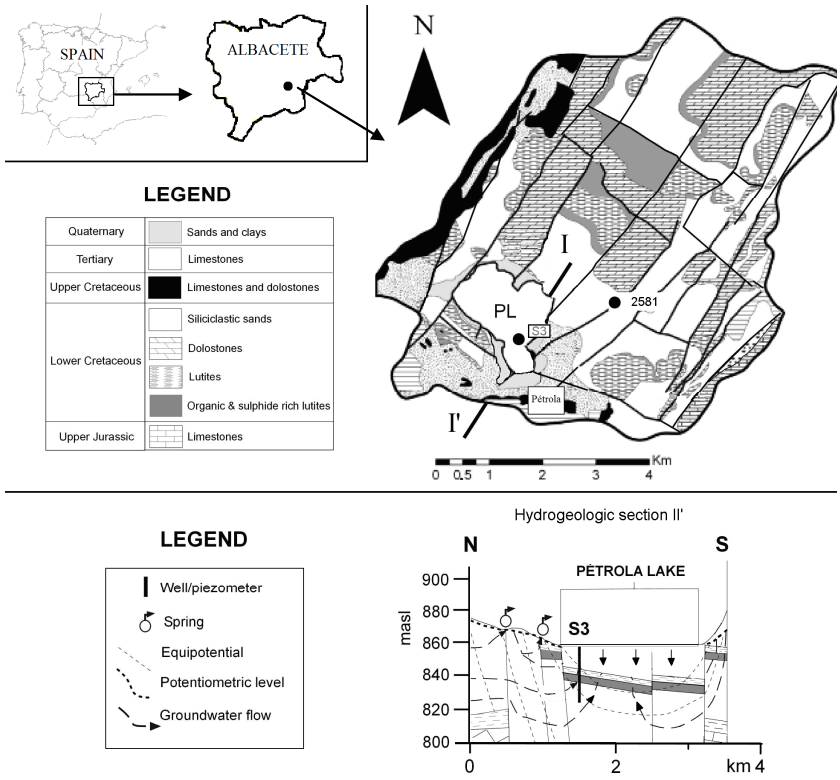

Figure 1. Geographic situation of Pétrola basin and simplified geological map with the lake located in the SW area. Sediment was obtained with piezometer S3 near the Pétrola Lake edge/shore. Water was sampled in well 2581; the NO_3^- concentration was 0.8 mM.

2. Methodology

2.1 Flow-through experiment

A flow-through reactor (FTR) experiment was carried out for ten months. The FTR consisted of a glass column (40 cm in length and 9 cm in inner diameter) placed in an anaerobic glove box. The reactor was equipped with 7 sampling ports at different heights (5, 12, 14, 17, 19, 22 and 24 cm from the sediment surface) (Fig. 2). The experiment was conducted at ambient temperature ranging from 16.4 ºC to 27.3 ºC, with an average value of 24.4 ºC. The atmosphere inside the glove box was mainly composed of argon to exclude O_2. Oxygen was removed once a day to maintain its partial pressure below 0.5%. The FTR was filled to a 24 cm height with 300 g of lake bottom sediment mixed with 1950 g of clean silica sand (1-2 mm) (Panreac®) to increase the permeability and achieve a homogenous flow inside the reactor. The total volume of water needed to saturate the sediment was 0.6 L, representing a porosity of approximately 0.30 - 0.35. The inflow and outflow rates were controlled by a peristaltic pump (Micropump Reglo Digital 4 channels ISMATEC) operating in the downflow mode. During the experiment, different flow rates were tested, ranging from 25 mL/d to 290 mL/d, providing residence times between 23 and 2 days, respectively.

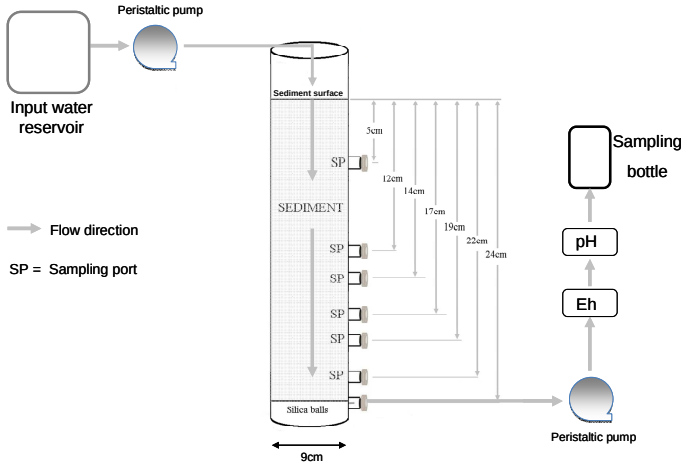

Figure. 2. Set-up of the flow-through experiment. The flow rate in the experiment was controlled by a peristaltic pump. Arrows indicate the flow direction in the flow-through experiment.

2.2 Batch experiments

Laboratory-scale batch experiments were performed to determine the N and O isotopic fractionation. A total of 9 sealed 0.5 L glass bottles were used as microcosms. Each glass bottle was filled with 75 g of sediment and 375 mL of the input water used in the FTR experiment. The reactors were set up inside a glove box with an argon atmosphere to remove any existing dissolved O_2. Then, the microcosms were removed from the glove box and wrapped with aluminum foil to prevent photodegradation, placed at room temperature and shaken twice a day. Once a day, 0.5 mL of water was sampled from each bottle to measure the NO_3^- concentration using a spectrophotometer (VVR Photometer Instrument Module V-1000, from CHEMetrics). Sampling was performed through a septum using a 3 mL syringe with a 25G needle (BD) to avoid oxygen diffusion into the system. Complete chemical and isotopic characterizations were performed according to the NO_3^- concentration evolution to characterize different reaction times.

2.3 Sediment and water description

The lake bottom sediment was sampled in September 2008 using a piezometer drilled close to the SE edge of the lake. The sediment used was sampled between depths of 0 m and 2 m below the ground surface. Immediately after sampling, the sediment was isolated from the atmosphere with polypropylene and frozen in the field with solid CO_2 to preserve it at -30 ºC. X-ray powder diffraction (XRD) analysis from the fine size (<40 μm) fraction indicated that the most abundant minerals were quartz, bassanite, gypsum, halite and magnesium sulfate. The total amounts (%) of nitrogen, carbon, sulfur and hydrogen in the sediment were determined by Elemental Analysis (EA 1108 CHNS-O Carlo Erba Instruments). The measured total C_{org} was approximately 1.2%, implying a total carbon mass of 3.6 g in the experiment. The sediment also included a significant percentage of sulfur (up to 5.7%), confirming the abundance of sulfate minerals observed with XRD.

The water used in the experiment was sampled at well 2581, screened in the Cretaceous aquifer, and can be considered representative of the groundwater composition that flows toward the lake. The physicochemical parameters measured in situ showed a conductivity of 1.2 mS/cm, a pH of 7.8 and an redox potential (Eh) of +88 mV. The input water was sampled periodically and analyzed during the experiment.

2.4 Analytical methods

During the 10 months of the FTR experiment, 115 samples were collected from the output point and from the 9 complete vertical profiles (2 mL from the 7 sampling points located throughout the column). In the batch experiments, 7 systems were analyzed. The Eh and temperature were measured every hour at the outlet of the column using portable electrodes (WTW pH-3310). The electrical conductivity was measured for all the samples using a WTW Cond-3310. Major element analyses were performed for all the samples except for the profile samples, for which, due to the lower volume extracted, analyses were restricted to the major anions. Isotopic analyses were performed on a subset of samples considered as representative. Samples were filtered through a 0.2 μm Millipore® filter. NH_4^+ was analyzed by spectrophotometry (ALPKEM, Flow Solution IV). The major anions (NO_3^-, SO_4^{2-}, Cl^- and NO_2^-) were analyzed by high-performance liquid chromatography (HPLC) using a WATERS 515 HPLC pump with IC-PAC Anion columns and WESCAN and UV/VIS KONTRON detectors. For the major cations and trace element analyses, filtered samples were acidified with 1% HNO_3^-, and Ca, Na, K and Mg were determined by inductively coupled plasma-atomic emission spectrometry (ICP-AES, Thermo Jarrel-Ash with CID detector), whereas Mn and Fe were analyzed with inductively coupled plasma-optical emission spectrometry (ICP-OES, Perkin-Elmer Optima 3200 RL.). The dissolved C_{org} (DOC) was measured by organic matter combustion (TOC 500 SHIMADZU). Analyses were performed in the Centres Científics i Tecnològics of the Universitat de Barcelona.

2.5 Isotopic analyses

Isotopic analyses during the experiment were performed on a subset of samples considered as representative based on their SO_4^{2-} and NO_3^- concentrations. A total of 9 samples were analyzed for their NO_3^- isotopic composition, including 5 samples from profile P7 at day 123, 3 samples from the batch experiment and the initial water for the experiments. The isotopic analyses included the $\delta^{34}S$ and $\delta^{18}O$ of the dissolved SO_4^{2-}, the $\delta^{34}S$ of S from the sediment and the $\delta^{15}N$ and $\delta^{18}O$ of the dissolved NO_3^-. To analyze $\delta^{34}S$ and $\delta^{18}O$, SO_4^{2-} was precipitated as $BaSO_4$ by adding $BaCl_2$ after acidifying the sample with HCl and boiling it to prevent $BaCO_3$ precipitation according to standard methods (Dogramaci et al., 2001). The $\delta^{34}S$ was analyzed in a Carlo Erba Elemental Analyzer (EA) coupled in continuous flow to a Finnigan Delta C IRMS. The $\delta^{18}O$ was analyzed in duplicate with a ThermoQuest high-temperature conversion analyzer (TC/EA) unit with a Finnigan Matt Delta C IRMS. The $\delta^{15}N$ and $\delta^{18}O$ from the dissolved NO_3^- were analyzed by the bacterial denitrifier method of Casciotti et al. (2002) and Sigman et al. (2001). Isotope ratios were calculated using 3 international standards and 1 internal laboratory standard. Notation is expressed in terms of δ per mL relative to

the international standards (Air for $\delta^{15}N$, V-SMOW for $\delta^{18}O$ and V-CDT for $\delta^{34}S$). The reproducibilities of the samples were ±0.2‰ for $\delta^{34}S$, ±0.5‰ for the $\delta^{18}O$ of SO_4^{2-}, 1‰ for the $\delta^{15}N$ of NO_3^- and ±2‰ for the $\delta^{18}O$ of NO_3^-. Isotopic analyses of $\delta^{34}S$ and $\delta^{18}O$ of SO_4^{2-} were prepared at the laboratory of the Mineralogia Aplicada i Medi Ambient research group and analyzed at the Centres Científics i Tecnològics of the Universitat de Barcelona, whereas isotopic analyses of $\delta^{15}N$ and $\delta^{18}O$ were analyzed at the Facility for Isotope Ratio Mass Spectrometry (FIRMS) at the University of California, Riverside.

2.6 Biogeochemical model construction

The Phreeqc-2 model code (Parkhurst and Appelo, 1999) was used to simulate the biodenitrification coupled to C_{org} transfer from the solid phase (organic sediment) to the liquid phase (DOC). The model was calibrated using the experimental data from the different vertical profiles (one for each velocity flow) of the FTR experiments measured at steady state.

Denitrification was modeled using the Monod equation (Monod et al., 1949). The Monod kinetic equation has been used to describe biological redox reactions; however, this equation must be considered purely descriptive and should not be used to predict transformation rates outside the range of concentrations used in the experiments (Bekins et al., 1998). Despite this limitation, Monod equations have been applied to biodenitrification models (Van Cappellen and Wang, 1996; Koenig and Liu, 2001; Hunter et al., 1998 and references therein). This equation has been utilized to describe the relationship between bacterial growth kinetics and substrate concentration (Rittmann and McCarty, 2001), and its use is justified when the organic substrate acts as a primary energy source for bacteria (Hunter et al., 1998). The model assumed that the input pH and temperature were constant during the experiment. The biomass was considered constant because the model was focused on steady-state conditions inside the FTR. The multiple-Monod expression was divided into two main equations: one for the electron donor (Eq. 3) and one for the electron acceptor (Eq. 4).

$$r_1 = \mu_{\max} \cdot [C]_t \cdot \left(\frac{[N]_t}{K_s + [N]_t} \right) \qquad (3)$$

$$r_2 = Q \cdot r_1 \qquad (4)$$

where [C] is the concentration of the soluble electron donor (mmol L^{-1}) (DOC), [N] is the concentration of the electron acceptor ($N\text{-}NO_x^-$, mmol L^{-1}), μ_{max} is the maximum specific growth rate (h^{-1}), K_s is the half saturation constant of $N\text{-}NO_x^-$ (mmol L^{-1}), and Q is the stoichiometric relationship between the electron acceptor and the electron donor; in the case of heterotrophic denitrification, Q is 0.8 (Knowles, 1982). To simplify the model, the denitrification rate was calculated for $N\text{-}NO_x^-$ ($N\text{-}NO_3^-$ + $N\text{-}NO_2^-$), which is appropriate when the denitrifier biomass concentration is not measured, as in the present study (Fu et al., 2009).

The proposed conceptual model for carbon species includes one immobile form of C_{org} (sediment) and one form of DOC. The immobilized sediment can be attached to the aquifer matrix and/or to the biofilms. From there, particulate organic matter will be successively solubilized and oxidized during denitrification (Janning et al., 1998). Solubilization, i.e., the mass transfer process, is assumed to be a rate-limited process, where the rate can also depend on the solubility of the dissolved organic compounds. We modeled this process following the instructions of Greskowiak et al. (2005), who slightly modified the model from Kinzelbach et al. (1991), as shown in Eq. 5:

$$r_{DOC,sol} = C_{SOM}\beta\frac{C_{sat} - C_{DOC}}{C_{sat}} \qquad (5)$$

where r is the mass transfer rate (mmol L^{-1} h^{-1}), C_{sat} is the saturation concentration (mmol L^{-1}), C_{DOC} is the soluble C_{org} (mmol L^{-1}), C_{SOM} is the solid C_{org} in the sediment normalized to the mass of water in the reactor (mol Kg^{-1}), and β is the maximum transfer rate (h^{-1}). The solubilization of filtered, immobilized sediment is thought to form a continuous and localized source of DOC. The initial conditions considered in the model are listed as supporting information (Table SI-1).

To enable a comparison with other values reported in the literature, the results of the model are shown as the net nitrogen ($N\text{-}NO_x^-$) reduction rate (NRR) (Laverman et al., 2012; Carrey et al., 2013; Abell et al., 2009). The NRR is defined as the nitrogen removed each day per volume of reactive sediment. The NRR values were determined from r_2 multiplied by the volume of water in the reactor (0.6

L) and normalized to the volume of the lake bottom sediment in the reactor (0.15 L^{-1}). Because the model focuses on N species, sulfate reduction reactions were not taken into account.

3. Results

3.1 FTR results

The bulk dataset from the FTR experiments is provided as supporting information (Table SI-2, 3 and 4). The input water composition did not vary significantly during the experiment, with an average pH of 7.8, an average Eh of +81 mV and concentrations of 0.88 mM NO_3^-, 3.54 mM SO_4^{2-}, 0.02 mM NH_4^+ and 0.17 mM DOC; NO_2^-, Fe and Mn were below the detection limit (<4.3x10^{-3} mM, <2 x10^{-3} mM and 4x10^{-4} mM, respectively).

Stage I: day 0 – 71 (flow rate of 150 mL/d)

At the beginning of the experiment, substantial leaching from the sediment was observed. As a consequence, an increase of two orders of magnitude in the major cations and certain anions was observed. The increased solute concentrations produced an increase in the electrical conductivity from 1.2 mS/cm (input water) to 88.3 mS/cm (outflow water) on day 1 and a gradual decrease to 3.0 mS/cm at the end of the stage (Fig. 3a). The concentrations of the major cations (Na^+, K^+, Ca^{2+}, Mg^{2+}) and anions (Cl^- and SO_4^{2-}) in the outflow showed similar trends, with the highest concentration at day 1 and decreases observed thereafter. The Eh varied from +88 mV to -300 mV, decreasing in the outflow rapidly to -192 mV (day 2) and subsequently increasing to -25 mV (day 15) (Fig. 3b). From day 15 to the end of Stage I, the Eh decreased to -300 mV (day 71). The pH measured in the outflow ranged from 7.8 to 8.6, increasing from an initial value of 7.8 (day 1) to 8.6 (day 10) and decreasing thereafter, ranging from 8.0 (day 15) to 8.3 at the end of the stage (Fig. 3c). The evolution of NO_3^- concentration in the outflow showed a decrease from 0.93 mM to 0.15 mM after 2 days (Fig. 3a). Complete NO_3^- attenuation in the outflow water was achieved at day 23 and remained below the detection limit (<3.2x10^{-3} mM) thereafter. As the NO_3^- decreased in the outflow, substantial NO_2^- and NH_4^+ accumulation occurred. The NO_2^- concentration in the outflow increased from day 1, reaching its highest level of 0.52 mM at day 2. Thereafter, the NO_2^- concentration decreased in the outflow, ranging from 0.24 mM to 0.01 mM, until day 15, when the NO_2^- was below the detection limit (4.3x10^{-3} mM) (Fig. 4a). During this stage, the NH_4^+

concentration in the outflow was higher than that in the input water (0.01 mM), varying from 0.07 mM to 0.88 mM (Fig. 4a). The NH_4^+ increased from 0.34 mM at day 1 to 0.88 mM (day 4) and then declined gradually to 0.07 mM at the end of the stage. A similar trend was observed for DOC in the outflow water, increasing initially to 17.5 mM (day 2) and then decreasing later to a concentration of 0.34 mM.

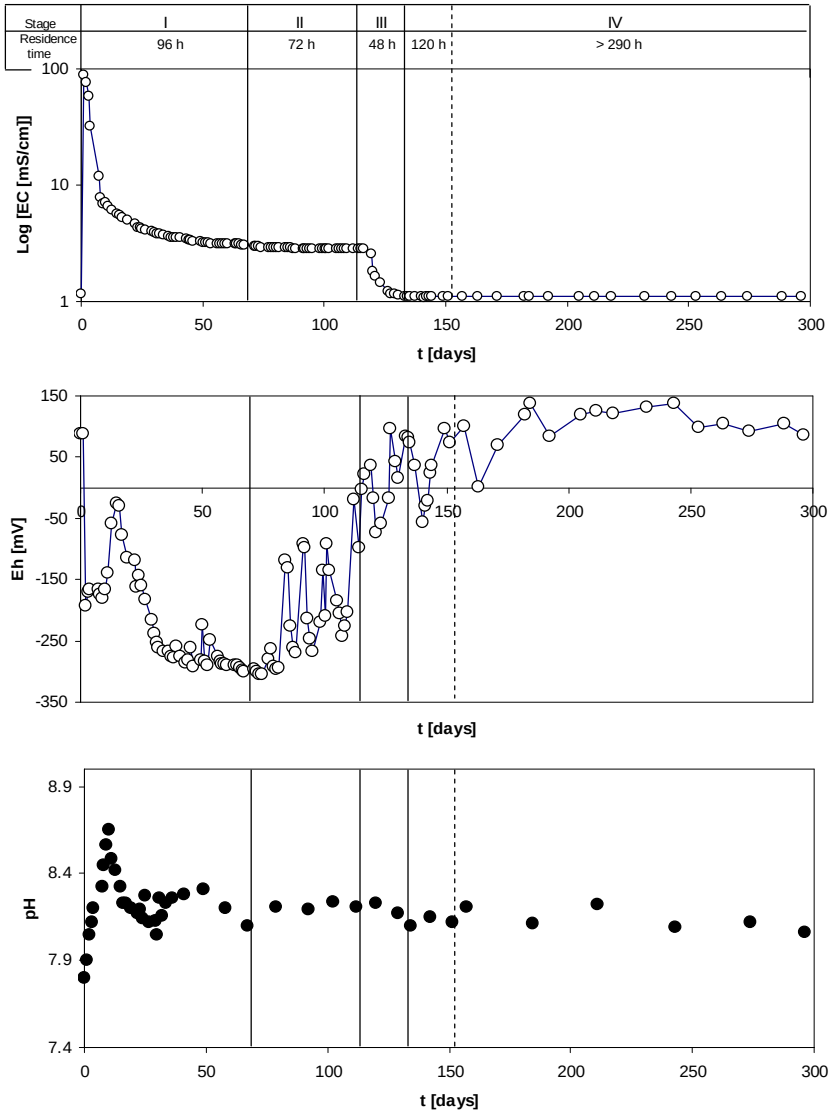

Figure 3. a) Electrical conductivity in the outflow water with time for the different stages; b) evolution of Eh; c) evolution of pH.

Two profile analyses were performed, at days 39 (P1) and 67 (P2) (Fig. 4a). The profile results showed that the NO_3^- concentration decreased mainly in the upper part of the FTR. Complete NO_3^- consumption was achieved in the first 12 cm. The NO_2^- concentration ranged from 0.07 mM to below the detection limit. The NO_2^- concentration increased in the upper part of the sediment, with the highest concentration observed 5 cm under the sediment surface.

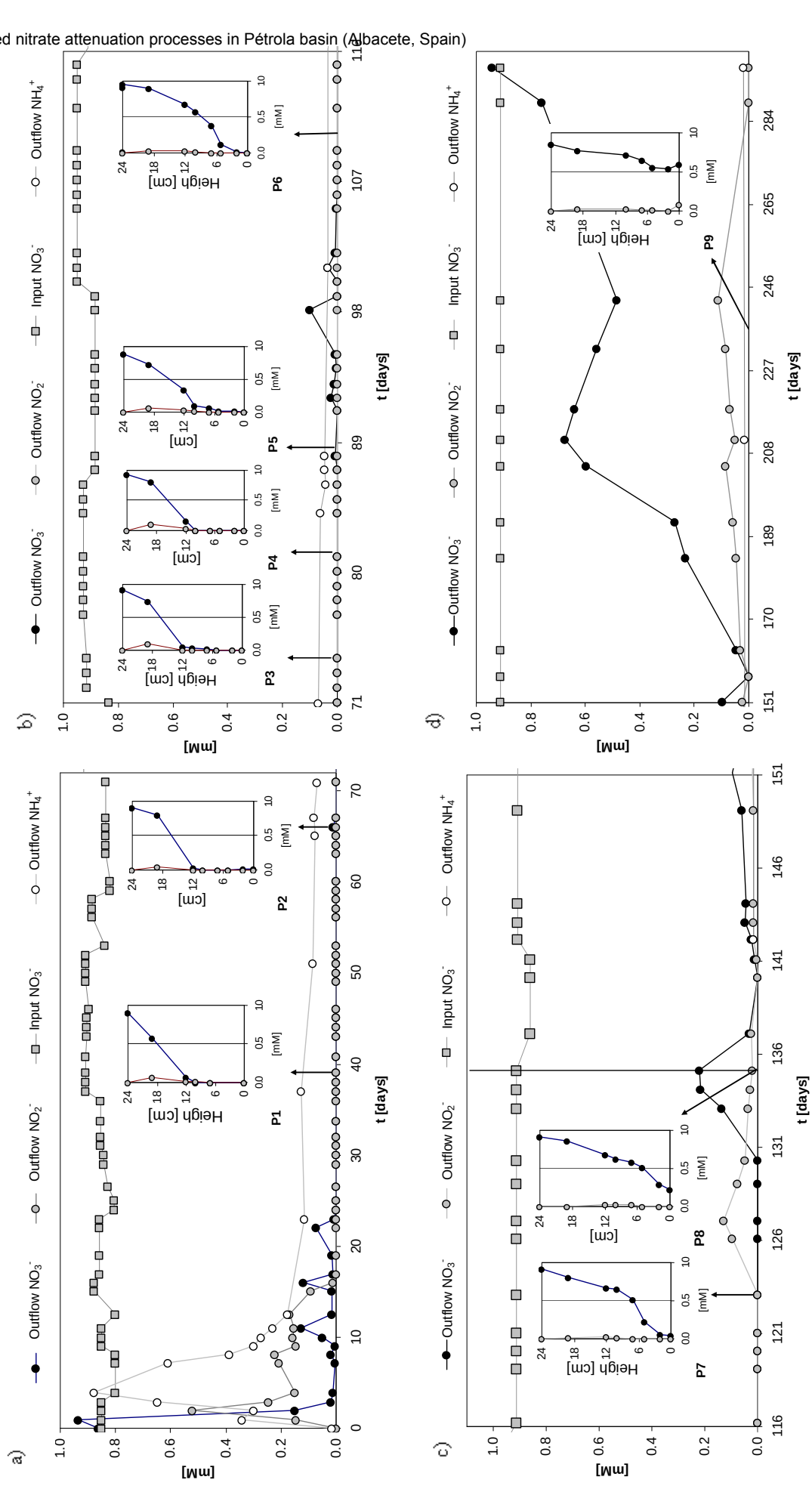

Figure 4. Evolution of nitrogen species during the flow-through experiment. a) Stage I, with a residence time of 4 days/96 hours; b) Stage II, with a residence time of 3 days; c) Stages III and IV, with a residence times of 2 days and 6 days, respectively, and d) the end of Stage IV, with a residence time of >12d

Stage II: Day 72 – 116 (flow rate of 200 mL/d)

During Stage II, the effects of leaching on the outflow water chemistry were less important. The electrical conductivity ranged from 3.0 mS/cm to 2.8 mS/cm but remained higher than the electrical conductivity of the input water (Fig. 3a). Some anions, such as Cl^-, K^+ and Mg^{2+}, had outflow concentrations similar to those in the input water. However, the Ca^{2+}, Na^+ and SO_4^{2-} concentrations remained higher than those in the input water during this stage. The Eh values increased from -304 mV at day 72 to +22.6 mV at the end of the phase (Fig. 3b). The pH measured in the outflow was about 8.2 (Fig. 3c). The NO_3^- concentration did not vary significantly during this stage, ranging from below the detection limit to 0.1 mM. The NO_2^- concentration in the outflow remained below the detection limit in all the samples, whereas the NH_4^+ concentration decreased from 0.08 mM, observed at the end of Stage I, to 0.03 mM at the end of Stage II (Fig. 4b). The DOC observed in the outflow ranged from 0.81 to 0.35 mM.

During the second stage, four profile analyses were performed, at days 74 (P3), 81 (P4), 88 (P5) and 112 (P6) (Fig. 4b). Similarly to Stage I, NO_3^- attenuation was achieved in the top of the sediment. In the upper 14 cm, P3 and P4 showed complete NO_3^- consumption, whereas in P5 and P6, the NO_3^- removal was approximately 90%. Coupled with NO_3^- attenuation, NO_2^- was also accumulated in the top of the sediment. The maximum NO_2^- concentration was observed at the first sampling point, located 5 cm under the surface sediment (ranging from 0.03 mM to 0.11 mM), and decreased to below the detection limit at a 12 cm depth from the surface in all the profiles.

Stage III: Day 116 – 135 (flow rate of 290 mL/d)

When the flow rate was increased, the electrical conductivity decreased to 1.2 mS/cm at day 127. This value is the same conductivity as that of the input water, illustrating the termination of the leaching from the sediment (Fig. 3a). The sulfate, Ca^{2+} and Na^+ concentrations in the outflow decreased during this stage to the same concentrations measured in the input water. The Eh decreased at the beginning of this stage to -204.7 mV (day 123) and then increased to +84.4 mV (day 135) (Fig. 3b). The pH observed in the outflow varied from 8.1 to 8.2 (Fig. 3c). Despite the flow rate increase, the NO_3^- concentration remained below the detection limit until day 133. Thereafter, the NO_3^- level increased to 0.22 mM. A substantial increase of NO_2^- was observed in the outflow after day 123. The NO_2^- concentration ranged from 0.03 mM to 0.13 mM, with the highest value reached at day 127. The increase in NO_2^- might have been influenced by the profile analysis performed at day 123, in which 7 mL was taken from each sampling point, modifying the residence time in the subsequent samples. Regarding the NH_4^+ observed in

the outflow, the measured concentration remained constant, with values of 0.01 mM, equal to the input water concentration (Fig. 4c). The DOC during this stage ranged from 0.49 mM to 0.30 mM.

Two profiles were collected during this stage: one at day 123 (P7) under steady-state conditions (Fig. 3c) and one at day 135 (P8), when the NO_3^- concentration in the outflow began to increase and could not be considered to be under steady-state conditions (Fig. 4c). In P7, NO_3^- attenuation was produced in the bottom of the FTR, with 95% of the NO_3^- consumed between the last two sample points (between 14 cm and 19 cm below the sediment surface) (Fig. 4c). The NO_3^- concentration in P8 decreased from 0.85 mM (first sampling point) to 0.22 mM (outflow). The NO_2^- concentration ranged from 0.01 mM to 0.03 mM. In both profiles, NO_2^- accumulated at the top of the reactor beginning at the onset of NO_3^- attenuation and then subsequently decreased to below the detection limit at the bottom of the reactor.

Stage IV: Day 135 – 295 (flow rate from 125 mL/d to 25 mL/d)

After day 135, the flow rate was gradually decreased to a minimum of 25 mL/d. The Eh increased during this stage with maximum value of +138.5 mV whereas pH remained almost constant ranged from 8.1 to 8.2 (Fig. 3b and c). The NO_3^- concentration tended to increase in the outflow. From day 135 to day 151, when the flow rate was lowered to 125 mL/d, the NO_3^- concentration ranged from below the detection limit up to 0.09 mM, lower than the values observed at the end of Stage III. During this period, the NO_2^- in the outflow water ranged from below the detection limit to 0.02 mM. After day 151, the flow rate was significantly decreased to 25 mL/d; nonetheless, the NO_3^- concentration increased from 0.09 mM to 0.94 mM at day 296. The NO_2^- concentration in the outflow water also increased to 0.11 mM at day 243 and then decreased to below the detection limit in the last samples (Fig. 4c and d). During this stage, the NH_4^+ concentration did not exhibit any variation, remaining at the input water concentration of 0.01 Mm. The DOC concentration ranged from 0.16 to 0.25 mM.

One profile was performed in non-steady-state conditions (P9) at day 243, showing incomplete NO_3^- attenuation. The NO_3^- concentration decreased from 0.85 mM to 0.55 mM, and the main attenuation was produced in the bottom of the FTR. NO_2^- accumulated in the bottom of the FTR, increasing to a concentration of 0.09 mM at the last sampling point (Fig. 4c and d).

3.2 Batch experiment results

The bulk dataset from the batch experiments is provided as supporting information (Table SI-5). All the systems showed a substantial increase in the electrical conductivity from that of initial water (1.3 mS/cm) to approximately 30 mS/cm in all the microcosms. The NO_3^- concentration ranged from below the detection limit to 0.60 mM. NO_2^- accumulation was observed in all the microcosms, ranging from 0.11 mM to 0.69 mM. The NH_4^+ concentration ranged from 0.01 mM to 0.08 mM. The DOC concentration varied from 0.65 mM to 1.17 mM.

3.3 Isotopic results

The isotopic composition of NO_3^- increased as the NO_3^- concentration decreased. $\delta^{15}N\text{-}NO_3^-$ ranged from +9.6‰ to +27.2‰, whereas $\delta^{18}O\text{-}NO_3^-$ varied from +8.6‰ to +28.9‰. In the batch experiments, $\delta^{15}N$ ranged from +15.0‰ to +28.9‰, whereas $\delta^{18}O$ varied from +20.1‰ to +31.0 ‰. The plot of $\delta^{15}N$ vs. $\delta^{18}O$ for all the samples showed a slope of 0.93 ($r^2 = 0.94$), typical of processes such as denitrification or DNRA, confirming that the observed NO_3^- attenuation could be achieved by these processes (Fig. 5). The isotopic composition of the sulfur from the lake bottom sediment was -22.5‰. The $\delta^{34}S_{SO4}$ and $\delta^{18}O_{SO4}$ from the input water were -17.0‰ and +5.5‰, respectively. The first sample of the outflow collected at Stage I showed a higher SO_4^{2-} concentration, with $\delta^{34}S$ of -20.0‰ and $\delta^{18}O$ of +4.3‰. The isotopic composition of $\delta^{34}S$ remained almost constant with time, ranging between -20.3‰ and -19.4‰. In the batch experiments, the isotopic composition of $\delta^{34}S$ also remained constant, with values ranging from -21.0‰ to -21.7 ‰.

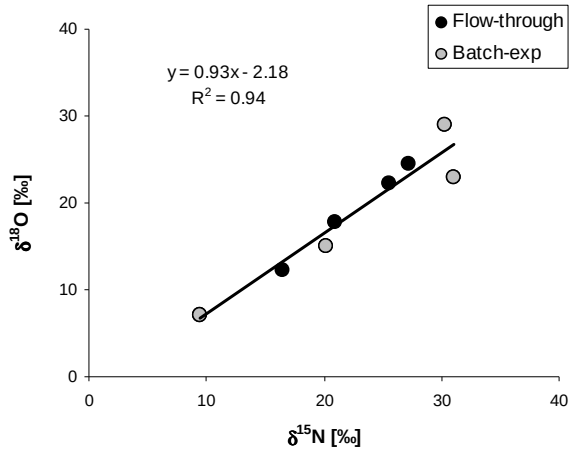

Figure 5. $\delta^{15}N$ vs. $\delta^{18}O$ for the flow-through and batch experiments, showing a slope of 0.93, typical of denitrification processes.

4. Discussion

4.1 NO_3^- attenuation processes

NO_3^- attenuation was produced quickly in the FTR experiment, beginning at day 2. The rapid decrease of NO_3^-, with a consumption of over 90% after 4 days, coupled with the substantial increase in the DOC in the outflow, indicated that the C_{org} from the sediment was easily degraded and acted as an electron donor. During the first 10 days, as the NO_3^- decreased, substantial NH_4^+ accumulation was produced. This increase in NH_4^+ may indicate the occurrence of DNRA in the FTR and may have been generated by the remineralization of organic nitrogen in the sediment as well as by NH_4^+ leached due to cation exchange. Remineralization can be ruled out because the amount of N in the sediment was below 0.01%. Increases in NH_4^+ due to cation exchange with Na^+ have been well established (Seitzinger et al., 1991; Rysgaard et al., 1999) and might have influenced the NH_4^+ increase in the outflow. The high cation concentrations observed at the beginning may have favored NH_4^+ mobility in the sediment. However, in the batch systems, the maximum detected NH_4^+ concentration was 0.08 mM, indicating low levels of NH_4^+ mobilized by cation-exchange in the sediment. Therefore, it is reasonable to assume that DNRA was the main source of NH_4^+ observed in the outflow. The amount of NO_3^- attenuated by DNRA with respect to the total NO_3^- removed after day 4 was 90%, decreasing gradually to approximately 2% after 17 days. The contributions of other reactions, such as Anammox, that could reduce the NH_4^+ concentration in the experiments is likely to be absent because Anammox is repressed in systems with excess organic C (Burgin and Hamilton, 2007). Therefore, the gradual decrease of NH_4^+ in the outflow was due to the repression of DNRA reactions over time. The evolution of the DNRA reactions in the FTR experiment might have been related to the variations in the C/N ratio observed in the initial stage. A high C/N ratio favors the development of DNRA reactions (Tiedje 1988; Nijburg 2000; Burgin and Hamilton 2007). The initial dominance of the DNRA reaction in the FTR experiment was not observed in the batch systems, where this reaction appeared to be negligible or absent. The lack of DNRA in the batch systems may be linked with the lower sediment-water ratio compared with that in the FTR experiment. A lower sediment-water ratio implies a lower C/N ratio. Therefore, a high C/N ratio might have favored the development of DNRA over denitrification in the FTR experiment, whereas when C/N decreased, denitrification became the main NO_3^- attenuation process. The high DOC values observed during the first days of the FTR experiment might have been promoted by the high salinity, which induced the mobilization of the sediment-bound organic matter (Laverman et al., 2007). The role of salinity in

different NO_3^- attenuation reactions is uncertain. Although some studies observed the inhibition of DNRA in highly saline environments (Dendooven et al., 2010), in the present study, DNRA seemed to be more important at the beginning of the FTR, when the salinity was highest. In this sense, the high salinity observed may have stressed the freshwater denitrifying bacteria, decreasing the denitrification rate (Rysgaard et al., 1999) and favoring the development of DNRA in the initial stage of the FTR experiment. After day 4, as the salinity decreased, denitrification became the dominant reaction. Overall, these FTR results and batch experiments showed that denitrification was the main reaction promoting NO_3^- attenuation, in agreement with other studies in lake systems, where DNRA generally does not play an important role (e.g., Mengis et al., 1997; Lehmann et al., 2003).

4.2 NO_2^- accumulation

Assuming that DNRA was the main NO_3^- reduction pathway during the first days (Stage I, Fig. 4a), it is also reasonable to assume that the NO_2^- accumulation during this period was linked to partial DNRA reactions. However, denitrification might have also contributed to the observed NO_2^- concentration. During denitrification, NO_2^- accumulation is produced due to the inhibition of NO_2^- reductase (Akunna et al., 1993). Because during DNRA, NO_2^- reduction is caused by the same reductase (Kraft et al., 2011), similar enzymatic behavior should be expected, resulting in the NO_2^- accumulation observed during Stage I. In addition, because NO_2^- reductase is a periplasmic enzyme, it is more sensitive to environmental conditions. Therefore, high salinity can stress this enzyme, affecting NO_2^- reduction processes (Zumft, 1997). Furthermore, NO_2^- accumulation may be related to the pH of the media. The observed NO_2^- accumulation during the experiment was correlated with the increase in the pH from 7.9 to 8.6 (Fig. 3c). The pH-values observed in this study were in the range of those reported by Glass and Silverstein (1998) to inhibit NO_2^- reduction during denitrification (8.5 to 9.0). Therefore, the pH conditions might have favored the lag in NO_2^- reduction compared with NO_3^- during the first days of the experiment. After day 15, NO_2^- accumulation was not observed in the outflow, despite the increase of the flow rates to 290 mL/d. At the end of the experiment, when organic C was limited in the sediment, the NO_3^- concentration began to increase, despite the decreasing flow rates tested in the FTR. Coupled with this increase in NO_3^-, NO_2^- accumulated again in the outflow but with a lower concentration than that observed during the first days of the experiment. Therefore, the substantial NO_2^- concentration in the outflow during Stage I may have been favored by competition among different bacterial communities,

whereas at the end, when the denitrifying bacteria were dominant, the NO_2^- accumulation was less important and was controlled by the lack of an electron donor in the sediment.

4.3 Sulfate reduction reaction

Once NO_3^- is completely consumed, if an electron donor is still available in the system, sulfate reduction can take place through a redox reaction sequence (Stumn and Morgan, 1996) because Fe and Mn concentrations are below the detection limit in the input water. Sulfate reduction should produce a decrease in the SO_4^{2-} concentration in the outflow water accompanied by an increase in the $\delta^{34}S$ values of the dissolved SO_4^{2-}. However, the possible variation in the SO_4^{2-} concentration was masked by both leaching and gypsum dissolution in the sediment, which increased the SO_4^{2-} content in the outflow water. In addition, the leaching masked variations in the isotopic composition of the dissolved SO_4^{2-} in the outflow water. The gypsum from the sediment had an average isotopic composition for $\delta^{34}S$ of -22.5‰, similar to the isotopic composition observed in the outflow (-20.3‰ to -19.1‰). Mainly during Stages I and II of the experiment, the redox conditions in the outflow were below the typical values at which sulfate reduction can be promoted (<-150 mV) (Connell and Patrick Jr., 1968) (Fig. 3b). Therefore, at the lab scale, sulfate reduction could be neither confirmed nor rejected; at the field scale, the migration of dissolved organic C coupled with the reducing environment might promote sulfate reduction.

4.4 Biogeochemical model and natural attenuation potential

The model simulates the dissolution of C_{org} into the aquifer and its subsequent oxidation due to denitrification. Fig. 6 shows the agreement of the model with the experimental data; each figure illustrates different flow velocities. The calibrated parameters used to produce the model are listed in Table 1. The denitrification parameters (μ_{max} and K_s) were in the same range as those of other similar natural attenuation processes and were similar to those of other enhanced denitrification studies at the lab scale (Table 1).

Table 1. Estimated values of different parameters used in this work compared to literature values.

Parameter	Unit	This work	Literature values	References
μ_{max}	$[h^{-1}]$	0.04	0.06	Killingstad et al., 2002
			0.42	Kinzelbach et al. 1991
			1.7	Lee et al., 2006
			1.6-3.3	Rodriguez-Escales et al., 2014
			0.014-0.054	An et al., 2011
$K_{sat,nit}$	[mmol/L]	$5x10^{-2}$	$8x10^{-3}$	Kinzelbach et al. 1991
			$4x10^{-2}$	Rodriguez-Escales et al., 2014
			$1.4x10^{1}$	Killingstad et al., 2002
			$2.2\text{-}2.7x10^{1}$	An et al., 2011
C_{sat}	[mmol/L]	4.65	4.65	Greskowiak et al. 2005
			0.13	Kinzelbach et al. 1991
β	$[h^{-1}]$	1.78×10^{-3}	4.63×10^{-3}	Greskowiak et al. 2005
			8.9×10^{-4}	Kinzelbach et al. 1991

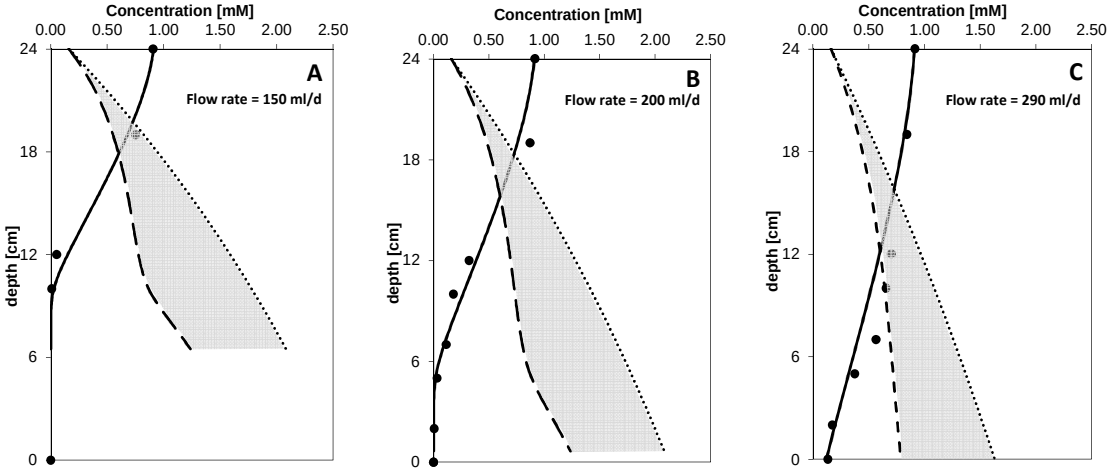

Figure 6. Modeling results (lines) vs. experimental data (solid circles). The solid line represents the NO_3^- concentration; the dashed line represents the calculated degraded C_{org}; the dotted line represents C_{org} transfer to the liquid from the solid phase without degradation; and the grey surface represents the C_{org} consumed due to denitrification processes.

Notably, certain values fit well with the three different flow conditions (Fig. 6). This finding indicates that the denitrification kinetics were not affected by the different flow rates with similar nitrogen reduction rates (NRRs) when steady-state conditions were reached. The average NRR during complete N-NO_x^- attenuation obtained in the model was 1.25 mmol d^{-1} L^{-1}, with a maximum value of 1.91 mmol d^{-1} L^{-1}. The results from the Pétrola Lake sediment were 50% lower than the NRR reported for other

hypersaline lakes, such as Mono lake (between 2.8 and 3.9 mmol d^{-1} L^{-1}) (Laverman et al., 2012). Furthermore, the NRR values obtained in the present study were within the range of values displayed by other brackish environments, such as estuaries, salt-marshes and near-shore environments (from 0.6 mmol d^{-1} L^{-1} to 7.3 mmol d^{-1} L^{-1}) (Laverman et al., 2012). The NRR values were two orders of magnitude higher than the values observed in an analogous FTR experiment using Cretaceous organic strata from the Pétrola area with C_{SOM} of 0.33 mol/Kg, which reached a maximum NRR of 0.02 mmol d^{-1} L^{-1} (Carrey et al., 2013). This remarkable difference may be related to the different reactivities of the C_{org} sources. The analysis of C_{org} in sediment provides only a rough indicator of electron donor availability due to the compositional variations of organic matter (Laverman et al., 2012). Therefore, the reactive C_{org} from the lake bottom sediment was obtained from chemical data from the outflow. The reactive C_{org} was obtained from the amount of C consumed by denitrification from day 10 to day 150. The total NO_3^- reduced to N_2 throughout the experiment was 23.0 mmol. Following the heterotrophic denitrification reactions, 1 mol of NO_3^- consumed 1.25 mol of C; hence, the total amount of C_{org} consumed during denitrification was 28.8 mmol. Moreover, the degradable C_{org} was calculated by adding the C_{org} released in the outflow as DOC from day 10 to day 150 with complete NO_3^- attenuation because after day 150, denitrification was limited by the low availability of organic C. The C_{org} released from the system was 24.7 mmol. The total amount of reactive C_{org} mobilized from the sediment was 53.5 mmol. Therefore, the reactive C_{org} represented 18% of the total SOM measured in the sediment (0.50 mol Kg^{-1}). These values are similar to those determined by Abell et al. (2009), where only 3-13% of the total organic C from intertidal freshwater sediments was degradable. Assuming a constant thickness of the lake bottom sediment of approximately 2 m and a C_{org} fraction of 1.2%, of which 18% is reactive, the lake bottom sediment can remove 1.6 mM (100 mg/L) of NO_3^- from a water flux of 5 $m^3/m^2/y$ over a period of 40 y. Utrillas Facies sediment showed the capacity to remove the same amount of NO_3^- considering the same flux for a period of 6 y. Therefore, the lake bottom sediment is an important source of electron donors that can remove input NO_3^- from the lake and can act as a source of C to underlying groundwater through different density-driven flows, as has been proposed previously by Gómez-Alday et al. (2013). In addition, the amount of organic matter in the lake bottom sediment is continuously increasing due to the high biological production in eutrophic lake water, which causes a continuous deposition of organic compounds (Hammer, 1986). Therefore, the key question for the sustainability of Pétrola N cycling is the actual rate of C_{org} accumulation in the lake bottom.

4.5 N and O isotopic fractionation

In this study, the isotopic fractionation for denitrification was calculated using samples from batch experiments as well as one profile performed in the FTR on day 123, when the NO_3^- removed by denitrification and DNRA was negligible. Variations in the isotopic compositions of both $\delta^{15}N$ and $\delta^{18}O$ during denitrification can be expressed as Rayleigh distillation processes (Aravena and Robertson, 1998; Mariotti et al., 1988):

$$\delta^{15}N_{residual} = \delta^{15}N_{initial} + \varepsilon \ln f \qquad (8)$$

$$\delta^{18}O_{residual} = \delta^{18}O_{initial} + \varepsilon \ln f \qquad (9)$$

where f is the residual NO_3^- concentration divided by the initial NO_3^- and ε is the fractionation. The value of ε was obtained using a linear regression between $\ln[NO_3^-]$ and both $\delta^{15}N$ and $\delta^{18}O$ (Fig. 7). If denitrification occurs, a linear correlation should be observed, where the slope corresponds with the ε (Kendall et al., 2007). The studied samples showed a good correlation between these parameters, with similar trends in both experiments ($r^2 = 0.80$ and 0.84 for $\delta^{15}N$ and $\delta^{18}O$, respectively). The fractionation values obtained were -14.7‰ for εN and -14.5‰ for εO (Fig. 7). The calculated isotopic fractionations from the lake bottom sediment were close to the values gathered from the Cretaceous strata of the region (-11.6‰ and -15.7‰ for εN and -12.1‰ and -13.8‰ for εO). Some authors have proposed that fractionation values decrease as denitrification rates increase (Mariotti et al., 1988), whereas others have observed that more negative values of fractionation were associated with higher denitrification rates (Korom et al., 2012). In the present study, the NO_3^- reduction rate in the lake bottom sediment was significantly higher than that observed in the Cretaceous strata; however, the isotopic fractionation values obtained in the two experiments were similar. Furthermore, the fractionation obtained from the batch systems agreed well with the fractionation determined from the FTR experiment (Fig. 7), even though the batch systems' denitrification rates were noticeably lower. Therefore, variations in $\delta^{15}N$ and $\delta^{18}O$ fractionation during denitrification cannot be explained only by variations in the reaction rate, and other factors play a role, such as the C_{org} type and availability or the bacterial community.

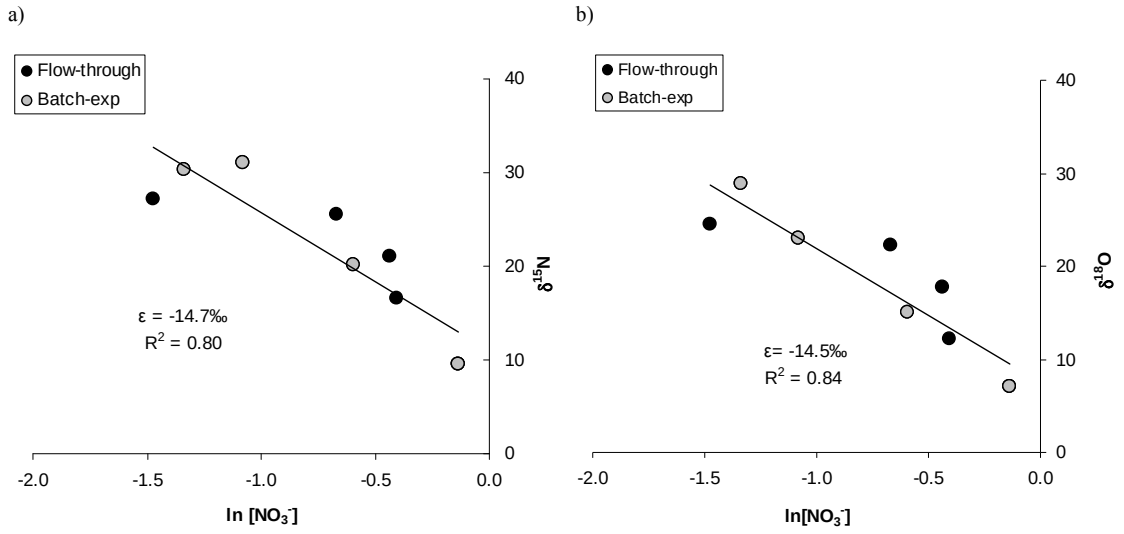

Figure 7. (a) Plot of $\delta^{15}N$ vs. $\ln[NO_3^-]$ values. The slopes correspond to the isotopic fractionation value of ^{15}N. (b) Plot of $\delta^{18}O$ vs. $\ln[NO_3^-]$ values. The slope corresponds to the isotopic fractionation of ^{18}O.

To the authors' knowledge, no isotopic fractionation values linked to denitrification produced exclusively by bottom sediments in hypersaline lakes have been reported. Brandes and Devol (1997, 2002) observed that sedimentary denitrification in the highly reactive sediments of Puget Sound did not produce apparent εN in the bottom water because denitrification was controlled by the diffusion of NO_3^- into reactive microsites, leading to the complete consumption of NO_3^- in the sediment. Because there was no significant fractionation during diffusion and NO_3^- was completely removed, no εN was observed. Some fractionation values have been reported for benthic denitrification. Lehmann et al. (2003) obtained variable εN and εO values from Lake Lugano (-11.2‰ and -20.7‰ for εN; -6.6‰ and 11.0‰ for εO) calculated using Rayleigh and diffusion models, respectively, in bottom waters. The isotopic fractionations obtained in the present study were in the range of the εN values obtained from both models, whereas the εO was higher in absolute value. Wunderlich et al. (2013) obtained fractionations in batch experiments with bottom sediments from freshwater lake Fohnsee of -19.5‰ for εN and -16.5‰ for εO, similar to the values obtained in the present study. In addition, the values obtained were in the range of the isotopic fractionation values previously reported in field and lab studies, which ranged from -4‰ to -30‰ for εN and from -2‰ to -18‰ for εO (Vogel et al,. 1981; Pauwels et al, 2000; Mengis et al., 1999; Otero et al., 2009). The εN/εO ratio for the lake bottom sediment was 1.01 ± 0.05, falling within the ratios from laboratory experiments using Cretaceous C_{org}-bearing strata (εN/εO ratios ranged from 0.96 to 1.14) (Carrey et al., 2013) and other lab-scale ratios reported by Torrentó et al. (2010, 2011) (in which εN/εO ratios ranged from = 1.13 to 1.30 in batch experiments with pure culture). In addition, this ratio was close

to the lower values of in situ field studies (in which εN/εO ratios ranged from 0.9 to 2.3; see Otero et al. 2009 and references therein). The low εN/εO observed is explained by the difference in εO linked to the variation observed in the $\delta^{18}O\text{-}NO_3^-$ between the experiment and field studies due to the exchange between $^{18}O\text{-}H_2O$ and $^{18}O\text{-}NO_2^-$ and the re-oxidation of NO_2^- to NO_3^-, resulting in low $\delta^{18}O\text{-}NO_3^-$ in the field data and therefore lower εO values than observed in the lab (Wunderlich et al., 2013).

5. Conclusions

FTR and batch experiments were designed to evaluate and quantify the different reactions affecting N compounds in lake bottom sediment from the Pétrola basin. The results showed that the lake bottom sediment has the potential to remove NO_3^- from the water through denitrification. The intrinsic NO_3^- attenuation potential of the lake bottom sediment was able to remove 95% of the NO_3^- input over 295 days under different flow conditions. DNRA reactions were observed at the beginning of the FTR experiment, favored by the high C/N ratio and the high salinity observed in the early days of the experiment. After 10 days, as the C/N ratio and salinity decreased, denitrification became the main NO_3^- attenuation reaction in the system. Substantial NO_2^- accumulation was observed at the beginning and at the end of the FTR experiment. The former occurred because of the enzymatic repression favored by the high salt content, whereas the latter accumulation was likely related to the exhaustion of the C_{org} supply. Sulfate reduction could be neither confirmed nor rejected during the FTR experiment because sediment leaching masked the chemical and isotopic signatures of this process. However, the Eh values measured were below the typical values for sulfate reduction, suggesting the possible development of this process at the field scale. The modeled average NRR was 1.25 mmol d^{-1} L^{-1}, with a maximum of 1.91 mmol d^{-1} L^{-1}, one order of magnitude higher than the NRR calculated for the C_{org} of the Cretaceous age. The calculated amount of reactive C_{org} consumed by denitrification during the experiment was approximately 28.8 mmol of C, representing approximately 10% of the total C in the sediment. The isotopic fractionation values obtained were -14.7‰ for εN and -14.5‰ for εO, similar to those calculated in the experiment using Cretaceous material. This finding indicates that the variations in the isotopic fractionation during denitrification cannot be explained only by variations in the reaction rate and that other factors, such as the bacterial community, also play a role. Overall, the important mobilization and transport of organic C observed in the FTR can influence the migration of this electron donor by density flow, promoting NO_3^- attenuation in the underlying contaminated aquifer. Because of the high biological production in the

eutrophic lake water, a key question for the sustainability of Pétrola N cycling is the actual rate of C_{org} accumulation in the lake bottom.

Acknowledgements

This work was financed by a grant (PEIC11-0135-8842) from the Castilla La Mancha Government, the CICYT-CGL2011-29975-C04-01 and CICYT-CGL2011-29975-C04-02 projects from the Spanish Government, the 2009SGR 103 project from the Catalan Government and MARSOL FP7-ENV-2013-WATER-INNO-DEMO from European Union. The authors would like to thank the "Centres Científics i Tecnològics" of the "Universitat de Barcelona" for the chemical and isotopic analyses.

References

Abell, J., Laverman, A.M., Van Cappellen, P., 2009. Bioavailability of organic matter in a freshwater estuarine sediment: long-term degradation experiments with and without nitrate supply. Biogeochem. 94 (1), 13–28.

Akunna, J.C., Bizeau, C., Moletta, R., 1993. Nitrate and Nitrite Reductions with Anaerobic Sludge Using Various Carbon Sources: Glucose, Acetic Acid, Lactic Acid and Methanol. Water Res. 27, 1303–1312.

An, S., Stone, H., Nemati, M., 2011. Biological removal of nitrat by an oil reservoir culture capable of atutrophic and heterotrophic activities: Kinetic evaluation and modeling of heterotrophic process. J. Hazard. Mater. 190 (1-3), 686–693.

Andre, L., Pauwels, H., Dictor, M.C., Parmentier, M., Azaroual, M., 2011. Experiments and numerical modelling of microbially-catalysed denitrification reactions. Chem. Geol. 287, 171–181.

Aravena, R., Robertson, W.D., 1998. Use of multiple isotope tracers to evaluate denitrification in ground water: Study of nitrate from a large-flux septic system plume. Ground Water 36, 975–982.

Bekins, B.A., Warren, E., Godsy, E.M., 1998. A comparison of zero-order, first-order, and monod biotransfromation models. Ground Water 36, 261–268.

Böttcher, J., Strebel, O.L., Voerkelus, S., Schmidt, H.L., 1990. Using isotope fractionation of nitrate–nitrogen and nitrate–oxygen for evaluation of microbial denitrification in sandy aquifer. J. Hydrol. 144, 413–424.

Brandes, J.A. & Devol, A.H. 1997. Isotopic fractionation of oxygen and nitrogen in coastal marine sediments. Geochim. Cosmochim. Acta, 61, 1793–1801.

Brandes J. A., and Devol A. H., 2002. A global marine fixed nitrogen isotopic budget: implications for Holocene nitrogen cycling. Global Biogeochem. Cycles 16, 1120.

Brinson, M. M., Hauer, F.R., Lee, L. C., Nutter, W. L., Rheinhardt, R. D., Smith, R. D., Whigham, D., 1995. A guidebook for application of hydrogeomorphic assessments to riverine wetlands. US Army Engineer. Waterw. Exp. Stn. Vicksburg, MS, USA.

Bulger, P.R., Kehew, A.E., Nelson, R.A., 1989. Dissimilatory nitrate reduction in a waste-water contaminated aquifer. Ground Water 27, 664–671.

Burgin, A.J., Hamilton, S.K., 2007. Have we overemphasized the role of denitrification in aquatic ecosystems? A review of nitrate removal pathways. Front. Ecol. Environ. 5, 89–96.

Carrey, R., Otero, N., Soler, A., Gómez-Alday, J.J., Ayora, C., 2013. The role of lower Cretaceous sediments in groundwater nitrate attenuation in central Spain: Column experiments. Appl. Geochem. 32, 142–152.

Casciotti, K.L., Sigman, D.M., Hastings, M.G., Böhlke, J.K., Hilkert, A., 2002. Measurement of the oxygen isotopic composition of nitrate in seawater and freshwater using the denitrifier method. Anal. Chem. 74, 4905–4912.

Clark, I.D., Fritz, P., 1997. Environmental isotopes in hydrogeology. Lewis Publishers, New York.

Clark, I., Timlin, R., Bourbonnais, A., Jones, K., Lafleur, D., Wickens, K., 2008. Origin and fate of industrial ammonium in anoxic ground water — ^{15}N evidence for anaerobic oxidation (Anammox). Ground Water Monit. Remediat. 28 (3), 73–82.

Connell, W.E., Patrick Jr., W.H., 1968. Sulfate reduction in soil: Effects of redox potential and pH. Sci. 159 (3810), 86–87.

Comly, H.H., 1945. Cyanosis in infants caused by nitrates in well water. J. Am. Med. Assoc. 129, 112–116.

De Beer, D., Schramm, A., Santegoeds, C., Küh, M., 1997. A nitrite microsensor for profiling environmental biofilms. Appl. Environ. Microbiol. 63, 973–977.

Dendooven, L., Alcántara-Hernández, R.J., Valenzuela-Encinas, C., Luna-Guido, M., Perez-Guevara, F., Marsch, R., 2010. Dynamics of carbon and nitrogen in an extreme alkaline saline soil: A review. Soil Biol. Biochem. 42, 865–877.

Dinçer, A., Kargi, F., 2000. Kinetics of sequential nitrification and denitrification processes. Enzyme Microb. Technol. 27, 37–42.

Dogramaci, S.S., Herczeg, A.L., Schiff, S.L., Bone, Y., 2001. Controls on $\delta^{34}S$ and $\delta^{18}O$ of dissolved sulfate in aquifers of the Murray Basin, Australia and their use as indicators of flow processes. Appl. Geochem. 16, 475–488.

Fu, Z., Yang, F., An, Y., Xue, Y., 2009. Bioresource technology characteristics of nitrite and nitrate in situ denitrification in landfill bioreactors. Bioresour. Technol. 100, 3015–3021.

Greskowiak, J., Prommer, H., Vanderzalm, J., Pavelic, P., Dillon, P., 2005. Modeling of carbon cycling and biogeochemical changes during injection and recovery of reclaimed water at Bolivar, South Australia. Water Resour. Res. 41(10): W10418.

Glass, C., Silverstein, J.A., 1998. Denitrification kinetics of high nitrate concentration water: pH effect on inhibition and nitrite accumulation. Water Res. 32, 831–839.

Gómez Alday, J.J., Carrey, R., Otero, N., Soler, A., Ayora C., Sanz, D., Castaño, S., Recio, C., Carnicero, A., 2011. Denitrification assessmeent in a high vulnerable area to nitrate pollution (Pétrola lake endorheic basin, SE Albacete, Spain. In: 9th Internat. Symp. Applied Isotope Geochemistry, p. 72 (Abstract).

Hammer, U., 1986. Saline lakes: their distribution and characteristics. Can. Plains Proc. 59, 1–22.

Harrison, J. A., Maranger, R.J., Alexander, R.B., Giblin, A.E., Jacinthe, P.-A., Mayorga, E., Seitzinger, S.P., Sobota, D.J., Wollheim, W.M., 2009. The regional and global significance of nitrogen removal in lakes and reservoirs. Biogeochem. 93, 143–157.

Hunter, K., Wang, Y., Van Cappellen, P., 1998. Kinetic modeling of microbially-driven redox chemistry of subsurface environments: coupling transport, microbial metabolism and geochemistry. J. Hydrol. 209, 53–80.

Janning, K.F., Le Tallez, X., Harremoës, P., 1998. Hydrolysis of organic wastewater particles in laboratory scale and pilot scale biofilm reactors under anoxic and aerobic conditions. Water Sci. and Technol. 38 (8-9), 179-188.

Jetten, M.S.M., Strous, M., 2007. Anammox, in: Bothe, H., Ferguson, S.J., Newton, W.E. (Eds.), Biol. Nitrogen Cycle, 245–262.

Jiazhong, Q., Jihong, L., Yong, L., 2009. Isolating and denitrification activity of the dominant bacterium in Chaohu wetland. in: Bioinformatics and Biomedical Engineering, 3rd International Conference on. IEEE, 1–4.

Joshi, K., Binnal, P., Srinikethan, G., 2007. Denitrification: Mass transfer and kinetic studies. In: Proceedings of the World Congress on Engineering and Computer Sicence (Lecture Notes) 188–193.

Kendall, C., Elliott, E.M., Wankel, S.D., 2007. Tracing antropogenic inputs of nitrogen to ecosystems, in: Michener, R.H., Lajtha, K. (Eds.), Stable Isotopes in Ecology and Environmental Science. Blackwell Publishing, 375–450.

Killingstad, M.W., Widdowson, M.A., Smith, R.L., 2002. Modeling enhanced in situ denitrification in groundwater. J. Environ. Eng. 128 (6), 491–504.

Kinzelbach, W., Schäfer, W., Herzer, J., 1991. Numerical modeling of natural and enhanced denitrification processes in aquifers. Water Resour. Res. 27 (6), 1123–1135.

Knowles, R., 1982. Denitrification. Microbiol. Rev. 46, 43–70.

Koenig, a, Liu, L.H., 2001. Kinetic model of autotrophic denitrification in sulphur packed-bed reactors. Water Res. 35, 1969–1978.

Korom, S.F., Schuh, W.M., Tesfay, T., Spencer, E.J., 2012. Aquifer denitrification and in situ mesocosms: Modeling electron donor contributions and measuring rates. J. Hydrol. 432–433, 112–126.

Kraft, B., Strous, M., Tegetmeyer, H.E., 2011. Microbial nitrate respiration--genes, enzymes and environmental distribution. J. Biotechnol. 155, 104–117.

Laverman, A.M., Canavan, R.W., Slomp, C.P., Van Cappellen, P., 2007. Potential nitrate removal in a coastal freshwater sediment (Haringvliet Lake, The Netherlands) and response to salinization. Water Res. 41, 3061–3068.

Laverman, A.M., Pallud, C., Abell, J., Van Cappellen, P., 2012. Comparative survey of potential nitrate and sulfate reduction rates in aquatic sediments. Geochim. Cosmochim. Acta 77, 474–488.

Lee, M.S., Lee, K.-K., Hyun, Y., Clement, T.P., Hamilton, D., 2006. Nitrogen transformation and transport modeling in groundwater aquifers. Ecol. Model. 192 (1–2), 143–159.

Lehmann, M.F., Reichert, P., Bernasconi, S.M., Barbieri, A., McKenzie, J. A., 2003. Modelling nitrogen and oxygen isotope fractionation during denitrification in a lacustrine redox-transition zone. Geochim. Cosmochim. Acta 67, 2529–2542.

Lehmann, M.F., Sigman, D.M., Berelson, W.M., 2004. Coupling the $^{15}N/^{14}N$ and $^{18}O/^{16}O$ of nitrate as a constraint on benthic nitrogen cycling. Mar. Chem. 88, 1–20.

Magee, P.N., Barnes, J.M., 1956. The production of malignant primary hepatic tumours in the rat by feeding dimethylnitrosamine. Br. J. Cancer 10, 114–122.

Mariotti, A., Landreau, A., Simon, B., 1988. ^{15}N isotope biogeochemistry and natural denitrification process in groundwater: Application to the chalk aquifer of northern France. Geochim. Cosmochim. Acta 52, 1869–1878.

Mathioudakis, V.L., Aivasidis, A., 2009. Heterotrophic denitrification kinetics in a pressurized sewer biofilm reactor. Desalination 248, 696–704.

Mengis, M., Gächter, R., Wehrli, B., 1997. Nitrogen elimination in two deep eutrophic lakes. Limnol. Oceanogr. 42 (7), 1530–1543.

Middelburg, J.J., 1989. A simple rate model for organic matter decomposition in marine sediments. Geochim. Cosmochim. Acta, 53 (7), 1577-1581.

Monod, J., 1949. The growth of bacterial cultures, Annu. Rev. Microbiol. 3, 371–394.

Nijburg, W.J., Gerards, S., Laanbroek, H.J., 1998. Competition for nitrate and glucose between Pseudomonas florescens and Bacillus licheniformis under continuous or fluctauating anoxic conditions. Mirobiol. Ecol. 26, 345–356.

Nielsen, P.H., Bjerg, P.L., Nielsen, P., Simth, P., Christensen, T.H., 1996. *In situ* and laboratory determined first-order degradation rate constants of specific organic compounds in an aerobic aquifer. Environ. Sci. Technol. 30, 31–37.

Nizzoli, D., Carraro, E., Nigro, V., Viaroli, P., 2010. Effect of organic enrichment and thermal regime on denitrification and dissimilatory nitrate reduction to ammonium (DNRA) in hypolimnetic sediments of two lowland lakes. Water Res. 44, 2715–2724.

Nolan, B., 2001. Relating nitrogen sources and aquifer susceptibility to nitrate in shallow ground waters of the United States. Ground Water 39, 290–299.

Otero, N., Torrentó, C., Soler, A., Menció,A., Mas-Pla, J., 2009. Monitoring groundwater nitrate attenuation in a regional system coupling hydrogeology with multi-isotopic methods: The case of Plana de Vic (Osona, Spain). Agric. Ecosyst. Environ. 133, 103–113.

Parkhurst, D.L., Appelo, C.A.J., 1999. User's guide to PHREEQC (version 2) - a computer program for speciation, reaction-path, 1D-transport, and inverse geochemical calculations., U.S. GEOLOGICAL SURVEY.

Pauwels, H., Foucher, J.C., Kloppmann, W., 2000. Denitrification and mixing in a schist aquifer: influence on water chemistry and isotopes. Chem. Geol. 168, 307–324.

Piña-Ochoa, E., Álvarez-Cobelas, M., 2006. Denitrification in aquatic environments: A cross-system analysis. Biogeochem. 81, 111–130.

Puckett, L.J., Tesoriero, A.J., Dubrovsky, N.M., 2011. Nitrogen contamination of surficial aquifers-a growing legacy. Environ. Sci. Technol. 45, 839–844.

Rittmann, B.E., McCarty, P.L., 2001. Environmental Biotechnology: Principles and Applications. McGraw-Hill Companies, Inc., New York (USA). pp. 754.

Rivett, M.O., Buss, S.R., Morgan, P., Smith, J.W.N., Bemment, C.D., 2008. Nitrate attenuation in groundwater: a review of biogeochemical controlling processes. Water Res. 42, 4215–32.

Rodríguez-Escales, P., Van Breukelen, B.M., Vidal-Gavilan, G., Soler, A., Folch, A., 2014. Integrated modeling of biogeochemical reactions and associated isotope fractionations at batch scale: A tool to monitor enhanced biodenitrification applications. Chem. Geol. 365, 20–29.

Roychoudhury, A., Viollier, E., 1998. A plug flow-through reactor for studying biogeochemical reactions in undisturbed aquatic sediments. Appl. Geochem. 13, 269–280.

Rysgaard, S., Thastum, P., Dalsgaard, T., Christensen, P.B., Sloth N.P., 1999: Effects of salinity on NH_4^+ adsorption capacity, nitrification, and denitrification in Danish estuarine sediments. Estuaries, 22, 21–31.

Schmidt, C.S., Richardson, D.J., Baggs, E.M., 2011. Constraining the conditions conducive to dissimilatory nitrate reduction to ammonium in temperate arable soils. Soil Biol. Biochem. 43, 1607–1611.

Schubert, C.J., Durisch-kaiser, E., Wehrli, B., Thamdrup, B., Lam, P., Kuypers, M.M., 2006. Brief report Anaerobic ammonium oxidation in a tropical freshwater system (Lake Tanganyika). Environ. Microbiol. 8, 1857–1863.

Seitzinger, S.P., Harrison, J. A., Böhlke, J.K., Bouwman, A. F., Lowrance, R., Peterson, B., Tobias, C., Van Drecht, G., 2006. Denitrification across landscapes and waterscapes: a synthesis. Ecol. Appl. 16, 2064–90.

Seitzinger, S.P., Gardner, W.S., Spratt, A.K., 1991. The effect of salinity on ammonium sorption in aquatic sediments. Implications for benthic nutrient recycling. Estuaries 14 (2), 167–174.

Seitzinger, S.P., 1988. Denitrification in freshwater and coastal marine ecosystems: Ecological and geochemical significance. Limno. Ocean. 33, 702–724.

Sigman, D.M., Casciotti, K.L., Andreani, M., Barford, C., Galanter, M., Böhlke, J.K., 2001. A bacterial method for the nitrogen isotopic analysis of nitrate in seawater and freshwater. Anal. Chem. 73, 4145–4153.

Smith, R.L., Howes, B.L., Duff, J.H., 1991. Denitrification in nitrate-contaminated groundwater: Occurrence in steep vertical geochemical gradients. Geochim. Cosmochim. Acta 55, 1815–1825.

Steefel, C.I., DePaolo, D.J., Lichtner, P.C., 2005. Reactive transport modeling: An essential tool and a new research approach for the Earth sciences. Earth Planet. Sci. Lett., 240 (3–4), 539-558.

Stumm, W., Morgan, J. J., 1996. Aquatic Chemistry: Chemical equilibria and rates in natural waters. in John Wiley and Sons, New York, 1022.

Tiedje, J.M., 1988. Ecology of denitrification and dissimilatory nitrate reduction to ammonium. Zehnder, A.J.B. (Ed.), Biology of Anaerobic Microorganisms. Wiley, New York, 179–244.

Van Cappellen, P., Wang, Y. 1996. Cycling of Irion and manganeses in surface sediment.pdf. Am. J. Sci. 296, 197–243.

Vasiliadou, I. a., Tziotzios, G., Vayenas, D.V., 2008. A kinetic study of combined aerobic biological phenol and nitrate removal in batch suspended growth cultures. Int. Biodeterior. Biodegrad. 61, 261–271.

Vitoria, L., Soler, A., Canals, A., Otero, N., 2008. Environmental isotopes (N, S, C, O, D) to determine natural attenuation processes in nitrate contaminated waters: Example of Osona (NE Spain). Appl. Geochem. 23, 3597–3611.

Vitousek, P.M., Aber, J.D., Howarth, R.W., Likens, G.E., Pamela, A., Schindler, D.W., Schlesinger, W.H., Tilman, D.G., 1997. Human alteration of the global nitrogen cycle: Sources and consequences. Ecol. Appl. 7, 737–750.

Ward, M.H., deKok, T.M., Levallois, P., Brender, J., Gulis, G., Nolan, B.T., VanDerslice, J., 2005. Workgroup report: Drinking-water nitrate and health-recent findings and research needs. Environ. Health Perspect. 113, 1607–1614.

Wetzel, R.G., 2001. Sediments and microflora, in: WETZEL, R.G. (Ed.), Limnology (Third Edition). Academic Press, San Diego. 631–664.

Woszczyk, M., Bechtel, A., Cieslinski, R., 2011. Interactions between microbial degradation of sedimentary organic matter and lake hydrodynamics in shallow water bodies: insights from Lake Sarbsko (northern Poland). J. Limnol. 70, 293–304.

Wunderich, A., Meckenstock, R.U., Einsiedl, Fl., 2013. A mixture of nitrite-oxidizing and denitrifying microorganisms affect the $\delta^{18}O$ of dissolved nitrate during anaerobic mircobial denitrification depending on the $\delta^{18}O$ of ambient water. Geochim. Cosmochim. Acta 119, 31–45.

Zimmermann, S., Bauer, P., Held, R., Kinzelbach, W., Walther, J.H., 2006. Salt transport on islands in the Okavango Delta: Numerical investigations. Adv. Water Resour. 29, 11–29.

Zumft,W.G., 1997. Cell biology and molecular basis of denitrification. Microbiol. Mol. Biol. Rev. 61 (4), 533–616.

Appendix A-3:

Denitrification processes in a hypersaline lake aquifer system (Pétrola basin, central Spain)

J.J. Gómez-Alday, R. Carrey, N. Valiente, D. Sanz, S. Castaño, N. Otero, A. Soler, C. Recio, A. Carnicero, C. Ayora, Muñoz-Martín, A. Cortijo

2014

(Supporting information of this paper is available in Appendix C-3)

Denitrification processes in a hypersaline lake-aquifer system (Pétrola basin, Central Spain)

Gómez-Alday, J.J.[1], Carrey, R.[2], Valiente, N.[1], Sanz, D.[1], Castaño, S.[1], Otero, N.[2], Soler, A.[2], Recio, C.[3], Carnicero, A.[3], Ayora, C.[4], Muñoz-Martín, A.[5], Cortijo, A.[1]

1 Hydrogeology Group. Institute for Regional Development (IRD). University of Castilla-La Mancha (UCLM) Campus Universitario de Albacete 02071 Albacete, España. JuanJose.Gomez@uclm.es

2 Grup de Mineralogia Aplicada i Medi Ambient, Facultat de Geologia, Universitat de Barcelona, C/ Martí i Franquès s/n, 08028, Barcelona, Spain. e-mail: raulcarrey@ub.edu, notero@ub.edu, albertsoler@ub.edu

3 Stable Isotope Laboratory. University of Salamanca. Plz. De los Caídos, s/n, 37008 Salamanca, Spain. crecio@usal.es

4 Grup d'Hidrologia Subterrània (GHS), Instituto de Diagnóstico Ambiental y Estudios del Agua, IDAEA- CSIC, C/Jordi Girona, 18, 08028 Barcelona, Spain, cayora1@gmail.com

5 Applied Tectonophysics Group, Departamento de Geodinámica, Universidad Complutense de Madrid, 28040, Madrid, Spain. amunoz@geo.ucm.es

Abstract

Agricultural regions placed at semiarid or arid climate zones with associated saline wetlands constitute one of the most vulnerable and exposed environments to nitrate pollution. The Pétrola basin was declared vulnerable to nitrate pollution by the Regional Government in 1998 and the hypersaline lake was classified as a heavily modified water body. This study was conducted in order to assess the fate of groundwater nitrate by means of the use of multi-isotopic tracers ($\delta^{15}N$, $\delta^{34}S$, $\delta^{13}C$, $\delta^{18}O$) coupled to hydrochemistry in the aquifer system connected to the Pétrola eutrophic saline lake. Hydrogeology of the basin showed two main flow components: regional groundwater flow, from the perimeter area/recharge areas (Zone 1) towards the lake (Zone 2) and the density driven flow from surface water from the lake towards the underlying aquifer (Zone 3) as was observed in Electrical Resistivity Tomography (ERT). In Zones 1 and 2, $\delta^{15}N_{NO3}$ and $\delta^{18}O_{NO3}$ is derived from synthetic fertilizers slightly volatilized. In addition, the observed trend in the isotopic composition of nitrate suggests the existence of denitrification processes controlling natural attenuation of the dissolved nitrate in the aquifer system. Nitrate reduction appears to be conducted by heterotrophic denitrification reactions as sulphate distribution and fate in the system can be explained by the dissolution of secondary gypsum from weathering of sulphide minerals. However, some samples the occurrence of autotrophic denitrification can not be ruled out. In zone 3, the saltwater-freshwater interface in the upper part of the aquifer (down to 12 m below ground surface)

constitutes a reactive zone for NO_3^- attenuation. On the other hand, tritium data suggest that the absence on nitrate in the deepest part of the aquifer under the lake can be attributed to regional flow with longer residence time. Consequently, the geometry of the density downflow plays an important role in denitrification processes under the lake.

1. Introduction

The European Groundwater Directive (EC 2006) considers nitrate (NO_3^-) as one of the most important contaminants that could prevent the achievement of the goals of the Water Framework Directive (EC 2000). Excessive use of synthetic and/or organic fertilizers in agriculture and the spill out of wastewaters are the major sources of NO_3^-. High NO_3^- concentration in groundwater is a matter of great concern due to the negative effects on health (Comly, 1945; Magee and Barnes 1956; Ward et al., 2005) and on the eutrophication of surface water bodies (Dassenakis et al. 1998; Mason 2002; Kraft and Stites 2003). The NO_3^- concentration threshold established by the Directive 98/83/CE for human water supplies is 50 mg/L NO_3^-.

At watershed scale, the identification of the pollution sources is helpful in order to design mitigation measures. The quantification of natural NO_3^- attenuation processes provides information about the system capacity for water resources renewal. Denitrification is considered the main process that irreversibly eliminates NO_3^- from groundwater. Denitrification is a redox reaction driven by specialized bacteria that utilize organic carbon disseminated in the sediment (heterotrophic denitrification) or reduced sulphur compounds (autotrophic denitrification) such as Fe^{2+} bearing minerals (i.e. Fe^{2+}-sulphides and Fe^{2+}-silicates), as electron donors for NO_3^- reduction to harmless N_2 (Korom, 1992; Appelo and Postma, 2005). Denitrification reactions can be represented by the following chemical reactions:

$$5CH_2O + 4NO_3^- \rightarrow 2N_2 + 4HCO_3^- + CO_2 + 3H_2O \quad (1)$$

$$5FeS_2 + 14NO_3^- + 4H^+ \rightarrow 7N_2 + 10SO_4^{2-} + 5Fe^{2+} + 2H_2O \quad (2)$$

The isotopic composition of dissolved NO_3^- can provide information about the source of the pollution (Kendall et al., 2007; Böttcher et al., 1990; Vitòria et al., 2004; Widory et al., 2004). In addition, a multi-isotopic approach coupled to hydrochemistry is a useful method for understanding denitrification

reactions in aquifers and surficial water systems (Aravena and Robertson, 1998; Mariotti et al., 1988; Pauwels et al., 2000; Vitòria et al., 2008; Wassenaar et al., 1995; among others). Stable isotopes are usually measured as the ratio between the less abundant isotope and the most abundant one (e.g. ^{15}N against ^{14}N). Stable isotope ratios are reported with respect to international standards using the delta notation (Eq. 3).

$$\delta^{15}N = [(R_{sample} - R_{std}) / R_{std}] \times 1000 \quad (3)$$

where $R = {}^{15}N/{}^{14}N$

During denitrification reaction, the isotopic composition of both, ^{15}N and ^{18}O in the residual NO_3^- fraction increase as denitrification proceeds (Mariotti et al., 1981). Denitrification can be considered as a single-step Rayleigh process and isotopic fractionation (ε) can be calculated employing the Eqs. 4 and 5 (Mariotti, 1986).

$$\delta^{15}N_{residual} = \delta^{15}N_{initial} + \varepsilon \ln f \quad (4)$$

$$\delta^{18}O_{residual} = \delta^{18}O_{initial} + \varepsilon \ln f \quad (5)$$

where f is the residual NO_3^- concentration divided by the initial NO_3^- and ε is the isotopic fractionation. Likewise, the isotopic composition of the reaction by-products (HCO_3^- and SO_4^{2-}) may be used to identify the metabolic processes involved in natural attenuation (Aravena and Robertson, 1998; Otero et al., 2009). In the case of heterotrophic denitrification an increase in HCO_3^- coupled with a decrease of $\delta^{13}C$ and NO_3^- concentration should be expected. In the other hand, autotrophic denitrification should produce an increase in SO_4^{2-} concentration and the $\delta^{34}S$ from dissolved sulphate should match with the isotopic composition of SO_4^{2-} from sulphide oxidation whereas the $\delta^{18}O$ would be related with the isotopic composition of $\delta^{18}O_{H2O}$.

Endorheic basins located in semiarid or arid regions are vulnerable areas to pollution due to their low precipitation and high evaporation rates. However, they have shown a high potential to remove nitrogen compounds from agricultural runoff (Brinson et al. 1995). In the Central Spain, the High Segura River Basin is located. This basin includes an important saline endorheic complex named the Pétrola-Corral Rubio-La Higuera Saline Complex, which is about 275 km^2 in extent. In this saline complex, a total of 19 wetlands have been identified (Cirujano et al., 1988). Usually, the final discharge point for

surface waters in these endorheic systems is a saline lake that can act as sink for dissolved nitrogen compounds. However, if the necessary conditions are met, NO_3^- can be reduced by denitrification in surface and/or groundwater (Seitzinger et al., 2006; Schubert et al., 2006; Harrison et al., 2009; Nizzoli et al., 2010). In endorheic systems the role of the lake in NO_3^- attenuation is linked with the interactions between high salinity lake water and fresh-groundwater. The different density between salty surface water from the lake and fresh groundwater can produce a density-driven downflow from the surface lake water towards the underlying aquifer (Zimmermann et al., 2006). The saltwater-freshwater interface is a favorable area to reduce NO_3^- in estuarine zones (Santoro et al., 2009 and references therein). However, to the authors' knowledge, less attention has been focused on nitrogen cycle studies on endorheic systems, especially to determine the relationship between saline lake-groundwater interface and NO_3^- attenuation processes.

A representative example from the Segura River Basin of such an endorheic system with a saline lake is the Pétrola Basin (Fig. 1). Pétrola Basin is located in a vulnerable zone to NO_3^- pollution, where the use of fertilizers is restricted and under the government supervision (Order 2011/7/2 CMA). However, the input of NO_3^- to the lake has been quantified, reaching 3.76 t/year (Cortijo et al., 2011). Furthermore, there is an additional NO_3^- input from the municipal wastewaters which are spilled directly to the lake. These NO_3^- inputs enhance eutrophication processes and produce harmful algal blooms in the Pétrola Lake. Previous laboratory work performed using different sediments present in the basin showed the potential to promote NO_3^- attenuation at field scale (Carrey et al., 2013, 2014). In these studies, the authors demonstrated the denitrification potential of sediments form the Utrillas Facies (a regional Formation rich in organic matter and sulphides such as pyrite) and the bottom lake sediment. In this context, the aim of the present work is to explain the hydrogeologic system of the Pétrola basin, focusing on the relationship between the saline lake and the regional-scale groundwater to confirm the occurrence and magnitude of density-driven downflow. A second aim is to identify the source of NO_3^- in groundwater and to understand the factors controlling NO_3^- distribution in the Pétrola basin. To do that NO_3^- attenuation processes in the basin will be studied by means of chemical and multi-isotopic techniques to confirm the role of the different electrons donors present in the basin. Results will be discussed integrating the laboratory experiments performed previously (Carrey et al., 2013 and 2014). Finally, this study aimed to describe the role of the surface lake water in the transport of the dissolved organic carbon into deep anoxic aquifer zones where denitrification can be produced. The study

represents a step forward in the study of the role of saline systems as natural barrier for nitrate pollution, adding a new value for their future study and conservation.

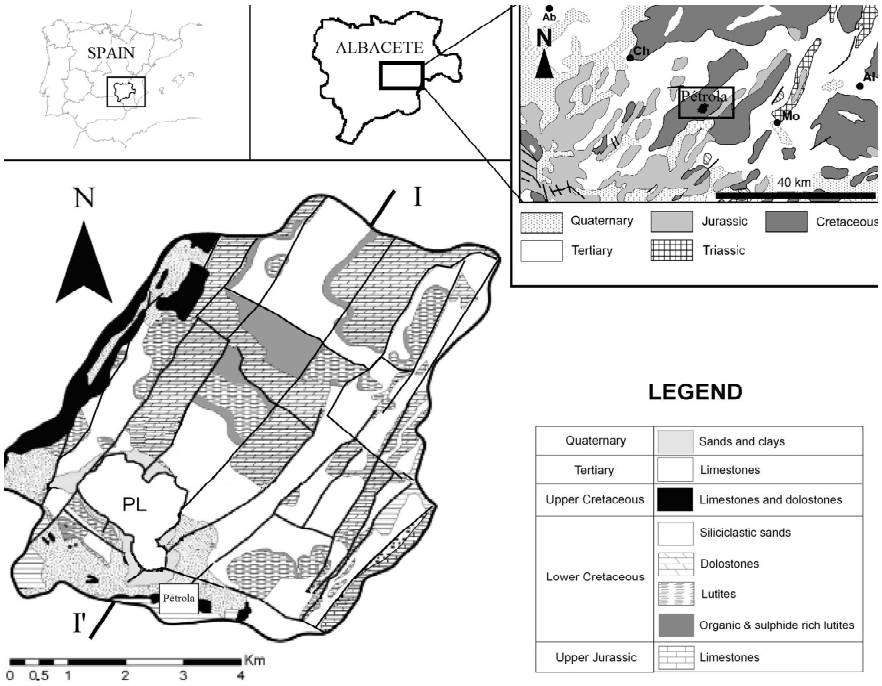

Figure 1. Location, regional geology and Simplified geological map of the Pétrola Lake endorheic basin (modified from Baena-Pérez and Jerez-Mir, 1982). Ab: Albacete, Ch: Chinchilla de Montearagón, Mo : Montealegre del Castillo, AL : Almansa, masl: meters above sea level.

2. The study area

The hydrogeologic boundary of the Pétrola saline lake-aquifer system extends over 43 km^2. The climate of the region is Mediterranean, continental, and semiarid. Mean annual precipitation is usually below 400 mm, and is mainly distributed during the spring and autumn seasons. Mean temperature values oscillate from 4.9 ºC (January) to 24.2 ºC (July). Farming (cultivation, livestock farming and cattle rising) are the main economic activities in the area. Irrigation and dry land occupies about 17 km^2 that represent 40% of the total surface of the basin (Database Corine Land Cover, 2000). The estimated nitrogen load from agricultural activities calculated was about 10 t/Km^2 $year^{-1}$ (year 2000) (ITAP, 2010). Furthermore, urban wastewaters, from a population of 777 inhabitants, are spilled directly to the lake, with no wastewater treatment. Crops are fertilized mainly using inorganic synthetic fertilizers and manure is not widely applied in the area.

Geology of the basin is formed mainly by Mesozoic materials (Fig. 1). The bottom of the sequence is formed by oolitic carbonate Jurassic rocks with porosity related with the fracture network. The base of the Lower Cretaceous unit corresponds to the Weald Facies and consists on lutite sediments, overlayed by sands and sandy-conglomerate sediments with intergranular porosity, which reaches the Barremian time. Aptian carbonates overlay Barremian terrigenous deposits. Albian deposits (Utrillas Facies) consist on siliciclastic sands, sandy-conglomerates and reddish to dark grey clay to lutite sediments deposited overlaying concordantly over Aptian sediments. The Utrillas Facies materials are interstratified by grey-to-black mudstones and sandy sediments with high contents in organic matter and sulphides. These deposits show noticeable lateral changes in thickness throughout the Pétrola Basin with an average thickness of about 7m. As consequence of sulphide oxidation processes, gypsum appears in the Lower Cretaceous lutitic sediments (Gómez-Alday et al., 2004).

During the late Miocene, pronounced compressional events related to the Alpine Orogeny, resulted in a general uplift of the region, accompanied by the development of NE-SW and NW-SE trending fractures which lead to a regional scale horst-and-graben structure. The tectonic framework exerts important controls on the hydrogeologic system in the study area where the Pétrola Lake occupies the lower topographic position in a horst-type tectonic structure.

3. Methods

3.1 Field survey

The sampling locations are shown in Figure 2. A total of 252 samples from 20 control points (springs, surface water including streams and lake, and agricultural wells) were collected in control points located in the Cretaceous aquifer, between April 2008 and December 2010. Additionally, four PVC piezometers (2623, 2624, 2625, 2626) were installed during 2008 nearby the lake border in order to measure vertical profiles of hydrogeochemical parameters at different depths in the aquifer system (Fig. 2). The piezometers were 5 cm in inner diameter, and were installed at different depths: 12.1 m (2626), 25.8 m (2625), 34.1 m (2624) and 37.9 m (2623). Screen lengths were 3 m (2623), 9 m (2624), 5 m

(2625) and 4 m (2626). Screening zones where isolated by means of the use of internal bentonite seals. Core sediments from the Utrillas Facies and bottom lake sediment were obtained during drilling operations. The core was isolated from the atmosphere with polypropylene and immediately frozen in the field with solid CO_2 to preserve it at -30ºC. These sediments were examined under scanning electron microscope using a DSM 940 model. In addition, eight thin sections were examined by standard microscopy methods, using Alizarin Red S and potassium ferricyanide staining (Dickson, 1965). In addition, several samples of gypsum, sulphides and dolomites from Utrillas Facies were collected from the basin and analyzed for sulphur, oxygen and carbon isotopic composition.

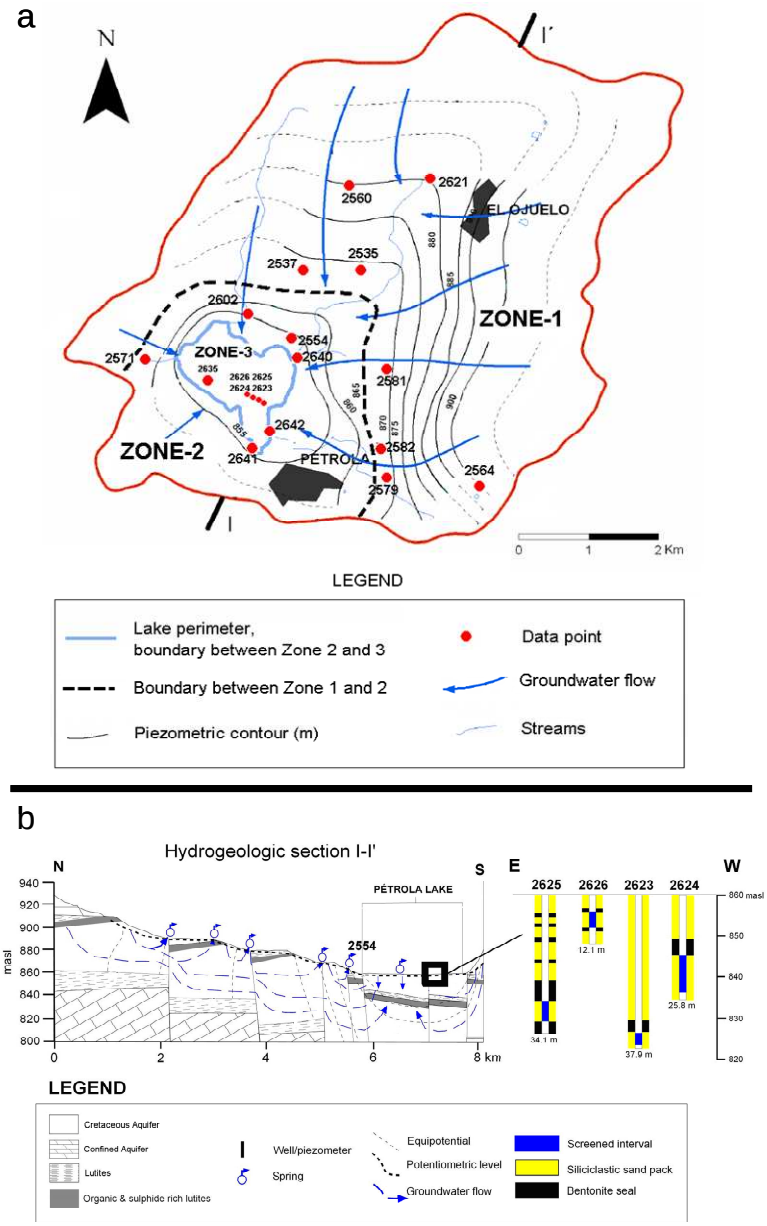

Figure 2. Map showing the distribution of piezometric surface (masl) of Cretaceous aquifer (2003) and sampling locations. C) Hydrostratigraphic cross-section with location and construction logs for the piezometers 2623, 2624, 2625 and 2626, installed in the lake.

3.2 Chemical analyses

Groundwater temperature (T), pH, redox potential (Eh), electrical conductivity (EC), and dissolved oxygen (DO) parameters were measured in situ with portable electrodes. In the springs, streams measurements were performed directly in the water flow whereas measurements in the four piezometers were made using a flow through-chamber to minimize the effect of air exchange. Agricultural wells were purged prior to sampling about a minimum of three well volumes and/or until EC was stabilized. Water samples were stored at 4 ºC in darkness previous to further analysis and following the official standard methods (APHA-AWWA-WEF, 1998). Water samples were filtered with a 0.45 µm nylon Millipore® filter. Alkalinity titrations were carried out in the laboratory by acid-base titration. NO_3^-, SO_4^{2-}, and Cl^- contents were measured by ion chromatography (DX120, Vertex). For avoiding chloride interferences in samples with high EC, the cadmium reduction method was employed for determining NO_3^- contents using a spectrophotometer (Perkin-Elmer, Lambda 650). Determination of NH_4^+ contents was carried out by distillation and volumetric methods (Koroleff method). Ca^{2+} and Mg^{2+} concentrations were measured by complexometry. TOC in solid samples (n=4) from drills core (2623) were performed in selected black to grey lutitic sediments at different depths using a Shimadzu Analyzer (A Coruña University). Dissolved organic carbon (DOC) concentration was determined using a Shimadzu Analyzer in the research services of the A Coruña University.

3.3 Isotopic analyses

Isotopic analyses were performed following standard methodology in a subset of samples according to their location and their hydrogeological context. The stable isotopic ratios $^{34}S/^{32}S$ and $^{18}O/^{16}O$ from dissolved SO_4^{2-} were measured on $BaSO_4$ precipitated from dissolved sulphate by the addition of 5% $BaCl_2$ after acidifying the sample with HCl and boiling it to prevent $BaCO_3$ precipitation, following standard methods (Dogramaci et al., 2001). The $^{34}S/^{32}S$ was also determined on Ag_2S evolved by reacting sulphides as described by Canfield et al. (1986) and Hall et al. (1988). The $\delta^{34}S$ from water samples was analyzed in a Carlo Erba Elemental Analyzer (EA) coupled in continuous flow to a Finnigan Delta C IRMS whereas the $\delta^{34}S$ from gypsums and sulphide were analyzed in a SIRA-II dual inlet spectrometer. The $\delta^{18}O$ from dissolved SO_4^{2-}, and gypsum was analyzed in duplicate with a ThermoQuest high-temperature conversion analyzer (TC/EA) unit with a Finnigan Matt Delta C IRMS. $^{18}O/^{16}O$ ratios from H_2O were measured by the CO_2 equilibration method using a Multiflow device coupled on line to a

continuous flow Isoprime Mass Spectrometer. $^{13}C/^{12}C$ ratios in DIC were determined on CO_2 evolved from the water by acidification with 103% H_3PO_4 employing the Multiflow device. Additionally, HCO_3^- of a few samples was precipitated as $SrCO_3$ by addition of 45% $SrCl_2$ to previously basified waters (to pH>10, using Na(OH)). These samples were reacted with 103% H_3PO_4 in a purpose-built vacuum extraction line, and the CO_2 evolved measured on a dual inlet SIRA-II mass spectrometer. These stable isotope analyses were performed at the Laboratorio de Isotopos Estables of Salamanca University (Spain). The isotopic composition of dissolved nitrate was analyzed by the bacterial denitrifier method described in Sigman et al. (2001) and Casciotti et al. (2002) at the Isotope Bioscience Laboratory (ISOFYS) of Ghent University (Belgium). Results are reported in δ values relative to international standards (Air for $\delta^{15}N$, Vienna Canyon del Diablo Triolite (VCDT) for $\delta^{34}S$, Vienna Pee Dee Belemnite (VPDB) for $\delta^{13}C$, and Vienna Standard Mean Ocean Water (VSMOW) for $\delta^{18}O$ and δD). Analytical reproducibility by repeated analysis of both international and internal reference samples of known isotopic composition was determined to be about ±1‰ for $\delta^{15}N$, ±0.2‰ for $\delta^{34}S$, ±2‰ for $\delta^{18}O$ of NO_3^-, ±0.5‰ for $\delta^{18}O$ of SO_4^{2-}, ±0.2‰ for $\delta^{13}C$, and ±0.3‰ and for $\delta^{18}O$ in waters. Radioactive isotope of H^3 (Tritium) in groundwater were determined by Liquid Scintillation Counting in the ^{14}C and Tritium Dating Service of the Universidad Autónoma de Barcelona with an analytical reproducibility of ±0.4 TU.

3.4 Electrical Resistivity Tomography (ERT)

The ERT survey was carried out in September 2008 using a RESECS DMT resistivity-meter, equipped with 72 electrodes. The selected electrode configuration was a Wenner array, because it has the highest signal-to-noise ratio and is more sensitive to the vertical variations of resistivity (Loke and Dahlin, 2002). Electrode spacing was 5 m, and 23 levels of investigation were used to reach 60 m depth in the central part of each section. Two cycles of injection were applied in each measurement, taking 700 potential differences and intensity values, and calculating root mean square (RMS) error for each apparent resistivity value. Three sections, lined up on the ground surface, were measured at Pétrola lake along dykes placed close to the east bank of the lake, coinciding with the industrial facilities (Fig. 3). ERT profile A, of about 355 m in length, was parallel to the location of the four piezometers installed in the lake eastern edge. ERT profiles B and C were allocated perpendicular to ERT profile A, and were about 310 m and 355 m in length, respectively. No noticeable differences in topography exist and, therefore, it was not necessary to normalize profile elevations to the ground surface. Individual measurement points were revised taking into account standard deviation, RMS and pooled standard deviation (SP). All values

with a standard deviation higher than 20% were removed. Field data inversion was performed with Res2Dinv software using the same the parameters in the inversion for all the profiles (De Groot-Hedlin and Constable 1990; Loke and Barker, 1996). A least-squares inversion algorithm was chosen for inversion, and the final calculated RMS errors for the three sections are between 12% and 17%. Finally, inversion results were exported to absolute XYZ coordinates, in order to compare with the rest of hydrogeological and geochemical data.

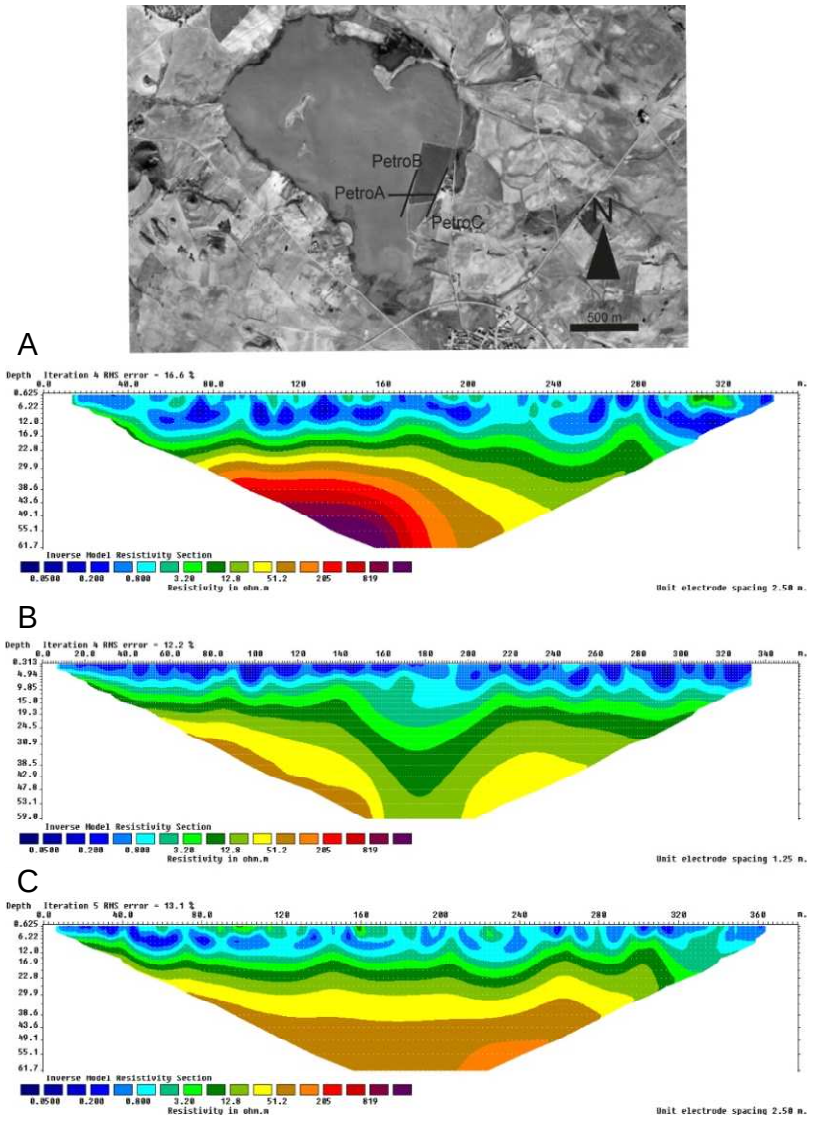

Figure 3. Inverted resistivity sections for two-dimensional ERT profiles: Location of the profiles in the edge of the Pétrola lake. A) Profile Pétrola A; B) Profile Pétrola B; C) Profile Pétrola C. Data were gathered with a 5 m spacing among electrodes. High resistivity (Red color) represents low EC values whereas low resistivity (Blue color) shows areas with high EC.

4. Hydrogeology of the Pétrola basin

Hydrogeologically, the system is formed by two unconnected aquifers (Gómez-Alday et al. 2004). A confined aquifer formed by highly permeable oolitic Jurassic carbonates is overlaid by a confining layer of lutitic Weald Facies. The upper aquifer is composed of siliciclastic sands, conglomerates and lutites (Utrillas Facies, Albian). Piezometric levels measured in the Cretaceous aquifer data points showed that groundwater flow in the unconfined aquifer converges to the Pétrola Lake (Fig. 2). Nearby the lake, the piezometric level of Cretaceous aquifer is close to the topographic surface and as consequence several springs and streams drain the aquifer in this area. Therefore, the lake can be considered as a terminal discharge zone for overland flow as small streams form a radial pattern (Fig. 2).

The relationship between the aquifer and the Pétrola lake has shown to be more complex. The ERT survey allowed visualizing the distribution of resistivity in sediments and rocks that is related to several parameters which include water content, EC, mineral content, porosity and temperature. Figure 3 shows the resistivity profiles performed on the lake. ERT was performed when Pétrola Lake was almost dry. Therefore, the first 2 m observed in profiles correspond to the height of the dykes where the ERT survey was performed showing unsaturated conditions. Below 2 m the system was saturated in water. The sedimentary sequence can be considered homogeneous in the three profiles performed. Changes in rock porosity can be negligible although the existence of preferential flow zones has been observed in the bottom of the lake. Thus, resistivity variations should mainly be related to changes in electrical conductivity of water. Resistivity values varied from lower than 0.2 Ohm·m, in the lake surface, to 20 Ohm·m at depths of about 50 m (Fig. 3). The observed differences in resistivity values are explained by the fact that superficial brines were underlying by fresh groundwater producing a hydro-dynamically unstable situation with dense brine perched on less dense fresh water. Thus, the resistivity gradient observed can be interpreted as the existence of a density-driven flow produced by the instability of the saline boundary layer (Zimmermann et al., 2006). The location of the piezometers 2626, 2625 2624 and 2623 coincided with this zone of density-driven groundwater flow.

The study area has been divided into three different zones (Fig. 2). Zone 1 corresponds with the recharge area of the upper aquifer in the North and East. Sample points in Zone 2 are located nearby the lake, discharge zone, following the groundwater flow direction from Zone 1. Therefore, Zones 1 and 2 will be discussed together in order to understand the chemical and isotopic evolution of groundwater in

the Pétrola Basin. In the other hand, Zone 3 represents the area of density-driven downflow from the lake to the underlying aquifer; the data points included are the piezometers 2623, 2624, 2625, 2626 and the surficial water (data point 2635).

5. Results

Complete chemical and isotopic characterization of the samples is available in appendix C.3. Despite that the sample points were not located along a groundwater flow line; the concentric pattern of the ion concentration distribution allowed to infer some conclusions on the hydrogeochemical behavior of the Pétrola lake-aquifer system.

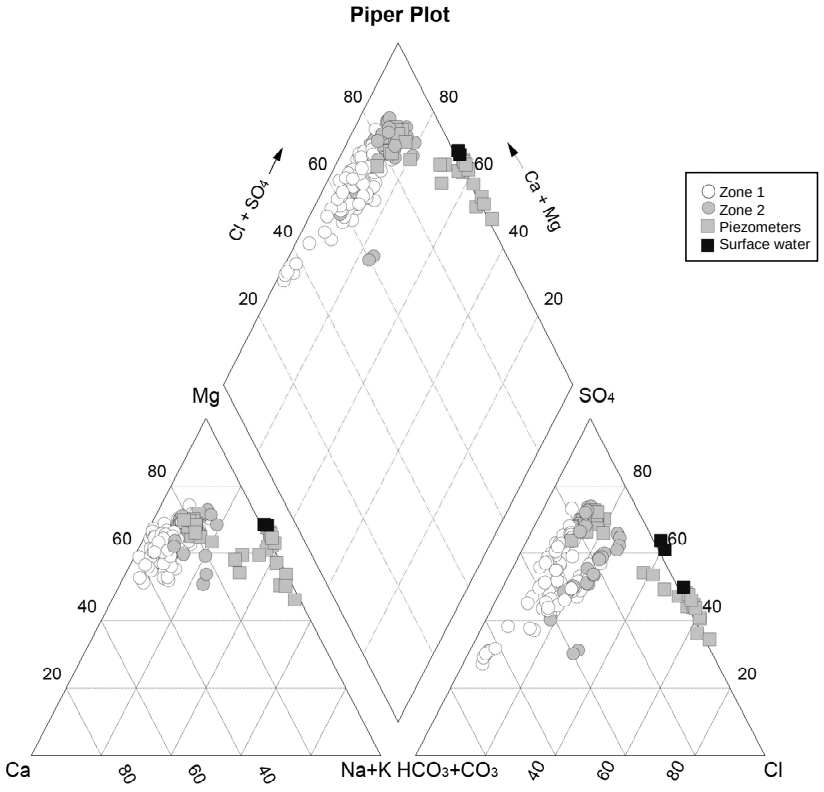

Figure 4. Piper diagram plotted the chemical composition of the surface and ground water sample points (Fig. 2) during 2008-2010.

5.1 Hydrochemistry of Zones 1 and 2

Zone 1 groundwater type varied between Mg-Ca-HCO_3 and Mg-Ca-SO_4 hydrofacies (8 control points; April 2008-December 2010; n=82). pH ranged from 7.3 to 8.4 and Eh values varied from +142 to +452 mV. In Zone 1 the electrical conductivity (EC) showed values, ranging from 507µS/cm to 2180 µS/cm and dissolved O_2 varied from 0.4 mg/L to 5.0 mg/L. The NO_3^- concentration ranged from below the detection limit (<0.1 mg/L) to 149 mg/L. The NH_4^+ contents oscillated between below the detection limit (<0.1 mg/L) and 0.2 mg/L. The SO_4^{2-} concentration varied from 33 mg/L to 803 mg/L whereas Cl^- changed in a range between 9 mg/L and 164 mg/L. The HCO_3^- contents showed a minimum value of 83 mg/L and a maximum value of 344 mg/L. DOC concentration ranged from below detection limit (0.2 mg/) to 4.9 mg/L.

Zone 2 hydrofacies were similar than in Zone 1, between Mg-Ca-SO_4-HCO_3 and Mg-Ca-SO_4 (5 control points; April 2008-December 2010; n=37) (Fig 4). Water samples had higher EC values than the measured in Zone 1, varying from 1046 µS/cm up to 3380 µS/cm. Dissolved O_2 showed values between 1.2 mg/L and 7.9 mg/L. Overall, the NO_3^- concentration in Zone 2 was slightly lower than in Zone 1, ranging from 5.6 mg/L to 96.0 mg/L. The NH_4^+ concentration ranged from below detection limit up to 2.1 mg/L. SO_4^{2-} ranged from 175 mg/L to 2009 mg/L whereas Cl^- oscillated from 34 mg/L up to 522 mg/L. The HCO_3^- values varied from 119 mg/L to 572 mg/L. DOC concentration observed ranged from 3.1 mg/L to 8.5 mg/L.

5.2 Hydrochemistry of Zone 3

Results from Zone 3 are presented in Table C.3.3, C.3.6 in appendix C.3. Chemical data are displayed separately between surface water of the lake and the groundwater results from the piezometers.

Surface waters of the lake were clearly different than in the Zones 1 and 2 (Fig 4). Hydrofacies can be classified as Mg-Na-SO_4-Cl during the study period (February 2010-November 2010; n=4). Surface waters of the lake showed a pH ranging from 7.6 to 9.1 and Eh varied from +63 mV to +292 mV. The EC values ranged from 59,300 (April) to 123,000 µS/cm (November). Dissolved O_2 was below 0.2 mg/L. The NO_3^- concentration was below detection limit (0.1 mg/L) in all the samples analyzed. The NH_4^+ concentration varied from 0.5 mg/L to 1.1 mg/L. SO_4^{2-} contents ranged from 43,200 mg/L to

122,880 mg/L and Cl^- varied between 21,799 mg/L and 102,960 mg/L. HCO_3^- concentration ranged from 327 mg/L to 2,134 mg/L. DOC values varied between 163 mg/L and 646 mg/L.

With regards to groundwater under the lake, the hydrofacies varied between Mg-Ca-SO_4-HCO_3 (2623) (Similar than Zones 1 and 2) to similar hydrofacies than surface lake water Mg-Na-Cl-SO_4 (2626) (September 2008-November 2010; n=30). The pH and Eh values ranged from 7.0 to 8.2 and from ‑100 mV to +318 mV, respectively. EC ranged from 2,410 µS/cm, in the deepest screened piezometer (2623), to 96,000 µS/cm in the shallowest one (2626). Therefore, in terms of groundwater chemistry, piezometers can be considered to be located in the saltwater-freshwater interface. Dissolved O_2 varied from 0.2 mg/L to 1.4 mg/L. The NO_3^- concentration was below detection limit (<0.1 mg/L) in most of the samples except for sample point (2623) where NO_3^- showed values up to 2.6 mg/L. The NH_4^+ contents varied between below detection limit (< 0.1 mg/L) to 1.8 mg/L. SO_4^{2-} changed between 510 mg/L, in the deepest screened piezometer (2623), and 38,808 mg/L, in the shallowest screened one (2626). Cl^- concentrations changed from 82.2 mg/L (2623), in the deepest screened piezometer to 42,071 mg/L (2626). Variations in HCO_3^- concentrations were not so noticeable: values oscillated from 207 mg/L (2623) to 499 mg/L (2626). DOC contents changed from a mean value of 21.3 (n=4; 2626) to 4.1 mg/L (n=4; 2623).

5.3 Stable isotope results

The isotopic analyses were performed on a subset of samples based on NO_3^- concentrations. The $\delta^{18}O_{H2O}$ in the water samples from Zone 1 and 2 varied from ‑5.4‰ to ‑7.6‰ (mean value of ‑6.5‰; n=25) whereas samples from piezometers ranged from ‑2.4‰ to ‑7.4‰ (mean value of ‑5.3‰; n=11). The $\delta^{15}N_{NO3}$ and $\delta^{18}O_{NO3}$ of the samples located in the Zone 1 varied between +6.1‰ and +7.6‰, and from +2.1‰ to +4.7‰ (n=7), respectively. In the Zone 2 the $\delta^{15}N_{NO3}$ varied from +6.6‰ and +19.9‰ whereas the $\delta^{18}O_{NO3}$ ranged from +5.3‰ to +16.2‰. The $\delta^{34}S_{SO4}$ values in the water samples from Zone 1 ranged from ‑17.4‰ to ‑13.2‰ whereas $\delta^{18}O_{SO4}$ varied between +2.3‰ and +4.8‰ (n=4). In Zone 2, $\delta^{34}S_{SO4}$ and $\delta^{18}O_{SO4}$ values varied from ‑22.5‰ to ‑14.3‰ and between +2.9‰ and +12.3‰ (n=6). The $\delta^{13}C_{DIC}$ data showed similar values in Zone 1 and 2 ranging from ‑12.7‰ to ‑8.0‰ (n=13).

Analyses from sulphides minerals, gypsum and dolomite from the basin are available in Table C.3.9, appendix C.3. $\delta^{34}S_{sulphide}$ from Utrillas Facies ranged from ‑40.5‰ to ‑12.2‰ (average value of ‑29.5‰, n=15). The $\delta^{34}S_{gypsum}$ ranged from ‑30.3‰ to +3.0‰ and the $\delta^{18}O_{gypsum}$ ranged from -3.2‰ to

+14.0‰ (n = 8). $\delta^{13}C_{dolomite}$ analysed from Utrillas Facies showed values oscillating from -7.2‰ to +1.9‰ (n = 21).

5.4 Tritium concentrations

Tritium is a short-lived isotope of hydrogen with a half-life of 12.43 years (Unterweger et al., 1980) and it is assumed that groundwater tritium contents reflect atmospheric levels of this isotope when the water was last in contact with the atmosphere (Clark and Fritz, 1997). Tritium content in water samples varied from 0.2 ±0.4 TU to 4.6 ±0.3 TU (n= 8). In the collected water samples the highest tritium concentration was detected in the surface water of the lake (data point 2635) reaching a value of 4.6 ±0.3 TU. The shallowest piezometer installed in the lake edge (2626) showed the highest tritium concentration (1.5 ±0.3 TU). Lower value of tritium were observed in wells 2623 and 2625 (0.8 ±0.4 TU), whereas 2625 showed 0.9 ±0.4TU.

6. Discussion

6.1 Nitrification and denitrification in Zones 1 and 2

Since groundwater level is usually close to the land surface, agrochemicals can rapidly reach the water table. However, the NH_4^+ concentration in Zones 1 and 2 was not significant with a mean value of 0.1 mg/L (n=147) indicating that NH_4^+ from agricultural activities was completely nitrified in the non-saturated zone to NO_3^-. In Zone 1, NO_3^- concentration increased coupled with EC (Fig. 5). Higher NO_3^- values were in agreement with the agricultural activities developed at the center and SW of the basin. Therefore, these agricultural activities affect to the heterogeneous spatial distribution of NO_3^- in the zone. Samples in Zone 2 showed a slightly decrease in NO_3^- concentration whereas EC values trend to increase compared with samples from Zone 1 (Fig. 5).

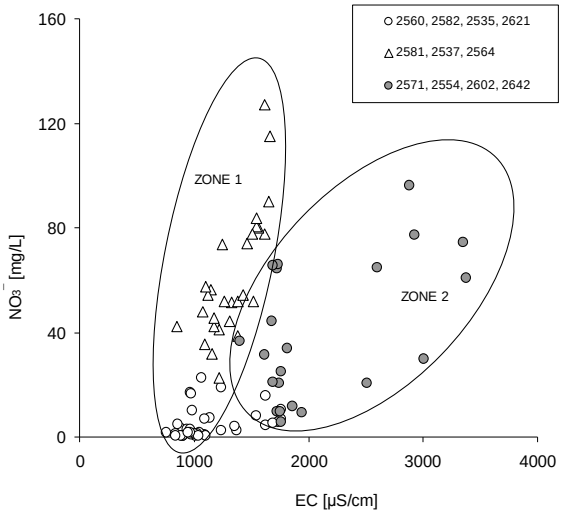

Figure 5. Scatter plot of electrical conductivity data against NO_3^- concentration from control points of the Cretaceous aquifer.

The decrease in NO_3^- concentration from Zone 1 to Zone 2 was produced coupled with an increase in the isotopic composition of $\delta^{15}N_{NO3}$ and $\delta^{18}O_{NO3}$. Figure 6 shows the $\delta^{15}N_{NO3}$ and $\delta^{18}O_{NO3}$ of dissolved NO_3^- of the samples together with the isotopic composition of the main nitrate sources: fertilizers (NO_3^- and nitrified NH_4^+ or urea), soil nitrate, and animal manure or sewage (Vitòria et al., 2004; Kendall et al., 2007; Xue et al., 2009). As Heaton (1986) pointed out, during nitrification processes no isotopic fractionation occurs between the $\delta^{15}N_{NH4}$ and $\delta^{15}N_{NO3}$ when NH_4^+ is completely nitrified. The $\delta^{18}O_{NO3}$ range for nitrification was calculated using Equation (5) (Anderson and Hooper 1983).

$$\delta^{18}O_{NO3} = 1/3\delta^{18}O_{O2} + 2/3\delta^{18}O_{H2O} \qquad (5)$$

This equation can be applied when NH_4^+ is abundant and nitrification rates are high. It also assumes negligible isotope fractionation effects during water and atmospheric O_2 ($O_{2(atm)}$) uptake (Mayer et al., 2001). It is also supposed that the $\delta^{18}O$ of O_2 used by the microorganisms is that of $O_{2(atm)}$. In this case, two-thirds of the oxygen atoms of NO_3^- produced are derived from water, whereas one-third is incorporated from atmospheric oxygen ($\delta^{18}O_{atm}$= +23.5‰; Dole et al., 1954). Thus the calculated $\delta^{18}O_{NO3}$ should range between +2.8‰ and +4.2‰.

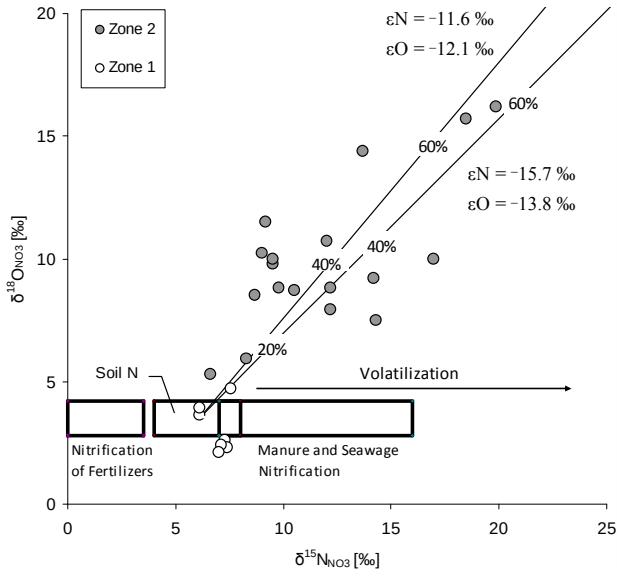

Figure 7. $\delta^{15}N_{NO3}$ and $\delta^{18}O_{NO3}$ (R^2= 0.65) of dissolved NO_3^- in the collected samples together with the isotopic composition of the main nitrate sources: fertilizers (NO_3^- and nitrified NH_4^+ or urea), soil nitrate, and animal manure or sewage (Vitòria et al., 2004).

The isotopic composition of NO_3^- from Pétrola samples showed $\delta^{15}N_{NO3}$ and $\delta^{18}O_{NO3}$ values, falling close or inside the literature box representing NO_3^- derived from soil organic N (Fig. 6). The lowest NO_3^- concentrations correspond to samples of Zone 1. Data points 2535 (mean value: 0.9 mg/L, n=12), 2579 (mean value: 1.9 mg/L, n=17) and 2621 (mean value: 3.4 mg/L, n=10) showed NO_3^- contents that could be related with soil-derived organic N (up to 2 mg/L, Foster et al., 1982). Nonetheless, the measured NO_3^- concentration in data points 2554 and 2564, was higher than the expected from a soil-derived organic N. An alternative explanation of NO_3^- origin could be nitrification of ammonium fertilizers slightly volatilized (Vitòria et al., 2004). Samples located in Zone 2 had higher values of both $\delta^{15}N_{NO3}$ and $\delta^{18}O_{NO3}$ (>10 ‰) and showed a positive correlation (r^2=0.65) between $\delta^{15}N_{NO3}$ and $\delta^{18}O_{NO3}$ (Fig. 6) pointing out that denitrification processes were taking place (Carrey et al., 2013). Denitrification was observed in samples with DO concentration above the threshold value of 2 mg/L. Denitrification can be justified by the presence of anoxic microsites, although the bulk groundwater may be well oxygenated (Mengis et al., 1999).

The isotopic fractionation (ε) allows to quantify NO_3^- losses due to denitrification independently of dilution and advection effects on NO_3^- concentrations. The value of ε calculated from NO_3^- isotopic composition and NO_3^- concentration can be applied to quantify the natural attenuation at field scale (Torrentó et al., 2010, Otero et al., 2009, among others). However, using field samples, the plots of

$\delta^{15}N_{NO3}$ and $\delta^{18}O_{NO3}$ *vs.* Ln[NO_3^-] showed poor correlations, R^2=0.26 and R^2=0.40, respectively (data not shown). This can be produced due to differences in the source origins, transport and reduction rates of NO_3^- in the aquifer system, the amount of volatilization occurred before nitrification, etc. Laboratory experiments allow to obtain reasonable isotopic fractionation values of denitrification at field scale. Carrey et al. (2013) reported values of isotopic fractionation obtained in laboratory experiments using organic and sulphides rich sediment from the Utrillas Facies (Pétrola Basin). These authors determined the isotopic fractionation during denitrification: −11.6‰ and −15.7‰ for εN, and −12.1‰ and −13.8‰ for εO. These values were used to quantify the amount of NO_3^- removed by denitrification at field scale ranging from 0% to 60% (Carrey et al., 2013). Reported average denitrification in Zone 1 reached a maximum of 10% whereas Zone 2 showed a higher denitrification percentage, between 10% and 60% (Fig. 6). Therefore, the observed denitrification was located in the area surrounding the lake but the attenuation was limited. In fact, samples in Zone 2 with higher denitrification, showed an average NO_3^- concentration of 44.8 mg/L, close to the human water supply threshold. For instance, sample 2602, where the observed denitrification during 2010 ranged from 30 - 40%, had a NO_3^- concentration between 46.8 and 50.4 mg/L. Even higher NO_3^- concentration was further observed at this site in the following surveys (96.1 mg/L in 2008 and 86.4 mg/L in 2009) illustrating that despite denitrification is acting in the study area, it has a limited capacity to remove NO_3^-. These data were in agreement with the observed limited capacity of Utrillas Facies to promote denitrification (Carrey et al., 2013). In this sense, the observed denitrification at field scale showed important spatial variability linked to variation in the amount and reactivity of labile organic matter availability, as well as NO_3^- supply. Also the higher DO measured pointed out the variability of the anoxic conditions in the aquifer. The resultant of these variables might be responsible of the observed spatial and temporal heterogeneity in NO_3^- attenuation at field scale.

6.2 Identifying the electron donor for denitrification

The presence of electron donors able to produce denitrification in Zone 2 is noticeable in the organic and sulphide-rich sediments from the Utrillas Facies (Carrey et al., 2013). Denitrification observed can be linked with organic matter oxidation or sulphide oxidation since both electron donors are present. In the case of heterotrophic denitrification (Eq. 1), although, the distribution of HCO_3^- seems to increase as $\delta^{15}N_{NO3}$ or $\delta^{18}O_{NO3}$ increase, no correlation was observed between $\delta^{13}C_{DIC}$ and HCO_3^-, $\delta^{15}N_{NO3}$ or $\delta^{18}O_{NO3}$. In addition to denitrification, variation of HCO_3^- and $\delta^{13}C_{DIC}$ might be affected by carbonate dissolution and/or precipitation processes. Despite the increase in HCO_3^- can be related with calcite

dissolution, $\delta^{13}C_{DIC}$ analyzed (-5.5‰ to -1.9‰, n=13) fell in the range of the isotopic values determined for carbonates present in the Utrillas Facies ($\delta^{13}C$= -7.2‰ to +1.9‰, n=21). Therefore, the observed variation in $\delta^{13}C$ might be hidden by other processes such as calcite precipitation. Calcite precipitation was supported by the calculated calcite saturation indexes, which varied from 0.0 to 1.1. Thus, the chemical equilibrium among the dissolved carbonate species masked any chemical and isotopic variation due to heterotrophic denitrification. As an alternative indicator of heterotrophic denitrification, a coupled decrease of both NO_3^- and DOC would be expected. However, in the present study higher DOC content matched up with a higher denitrification percentage (Fig. 7). The observed DOC increase pointed out the degradation of organic carbon compounds that, hence, increased the electron donor availability for denitrification. The variation in DOC concentration and denitrification can be attributed to the heterogeneous distribution of both, sources of organic matter and NO_3^- pollution of the basin. Therefore, although HCO_3^- and $\delta^{13}C$ data were not conclusive, chemical evolution of DOC pointed out that organic matter played a role in NO_3^- attenuation observed at field scale.

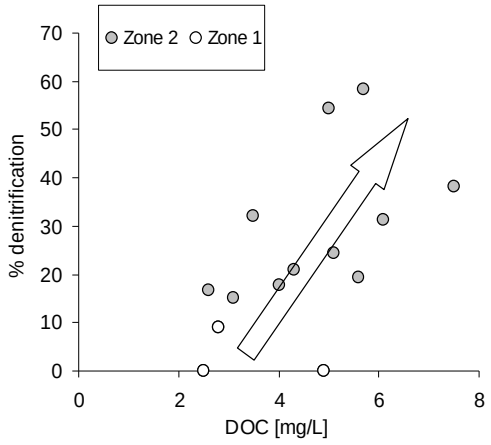

Figure 8. DOC contents against HCO_3^- concentrations scatter plot from water samples collected from the Cretaceous aquifer.

Regarding the oxidation of sulphides minerals, NO_3^- attenuation by autotrophic denitrification processes could also take place (Eq. 2). Either $O_{2(atm)}$ or water oxygen can be used during sulphide oxidation processes as electron acceptor (Taylor et al. 1984, Nordstrom & Alpers 1999). In Zone 1, located in the North and North-East where denitrification was not observed, the SO_4^{2-} concentration showed differences in the spatial distribution. Most of the samples located in the North showed an increase in SO_4^{2-} with low NO_3^- concentration (Fig. 9). On other hand, sample points located in the East (2581, and 2564) showed a coupled increase in NO_3^- and SO_4^{2-} concentration (Fig. 9). Groundwater flow

through Zone 2 produced an increase in SO_4^{2-} concentration and the higher values of SO_4^{2-} matched out with the samples with higher denitrification. In the studied area, the distribution of SO_4^{2-} in groundwater can be explained by 1) dissolution of gypsum, 2) the oxidation of sulphides minerals during denitrification.

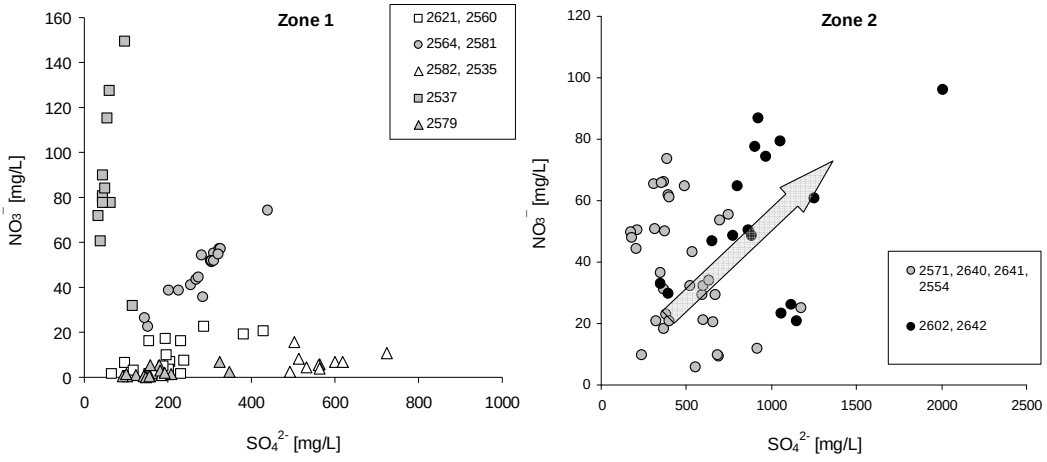

Figure 9. Scatter plots of NO_3^- and SO_4^{2-} concentrations in Zone 1(A) and Zone 2 (B).

The $\delta^{34}S_{SO4}$ and $\delta^{18}O_{SO4}$ isotopic composition of the dissolved SO_4^{2-} can be used to distinguish between different SO_4^{2-} sources such as sulphide oxidation or evaporitic sulphate minerals dissolution (Krouse, 1980; van Stempvoort and Krouse 1994). The Utrillas Facies is rich in reduced sulphur compounds, however in some areas, secondary gypsum occurs from the weathering of these sulphides. The isotopic composition of disseminated sulphides present in the Utrillas Facies ranges from –11.7‰ to –40.5‰. The $\delta^{34}S$ measured in gypsum from the Utrillas Facies sediment (+3.0‰ to –30.3‰), pointing out that sulphide oxidation was the main source of gypsum (Gómez-Alday et al., 2004). Likewise, $\delta^{18}O_{gypsum}$ formed via sulphide oxidation must show a relationship with $\delta^{18}O_{H2O}$. Van Stempvoort and Krouse (1994) defined the area, in a $\delta^{18}O_{SO4}$ vs. $\delta^{18}O_{H2O}$ diagram, where SO_4^{2-} derived from sulphide oxidation must fall. The lower line of the area is represented for the $\delta^{18}O_{SO4}$ considering no fractionation during the incorporation of oxygen from H_2O; the upper limit was calculated following the equation defined as:

$$\delta^{18}O_{SO4} = 0.62 * \delta^{18}O_{H2O} + 9 \qquad (8)$$

Following equation (8), using similar $\delta^{18}O_{H2O}$ than current groundwater (ranging from –5.0‰ to –8.0‰), most of the gypsum samples from the Utrillas Facies fall inside the area derived from sulphide

oxidation (Fig. 10). However, some values with higher $\delta^{18}O_{gypsum}$, plotted outside of this area, and could be interpreted gypsum formed from subaerial sulphide oxidation, or by secondary precipitation processes that should be enriched in ^{18}O due to the influence of atmospheric $\delta^{18}O$ (+23.8‰) in the non-saturated zone.

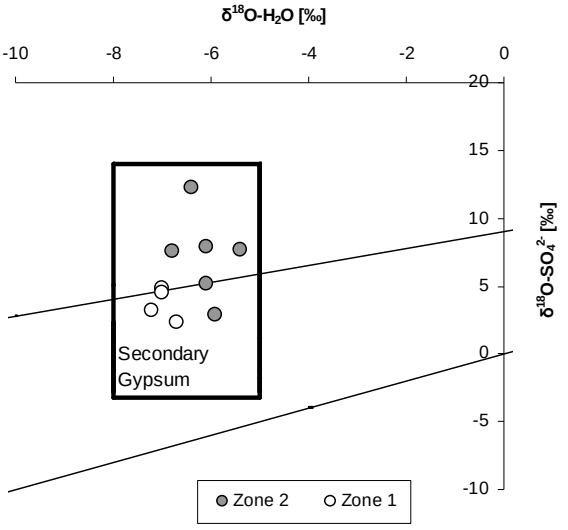

Figure 10. The $\delta^{18}O_{H2O}$ against $\delta^{18}O_{SO4}$ in secondary gypsum (Square area) from Utrillas Facies and water samples (circles) collected from the Cretaceous aquifer.

In this context, where the gypsum samples are derived from sulphide oxidation it is impossible to determine if the isotopic composition of dissolved sulphate is derived from sulphide oxidation or from secondary gypsum dissolution, since both the $\delta^{34}S_{SO4}$ and $\delta^{18}O_{SO4}$ will be same. Indeed the studied groundwater samples had $\delta^{34}S_{SO4}$ ranging form -1.9‰ and -22.5‰ and $\delta^{18}O_{SO4}$ values between +2.3‰ and -12.3‰ overlapping both the $\delta^{34}S$ of disseminated sulphides and the $\delta^{34}S_{SO4}$ and $\delta^{18}O_{SO4}$ of gypsum. Even in those samples affected by denitrification (2571 and 2602 from Zone 2), where sulphate could be derived form sulphide oxidation linked to denitrification, dissolved sulphate could no be isotopically distinguished from gypsum dissolution (Fig. 10). Hence, neither chemical nor isotopic field data could completely confirm or discard the role of sulphide in NO_3^- attenuation. Overall, chemical and isotopic data from the field were in agreement with the results obtained in the flow-through experiment using Utrillas Facies, where denitrification was mainly linked with organic matter, and sulphide had a secondary role. Detailed isotopic characterization of SO_4^{2-} water should be needed to give further insight about the role of sulphides to promote denitrification in some areas of Pétrola basin.

6.3 Nitrate reduction in Zone 3

The important NO_3^- input from both farming activities and the wastewater spilled out directly to the lake coupled with the increase nitrogen load from groundwater discharge have contributed to the eutrophication of the lake. In continental lakes nitrogen is one of the limiting nutrients which promote eutrophication (Vitousek et al., 1997). In the case of Pétrola Lake, NO_3^- concentration measured in surface water was below the detection limit. Therefore, NO_3^- was mainly consumed in surface waters for primary production, promoting the development of algal blooms observed seasonally in the lake. DOC concentrations increased with salinity. High values of DOC matched with the lowest water level in the lake, corresponding to the dry periods, and probably influenced by an important evaporation. This increase in organic C in surface lake water enhances the appearance of anoxic conditions (Ryther and Dunstan, 1971; Van Luijn et al., 1996). Under these conditions organic matter is preserved and accumulated in the bottom of the lake as organic rich sediment. This important amount of organic C available in surface waters can also promote NO_3^- reduction by denitrification or dissimilatory NO_3^- reduction to ammonium (DNRA) (Laverman et al., 2007). However, despite DNRA could be favored by the high C/N ratio observed (Carrey et al., 2014), the NH_4^+ concentration in surface waters showed around 1.1 mg/L, similar values to those samples collected nearby the lake. In addition, NH_4^+ can also be directly derived from the Pétrola town wastewater. All these evidences suggested that the occurrence of DNRA could be ruled out in the Pétrola Lake. Regarding denitrification this reaction has been observed in lakes in benthic environments or linked with bottom lake sediments (Mengis et al., 1997; Lehmann et al., 2003). However, due to the lack of chemical data of surface lake waters, the role of denitrification as responsible of NO_3^- elimination from surface water could not be neither confirmed nor discarded.

In the saltwater-freshwater interface, the hydrogeologic model suggested that saline lake water (with no NO_3^-) is mixed with fresh-groundwater (contaminated by NO_3^-). However, NO_3^- concentration measured in the piezometers under the lake during the year 2010 was below the detection limit. Therefore, the hypothesis is that organic matter from the bottom lake sediment could be transported by the density driven flow, provoking the development of reducing conditions and the availability of electron donors in the freshwater-saltwater interface. NO_3^- could be therefore completely removed in the fresh-water-saltwater interface. This is in agreement with the laboratory experiments performed using bottom lake sediment as electron donor for denitrification (Carrey et al., 2014). The freshwater-saltwater interface may be a reactive zone to promote NO_3^- reduction. The distribution of DOC in the piezometers

showed a positive correlation with EC (R^2=0.84, Fig. 11)**,** suggesting that labile organic matter for denitrification is available where the influence of the saline water from the lake is more pronounced.

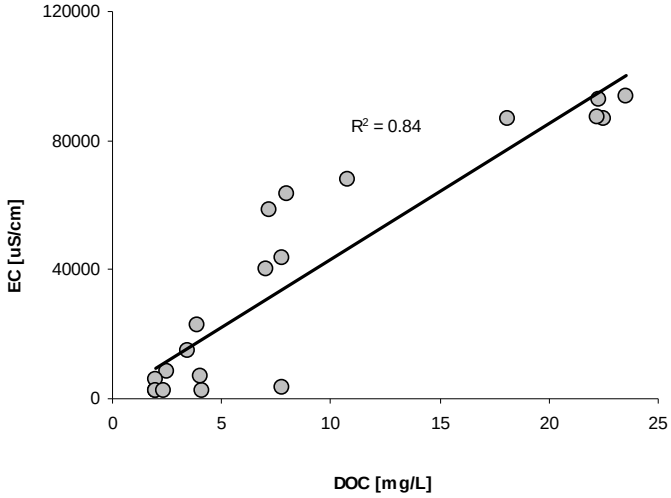

Figure 11. DOC contents against EC values scatter plot from water samples collected from piezometers in Zone 3.

ERT results indicated that the saltwater-freshwater interface extents down to 12-16m (Fig. 3A). The density driven downflow therefore could not explain the absence of NO_3^- measured in the deepest piezometers. An alternative explanation is that the deepest piezometers are influenced by regional groundwater flow with longer residence time and absence of NO_3^-. Tritium in piezometer samples showed values close to the detection limit, suggesting waters infiltrating before 1950, meanwhile surficial waters of the lake show higher tritium values (4.6 ±0.3 TU), corresponding to recent recharge. Piezometer 2626 (12 m) with 1.5 ±0.3 TU represented the mix between surface lake water and regional groundwater, pointing out the influence of surface lake at this depth. On the other hand values close to the detection limit (~0.8 TU) indicated pre-bomb water (prior to 1950s) reflecting groundwater without lake influence. Since in the Castilla-La Mancha Region, the surface of irrigation crops began to be noticeable at the beginning of the 80´s of the past century (Calera and Martín, 2005), the absence of NO_3^- in the deepest part of the aquifer under the lake is related to regional groundwater flow with longer residence time and it was not linked to denitrification. Therefore, tritium data confirmed that the role of DOC transported by the density-driven downflow would be restricted to the freshwater-saltwater interface in the upper part of the aquifer (down to 12 m below ground surface), in agreement with ERT results. Consequently, the geometry of the density downflow plays an important role in denitrification under the lake.

7. Conclusions

The obtained results have important implications for understanding the role of hypersaline systems in groundwater denitrification. The hydrogeologic study has shown that the groundwater flow in the Pétrola basin can be considered as the result of two main flow components: regional groundwater flow, from the perimeter area/recharge areas (Zone 1) towards the lake (Zone 2) and the density driven flow from surface water from the lake towards the underlying aquifer (Zone 3). Hydro-chemical and isotopic results suggested that NO_3^- in the basin is derived from synthetic fertilizers slightly volatilized, and denitrification is taking place although restricted to the area surrounding and under the lake. In agreement with the results from Carrey et al., (2013), the observed denitrification in the Cretaceous aquifer is likely to be produced by organic carbon oxidation, since dissolved SO_4^{2-} distribution can be explained by dissolution processes. However, in specific wells sulphide minerals could not be discarded as potential electron donors. The observed denitrification was limited and presented important spatial variability due to the amount, availability and reactivity of labile organic matter, as well as to the spatial variation of NO_3^- supply. The saltwater-freshwater interface (Zone 3) constitutes a reactive zone for NO_3^- attenuation. In this sense, attenuation processes by heterotrophic denitrification reactions were more likely to occur in zones of the saline lake-aquifer system where density driven flow effectively transported the DOC into aquifer zones under reducing conditions. The role of DOC transported by the density-driven down flow would be restricted to the freshwater-saltwater interface in the upper part of the aquifer (down to 12 m below ground surface) whereas the absence on nitrate in the deepest part of the aquifer is attributed to regional flow with longer residence time. Consequently, the geometry of the density downflow plays an important role in denitrification processes under the lake.

Overall, the hydrodynamic equilibrium is not equally distributed in Pétrola basin because of heterogeneities in the physical properties of the aquifer media. In addition to this variability, the amount and reactivity of labile organic matter availability as well as NO_3^- supply can also show spatial variability. These results in the spatial heterogeneity in nitrate attenuation observed at field scale. Significant spatial and temporal variability of denitrification processes within the Pétrola Basin suggests that accurate estimates of denitrification will require more extensive studies.

Acknowledgements

This work was financed by a grant (PEIC11-0135-8842) from the Castilla La Mancha Government, the CICYT-CGL2011-29975-C04-01 and CICYT-CGL2011-29975-C04-02 projects from the Spanish Government, and the 2009SGR 103 project from the Catalan Government. The authors would like to thank the "Centres Científics i Tecnològics" of the "Universitat de Barcelona" for the chemical and isotopic analyses.

References

Anderson, K.K., Hooper, A.B., 1983. O^2 and H_2O are each the source of one O in NO_2 produced from NH_3 by *Nitrosomonas*: ^{15}N evidence. FEBS Lett. 164, 236–240

APHA-AWWA-WEF, 1998. Standard Methods for the Examination of Water and Wastewater. 20th edn. Washington: American Public Health Association.

Appelo, C.A.J., Postma, D., 2005. Geochemistry, groundwater and pollution. 2nd Edition, Balkema: Rotterdam, The Netherlands.

Aravena, R., Robertson, W.D., 1998. Use of multiple isotope tracers to evaluate denitrification in ground water: study of nitrate from a large-flux septic system plume. Ground Water 36, 975–981.

Baena-Pérez, J., Jerez-Mir, L., 1982. (IGME) Síntesis para un ensayo paleogeográfico entre la Meseta y la Zona Bética (s:srt). Col. Informe. Madrid, pp 256.

Böttcher, J., Strebel, O., Voerkelius, S., Schmidt, H.J. 1990. Using isotope fractionation of nitrate-nitrogen and nitrate-oxygen for evaluation of microbial denitrification in a sandy aquifer. J. Hydrol. 114, 413-424.

Brinson, M. M., Hauer, F.R., Lee, L. C., Nutter, W. L., Rheinhardt, R. D., Smith, R. D., Whigham, D., 1995. A guidebook for application of hydrogeomorphic assessments to riverine wetlands. US Army Engineer. Waterw. Exp. Stn. Vicksburg, MS, USA.

Calera, A., Martín, F., 2005. Uso de la teledetección en el seguimiento de los cultivos de regadío. In Martín F, López P, Calera A. (eds), Agua y Agronomía. Mundi-Prensa, Madrid.

Canfield, D., Raiswellr, E., Westrichj, T., Reave, C.M., Bener, R.A., 1986. The use of chromium reduction in the analysis of reduced sulfur in sediments and shales. Chem. Geol. 54, 149–155.

Carrey, R., Otero, N., Soler, A., Gómez-Alday, J.J., Ayora, C., 2013. The role of Lower Cretaceous sediments in groundwater nitrate attenuation in central Spain: column experiments, Appl. Geochem. 32, 142–152.

Carrey, R., Rodríguez-Escales, P., Otero, N., Ayora, C., Soler, A., Gómez-Alday, J.J., 2014. Nitrate attenuation potential of hypersaline lake sediments in central Spain: Flow-through and batch experiments. J. Contam. Hydrol. submitted for publication.

Casciotti, K.L., Sigman, D.M., Hastings, M.G., Böhlke, J.K., Hilkert, A., 2002. Measurement of the oxygen isotopic composition of nitrate in seawater and freshwater using the denitrifier method. Anal. Chem. 74, 4905–4912.

Cirujano, S., Montes, C., García, L.I., 1988. Los humedales de la provincia de Albacete. Una panorámica general. Al-Basit 24, 77–95.

Clark, I.D., Fritz, P., 1997. Environmental isotopes in hydrogeology. Lewis Publishers, New York.

Comly, H.H., 1945. Cyanosis in infants caused by nitrates in well water. J. Am. Med. Assoc. 129. 112-116.

Cortijo, A., Carrey, R., Gómez-Alday, J.J., Otero, N., Soler, A., Sanz, D., Castaño, S., Recio, C., Carnicero, A., Ayora, C., Gómez-Sánchez, E., 2011. Aportes de nitrato a la laguna de Pétrola (SE, Albacete). Impacto de la agricultura y de los vertidos de agua residuales. In: Congreso Ibérico sobre las aguas subterráneas (AIH-GE).

Dassenakis, M., Scoullos, M., Foufa, E., Krasakopoulou, E., Pavlidou, A., Kloukiniotou, M., 1998. Effects of multiple source pollution on a small Mediterranean river. Appl. Geochem. 13 (2), 197–211.

De Groot-Hedlin, C. Constable, S., 1990. Occam's inversion to generate smooth, two-dimensional models form magnetotelluric data. Geophysics, 55, 1613–1624.

Dickson, J.A.D. 1965. A modified staining technique for carbonates in thin section. Nature 205, 587.

Dogramaci, S.S., Herczeg, A.L., Schiff, S.L., Bone, Y., 2001. Controls on $\delta^{34}S$ and $\delta^{18}O$ of dissolved sulfate in aquifers of the Murray Basin, Australia and their use as indicators of flow processes. Appl. Geochem. 16, 475–488.

Dole, M., Lane, G., Rudd, D., Zaukelies, D.A., 1954. Isotopic composition of atmospheric oxygen and nitrogen. Geochim. Cosmochim. Acta 6, 65–78.

EC, 2000. Council Directive 2000/60/EC, of 23 October 2000, establishing a frame- work fro Community action inthe field of water policy [online].Off. J. Eur. Comm. L 327, 1–73 (Brussels). Available from: <http://www.europa.eu.int/eur-lex> (22.12.2000).

EC, 2006. Council Directive 2006/118/EC, of 12December 2006, on the protection of groundwater against pollution and deterioration [online]. Off. J. Eur. Comm. L 372, 19–31 (Brussels). Available from: <http://www.europa.eu.int/eur-lex> (27.12.2006).

Foster, S.S.D., Cripps, A.C., Smith-Carington, A., 1982. Nitrate leaching to groundwater. Phil. Trans. R. Soc. Lond. 296, 477-489.

Gómez-Alday, J.J., Castaño, S., Sanz, D., 2004. Origen geológico de los contaminantes (sulfatos) presentes en las aguas subterráneas de la laguna de Pétrola. (Albacete, España). Resultados preliminares. Geogaceta. 35, 167-170.

Hall, G.E.M., Pelchat, JC, Loop J., 1988. Separation and recovery of various sulphur species in sedimentary rocks for stable sulphurisotopic determination. Chem. Geol. 67, 35–45.

Harrison, J., Maranger, R., Alexander, R., Giblin, A., Jacinthe, P.A., Mayorga, E., Seitzinger, S., Sobota, D., Wollheim, W., 2009. The regional and global significance of nitrogen removal in lakes and reservoirs. Biogeochem. 93 (1), 143–157.

Heaton, T.H.E., 1986. Isotopic studies of nitrogen pollution in the hydrosphere and atmosphere: a review. Chem. Geol. 59, 87–102.

ITAP, 2010. Datos sobre resultados de ensayos de cultivos. Instituto Técnico Agronómico y Provincial. Obtenido de http://www.itap.es/ITAP-Ensayos/Experimentos/Resultados1.asp.

Kendall, C., Elliott, E.M., Wankel, S.D., 2007. Tracing antropogenic inputs of nitrogen to ecosystems, in: Michener, R.H., Lajtha, K. (Eds.), Stable Isotopes in Ecology and Environmental Science. Blackwell Publishing, 375–450.

Korom, S.F., 1992. Natural denitrification in the saturated zone: A review, Water Resour. Res. 28 (6), 1657–1668.

Kraft, G.J., Stites, W., 2003. Nitrate impacts on groundwater from irrigated-vegetable systems in a humid north-central US sand plain. Agr. Ecosyst. Environ. 100 (1), 63–74.

Krouse, H.R., 1980. Sulphur isotopes in our environment. In Fritz, P. and Fontes J.C. (eds.), Handbook of Environmental Isotopes Geochemistry, Elsevier, Amsterdam, pp.435–471.

Laverman, A.M., Canavan, R.W., Slomp, C.P., Van Cappellen, P., 2007. Potential nitrate removal in a coastal freshwater sediment (Haringvliet Lake, The Netherlands) and response to salinization. Water Res. 41, 3061–3068.

Lehmann, M.F., Reichert, P., Bernasconi, M.S., Barbieri, A., McKenzie, J.A., 2003. Modelling nitrogen and oxygen isotope fractionation during denitrification in a lacustrine redox-transition zone. Geochim. Cosmochim. Acta 67 (14), 2529-2542.

Loke, M.H., Barker, R.D., 1996. Rapid least-squares inversion of apparent resistivity pseudosections by a quasi-Newton method. Geophys. Prospect. 44, 131–152.

Loke, M.H., Dahlin, T., 2002. A comparison of the Gauss-Newton and quasi-Newton methods in resistivity imaging inversion. J. Appl. Geophys. 49, 149-162.

Magee, P.N., Barnes, J.M., 1956. The production of malignant primary hepatic tumours in the rat by feeding dimethylnitrosamine. Br. J. Cancer 10, 114–122.

Mariotti, A., Landreau, A., Simon, B., 1988. ^{15}N isotope biogeochemistry and natural denitrification process in groundwater: Application to the chalk aquifer of northern France. Geochim. Cosmochim. Acta 52, 1869–1878.

Mariotti, A., 1986. Denitrification in groundwaters, principles and methods for its identification: a review. J. Hydrol. 88 (1–2), 1–23.

Mariotti, A., Germon, J.C., Hubert, P., Kaiser, P., Letolle, R., Tardieux, A.,Tardieux, P., 1981. Experimental determination of nitrogen kinetic isotope fractionation: some principles; illustration for the denitrification and nitrification processes. Plant Soil 62, 423–430.

Mason, C.F., 2002. Biology of freshwater pollution. 4th ed. Prentice Hall, Harlow.

Mayer, B., Bollwerk, S.M., Mansfeldt, T., Hütter, B., Veizer, J., 2001. The oxygen isotope composition of nitrate generated by nitrification in acid forest floors. Geochim. Cosmochim. Acta 65, 2743–2756.

Mengis, M., Gächter, R., Wehrli, B., 1997. Nitrogen elimination in two deep eutrophic lakes. Limnol. Oceanogr. 42 (7), 1530–1543.

Mengis, M., Schiff, S.L., Harris, M., English, M.C., Aravena, R., Elgood, R.J., Maclean, A., 1999. Multiple geochemical and isotopic approaches fro assessing ground water NO_3^- elimination in a riparian zone. Ground Water 37, 448-457.

Nizzoli, D., Carraro, E., Nigro, V., Viaroli, P., 2010. Effect of organic enrichment and thermal regime on denitrification and dissimilatory nitrate reduction to ammonium (DNRA) in hypolimnetic sediments of two lowland lakes. Water Res. 44, 2715–2724.

Nordstrom, D.K., Alpers, C.N., 1999. Geochemistry of acid mine waters. In The Environmental Geochemistry of Mineral Deposist, G. S. Plumlee and M. J. Logsdon, eds., Rev. Econ. Geol. V. 6A, Soc. Econ. Geol. Inc., Littleton, CO (1999). Chapter 6. 133-160.

Otero, N., Torrentó, C., Soler, A.,Menció, A., Mas-Pla, J., 2009 Monitoring groundwater nitrate attenuation in a regional system coupling hydrogeology with multi-isotopic methods: the case of Plana de Vic (Osona, Spain). Agric. Ecosyst. Environ. 133 (1-2), 103–113.

Pauwels, H., Foucher, J.C., Kloppmann, W., 2000. Denitrification and mixing in a schist aquifer: influence on water chemistry and isotopes. Chem. Geol. 168, 307–324.

Ryther, J.H., Dunstan, W.M., 1971. Nitrogen, phosphorus, and eutrophication in the coastal marine environment. Sci. 171 (3975), 1008–1013.

Santoro, A.E., 2009. Microbial nitrogen cycling at the saltwater-freshwater interface. Hydrogeol. J. 18 (1), 187–202.

Schubert, C.J., Durisch-kaiser, E., Wehrli, B., Thamdrup, B., Lam, P., Kuypers, M.M., 2006. Brief report Anaerobic ammonium oxidation in a tropical freshwater system (Lake Tanganyika). Environ. Microbiol. 8, 1857–1863.

Seitzinger, S., Harrison, J.A., Böhlke, J.K., Bouwman, A.F., Lowrance, R., Peterson, B., Tobias, C., Van Drecht, G., 2006. Denitrification across landscapes and waterscapes: A synthesis. Ecol. Appl. 16 (6), 2064-2090.

Sigman, D.M., Casciotti, K.L., Andrean, M., Barford, C., Galanter, M., Böhlke, J.K., 2001. A bacterial method for the nitrogen isotopic analysis of nitrate in seawater and freshwater. Analytical Chem. 73 (17), 4145-4153.

Taylor, B.E., Wheeler, M.C., 1984. Stable isotope geochemistry of acid mine drainage: Experimental oxidation of pyrite. Geochim. Cosmochim. Acta 48 (12), 2669-2678.

Torrentó, C., Cama, J., Urmeneta, J., Otero, N., Soler, A., 2010. Autotrophic denitrification with pyrite: implications for bioremediation of nitrate contaminated groundwater. Chem. Geol. 278, 80–91.

Unterweger, M.P., Coursey, B.M., Schima, F.J., Mann, W.B., 1980. Preparation and calibration of the 1978 National Bureau of Standards tritiated-water standards. Int. J. Appl. Radiation Isotopes 31 (10) 611-614.

Van Luijn, F., Boers, P.C.M., Lijklema, L., 1996. Comparison of denitrification rates in lake sediments obtained by the N, flux method, the I5N isotope pairing technique and the mass balance approach. Water Res 30:863-900.

Van Stempvoort, D.R., Krouse, H.R., 1994. Controls of $\delta^{18}O$ in sulphate. In: Alpers, C.N., Blowes, D.W. (Eds.), Environmental Geochemistry of Sulphide Oxidation. American Chemical Society, Washington, pp. 446–480.

Vitòria, L., Soler, A., Canals, A., Otero, N., 2008. Environmental isotopes (N, S, C, O, D) to determine natural attenuation processes in nitrate contaminated waters: example of Osona (NE Spain). Appl. Geochem. 23, 3597–3611.

Vitòria, L., Otero, N., Soler, A., Canals, A., 2004. Fertilizer characterization: Isotopic data (N, S, O, C, and Sr). Environ. Sci. Technol. 38, 3254–3262.

Vitousek, P.M., Aber, J.D., Howarth, R.W., Likens, G.E., Matson, P.a., Shindler, D.W., Schelesinger, W.H., Tilman, D.G., 1997. Human alteration of the global nitrogen cycle: source and consequence. Ecol. Appl. 7, 737–750.

Ward, M.H., deKok, T.M., Levallois, P., Brender, J., Gulis, G., Nolan, B.T., VanDerslice, J., 2005. Workgroup Report: Drinking-Water Nitrate and Health—Recent Findings and Research Needs. Environ. Health Perspect. 113, 1607–1614.

Wassenaar, L.I., 1995. Evaluation of the origin and fate of nitrate in Abbostsford aquifer using the isotopes of ^{15}N and ^{18}O in NO_3^-. Appl. Geochem. 10, 391–405.

Widory, D., Kloppmann, W., Chery, L., Bonnin, J., Rochdi, H., Guinamant, J.L., 2004. Nitrate in groundwater an isotopic multi-tracer approach. J. Contam. Hydrol. 74 (1-4), 165-188.

Xue, D., Botte, J., De Baets, B., Accoe, F., Nestler, A., Taylor, P., Van Cleemput, O., Berglund, M., Boeckx, P., 2009. Present limitations and future prospects of stable isotope methods for nitrate source identification in surface- and groundwater. Water Res. 43, 1159–1170.

Zimmermann, S., Bauer, P., Held, R., Kinzelbach, W., Walther, J.H., 2006. Salt transport on islands in the Okavango Delta: Numerical investigations. Adv. Water Resour. 29 11–29.

Appendix A-4:

Induced nitrate attenuation by glucose in groundwater: Flow-through experiment

R. Carrey, N. Otero, G. Vidal-Gavilan, C. Ayora, A. Soler, J.J. Gómez-Alday

2014

Chemical Geology 370, 19-28

(Supporting information of this paper is available in Appendix C-4)

Induced Nitrate Attenuation by Glucose in Groundwater: Flow-Through Experiment

Raúl Carrey[1], Neus Otero[1], Georgina Vidal[1], Carlos Ayora[2], Albert Soler[1], Juan José Gómez-Alday[3]

1 Grup de Mineralogia Aplicada i Medi Ambient, Facultat de Geologia, Universitat de Barcelona, C/ Martí i Franquès s/n, 08028, Barcelona, Spain. e-mail: raulcarrey@ub.edu, notero@ub.edu, albertsoler@ub.edu, georginavidal@biorem.cat

2 Instituto de Diagnóstico Ambiental y Estudios del Agua, IDAEA- CSIC, C/Jordi Girona, 18, 08028 Barcelona, España, cayora1@gmail.com

3 Hydrogeology Group. Institute for Regional Development (IRD). University of Castilla-La Mancha (UCLM) Campus Universitario de Albacete 02071 Albacete, España. JuanJose.Gomez@uclm.es

Abstract

Endorheic basins are frequently exposed environments to nitrate (NO_3^-) pollution where groundwater may be the primary fresh water resource. The Pétrola basin (Central Spain) is an outstanding example of this type of basin that is affected by NO_3^- pollution where natural attenuation capacity observed in the field is limited. A three-stage flow-through experiment was developed to evaluate the viability of induced heterotrophic denitrification to remove NO_3^- using chemical, microbial and isotopic tools. The proposed biostimulation involves periodically injecting glucose to act as an electron donor to promote complete NO_3^- removal. The C/N ratio tested is nearly stoichiometric to avoid the generation of undesirable compounds such as NO_2^- or H_2S. Nitrate reduction was achieved after 13 days, along with transient NO_2^- accumulation that was observed until day 27. In addition to attenuating NO_3^-, the glucose injection also represses the dissimilatory nitrate reduction to ammonium (DNRA), reducing the NH_4^+ concentration in the outflow. Changes in the C/N ratio during the experiment reduced the amount of glucose discharged from the system. However, despite these changes, NO_3^- attenuation continued because secondary carbon sources (dissolved organic carbon in the input water or biomass) were present during the experiment and accounted for approximately 30% of the total attenuated NO_3^-. Isotopic characterisation of the sulphate (SO_4^{2-}) proved that the SO_4^{2-} reduction did not occur, even though carbon excess and low redox conditions were present. This is attributed to the lack of time for SO_4^{2-} reduction to occur inside the column. The N and O isotopic fractionation obtained during the induced attenuation were −8.8‰ and −8.0‰, respectively; these values were lower (in absolute values) than the fractionation from natural denitrification processes observed in Pétrola basin. This variation was caused by differences in the

experimental conditions that affected the denitrification rate. Overall, periodically injecting glucose might be a feasible method to remove NO_3^- from groundwater; a pilot-scale test should be performed to verify its applicability during long-term treatments in the field.

1. Introduction

Nitrate (NO_3^-) is one of the most common groundwater pollutants. Anthropogenic activities increase the NO_3^- concentration, reducing water quality. Frequently, the sources for the NO_3^- pollution in groundwater are linked to the extensive use of synthetic and organic fertilisers, inappropriate placement of animal waste, and spills from septic system effluents. High NO_3^- ingestion causes adverse health effects, such as methemoglobinemia, in infants and young children (Comly et al., 1945, Magee and Barnes, 1956) and may also promote cancer (Ward et al., 2005). Moreover, NO_3^- impacts the environment, contributing to the eutrophication of surface water bodies (Vitousek et al., 1997). The NO_3^- concentration threshold established by Directive 98/83/CE for human water supplies is 0.81 mM. This limit is exceeded by many aquifers worldwide because NO_3^- is highly mobile in groundwater and often persists in aquifers where the concentration of dissolved oxygen is over 0.06 mM and/or there are few electron donors available, such as labile organic carbon, sulphides and Fe(II)-bearing minerals (Korom, 1992). Consequently, Europe has proposed actions to reduce NO_3^- pollution (Directive 91/976/ECC). Of the different strategies, one of the most efficient treatments for removing NO_3^- involves enhanced biological denitrification within the aquifer using biodenitrification technologies (Khan and Spalding, 2004; Tartakovsky et al., 2002; Vidal-Gavilan et al., 2013; among others).

Denitrification is a redox reaction driven by autotrophic or heterotrophic bacteria that reduce NO_3^- to nitrogen gas (N_2) under suboxic conditions. Autotrophic bacteria promote denitrification using reduced sulphur compounds. Heterotrophic denitrification occurs through a number of sequential reactions where bacteria use organic matter as the electron donors for NO_3^- reduction. In both processes, NO_3^- is initially converted to nitrite (NO_2^-), which is more toxic than NO_3^- (De Beer et al., 1997). The maximum allowed NO_2^- concentration in drinking water is 0.01 mM (Directive 98/83/CE). The next reaction transforms NO_2^- into nitric oxide gas (NO), and NO is subsequently converted into nitrous oxide gas (N_2O); both species are greenhouse gases. Finally, N_2O is transformed into N_2. Usually, this reaction sequence is presented as a single reaction (Eqs. 1 and 2).

$$5FeS_2 + 15NO_3^- + 5H_2O \rightarrow 10SO_4^{2-} + 7.5N_2 + 5FeOOH + 5H^+ \quad (1)$$

$$5CH_2O + 4NO_3^- \rightarrow 2N_2 + 4HCO_3^- + CO_2 + 3H_2O \qquad (2)$$

Chemical data, when coupled with multi-isotopic studies of the solutes involved in the reactions, are an effective tool to identify and describe heterotrophic and autotrophic denitrification, as well as secondary processes, such as SO_4^{2-} reduction (Aravena and Robertson, 1998; Mariotti et al., 1988; Pauwels et al., 2000; Vitòria et al., 2008). Stable isotopes are commonly measured as the ratio between the heavier and the most-abundant isotope (lighter isotope), e.g., ^{15}N against ^{14}N. These ratios are established in accordance with international standards using delta notation (δ) (Eq. 3).

$$\delta^{15}N = [(R_{sa} - R_{std}) / R_{std}] \times 1000 \qquad (3)$$

where $R = {}^{15}N/{}^{14}N$ in the sample (sa) and the standard (std)

In addition, the isotopic fractionation (ε) of the N and O in dissolved NO_3^- is essential for determining the rate of denitrification. During denitrification, while NO_3^- is consumed, any residual NO_3^- becomes enriched in the heavier isotopes (^{15}N and ^{18}O). This process can be expressed as a Rayleigh distillation process (Eqs. 4 and 5) (Mariotti et al., 1988).

$$\delta^{15}N_{residual} = \delta^{15}N_{initial} + \varepsilon \ln f \qquad (4)$$

$$\delta^{18}O_{residual} = \delta^{18}O_{initial} + \varepsilon \ln f \qquad (5)$$

where f is the residual NO_3^- divided by the initial NO_3^- concentration and ε is the fractionation factor that depends on the aquifer's materials and media characteristics.

In natural systems, denitrification is predominantly restricted by the availability of electron donors (Knowles, 1982). To overcome this natural limitation, different field-scale treatments were tested to remove NO_3^- from both ground- and wastewaters by adding an external electron donor to promote denitrification with significant success (Borden et al., 2011; Istok et al., 2004; Leverenz et al., 2010; Tartakovsky et al., 2002; Vidal-Gavilan et al., 2013). From the different remedial strategies tested, biostimulation of heterotrophic denitrification has seen common use because it is the most economical and easily performed technique. However, some issues must be taken into account during induced treatments to avoid increasing the toxicity of the treated water by generating undesirable compounds, such as NO_2^-, N_2O or hydrogen sulphide (H_2S). Furthermore, the processes

that reduce NO_3^- beyond denitrification, such as the dissimilatory nitrate reduction to ammonium (DNRA or ammonification), should be avoided. DNRA is enacted by fermentative bacteria, reducing NO_3^- to NO_2^- before the final reduction to NH_4^+. Therefore, before any field treatment, exhaustive laboratory experiments must be performed to avoid these adverse effects. Consequently, in recent decades, several studies have introduced different carbon sources as electron donors and/or a specific bacterial strain to promote heterotrophic denitrification. Frequently tested electron donors included alcohols, sugars, or other organic compounds (Aesoy et al., 1998; Akunna et al., 1993; Fernández-Nava et al., 2010; Ge et al., 2012; Gómez et al., 2000; Lee and Welander, 1996; Martin et al., 2009; Osaka et al., 2008; Peng et al., 2007; Vidal-Gavilan et al., 2013; among others). Complex organic compounds, such as pine bark, compost or sawdust have also been studied (Schipper and Vojvodic, 2000; Trois et al., 2010). Few of the induced studies have utilised multi-isotopic characterisation to identify and describe the denitrification reactions (Vidal-Gavilan et al., 2013; Barford et al., 1999; Delwiche and Steyn, 1970; Torrentó et al., 2011).

Enhanced denitrification may be applied in areas affected by NO_3^- pollution where attenuation is absent or limited but environmental conditions in the natural system are met. Examples of areas exposed to NO_3^- pollution include the endorheic basins located in arid and semiarid regions. These basins are common in central Spain. The Pétrola basin is an excellent example of an endorheic system affected by NO_3^- pollution. Previous work performed in this basin has indicated that, although heterotrophic denitrification occurs naturally, it is limited; the NO_3^- attenuation ranges from 15% to 60% with an average value of approximately 20% (Carrey et al., 2013). To enhance the heterotrophic denitrification in the Pétrola basin, a biostimulation treatment is proposed. Before any field application, a detailed laboratory characterisation is required. Consequently, the present work sought to design an efficient strategy for inducing biostimulation. To simulate field conditions, the experiment was performed on a flow-through system. The selected carbon source was glucose which has been previously used as an electron donor in denitrification batch experiments (Akunna et al., 1993; Ge et al., 2012; Vidal-Gavilan et al., 2013). However, to the best of our knowledge, long-term denitrification experiments using glucose have not been assessed. The major goal of this experiment was to evaluate the viability of periodically injecting glucose to promote denitrification in ground water. Different C/N ratios were tested to achieve complete NO_3^- elimination while preventing the generation of undesirable compounds, such as NO_2^- or H_2S. The

second goal of this study was to obtain the isotopic fractionation factor (ε) for N and O during the induced denitrification reaction to evaluate the efficiency of future field tests.

2. Methodology / Methods

2.1 Experimental set-up

The experiment consisted of a glass cylindrical column (40 cm high, 9 cm inner diameter) filled with a homogeneous mix of sediment and clean silica (siliceous) sand (Panreac®) (Fig. 1). Before the biostimulation experiment, the system's natural denitrification potential was evaluated. The sediment had a limited capacity for inducing denitrification. This preliminary experiment lasted for one year, ending when the electron donors were exhausted (Carrey et al., 2013). After that interval but before the biostimulation experiment was set-up, the column was operated for 3 months at 0.1 mL/min and with constant NO_3^- input (0.88 mM) to verify that the sediment was no longer able to naturally undergo denitrification.

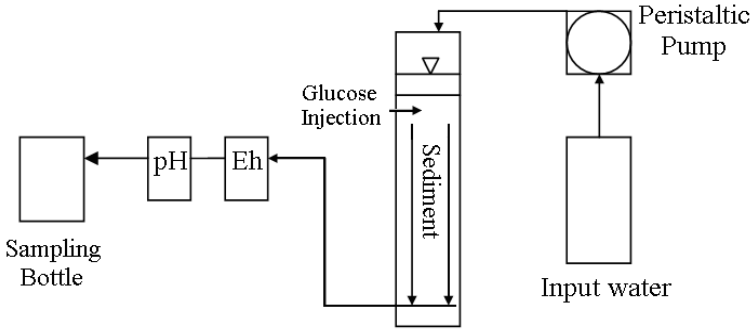

Figure 1. Set-up of the column experiment. Glucose injection was performed in the top of the sediment. Water was sampled in agricultural well; NO_3^- concentration was 0.88 mM. Flow rate in the experiment was controlled by a peristaltic pump.

The experiment was developed in an anaerobic glove box filled predominantly with argon. The temperature ranged from 18 to 27 ºC. Oxygen was removed once a day to maintain a partial pressure between 0.0% and 0.4%. The inflow and outflow rate was controlled with a peristaltic pump (Micropump Reglo Digital 4 channels ISMATEC). The flow rate was 0.1 mL/min for 87 days and 0.11 mL/min from day 87 to day 124, meaning the retention times were 72 and 67 hours, respectively. The input water used in this experiment was collected in 2008 from an agricultural well and can be considered as representative of contaminated groundwater from the Pétrola basin. This water contained, on average, 0.88 mM NO_3^-, 3.54 mM SO_4^{2-}, 0.02

mM NH_4^+, 0.21 mM dissolved organic carbon (DOC), and NO_2^- was below the detection limit (< $4x10^{-3}$ mM). The outflowing water was sampled every 12 hours for 60 days and once a day thereafter.

2.2 Carbon source and C/N ratio during the biostimulation experiment

Anhydrous glucose ($C_6H_{12}O_6$) Panreac® was used as the carbon source because it was accessible and easy to handle. The solid glucose was dissolved in 10 mL input groundwater. The solution was injected at the top of the column 2 cm below the surface sediment using a spinal needle (BD spinal Needle 25G). The injection was carried out every 3 days (72 hours), corresponding to the retention time calculated for the flow rate (0.1 mL/min). The molar ratio of C/N (C-$C_6H_{12}O_6$ / N-NO_3^-) was varied during the experiment. The minimum required C/N ratio was calculated based on a stoichiometric heterotrophic denitrification reaction (Eq. 2). Following this equation, 5 mol C-$C_6H_{12}O_6$ are consumed to remove 4 mol of N-NO_3^-, suggesting a C/N ratio of 1.25. During the experiment, three different stages with varied C/N ratios were tested. Initially (stage I, days 0 to 39), the C/N molar ratio was approximately 1.6, corresponding to 0.60 mmol C-$C_6H_{12}O_6$ per injection. The excess carbon source was added to reach complete NO_3^- attenuation more rapidly. From day 39 to day 87 (stage II), the stoichiometric ratio was 1.25 (0.46 mmol C-$C_6H_{12}O_6$ per injection). Finally, from day 87 to day 124 (stage III), the flow rate was changed from 0.1 to 0.11 mL/min, changing the molar ratio to 1.12.

2.3 Analytical methods

Chemical analyses

The experiment was run over 4 months to collect 133 samples. The redox potential (Eh) and pH were measured every hour at the outflow with portable electrodes (WTW-3310). Chemical analyses were performed for all samples, but the isotopic data were only analysed in a subset of representative samples according to the measured NO_3^- concentrations. The samples were filtered through a 0.20 μm Millipore® filter and 1% 0.1 M $HgCl_2$ was added to stop all microbial activity. NH_4^+ was analysed using spectrophotometry (ALPKEM, Flow Solution IV). NO_3^-, SO_4^{2-}, Cl^-, and NO_2^- were analysed using high performance liquid chromatography (HPLC) with a WATERS 515 HPLC pump and IC-PAC Anions columns, as well as WESCAN and UV/VIS KONTRON detectors. Mn- and Fe-containing samples were acidified with 1% HNO_3^- and analysed with inductively coupled plasma-optical emission spectrometry (ICP-OES, Perkin-Elmer Optima 3200 RL). DOC was measured using organic matter combustion (TOC 500 SHIMADZU).

Glucose was analysed by HPLC with a Waters Alliance 2695 system. Chemical analyses were conducted at the Centres Cientifics i Tecnològics of the Universitat de Barcelona.

Isotopic analyses

The isotopic analyses included the $\delta^{15}N$ and $\delta^{18}O$ of the dissolved NO_3^- and the $\delta^{34}S$ and $\delta^{18}O$ of the dissolved SO_4^{2-}. The $\delta^{15}N$ and $\delta^{18}O$ from the dissolved NO_3^- were analysed using the bacterial denitrifier method described by Casciotti et al. (2002) and Sigman et al. (2001). Bacterial cultures of *"Pseudomonas aureofaciens"* (LMG1245; ATCC 13985) were used to convert NO_3^- to $N_2O_{(g)}$. Before the isotopic analyses, the samples were treated with sulfamic acid to remove the dissolved NO_2^- according to the methodology detailed by Granger and Sigman (2009). Simultaneous $\delta^{15}N$ and $\delta^{18}O$ analysis of the produced N_2O was carried out using a Trace gas-preparation unit (ANCA TGII, PDZ Europa Ltd.) coupled with an IRMS instrument (20-20, SerCon Ltd.). For $\delta^{34}S$ and $\delta^{18}O$ analyses, SO_4^{2-} was precipitated as $BaSO_4$ by adding $BaCl_2$ after acidifying the sample with HCl and boiling it to prevent $BaCO_3$ precipitation, as prescribed by the standard method (Dogramaci et al., 2001). The $\delta^{34}S$ was analysed with a Carlo Erba Elemental Analyzer (EA) coupled in continuous flow with a Finnigan Delta C IRMS. The $\delta^{18}O$ was analysed in duplicate with a ThermoQuest high temperature conversion elemental analyser (TC/EA) coupled in continuos flow with a Finnigan Matt Delta C IRMS. The isotope ratios were calculated using international and internal laboratory standards. The notation is expressed as δ per mil relative to the international standards (Air for $\delta^{15}N$, V-SMOW for $\delta^{18}O$ and V-CDT for $\delta^{34}S$). The reproducibility of the samples was ±0.2‰ for the $\delta^{34}S$, ±0.5‰ for the $\delta^{18}O$ of SO_4^{2-}, ±1‰ for the $\delta^{15}N$ of NO_3^-, and ±2‰ for the $\delta^{18}O$ of NO_3^-. The isotopic analyses of the $\delta^{34}S$ and $\delta^{18}O$ were prepared at the laboratory of the Mineralogia Aplicada i Medi Ambient research group and analysed at the Centres Científics i Tecnològics of the Universitat de Barcelona; the isotopic analyses of $\delta^{15}N$ and $\delta^{18}O$ were prepared and analysed at the laboratory of the ISOFYS research group at Gent University.

Microbial analysis

During the experiment, the denitrifying population was quantified using the most probable number (MPN) method published by Saitoh et al. (2003). In addition, the total aerobic heterotrophic population was obtained using the miniaturised MPN method. Five millilitres of water was removed from the middle of the bioreactor until day 23 and processed within 6 hours of collection. To estimate the population density of the denitrifying

bacteria, the water sample was diluted up to a maximum of $1/10^{12}$. Nine 0.25-mL replicates of each dilution were placed in Eppendorf vials with 0.25 mL sterilised Nutrient Broth (NB) medium. The NB solution contained 6 g/L beef extract, 10 g/L peptone, 2 g/L $NaNO_3$, 0.05 g/L $NaNO_2$, 2 g/L agar, and 2.5 g/L HEPES. The pH of the NB was adjusted to 7.0 using a 0.1 M NaOH. Eppendorf vials containing the diluted sample and NB, were individually sealed with 1 mL overlaying solution containing 5 g/L agar and 8 g/L gellan gum to preserve the N_2 bubbles formed by the denitrifying bacteria. To calculate the population density of the heterotrophic bacteria, the diluted samples were added to microtiter plates using sterilised Tryptic Soy Broth (TSB) solution as a culture medium. Twenty-five microlitres of TSB was placed in each well and mixed with 25 μL diluted sample. Eight replicate wells per dilution were constructed. The positive tests were used to calculate the MPN of the heterotrophic organisms per millilitre of water.

3. Results

3.1 Outflow water before biostimulation

Before biostimulation, the experiment ran for 3 months. During this time, the outflow water was analysed to confirm that the sediment could not perform denitrification. The input water was described in Section 2.1. The outflow water before biostimulation had Eh of +180 mV and pH 8.5, similar to the input water. The NO_3^- concentration ranged from 0.77 mM to 0.84 mM, NO_2^- varied from 0.02 mM to 0.03 mM, SO_4^{2-} ranged from 3.23 mM to 3.54 mM, NH_4^+ varied from 0.09 mM to 0.1 mM and DOC concentration changed between 0.20 and 0.22 mM.

3.2 Outflow water during biostimulation

3.2.1 Redox potential and pH evolution

The Eh and pH during the experiment were measured every hour. The daily Eh average in the outflow displayed several increase-decrease steps varying from +170 mV to −370 mV with an overall trend towards the lower values (Fig. 2a). At stage I (C/N= 1.6), the Eh values decreased from +170 mV in the first sample to approximately −270 mV. During stage II (C/N=1.25), the Eh values ranged between −117 mV and −262 mV, and during stage III (C/N=1.12), the Eh varied from −186 to −370 mV (Fig. 2a). The daily average pH in the outflow ranged from 8.0 to 8.7 (Fig. 2b), remaining within the optimal range for denitrification (pH 7 – 9) (Aesoy et al., 1998). From the beginning of the experiment until day 18, the pH varied from 8.5 to 8.7. After

day 18, the pH decreased from 8.5 to approximately 8.1 at day 39. During the second stage, the pH in the outflow ranged from 8.0 to 8.3, while during the final stage, the pH varied from 8.0 to 8.4. (Fig. 2b)

a

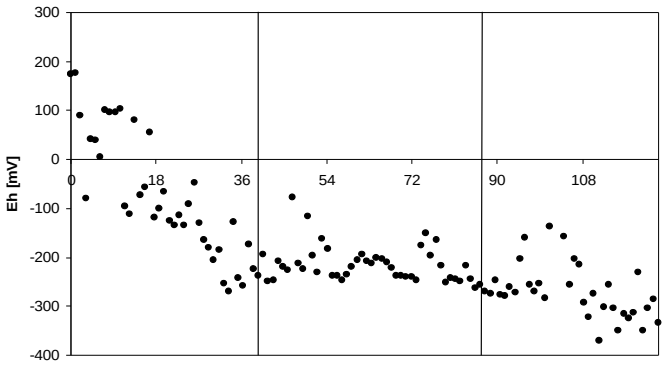

b

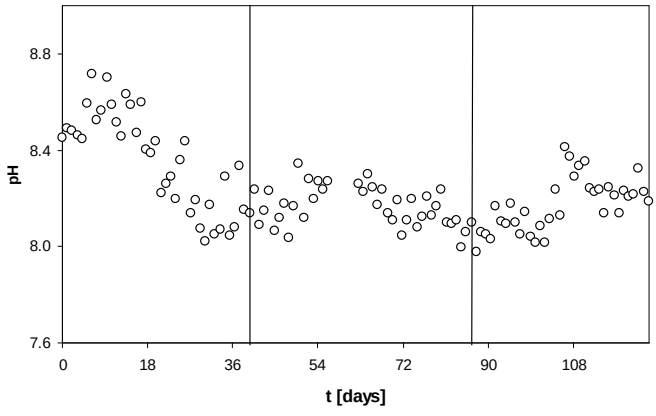

Figure 2. a,b: Average daily Eh (a) and pH (b) along the experiment.

3.2.2 Chemical data

The NO_3^- concentration in the outflow water varied from below the detection limit (< $3x10^{-3}$ mM) to 0.84 mM. During stage I, the NO_3^- concentration displayed several increase-decrease cycles (Fig. 3a). A cycle was observed after every glucose addition until day 18. A peak concentration of NO_3^- was observed during the first 36 hours, while from 36 to 72 hours, the lowest NO_3^- concentration was observed for each injection (Fig. 3a). Over time, the NO_3^- peak for each injection was lower than the previous peak until the 7^{th} injection (from day 18 to day 21); thereafter, NO_3^- was permanently below the detection limit in the outflow. During stage II, the C/N ratio was lowered to 1.25 to prevent sulphate reduction once NO_3^- was completely reduced. During this

period, the detected NO_3^- concentrations ranged from below the detection limit to 0.02 mM (Fig. 3b). At stage III, similar NO_3^- values were obtained at the outflow, ranging from below the detection limit to 0.02 mM (Fig. 3c).

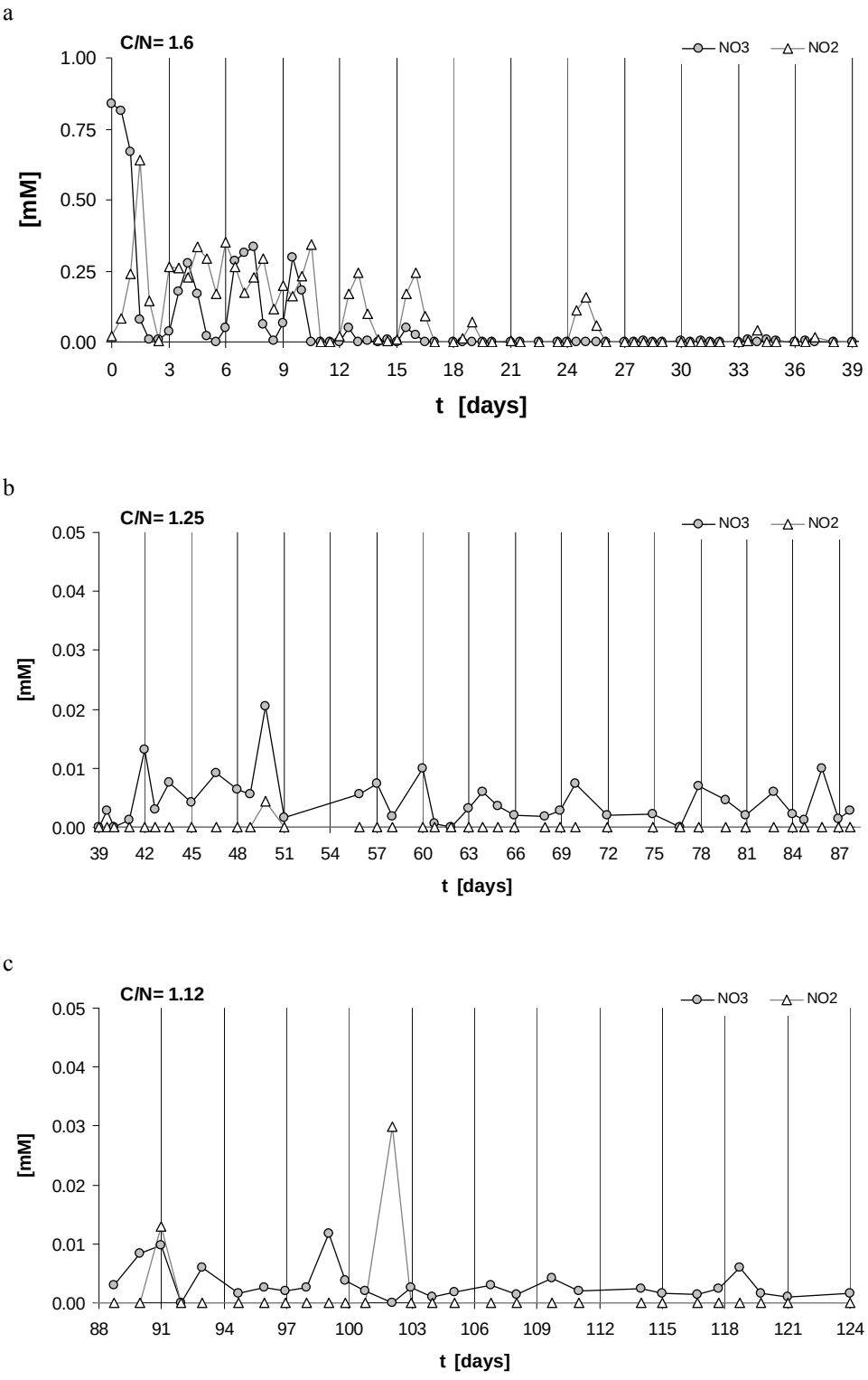

Figure 3. a, b c: NO_3^- and NO_2^- evolution during the experiment. a) Stage I C/N = 1.6, b) Stage II C/N = 1.25, c) Stage III C/N =1.12. *Note that the graph (a) has a different y-axis scale. Vertical lines represent the glucose injections.

Because it is associated with the NO_3^- reduction, NO_2^- was accumulated in the outflow during the first stage (up to day 27) but was observed infrequently after that day (Fig. 3). The NO_2^- concentration of the outflow samples ranged from below the detection limit (< $4x10^{-3}$ mM) to 0.64 mM. After the first injection, a NO_2^- peak was detected on day 1 (36 hours after the injection) that reached the highest NO_2^- concentration value during the experiment. Afterwards, the NO_2^- concentration decreased on day 2 (after 60 hours of glucose addition) and increased again until day 3 (24 hours after second injection). From day 3 to day 11, NO_2^- was observed in the outflow at a concentration ranging from 0.11 mM to 0.33 mM. Between days 12 and 27, the NO_2^- concentration increased during the first 24 hours after each glucose addition and decreased between 24 and 72 hours. From day 27 until the end of the experiment (including stages II and III), most of the samples (90%) showed NO_2^- contents below the detection limit, and the samples with detectable NO_2^- had concentrations up to 0.04 mM (Fig. 3b and c).

During the experiment, the NH_4^+ content decreased in the outflow samples from 0.10 mM (measured in the first sample) down to 0.04 mM at day 3. From day 3 to day 10, NH_4^+ increased to 0.07 mM and decreased thereafter to 0.02 mM; the NH_4^+ content remained between 0.01 mM and 0.02 mM in the samples analysed until the end of the experiment (Fig. 4). The SO_4^{2-} concentration in the outflow during stage I ranged from 3.23 mM to 3.62 mM. During stage II, the SO_4^{2-} varied from 3.15 mM to 3.58 mM, and in stage III, it varied from 3.25 mM to 3.53 mM (not shown).

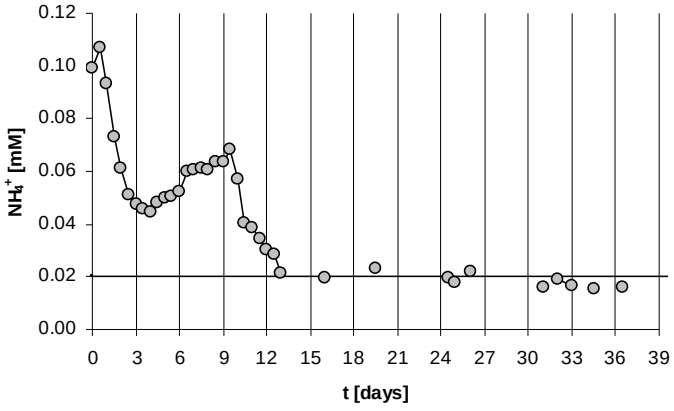

Figure 4. NH_4^+ concentration in the outflow during the first period (C/N =1.6). Horizontal line represents the input concentration, and the vertical lines represent the glucose injections.

3.2.3 Isotopic results

A subset containing 16 samples was selected based on the NO_3^- concentrations and isotopically analysed. During NO_3^- reduction, the isotopic composition increased from +9.5‰ to +39.5‰ for $\delta^{15}N\text{-}NO_3^-$ and from +3.3‰ to +39.9‰ for $\delta^{18}O\text{-}NO_3^-$ (Fig. 5). The observed increase in δ values agrees with a NO_3^- concentration decrease from 0.88 mM to 0.05 mM. Furthermore, $\delta^{15}N$ was linearly related to $\delta^{18}O$ and had a slope of 0.95 (R^2=0.88) (Fig. 5); this value is common for denitrification reactions (Böttcher et al., 1990). For SO_4^{2-}, a subset containing 9 samples with different SO_4^{2-} concentrations was analysed to determine the isotopic composition of $^{34}S_{SO4}$ and $^{18}O_{SO4}$. The initial isotopic composition of sulphate was −17.0‰ for $\delta^{34}S$ and +5.1‰ for $\delta^{18}O$. The analysed outflow water revealed a narrow range of $\delta^{34}S$ between −17.1‰ and −17.2‰, while $\delta^{18}O$ varied from +5.2 ‰ to +5.8 ‰ (Fig. 6).

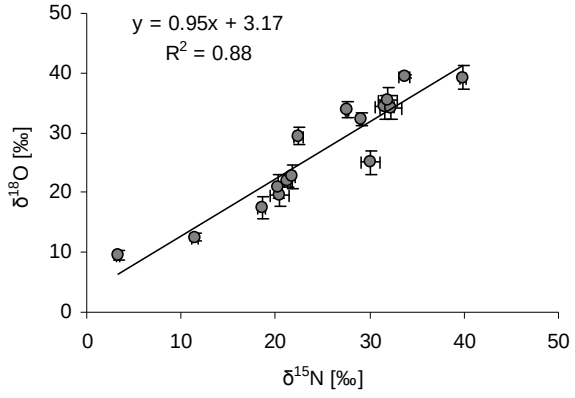

Figure 5. $\delta^{15}N$ plotted against $\delta^{18}O$ to display a positive linear trend with a slope of 0.92 (typical for the denitrification process).

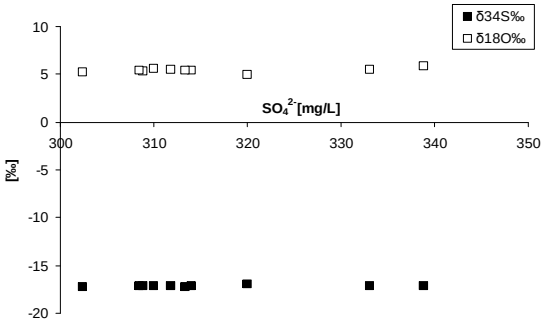

Figure 6. $\delta^{34}S\text{-}SO_4^{2-}$ and $\delta^{18}O\text{-}SO_4^{2-}$ for samples with different SO_4^{2-} concentrations.

3.3 C-$C_6H_{12}O_6$ concentration

Glucose concentrations were measured in the outflow during the first 72 hours after selected injections during the experiment (the 1st, 7th, 10th, 14th, 17th, 19th, 30th, 34th and 39th injections). The $C\text{-}C_6H_{12}O_6$ concentration in

the outflow varied from below the detection limit (<0.06 mM) to 1.07 mM. The concentration of C-$C_6H_{12}O_6$ revealed a linear increase starting from the injection and lasting 48 hours until a C-$C_6H_{12}O_6$ concentration peak was observed. Then, the concentration decreased until the next glucose injection (72 hours later). During stage I, the C-$C_6H_{12}O_6$ peak ranged from below 0.95 mM to 1.07 mM; whereas 72 hours after every injection, the C-$C_6H_{12}O_6$ concentration ranged from 0.08 mM to 0.43 mM (Fig. 7a). During stage II, the peak of C-$C_6H_{12}O_6$ in the outflow samples ranged from 0.53 mM to 0.71 mM, and the concentration after 72 hours from each injection ranged from 0.32 mM to 0.50 mM (Fig. 7b). With regards to stage III, the peak was not observed and the C-$C_6H_{12}O_6$ concentration in the outflow samples ranged from below the detection limit to 0.35 Mm (Fig. 7c).

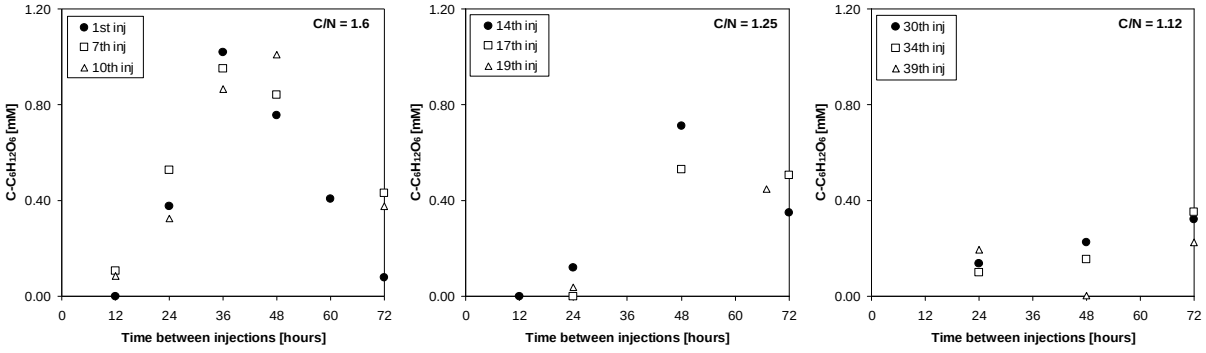

Figure 7. a, b, c: C-$C_6H_{12}O_6$ concentration measured every 12 hours for the 72 hours after the selected injections. a) C/N =1.6 (1st, 7th, and 10th injections), b) C/N =1.25 (14th, 17th, and 19th), c) C/N =1.12 (30th, 34th, and 39th).

3.4 MPN results

The first sample used for MPN analysis was removed before the first glucose injection to establish the initial number of denitrifying and heterotrophic bacteria in the system. Subsequent sampling was performed on days 2, 5, 8, and 23. Before biostimulation, the denitrifying bacteria population contained $4.4x10^0$ MPN cells mL^{-1}, representing 0.2% of the total heterotrophic bacteria. After the first injection, the denitrifying bacteria increased drastically. At day 23 (540 hours), when the NO_3^- attenuation was nearly complete, the denitrifying bacteria population was $1.2x10^6$ MPN cells/mL, reaching 28% of the total heterotrophic bacteria. The heterotrophic population displayed a similar increase from $2.5x10^3$ MPN cells/mL at the beginning of the experiment to over $4.3x10^6$ MPN cells/mL after 23 days (Table 1).

Table 1: Bacteria enumeration results. T: time. Den.: denitrifying bacteria, MPN cells/*mL. Het: heterotrophic bacteria,* MPN cells/*mL. %Den.:* percentage of denitrifying organisms

T [day]	Den.	Het.	% Den.
0	$4.40x10^{0}$	$2.50x10^{3}$	0.2
2	$3.20x10^{2}$	$1.80x10^{4}$	2
5	$2.70x10^{4}$	$1.50x10^{5}$	18
8	$6.70x10^{5}$	$3.30x10^{6}$	20
23	$1.20x10^{6}$	$4.30x10^{6}$	28

4 Discussion

4.1 NH_4^+ generation before biostimulation

Before glucose biostimulation, the NH_4^+ concentration measured in the outflow water was higher than the input water concentration. This increase in NH_4^+ could indicate the occurrence of DNRA in the reactor but could also be generated by remineralisation of organic matter in the sediment. Remineralisation can be ruled out since this process should not be affected once glucose was injected in the system in contrast with the NH_4^+ trend observed in the outflow after the glucose inoculation. Therefore, it is reasonable to assume that DNRA reaction was the main source of the NH_4^+ generated in the system previous biostimulation. In addition, the NO_2^- detected in the outflow was likely produced by an incomplete DNRA reaction. DNRA occurs in environments with high C and low NO_3^- contents (Burgin and Hamilton, 2007; Lind et al., 2013). In the present study, NH_4^+ was produced with a lower C content and NO_3^- in excess. The NO_3^- reduction pathway depends on the biomass present in the system, that is controlled by the type of organic carbon available (Nijburg et al., 1998). In addition, Abell et al. (2009) reported that fermentative bacteria are able to use organic substrates that are unavailable for nitrate reducers. The reactive organic carbon available for denitrification in the sediment was completely consumed in the natural attenuation experiment but it represented only the 3% of total carbon from the sediment (Carrey et al., 2013). Therefore, the remaining organic carbon present in the sediment could not promote denitrification, although fermentative bacteria were able to use it to promote DNRA despite the low C/N ratio. The amount of NO_3^- reduced before the biostimulation began was calculated using a stoichiometric reaction of DNRA: 1 mol of NO_3^- produces 1 mol of NH_4^+. The amount of NO_3^- reduced by the DNRA in the column before the first glucose injection was approximately 0.10 mM, agreeing with the difference between the input (0.88 mM) and outflow NO_3^- concentrations (which ranged from 0.77 mM to 0.84 mM).

4.2 Denitrification enhanced by biostimulation

Once glucose was added to the system, NO_3^- reduction increased rapidly, implying that bacteria capable of using carbon to reduce NO_3^- were present in the sediment. Therefore, autochthonous bacteria adapted rapidly once a carbon source was available. Successive glucose injections produced an exponential increase in both heterotrophic and denitrifying bacteria. The proportion of denitrifying organisms increased from almost negligible levels (<1%) to approximately 28% (Table 1). The bacteria enumeration measured in this study was significantly lower than in previous studies. For instance, Vidal-Gavilan et al. (2013) obtained approximately 10^8 MPN cells/mL of denitrifying bacteria in glucose-amended batch experiments; this result was two orders of magnitude higher than the MPN found in our experiment. This disparity in the bacteria count might be caused by differences in the experimental design (batch versus flow-through) and conditions, such as nitrogen and carbon supply. Along with this increase in denitrifying bacteria, the NO_3^- and NH_4^+ concentrations decreased in the outflow. As described in section 4.1, DNRA reaction consumed 0.1 mM of NO_3^- previous to biostimulation. When glucose was injected, the generated NH_4^+ decreased likely because the reaction was repressed, and therefore the amount of NO_3^- consumed by this reaction also decreased. If the DNRA reaction is enhanced by glucose injection an increase in NH_4^+ concentration in the outflow should be observed. In the experiment after 13 days the NH_4^+ concentration in the outflow showed similar values than the input water, supporting that DNRA was completely repressed (Fig. 4). This finding suggests that the role of DNRA in the removal of NO_3^- during the experiment was limited and decreased over time. Therefore, NO_3^- attenuation was mostly linked to denitrification. Because denitrification is the main NO_3^- reduction process, NO_2^- observed at the first stage was predominantly attributed to incomplete denitrification. During the experiment, NO_2^- persisted until day 27, remaining in the outflow even after NO_3^- was completely removed. This lag in the NO_2^- reduction was produced because bacteria preferentially use NO_3^- at the beginning of the induced denitrification processes when NO_3^- and NO_2^- were available, accumulating NO_2^- when the nitrite reductase was repressed (Kraft et al., 2011; Strohm et al., 2007 and references therein). Similar NO_2^- accumulation was reported when glucose was used as an electron donor instead of other carbon sources, such as methanol or acetate (Ge et al., 2012). In addition, NO_2^- accumulation may also be related to pH. Samples with detectable NO_2^- concentrations had a pH ranging from 8.4 to 8.7; these values are within the range that inhibits the NO_2^- reduction (between 8.5 and 9.0) (Glass and Silverstein, 1998). However, when the pH in the outflow was lower than 8.4, the NO_2^- content was below the detection limit (Fig. 8). Changing the C/N ratio did not affect the complete NO_3^- reduction, revealing that stable

conditions were reached inside the reactor. With regards N_2O generation, the presence of easily degradable C substrates has been reported to increase denitrification and may decrease the N_2O/N_2 product ratio of denitrification (Senbaryram et al., 2012, Weier et al, 1993, Welti et al, 2012). As in the present work organic carbon is periodically inoculated, and denitrification increased achieving complete NO_3^- consumption, N_2O should be converted to N_2 and not be accumulated and/or expelled during the experiment.

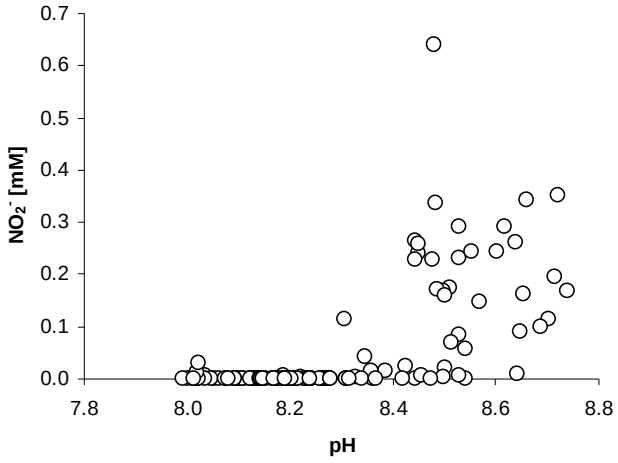

Figure 8. NO_2^- accumulation vs. pH. NO_2^- was usually detected on samples with pH > 8.4.

In addition to NO_2^-, H_2S is also an undesirable compound in biostimulation processes. Sulphate reduction may be promoted when NO_3^-, as well as the dissolved Mn and Fe, have been entirely consumed but organic carbon is still available. The input water contained Fe and Mn concentrations below the detection limit ($<2x10^{-3}$ mM and $<2x10^{-4}$ mM, respectively); therefore, once the NO_3^- was completely consumed, SO_4^{2-} reduction could occur according to the redox sequence in natural systems (Stumn and Morgan, 1996). During the experiment, the NO_3^- concentration in the outflow water was below the detection limit after day 10. Most of these samples appeared during the first stage (when more glucose was injected). In addition, the Eh was below the values reported to promote SO_4^{2-} reduction (<–150 mV) (Connell and Patrick Jr. 1968). Therefore, once NO_3^- was completely removed, the excess glucose could be used to promote SO_4^{2-} reduction, producing variations in the SO_4^{2-} concentration between the input (3.54 mM) and outflow water (3.15 mM). If this variation in the SO_4^{2-} concentration was caused by SO_4^{2-} reduction reactions, then changes in $\delta^{34}S_{SO4}$ and $\delta^{18}O_{SO4}$ should be produced. Isotopic fractionation values of the S_{SO4} reported in groundwater studies ranges from –33.1‰ (Massmann et al., 2003) to –9.7‰ (Strebel et al., 1990). After accounting for these isotopic fractionation

factors, a Rayleigh distillation process (similar to Eq. 4 or 5 using SO_4^{2-} instead of NO_3^-) was applied. If SO_4^{2-} reduction processes took place in the column, an increase in the isotopic composition of $\delta^{34}S_{SO4}$ between 1‰ and 4‰ should be observed in the outflow samples. However, the measured $\delta^{34}S_{SO4}$ remained constant at −17.1‰ ±0.2‰ (Fig. 6), indicating that the SO_4^{2-} reduction was not occurring; this result occurred even though glucose remained in most of the outflow samples, revealing an excess of labile carbon. Once NO_3^- was completely consumed, the residence time of water inside the reactor was too short to promote sulphate reduction. Although in the present work the SO_4^{2-} reduction was not observed, an excess of available glucose is undesirable because this reaction could occur during field-tests.

4.3 Organic carbon balance

The C-$C_6H_{12}O_6$ concentration in the outflow decreased over time (Fig. 5). The mass of the C-$C_6H_{12}O_6$ discharged between two successive injections may be obtained by adding the glucose concentration multiplied by the volume of each sample during that period (L). The mass of the discharged C-$C_6H_{12}O_6$ ranged from 0.21 mmol to 0.24 mmol during stage I, from 0.12 mmol to 0.21 mmol for stage II and between 0.06 mmol and 0.12 mmol for stage III. This progressive depletion was caused by the increasing success of the NO_3^- removal, as well as by changes in the mass of the injected glucose. However, glucose was detected in most of the outflow samples, regardless of whether the C/N ratio was stoichiometric or lower, and NO_3^- was completely removed. The amount of secondary C was obtained by subtracting the reactive C from glucose (C-$C_6H_{12}O_6$ injected – C-$C_6H_{12}O_6$ discharge) over 72 hours from the C used to reduce NO_3^-, following Eq. 2. The results indicated that a supplementary C source was necessary to promote the observed NO_3^- attenuation for every injection, except for the first one (Table 2). The additional mass of C required ranged from 0.08 mmol to 0.17 mmol for every injection, representing between 20% and 35% of the total C used to remove NO_3^-. Apart from glucose, the secondary C-sources in the system might include i) the DOC from the input water with a concentration of 0.21 mM; or ii) the C from the biomass growing inside the reactor. The use of dead and lysed cells as the C-source has been reported during studies of induced denitrification (Koenig et al., 2005; Torrentó et al., 2011). The NO_3^- removal by heterotrophic denitrification in these studies using biomass as the secondary C source was approximately 35%, agreeing with the percentage of NO_3^- removed by the secondary source in the current work. However, the DOC in the input water cannot be ruled out as a secondary C source. The presence of

different C sources must be accounted for minimising the glucose concentration after NO_3^- has been completely consumed in groundwater.

Table 2: C balance of the system for the injections analyzed. C_{inj}: $C_{C6H12O6}$ Injected; C_{dis}; $C_{C6H12O6}$ Discharged; C_{NO3} ; $C_{C6H12O6}$consumed

Nº injection C/N 1.6	$C_{C6H12O6}$ injected [mmol]	$C_{C6H12O6}$ Discharged [mmol]	C_{NO3} consumed [mmol]	Secondary C = C_{NO3} – (C_{inj} – C_{dis}) [mmol]
1st	0.60	0.20	0.32	-0.08
7th	0.60	0.25	0.47	+0.12
10th	0.60	0.22	0.46	+0.09
C/N 1.25				
14th	0.47	0.14	0.45	+0.12
17th	0.47	0.16	0.47	+0.17
19th	0.47	0.12	0.42	+0.08
C/N 1.12				
30th	0.47	0.10	0.50	+0.13
34th	0.47	0.09	0.50	+0.12
39th	0.47	0.07	0.51	+0.11

4.4 Fractionation of N and O

Induced denitrification at field scale may be masked by several processes, such as dispersion, diffusion, or dilution (mixing) that change the NO_3^- concentration in the groundwater. The isotopic fractionation factor (ε) of N and O for dissolved NO_3^- allows the biodegradation rate produced by biostimulation to be quantified. The ε value was obtained using a linear regression between ln[NO_3^-] and both $\delta^{15}N$ and $\delta^{18}O$ (Fig. 9). A plot of $\delta^{15}N$ or $\delta^{18}O$ versus ln[NO_3^-] should reveal a linear correlation if denitrification occurs (Kendall et al., 2007). The studied samples displayed an acceptable correlation of these parameters (R^2=0.90 for εN and R^2=0.80 for εO) (Fig. 9). The ε values attained were ‒8.8‰ ±1‰ for $\delta^{15}N$ and ‒8.0‰ ±2‰ for εO.

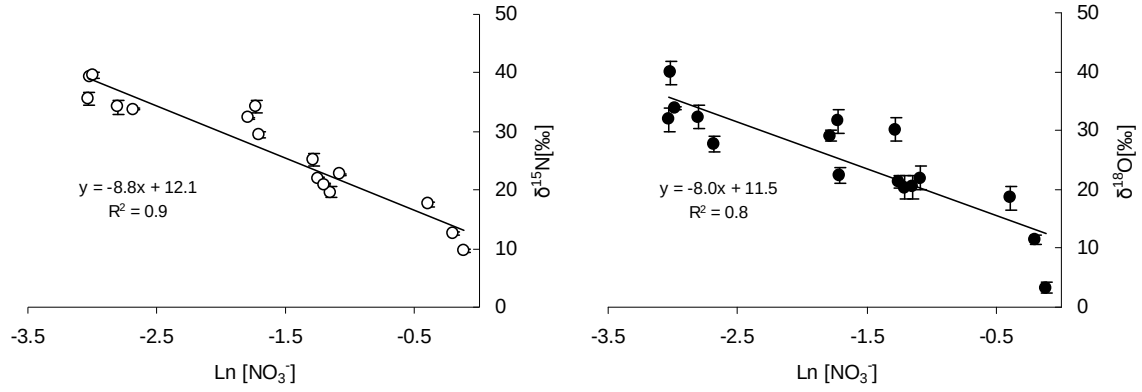

Figure 9. $\delta^{15}N$ and $\delta^{18}O$ of NO_3^- against the natural logarithm of the NO_3^- concentration [mM]. Slopes of the regression lines represent the isotopic fractionation factor for N and O. Error bars represent the standard deviation of the replicates.

As was stated above, before the biostimulation experiment was carried out, the intrinsic potential of the sediment to promote denitrification was isotopically characterised. The isotope fractionation values for natural denitrification obtained varied between ‑15.7‰ and ‑11.6‰ for εN and ‑13.8‰ and ‑12.1‰ for εO (Carrey et al., 2013). Therefore, the isotopic fractionation values for both N and O calculated during natural attenuation were significantly higher (in absolute values) than the values calculated during the induced attenuation experiment, most likely because the natural process displayed slower kinetics. Different isotope effects may be related to the variations in the denitrification rate constant (Mariotti et al., 1988). The denitrification rate was higher during induced denitrification, producing the observed lower isotopic effect. These variations in the denitrification rate might be related to the specific C source used for biostimulation being different than the C-natural sources present in the sediment, affecting the evolution of the microbial populations and, consequently, the denitrification kinetics (Song and Tobias, 2011).

The isotopic fractionation factor of induced heterotrophic denitrification in flow-through experiments has not yet been reported. The εN and εO values obtained during this study were lower (in absolute values) than the values calculated for biostimulation batch experiments using glucose as the C source. For instance, Vidal-Gavilan et al. (2013) obtained εN values of ‑17.1‰ and εO of ‑15.2‰, but Delwiche and Steyn (1970) used glucose as the electron donor for the *Pseudomonas denitrificans* strain and obtained εN values ranging from ‑13.4‰ to ‑20.8‰. The observed differences might be linked to the differences in the experimental protocol. Therefore, the conditions inside the reactor, such as the pH, C/N ratio,

temperature, or soil characteristics, might affect the community structure of the denitrifying bacteria that control the denitrification rate constant (Braker et al., 2001; Cavigelli and Robertson, 2000; Holtan-Hartwig et al., 2000) and, therefore, the isotopic fractionation (Mariotti et al., 1988).

Compared to other fractionation factors reported in the literature, in the current study, the εN values fall inside the range for biostimulation experiments using alternative carbon sources that varied from –5‰, reported by Bryan et al. (2013) using succinate, to –39‰ attained by Toyoda et al. (2005) using acetylated citrate. With respect to εO, fewer values have been reported in the literature. Isotopic fractionation performed in lab-scale experiments using different denitrifying bacteria species and electron donors ranged from -27.6‰, obtained during an induced autotrophic denitrification (Torrentó et al., 2011), to +32‰ measured in pure cultures with inversed isotopic fractionation (Toyoda et al., 2005). The εN/εO obtained in the present biostimulation study was 1.08 ±0.04. This value agreed with the ratios determined for the natural denitrification in the Pétrola basin; these values oscillated between 0.96 and 1.14 (Carrey et al., 2013) and were also similar to the ratio obtained by (Vidal-Gavilan et al., 2013) during their glucose experiments (εN/εO=1.13). Furthermore, the value obtained in the present study fell within the range of field-scale εN/εO ratios (0.9 – 2.3) (Otero et al., 2009 and references therein).

5 Conclusions

The viability of periodically injecting glucose to remove NO_3^- from groundwater was tested with flow-through experiments using a nearly stoichiometric C/N ratio. The glucose inoculation enhanced the denitrification and repressed the DNRA observed before biostimulation. The NO_3^- was completely attenuated 13 days after the beginning of biostimulation. However, significant NO_2^- accumulation was observed in the outflow water until day 27, most likely because the nitrite reductase was enzymatically repressed and the pH was high during the first stage of the experiment. Controlling the pH might be useful for decreasing the lag time for NO_2^- accumulation. The isotopic results for $\delta^{34}S\text{-}SO_4^{2-}$ indicated that the SO_4^{2-} reduction did not generate H_2S during the experiment, even though glucose was available after complete NO_3^- removal, due to kinetic effects/reasons. Using a substoichiometric C/N ratio reduced the glucose outflow; however, complete NO_3^- attenuation was still achieved because secondary C sources such as DOC of input water and the biomass were available. Nitrate was isotopically fractionated: εN = 8.8‰ and εO = 8.0‰, with a εN/εO ratio = 1.08. These values were lower (in absolute values) than those

observed during the natural sediment denitrification and in other induced attenuation experiments using glucose. Overall, periodically injecting an organic carbon source might be a suitable method to remove NO_3^- from groundwater during long-term treatments. The strategy tested at laboratory-scale reliably removed all NO_3^- after 13 days when the C/N ratio was close to or slightly below the stoichiometric value. The data obtained in this study support a continuing investigation using a field-scale/pilot-test assay.

Acknowledgments

This work was financed by a grant (PEIC11-0135-8842) from the Castilla La Mancha Government, the CICYT-CGL2011-29975-C04-01 and CICYT-CGL2011-29975-C04-02 projects from the Spanish Government, and the 2009SGR 103 project from the Catalan Government. The authors would like to thank the "Centres Científics i Tecnològics" of the "Universitat de Barcelona" for the chemical and isotopic analyses.

References

Abell, J., Laverman, A.M., Cappellen, P., 2009. Bioavailability of organic matter in a freshwater estuarine sediment: long-term degradation experiments with and without nitrate supply. Biogeochemistry 94, 13–28.

Aesoy, A., Odegaard, H., Bach, K., Pujol, R., Hamon, M., 1998. Denitrification in a packed bed biofilm reactor (Biofor) - Experiments with different carbon sources. Water Res. 32, 1463–1470.

Akunna, J.C., Bizeau, C., Moletta, R., 1993. Nitrate and nitrite reductions with anaerobic sludge using various carbon sources: glucose, acetic acid, lactic acid and methanol. Water Res. 27, 1303–1312.

Aravena, R., Robertson, W.D., 1998. Use of multiple isotope tracers to evaluate denitrification in ground water: Study of nitrate from a large-flux septic system plume. Ground Water 36, 975–982.

Barford, C.C., Montoya, J.P., Altabet, M. a, Mitchell, R., 1999. Steady-state nitrogen isotope effects of N_2 and N_2O production in Paracoccus denitrificans. Appl. Environ. Microbiol. 65, 989–94.

Borden, A.K., Brusseau, M.L., Carroll, K.C., McMillan, A., Akyol, N.H., Berkompas, J., Miao, Z., Jordan, F., Tick, G., Waugh, W.J., Glenn, E.P., 2011. Ethanol addition for enhancing denitrification at the uranium mill tailing site in monument valley, AZ. Water Air Soil Pollut. 223, 755–763.

Böttcher, J., Strebel, O., Voerkelius, S., Schmidt, H.L., 1990. Using isotope fractionation of nitrate-nitrogen and nitrate-oxygen for evaluation of microbial denitrification in a sandy aquifer. J. Hydrol. 114, 413–424.

Braker, G., Ayala-del-Río, H.L., Devol, A.H., Fesefeldt, A., Tiedje, J.M., 2001. Community structure of denitrifiers, bacteria, and archaea along redox gradients in Pacific Northwest marine sediments by terminal restriction fragment length polymorphism analysis of amplified nitrite reductase (nirS) and 16S rRNA genes. Appl. Environ. Microbiol. 67 (4), 1893-1901.

Bryan, B.A., Shearer, G., Skeeters, L., Kohl, D.H., 2013. Variable expression of the nitrogen isotope effect associated with denitrification of nitrite. J. Biol.Chem. 258 (14), 8613–8617.

Burgin, A.J., Hamilton, S.K., 2007. Have we overemphasized the role of denitrification in aquatic ecosystems? A review of nitrate removal pathways. Front. Ecol. Environ. 5, 89–96.

Carrey, R., Otero, N., Soler, A., Gómez-Alday, J.J., Ayora, C., 2013. The role of lower Cretaceous sediments in groundwater nitrate attenuation in central Spain: Column experiments. Appl. Geochem. 32, 142–152.

Casciotti, K.L., Sigman, D.M., Hastings, M.G., Böhlke, J.K., Hilkert, A., 2002. Measurement of the oxygen isotopic composition of nitrate in seawater and freshwater using the denitrifier method. Anal. Chem. 74 (19), 4905–12.

Cavigelli, M., Robertson, G., 2000. The functional significance of denitrifier community composition in a terrestrial ecosystem. Ecol. 81 (5), 1402–1414.

Comly, H.H., 1945. Cyanosis in infants caused by nitrates in well water. J. Am. Med. Assoc. 129, 112–116.

Connell, W.E., Patrick Jr., W.H., 1968. Sulfate reduction in soil: Effects of redox potential and pH. Sci. 159, 86–87.

De Beer, D., Schramm, a, Santegoeds, C.M., Kuhl, M., 1997. A nitrite microsensor for profiling environmental biofilms. Appl. Environ. Microbiol. 63, 973–977.

Delwiche, C.C., Steyn, P.L., 1970. Nitrogen isotope fractionation in soils and microbial reactions. Environ. Sci. & Technol. 4, 929–935.

Dogramaci, S.S., Herczeg, A.L., Schi, S.L., Bone, Y., 2001. Controls on $\delta^{34}S$ and $\delta^{18}O$ of dissolved sulfate in aquifers of the Murray Basin, Australia and their use as indicators of flow processes. Appl. Geochem. 16, 475-488.

Fernández-Nava, Y., Marañón, E., Soons, J., Castrillón, L., 2010. Denitrification of high nitrate concentration wastewater using alternative carbon sources. J. Hazard. Mater. 173, 682–8.

Ge, S., Peng, Y., Wang, S., Lu, C., Cao, X., Zhu, Y., 2012. Nitrite accumulation under constant temperature in anoxic denitrification process: The effects of carbon sources and COD/NO_3-N. Bioresource Technol. 114, 137–43.

Glass, C., Silverstein, J.A., 1998. Denitrification kinetics of high nitrate concentration water: pH effect on inhibition and nitrite accumulation. Water Res. 32, 831–839.

Gómez, M. A., González-López, J., Hontoria-García, E., 2000. Influence of carbon source on nitrate removal of contaminated groundwater in a denitrifying submerged filter. J. Hazard. Mater. 80, 69–80.

Granger, J., Sigman, D.M., 2009. Removal of nitrite with sulfamic acid for nitrate N and O isotope analysis with the denitrifier method. Rapid Commun. Mass Spectrom. 23, 3753–3762.

Holtan-Hartwig, L., Do, P., Reier, L., 2000. Comparison of denitrifying communities in organic soils: kinetics of NO_3^- and N_2O reduction. Soil Biol. Biochem. 32, 833–843.

Istok, J.D., Senko, J.M., Krumholz, L.R., Watson, D., Bogle, M. A., Peacock, A, Chang, Y.J., White, D.C., 2004. In situ bioreduction of technetium and uranium in a nitrate-contaminated aquifer. Environ. Sci. & Technol. 38, 468–75.

Kendall, C., Elliott, E.M., Wankel, S.D., 2007. Tracing antropogenic inputs of nitrogen to ecosystems, Chapter 12, In: Michener, R.H., Lajtha, K. (Eds.), Stable Isotopes in Ecol. and Environ. Sci.. second ed. Blackwell, 375–450.

Khan, I. A., Spalding, R.F., 2004. Enhanced in situ denitrification for a municipal well. Water Res. 38, 3382–8.

Knowles, R., 1982. Denitrification. Microbiol. Rev. 46, 43–70.

Koenig, A., Zhang, T., Liu, L.-H., Fang, H.H.P., 2005. Microbial community and biochemistry process in autosulfurotrophic denitrifying biofilm. Chemosphere 58 (8), 1041–1047.

Korom, S.F., 1992. Natural denitrification in the saturated zone: A review. Water Resour. Res. 28 (6), 1657–1668.

Kraft, B., Strous, M., Tegetmeyer, H.E., 2011. Microbial nitrate respiration-genes, enzymes and environmental distribution. J. Biotechnol. 155, 104–117.

Lee, N.M., Welander, T., 1996. The effect of different carbon sources on respiratory denitrification in Biol. wastewater treatment. J. Ferment. Bioeng. 82, 277–285.

Leverenz, H.L., Haunschild, K., Hopes, G., Tchobanoglous, G., Darby, J.L., 2010. Anoxic treatment wetlands for denitrification. Ecol. Eng. 36, 1544–1551.

Lind, L.P.D., Audet, J., Tonderski, K., Hoffmann, C.C., 2013. Nitrate removal capacity and nitrous oxide production in soil profiles of nitrogen loaded riparian wetlands inferred by laboratory microcosms. Soil Biol. Biochem. 60, 156–164.

Magee, P.N., Barnes, J.M., 1956. The production of malignant primary hepatic tumours in the rat by feeding dimethylnitrosamine. British J. Cancer 10, 114–22.

Mariotti, A., Landreau, A., Simon, B., 1988. ^{15}N isotope biogeochemistry and natural denitrification process in groundwater: Application to the chalk aquifer of northern France. Geochim. Cosmochim. Acta 52, 1869–1878.

Martin, D., Salminen, J.M., Niemi, R.M., Heiskanen, I.M., Valve, M.J., Hellstén, P.P., Nystén, T.H., 2009. Acetate and ethanol as potential enhancers of low temperature denitrification in soil contaminated by fur farms: A pilot-scale study. J. Hazard. Mater. 163 (2-3), 1230–1238.

Massmann, G., Tichomirowa, M., Merz, C., Pekdeger, a., 2003. Sulfide oxidation and sulfate reduction in a shallow groundwater system (Oderbruch Aquifer, Germany). J. Hydrol. 278, 231–243.

Nijburg, J.W., Gerards, S., Laanbroek, H.J., 1998. Competition for nitrate and glucose between *Pseudomonas Fluorescens* and *Bacillus Licheniformis* under continuous or fluctuating anoxic conditions. Microbiol. Ecol. 26, 345–356.

Osaka, T., Shirotani, K., Yoshie, S., Tsuneda, S., 2008. Effects of carbon source on denitrification efficiency and microbial community structure in a saline wastewater treatment process. Water Res. 42, 3709–3718.

Otero, N., Torrentó, C., Soler, A., Menció, A., Mas-Pla, J., 2009. Monitoring groundwater nitrate attenuation in a regional system coupling hydrogeology with multi-isotopic methods: The case of Plana de Vic (Osona, Spain). Agric. Ecosyst. Environ. 133, 103–113.

Pauwels, H., Foucher, J.C., Kloppmann, W., 2000. Denitrification and mixing in a schist aquifer: influence on water chemistry and isotopes. Chem. Geol. 168, 307–324.

Peng, Y.Z., Ma, Y., Wang, S.Y., 2007. Denitrification potential enhancement by addition of external carbon sources in a pre-denitrification process. J. Environ. Sci. 19, 284–289.

Saitoh, S., Iwasaki, K., Yagi, O., 2003. Development of a most-probable-number method for enumerating denitrifying bacteria by using 96-well microtiter plates and anaerobic culture system. Microbes Environ. 18, 210─215.

Schipper, L.A., Vojvodic, M., 2000. Nitrate removal from groundwater and denitrification rates in a porous treatment wall amended with sawdust. Ecol. Eng. 14, 269–278.

Senbayram, M., Chen, R., Budai, A., Bakken, L., Dittert, K., 2011. N_2O emission and the $N_2O/(N_2O + N_2)$ product ratio of denitrification as controlled by available carbon substrates and nitrate concentrations. Agri. Ecosyst. Environ. 147, 4-12

Sigman, D.M., Casciotti, K.L., Andreani, M., Barford, C., Galanter, M., Böhlke, J.K., 2001. A bacterial method for the nitrogen isotopic analysis of nitrate in seawater and freshwater. Anal. Chem. 73, 4145–53.

Song, B., Tobias, C.R., 2011. Molecular and stable isotope methods to detect and measure anaerobic ammonium oxidation (anammox) in aquatic ecosystems. Methods Enzymol. 496, 63–89 .

Strebel, O., Böttcher, J., Fritz, P., 1990. Use of isotope fractionation of sulfate-sulfur and sulfate-oxygen to assess bacterial desulfurication in a sandy aquifer. J. Hydrol. 121, 155–172.

Strohm, T.O., Griffin, B., Zumft, W.G., Schink, B., 2007. Growth yields in bacterial denitrification and nitrate ammonification. Appl. Environ. Microbiol. 73, 1420–1424.

Stumm, W., Morgan, J.J., 1996. Aquatic chemistry: chemical equilibria and rates in natural waters. John Wiley and Sons. New York, 1022 pp.

Tartakovsky, B., Millette, D., Delisle, S., Guiot, S.R., 2002. Ethanol-stimulated bioremediation of nitrate-contaminated ground water. Ground Water Monit. Remediat. 22, 78–87.

Torrentó, C., Urmeneta, J., Otero, N., Soler, A., Viñas, M., Cama, J., 2011. Enhanced denitrification in groundwater and sediments from a nitrate-contaminated aquifer after addition of pyrite. Chem. Geol. 287, 90–101.

Toyoda, S., Mutobe, H., Yamagishi, H., Yoshida, N., Tanji, Y., 2005. Fractionation of N_2O isotopomers during production by denitrifier. Soil Biol. Biochem. 37, 1535–1545.

Trois, C., Pisano, G., Oxarango, L., 2010. Alternative solutions for the bio-denitrification of landfill leachates using pine bark and compost. J. Hazard. Mater. 178 (1-3), 1100–1105.

Vidal-Gavilan, G., Folch, A., Otero, N., Solanas, A. M., Soler, A., 2013. Isotope characterization of an in situ biodenitrification pilot-test in a fractured aquifer. Appl. Geochem. 32, 153–163.

Vitòria, L., Soler, A, Canals, A, Otero, N., 2008. Environmental isotopes (N, S, C, O, D) to determine natural attenuation processes in nitrate contaminated waters: Example of Osona (NE Spain). Appl. Geochem. 23, 3597–3611.

Vitousek, P.M., Aber, J.D., Howarth, R.W., Likens, G.E., Pamela, A., Schindler, D.W., Schlesinger, W.H., Tilman, D.G., 1997. Human alteration of the global nitrogen cycle: Sources and consequences. Ecol. Appl. 7, 737–750.

Ward, M.H., deKok, T.M., Levallois, P., Brender, J., Gulis, G., Nolan, B.T., VanDerslice, J., 2005. Workgroup Report: Drinking-water nitrate and health—recent findings and research needs. Environ. Health Perspect. 113, 1607–1614.

Weier, K.L., Doran, J.W., Power, J.F., Walters, D.T., 1993. Denitrification and the dinitrogen nitrous-oxide ratio as affected by soil-water, available carbon, and nitrate. Soil Sci. Soc. Am. J. 57, 66-72

Welti, N., Bondar-Kunze, E., Mair, M., Bonin, P.,Wanek, W., Pinay, G., Hein, T., 2012. Mimicking floodplain reconnection and disconnection using ^{15}N mesocosm incubations. Biogeosciences 9, 4263-4278

Appendix B:

Laboratory and Field Methods

In this appendix of the thesis the main laboratory and field methods and protocols used are described. The analyses performed in solid and aqueous samples were carried out according to standard methodologies described elsewhere.

1. Water sampling and preservation

1.1 Field samples

A total of 20 control points including springs, streams, agricultural wells and piezometers were analyzed between April 2008 and December 2010. Springs and streams samples were collected directly whereas for well and piezometer samples a portable pump was used. Physicochemical parameters pH, redox potential (Eh), dissolve O_2 (DO), and conductivity (EC) were measured in situ, directly in the water flow in springs and streams, whereas in well and piezometers measurements were performed using a flow cell to avoid contact with the atmosphere. Water samples were stored in plastic bottles filled completely to avoid oxidation of species in contact with atmosphere. Samples were preserved at 4 ºC in darkness prior to further analysis.

1.2 Laboratory experiment samples

Aqueous samples from flow-through experiments were obtained at periodical intervals depending of the flow rate using glass bottles. Batch experiments were sampled depending of the reaction kinetics using sterile syringes. In natural attenuation experiments samples were filtered through a 0.45 μm Millipore® filter. In the induced attenuation experiment, the samples were filtered through a 0.20 μm Millipore® filter and 1% 0.1 M $HgCl_2$ was added to stop all microbial activity.

In flow through experiments pH and Eh were measured in the outflow every hour by means portable electrodes (WTW-3310) connected to the experimental set up. In batch experiments pH and Eh measurement were performed in aliquots previously filtered through a 0.45μm Millipore® filter.

2 Chemical analyses

2.1 Anion analyses

Water samples filtered at 0.45μm were diluted until EC was below 1000 μS/cm and subsequent analysed. Major anions (NO_3^-, SO_4^{2-}, Cl^-, and NO_2^-) were analysed by high performance liquid chromatography (HPLC) using a WATERS 515 HPLC pump with IC-PAC Anions columns. For NO_3^- and NO_2^- determinations WESCAN and UV/VIS KONTRON detectors were used in order to measure low concentrations. Samples for NH_4^+ analyses were preserved with phenol. NH_4^+ concentration was analysed using spectrophotometry (ALPKEM, Flow Solution IV).

2.2 Cation analyses

Samples were filtered through a 0.2 μm Millipore® filter and acidified with 1% HNO_3^- (67%). Samples were diluted in order to decrease EC under 1000 μS/cm. Ca, Na, K, Mg, S, total Fe and P were determined by inductively coupled plasma-optical emission spectrometry (ICP-OES, Perkin-Elmer Optima 3200 RL). Trace metals (As, Ba, Cd, Cr, Cu, Hg, Mn, Ni, Pb, Se, V and Zn were analysed using inductively coupled plasma-mass spectrometry (ICP-MS) Perkim-Elmer, model Elan-6000. The detection limits for undiluted sample are listed in Table 1. Analyses were performed at the Centres Científics i Tecnològics of the Universitat de Barcelona.

Table 1: Detection limits of ICP-OES and ICP-MS

Detection limit ICP-OES			ICP-MS		Confidence limits (ppm)		
	ppm	ppb		ppb		Limit	Accepted
Ca	0.025	25	As	10	Ca	200	220
Mg	0.025	25	Se	50	Mg	100	123-130
Na	0.05	50	Cd	1	Na	500	510
K	0.5	500	V	10	K	100	120-130
Sr	0.005	5	Hg	1	Sr	5	6
Ni	0.025	25	Zn	10	Ni	0.5	
Fe	0.005	5	Mn	1	Fe	0.5	2
B	0.025	25	Ba	1	B	1	2
Cr	0.025	25	Pb	1	Dilution		
Co	0.025	25	Cr	10	2000 < EC < 4000		1:2
Zn	0.05	50	Cu	10	4000 < EC < 5000		1:5
			Ni	20	5000 < EC < 10000		1:10

2.3 Organic carbon analyses

20 mL of filtered (for DOC) and unfiltered (for TOC) samples were placed in combusted (2 hours at 450ºC) glass bottles and acidified with HCl (14%) to reach pH < 3. The analyses were performed by organic matter combustion (TOC 500 SHIMADZU).

Samples for Glucose analyses were filtered at 0.2 μm and preserved with 1% of $HgCl_2$ 0.1 M. Glucose was analysed by HPLC with a Waters Alliance 2695 system.

2.4 Dissolved inorganic carbon analyses

The dissolved inorganic carbon (DIC) was measured in the 0.45 μm filtered samples by titration (METROHM 702 SM Titrino).

3. Isotopic analyses

Stable isotopes are measured as the ratio between the desired isotope and the most-abundant one. Because measuring such a small difference cannot be feasibly done in an absolute way, these ratios are almost always established with respect to international standards. As a result, measures are usually expressed in terms of δ per mil relative to the international standards: V-SMOW (Vienna Standard Mean Oceanic Water) for $\delta^{18}O$, AIR (Atmospheric N_2) for $\delta^{15}N$, V-CDT (Vienna Canyon Diablo Troilite) for $\delta^{34}S$ and V-PDB (Vienna Peedee Belemnite) for $\delta^{13}C$.

The isotope ratios were calculated using international and internal laboratory standards (Table 2). The reproducibility of the samples was ±0.2‰ for the $\delta^{34}S$, ±0.5‰ for the $\delta^{18}O$ of SO_4^{2-}, ±0.2‰ for $\delta^{13}C$, from ±0.3‰ to ±1‰ for the $\delta^{15}N$ of NO_3^-, and from ± 0.5‰ to ±2‰ for the $\delta^{18}O$ of NO_3^-. The differences in the reproducibility of $\delta^{15}N$ and $\delta^{18}O$ of dissolved NO_3^- are due to the reproducibility of two different techniques performed in different laboratories.

Table 2: Standards used in the isotopic determinations

Ratio	Scale	Reference material	Matrix	δ [‰]	Used for the determination of	
$^{13}C/^{12}C$	VPDB (Vienna Peedee Belemnite	IAEA-CH3 (1)	Cellulose	-24.72	$\delta^{13}C_{DIC}$	
		IAEA-CH6 (1)	Sucrose	-10.43 ±0.13	$\delta^{13}C_{DIC}$	
		IAEA-CH7 (1)	Polyethylene	-31.83 ±0.11	$\delta^{13}C_{DIC}$	
		USGS 24 (1)	C (graphite	-15.99 ±0.11	$\delta^{13}C_{DIC}$	
$^{15}N/^{14}N$	AIR-N_2 (Atmospheric N_2)	IAEA-N1 (1)	$(NH_4)_2SO_4$	+0.43 ±0.07	$\delta^{15}N_{NO3}$	
		IAEA-N2 (1)	$(NH_4)_2SO_4$	+20.41 ±0.12	$\delta^{15}N_{NO3}$	
		IAEA-NO3 (1)	KNO_3	+4.72 ±0.13	$\delta^{15}N_{NO3}$	
		USGS-25 (1)	$(NH_4)_2SO_4$	-30.25 ±0.38	$\delta^{15}N_{NO3}$	
		USGS-32 (1)	KNO_3	+180 ±1.0	$\delta^{15}N_{NO3}$	
		USGS-34 (1)	KNO_3	-1.8 ±0.2	$\delta^{15}N_{NO3}$	
		USGS-35 (1)	$NaNO_3$	+2.7 ±0.2	$\delta^{15}N_{NO3}$	
		IWS (2)	KNO_3	+16.9±0.2	$\delta^{15}N_{NO3}$	
$^{18}O/^{16}O$	VSMOW (Vienna Standard Mean Ocean Water)	NBS127 (1)	$BaSO_4$	+9.3 ±0.4	$\delta^{18}O_{NO3}$	$\delta^{18}O_{SO4}$
		YCEM (2)	$BaSO_4$	+17.6 ±0.5	$\delta^{18}O_{NO3}$	$\delta^{18}O_{SO4}$
		H_2SO_4 (2)	$BaSO_4$	+12.9 ±0.6	$\delta^{18}O_{NO3}$	$\delta^{18}O_{SO4}$
		USGS-32 (1)	KNO_3	+25.7 ±0.4	$\delta^{18}O_{NO3}$	
		USGS-34 (1)	KNO_3	-27.9 ±0.6	$\delta^{18}O_{NO3}$	
		USGS-35 (1)	$NaNO_3$	+57.5 ±0.6	$\delta^{18}O_{NO3}$	
		EGC-1 (3)	KNO_3	+28.0	$\delta^{18}O_{NO3}$	
		EIL 61 (3)	KNO_3	+11.0	$\delta^{18}O_{NO3}$	
		EIL 62 (3)	$AgNO_3$	+20.5	$\delta^{18}O_{NO3}$	
		IWS (2)	KNO_3	+28.5±0.4	$\delta^{18}O_{NO3}$	
$^{34}S/^{32}S$	V-CDT (Vienna Canyon Diablo Troilite)	IAEA-S1 (1)	Ag_2S	-0.30 (exact.)	$\delta^{34}S_{SO4}$	
		IAEA-S2 (1)	Ag_2S	+22.67 ±0.15	$\delta^{34}S_{SO4}$	
		IAEA-S3 (1)	Ag_2S	-32.55 ±0.12	$\delta^{34}S_{SO4}$	
		NBS127 (1)	$BaSO_4$	+21.1	$\delta^{34}S_{SO4}$	
		YCEM (2)	$BaSO_4$	+12.5	$\delta^{34}S_{SO4}$	

(1) International standard
(2) Internal standard (Centres Científics i Tecnològics of the Universitat de Barcelona)
(3) Environmental Isotopes Laboratory, University of Waterloo, Canada

The isotopic analyses of the $\delta^{34}S$ and $\delta^{18}O$ of SO_4^{2-} and $\delta^{13}C$ were prepared at the laboratory of the Mineralogia Aplicada i Medi Ambient research group and analysed at the Centres Científics i Tecnològics of the Universitat de Barcelona; the isotopic analyses of $\delta^{15}N$ and $\delta^{18}O$ were prepared and analysed at the

laboratory of the ISOFYS research group at Gent University, in the Woods Hole Oceanographic Institution (Woods Hole, MA, US) and at the laboratory of Facility for Isotope Ratio Mass Spectrometry (FIRMS) at University of California, Riverside.

3.1 $\delta^{15}N$ and $\delta^{18}O$ of dissolved NO_3^-

Samples for the $\delta^{15}N$ and $\delta^{18}O$ analysis of dissolved NO_3^- were preserved filtered at 0.2 µm and either basified to pH >11 by adding 0.5 mL of K(OH) (10 mg/L) or frozen. The isotopic analyses were obtained following the denitrifier method at three different laboratories: the Woods Hole Oceanographic Institution, Riverside University and ISOFYS research group at Gent University. The protocol of the denitrifier method employed in Gent is explained in detail.

Before the isotopic analyses, the samples were treated with sulfamic acid to remove the dissolved NO_2^- according to the methodology detailed by (Granger and Sigman, 2009) . Briefly, the sulfamic method consisted on the addition of 0.8mL of 40 mM sulphamic acid ($(H_2N)HSO_3$) solution. Then, the sample pH must be adjusted to 1.6 - 1.9 pH units in order to promote NO_2^- transformation to N_2 following the Eq. 1.

$$HNO_2^- + (H_2N)HSO_3 \rightarrow H_2SO_4 + N_2 + H_2O \qquad (1)$$

After 10 minutes all the NO_2^- is completely removed. Thereafter, samples are neutralized by adding ~1mL of Na(OH) 1M solution and then are subsequently analyzed. This method allows to remove dissolved NO_2^- concentrations up to 7-fold the ambient NO_3^- without detectably compromising the isotopic composition of dissolved NO_3^-.

The bacterial denitrifier method was described by Casciotti et al. (2002) and Sigman et al. (2001). This method is based in the conversion of NO_3^- to N_2O by denitrifying bacteria that lack an active N_2O reductase. All the steps must be performed in a sterilized laminar flow hood and the material must be sterile to avoid bacterial contamination.

Denitrifier strain of *"Pseudomonas aureofaciens"* (LMG1245; ATCC 13985), which naturally lack active N_2O reductase, is cultured in 40g/L Tryptic soy Agar amended with 10 mM KNO_3 in a Petri

Plate following a 4x4 dilution method to get an isolate colony. After one day, an isolate colony is inoculated in a starter culture (10 mL Tryptic Soy Broth or TBS) and grown overnight in a reciprocal shaker. TSB solution is amended with 10mM KNO_3, 7,5mM NH_4Cl and 36Mm KH_2PO_4 and 0.25mL/L of antifoam, the solution is poured in glass bottles and autoclaved. 3mL of starter culture is inoculated into the working cultures. Working cultures are grown in 1L batches with Tryptic Soy Broth during 6 – 10 days in a reciprocal shaker at 200rpm and 25ºC. On the day of sample preparation the culture is divided into 40 mL aliquots in falcon tubes and centrifuged for 20 minutes at 4000rpm in a fixed-angle. The supernatant medium is then decanted and reserved and 4 mL of spent medium is pipetted back into the falcon tubes with each cell pellet, representing 10-fold bacteria concentration. These tubes are then vortexed to ensure homogenized cultures and the content is transferred as 2 x 2 aliquots into 20 mL headspace vials. The vials are sealed with screw-topped Teflon-backed silicone septa. To ensure anaerobic conditions and remove N_2O formed during bacteria grown, each sealed vial is purged during 3 hours with N_2 gas. The purging gas is introduced through a 22-gauge spinal needle, inserted through the septum so as to bubble the medium, and is vented through a 27-gauge needle that is inserted above the liquid level. At the end of the purging time, the vent needle is removed, followed immediately by the bubbling needle. Samples of dissolved NO_3^- are then injected into the headspace vials and incubated overnight to allow complete NO_3^- conversion into N_2O. The volume of sample injected is adjusted to achieve a final sample size of 100 nmols of N_2O although the volume can not be over 1mL to avoid overpressure in the vials. On the following day, 0.1 mL of 10N Na(OH) is injected into the headspace vials to stop bacterial activity and to scrub any CO_2 gas in the vial which could interfere with N_2O measurement. Finally, simultaneous $\delta^{15}N$ and $\delta^{18}O$ analysis of the produced N_2O is carried out using a Trace gas-preparation unit (ANCA TGII, PDZ Europa Ltd.) coupled with an IRMS instrument (20-20, SerCon Ltd.).

3.2 $\delta^{34}S$ and $\delta^{18}O$ of dissolved SO_4^{2-}

The dissolved SO_4^{2-} was precipitated as $BaSO_4$ by adding $BaCl_2 \cdot 2H_2O$ after acidifying the sample with HCl and boiling it to remove HCO_3^- and CO_3^{2-} and, therefore, prevent $BaCO_3$ precipitation, as prescribed by the standard method (Dogramaci et al., 2001). Samples were filtered at 3µm and the precipitate was dried in an oven at <60ºC. The precipitate was subsequent scraped off the filter paper and stored in a desiccator until analysis. The solid precipitated was analysed for the $\delta^{34}S$ using a Carlo Erba Elemental Analyzer (EA) coupled in continuous flow (Conflo II Finningan MAT) with a Finnigan Delta C IRMS. Previously to analyse the $\delta^{18}O$,

the precipitated $BaSO_4$ must be dried in an oven at ~100ºC to remove H_2O. $\delta^{18}O$ was analysed in duplicate with a ThermoQuest TC/EA (high temperature conversion elemental analyser) unit coupled in continous flow (Conflo III Finningan MAT) with a Mass Spectometer (Finnigan Matt Delta C IRMS).

3.3 $\delta^{13}C$ of dissolved inorganic carbon

For the $\delta^{13}C_{DIC}$ determination, filtered samples were treated with NaOH-$BaCl_2$ solution to precipitate $BaCO_3$ together with $BaSO_4$. Sample was filtered and recovered following the same methodology as in the case of $BaSO_4$. $\delta^{13}C$ was analysed in a Carlo Erba Elemental Analyzer (EA) coupled in continuous flow to a Finnigan Delta C IRMS.

4. Microbial analyses

During the induced denitrification experiment, the denitrifying population was quantified using the most probable number (MPN) method published by Saitoh et al. (2003). In addition, the total aerobic heterotrophic population was obtained using the miniaturised MPN method. Five millilitres of water were removed from the middle of the bioreactor and processed within 6 hours of collection. To estimate the population density of the denitrifying bacteria, the water sample was diluted up to a maximum of $1/10^{12}$. Nine 0.25-mL replicates of each dilution were placed in Eppendorf vials with 0.25 mL sterilised Nutrient Broth (NB) medium. The NB solution contained 6 g/L beef extract, 10 g/L peptone, 2 g/L $NaNO_3$, 0.05 g/L $NaNO_2$, 2 g/L agar, and 2.5 g/L HEPES. The pH of the NB was adjusted to 7.0 using a 0.1 M NaOH. Eppendorf vials containing the diluted sample and NB, were individually sealed with 1 mL of overlaying solution containing 5 g/L agar and 8 g/L gellan gum to preserve the N_2 bubbles formed by the denitrifying bacteria. To calculate the population density of the heterotrophic bacteria, the diluted samples were added to microtiter plates using sterilised Tryptic Soy Broth (TSB) solution as a culture medium. Twenty-five microlitres of TSB was placed in each well and mixed with 25 µL diluted sample. Eight replicate wells per dilution were constructed. The positive tests were used to calculate the MPN of the heterotrophic organisms per millilitre of water.

5. Set up of new isotopic methods

During the thesis new methodologies to analyses of $\delta^{15}N$ from NH_4^+, by diffusion method and $\delta^{15}N$ and $\delta^{18}O$ from NO_3^- and NO_2^- by cadmium reduction method were set up in the laboratory of MAiMA group.

5.1 $\delta^{15}N$-NH_4^+ analyses by diffusion method

The method is based on the protocol explained by Sebilo et al., (2004) and Holmes et al., (1998). The method consists on the conversion of dissolved NH_4^+ to $(NH_4^+)_2SO_4$. Prior to perform the analysis samples must be keep at Ph < 2.5 adding 1 drop of H_2SO_4 (99%).

During the set up of the method different tests were performed in order to achieve the best reproducibility. Two different filters: GF/D and GF/C with different sealed material (Teflon or Polypropylene) were utilized. In addition, the volume of water and the amount of NH_4^+ were also checked. Finally different shaker (orbital or magnetic) were also evaluated (Table 3). The best results of the different approaches performed were obtained with the following methodology:

Samples are placed in acid-washed amber glass bottles of 250 mL and deionized water is added to each bottle, if necessary, to bring the total liquid volume of 100 mL. Over the water sample a filter-pack is placed. Filter-packs consist on a 1 cm-diameter GF/D filter (WHATMAN) containing 30 µL of 8N H_2SO_4 solution and sandwiched between two Teflon sheets. The Teflon sheets were sealed making pressure using a stainless steel tube pressed down on the filters and rotated slightly to form a circular compression around the enclosed filter. Once the filter-pack was placed over the water 2mL of Na(OH) 5N solution was added in order to increase pH to a value above 12 pH units. The raises in pH will produce the NH_4^+ conversion to NH_3. The bottle was quickly sealed and placed in an orbital shaker during 7 days at room temperature in order to favor the NH_3 diffusion into the headspace. NH_3 was then trapped into the filter and converted to $(NH_4^+)_2SO_4$. After one week the filter-pack was placed in an acid-washed glass bottle and placed in a freezer-drier during 2 hours to remove any water from the filter. Then the GF/D filter was removed and placed in a silver-cup to immediately analyze in an EA-IRMS.

Table 3: Results of different diffusion method approaches

Compound	Filter-pack	Shaker	NH_4^+ (μg)	Volume (mL)	Avg $\delta^{15}N_{AIR}$ [‰]	SD	n
$(NH_4^+)_2SO_4$	GF/C + Polyp	Orbital	150	100	-7.2	2.9	n = 2
$(NH_4^+)_2SO_4$	GF/C + Polyp	Orbital	100	50	-2.1	0.5	n = 8
$(NH_4^+)_2SO_4$	GF/C + Polyp	Orbital	75	50	-3.5	1.3	n = 5
$(NH_4^+)_2SO_4$	GF/C + Polyp	Magnetic	100	100	-2.4	0.7	n = 4
$(NH_4^+)_2SO_4$	GF/C + Polyp	Magnetic	100	50	-2.0	0.4	n = 2
$(NH_4^+)_2SO_4$	GF/D + Teflon	Orbital	150	100	-1.6	0.9	n = 6
$(NH_4^+)_2SO_4$	**GF/D + Teflon**	**Orbital**	**100**	**100**	**-0.8**	**0.1**	**n = 10**
$(NH_4^+)_2SO_4$	GF/D + Teflon	Orbital	75	50	-0.9	0.9	n = 4
$(NH_4^+)_2SO_4$	GF/D + Teflon	Magnetic	100	150	-0.8	0.0	n = 2
$\delta^{15}N$-$(NH_4^+)_2SO_4$ = -0.8 ±0.1							

5.2 $\delta^{15}N$ and $\delta^{18}O$ analyses by cadmium method

This method was described by McIlvin and Altabet (2005). The method involves the chemical reduction of NO_3^- to NO_2^- using spongy cadmium with further reduction to N_2O using sodium azide in an acetic acid buffer. Different tests were made in order to achieve the best reproducibility. Different NO_3^- concentration and timing of the reduction steps were tested using international and internal standards. The best results were obtained with the following protocol.

5.2.1 Cadmium preparation

Spongy cadmium was prepared by whasing with 10% HCl to activate particle surface followed by a reaction with a 2% $CuSO_4$ solution in order to create Cu-Cd reactive. Then, the spongy cadmium was rinsed multiple times with deionized water previously bubbled with Argon until the pH became neutral. 12-13 g of Cu-Cd was placed in each plastic columns filled with De-Ionized Water (DIW) and stored in a container with an Argon atmosphere until their utilization. After four batchs of samples were processed, the cadmium columns can be reused by repeating the acid wash, Cu reactivation and rinse steps. All the steps were performed at room temperature.

5.2.2 Conversion of NO_3^- to NO_2^-

A sample volume containing 50 nmol of N was added to the Cd-column followed by 0.2 mL of 1M imidazole solution with a resultant pH close to 9. In the case of freshwater, 2 mL of 2.5M of NaCl solution is added to avoid overreduction of NO_2^- to N_2 follwing the recommendations of (Ryabenko et al., 2009). Columns were then shaken during 3 hours on a rotator shaker to complete NO_3^- reduction to NO_2^-.

5.2.3 Conversion of NO_2^- to N_2O

Samples were then removed from the column and placed in a headspace vials capped tightly with Teflon-lined septa that have been previously purged with helium (He) during 5 minutes. Samples were removed from the column through a 0.45µm filter connected to a 27g needle for injecting into the headspace vial. Then 2 mL of the azide/acetic acid buffer was added to each vial via a syringe. To prepare 50 mL of the buffer, 25 mL of 2 M sodium azide solution was mixed with 25mL of 20% acetic acid solution. Thereafter the headspace vials were placed in an orbital shaker during 10 minutes. Following, 1mL of 6 M Na(OH) solution were added and shaken to neutralize the solution. Then 1mL of headspace gas was removed using a gas tight syringe and placed in a 12 mL tube previously purged with He. Simultaneous $\delta^{15}N$ and $\delta^{18}O$ analysis of the N_2O produced was carried out using Pre-Con system (Thermo Scientific) coupled to an IRMS Finnigan MAT-253 (Thermo Scientific). Precision of the system was ±0.3‰ for ^{15}N and ^{18}O analyses. Precision calculated from the reproducibility of standards interspersed in the analytical batches achieved for $\delta^{15}N$ and $\delta^{18}O$ of NO_3^- are listed in Table 4.

Table 4: Results of international and internal standards analyzed by Cadmium method.

Standard	Avg. $\delta^{15}N_{AIR}$ [‰]	SD	Avg. $\delta^{18}O_{AIR}$ [‰]	SD	n
USGS-32	+180.8	1.5	26.1	0.5	n = 30
USGS-34	-2.6	0.5	-26.1	0.6	n = 30
USGS-35	+3.8	0.5	+57.2	0.6	n = 30
IWS	+16.5	0.5	+28.4	0.7	n =19

Isotopic composition of Standards are listed in Table 2

References

Casciotti, K.L., Sigman, D.M., Hastings, M.G., Böhlke, J.K., Hilkert, A., 2002. Measurement of the oxygen isotopic composition of nitrate in seawater and freshwater using the denitrifier method. Anal. Chem. 74, 4905–4912.

Dogramaci, S.S., Herczeg, A.L., Schiff, S.L., Bone, Y., 2001. Controls on $\delta^{34}S$ and $\delta^{18}O$ of dissolved sulfate in aquifers of the Murray Basin, Australia and their use as indicators of flow processes. Appl. Geochemistry 16, 475–488.

Granger, J., Sigman, D.M., 2009. Removal of nitrite with sulfamic acid for nitrate N and O isotope analysis with the denitrifier method. Rapid Commun. mass Spectrom. 23, 3753–3762.

Holmes, R.M., McClelland, J.W., Sigman, D.M., Fry, B., Peterson, B.J., 1998. Measuring $^{15}N\text{-}NH_4^+$ in marine, estuarine and fresh waters: An adaptation of the ammonia diffusion method. Mar. Chem. 60, 235–243.

McIlvin, M.R., Altabe, M.A., 2005. Chemical conversion of nitrate and nitrite to nitrous oxide for nitrogen and oxygen isotopic analysis in freshwater and seawater. Anal. Chem. 77 (17), 5589–5595.

Ryabenko, E., Altabet, M.A., Wallace, D.W.R., 2009. Effect of chloride on the chemical conversion of nitrate to nitrous oxide for $\delta^{15}N$ analysis. Limno. Ocean. 7, 545–552.

Saitoh, S., Iwasaki, K., Yagi, O., 2003. Deveopment of a most-probable-number method for enumerating denitrifying bacteria by using 96-well microtiter plates and an anaerobic culture system. Microbes Environ. 18 (4), 210–215.

Sebilo, M., Mayer, B., Grably, M., Bildou, D., Mariotti, A., 2004. The use of the ammonium diffusion method for $\delta^{15}N\text{-}NH_4^+$ and $\delta^{15}N\text{-}NO_3^-$. Environ. Chem. 1, 1–5.

Sigman, D.M., Casciotti, K.L., Andreani, M., Barford, C., Galanter, M., Böhlke, J.K., 2001. A bacterial method for the nitrogen isotopic analysis of nitrate in seawater and freshwater. Anal. Chem. 73, 4145–4153.

Appendix C:

C-1 Chemical and Isotopic data of Utrillas experiments

C-2 Chemical and isotopic data of Bottom lake sediment experiments

C-3 Chemical and isotopic data of Pétrola groundwater

C-4 Chemical and isotopic dada of biostimulation experiments

Appendix C.1:

Chemical and Isotopic data from
flow-through experiment of
Appendix A-1

Table C.1.1. Results of chemical characterization for column experiment. (b.d.l.: below detection limit. n.d.: not determined)

Sample	t (days)	Sample Volume (mL)	Retention time (days)	Cl^- (mM)	SO_4^{2-} (mM)	NO_3^- (mM)	NO_2^- (mM)	DOC (mM)	DIC (mM)	$\%NO_3^-$ Removed
First denitrification stage										
Input water	-	-	-	1.23	3.38	0.74	0.00	0.16	6.29	46
Ini-1	1	140	1	136.79	44.96	0.40	0.38	0.68	n.d	91
Ini -2	5	50	5	75.89	29.46	0.07	0.50	n.d	n.d	94
Ini -3	7	140	7	59.27	22.66	0.05	0.49	0.51	3.55	70
Ini -4	8	150	8	22.59	11.53	0.22	0.37	0.36	n.d	43
Ini -5	11	150	8	8.54	5.98	0.42	0.22	0.34	6.12	12
Ini -6	12	250	4	2.67	4.54	0.65	0.13	0.25	n.d	22
Col-1	13	150	5	2.82	4.44	0.58	0.19	n.d	3.62	21
Col-2	15	150	5	3.23	4.70	0.59	0.19	n.d	n.d	45
Col-3	18	150	6	2.99	4.63	0.41	0.17	n.d	3.21	5
Col-4	19	150	6	1.93	4.25	0.70	0.06	n.d	n.d	11
Col-5	20	150	5	2.03	4.29	0.66	0.06	n.d	n.d	0
Col-6	21	140	3	1.73	4.15	0.76	0.04	n.d	n.d	46
Second denitrification stage										
Col-7	22	150	3	1.94	3.61	0.64	0.05	0.27	2.69	13
Col-8	23	140	3	1.74	3.35	0.73	0.04	n.d	n.d	2
Col-9	26	150	5	1.72	3.64	0.83	0.04	n.d	n.d	0
Col-10	27	150	5	1.81	3.17	0.76	0.05	n.d	n.d	0
Col-11	29	150	7	1.91	3.12	0.64	0.05	n.d	n.d	15
Col-12	32	750	1	1.62	3.14	0.80	0.03	n.d	n.d	0
Col-13	34	250	2	1.77	3.16	0.71	0.06	n.d	n.d	4
Col-14	36	200	4	1.58	3.49	0.85	0.05	n.d	2.76	0
Col-15	37	170	4	1.54	3.45	0.85	0.06	n.d	n.d	0
Col-16	39	190	4	1.57	3.47	0.82	0.05	n.d	n.d	0
Col-17	40	150	4	1.47	3.43	0.89	0.05	n.d	2.78	0
Col-18	41	160	4	1.61	3.54	0.90	0.06	n.d	n.d	0
Col-19	42	170	3	1.40	3.48	0.76	0.06	n.d	n.d	0
Col-20	43	150	3	1.75	3.48	0.89	0.04	n.d	n.d	0
Col-21	46	150	5	2.65	3.46	0.74	0.10	n.d	n.d	0
Col-22	47	160	5	1.46	3.44	0.54	0.13	n.d	n.d	27
Col-23	48	160	5	1.67	3.46	0.65	0.13	0.18	n.d	13
Col-24	50	150	4	1.93	3.25	0.61	0.14	0.19	2.67	18
Col-26	55	220	6	2.02	3.76	0.59	0.15	0.14	n.d	20
Col-27	57	160	6	2.03	3.45	0.62	0.11	0.13	n.d	16
Col-28	60	215	6	1.98	3.77	0.59	0.10	0.16	n.d	20
Col-29	62	160	6	1.97	3.35	0.57	0.09	0.15	n.d	24
Col-30	64	150	6	2.16	3.74	0.59	0.08	0.16	2.80	20
Col-31	67	210	6	2.01	3.32	0.54	0.09	0.15	n.d	27
Col-32	69	180	6	2.00	3.35	0.51	0.09	0.15	n.d	32
Col-33	71	160	6	2.05	3.13	0.43	0.09	0.16	n.d	42
Col-34	74	160	6	2.01	3.27	0.47	0.09	0.17	n.d	37
Col-35	76	160	6	1.95	3.28	0.50	0.09	0.17	2.47	33
Col-36	78	160	6	2.02	3.34	0.52	0.09	0.18	n.d	30
Col-37	81	160	6	2.28	3.40	0.54	0.08	0.22	n.d	27
Col-38	85	150	6	2.12	3.34	0.44	0.08	0.25	n.d	41
Col-39	92	150	6	1.92	3.25	0.39	0.09	0.20	n.d	48
Col-40	96	150	6	1.90	3.31	0.44	0.07	0.19	n.d	41
Col-41	104	140	12	3.22	3.38	0.01	b.d.l	0.40	n.d	99
Col-42	115	150	21	2.94	3.66	b.d.l	b.d.l	0.76	n.d	100

Table C.1.1. (continued)

Sample	t	Sample Volume (mL)	Retention time (days)	Cl^- (mM)	SO_4^{2-} (mM)	NO_3^- (mM)	NO_2^- (mM)	DOC (mM)	DIC (mM)	% NO_3^- Remov
Col-43	133	250	33	3.50	3.68	b.d.l	b.d.l	0.42	2.52	100
Col-44	145	170	32	3.47	3.77	b.d.l	b.d.l	0.38	n.d	100
Col-45	158	180	32	3.67	3.73	0.04	b.d.l	0.36	2.52	95
Col-46	160	150	6	1.85	3.64	0.31	0.14	0.31	n.d	58
Col-47	162	150	4	1.83	3.63	0.34	0.16	0.28	2.52	54
Col-48	167	150	9	2.43	3.45	0.53	0.09	0.29	n.d	29
Col-49	169	150	9	1.85	3.78	0.64	0.06	0.23	n.d	14
Col-50	172	225	10	1.59	3.39	0.58	0.05	0.24	2.64	22
Col-51	174	150	7	1.54	3.39	0.58	0.06	0.21	n.d	22
Col-52	176	170	7	1.84	3.69	0.64	0.09	0.23	3.12	14
Col-53	179	230	7	1.62	3.39	0.54	0.08	0.24	n.d	27
Col-54	183	225	8	1.63	3.55	0.55	0.12	0.25	n.d	26
Col-55	186	225	7	1.91	3.71	0.54	0.12	0.24	2.49	27
Col-56	189	225	6	1.59	3.40	0.41	0.12	0.27	2.70	45
Col-57	194	150	5	2.32	3.52	0.44	0.15	0.32	n.d	40
Col-58	195	150	6	1.69	3.60	0.58	0.11	0.22	n.d	22
Col-59	196	150	7	1.70	4.12	0.58	0.10	0.22	n.d	22
Col-60	199	225	5	1.69	3.64	0.53	0.12	0.23	n.d	29
Col-61	200	150	5	2.12	3.65	0.45	0.12	0.26	2.44	39
Col-62	201	150	5	1.56	3.60	0.52	0.08	0.22	n.d	30
Col-63	202	150	3	1.66	3.66	0.61	0.08	0.22	2.44	18
Col-64	203	150	3	1.66	3.47	0.63	0.09	0.20	n.d	15
Col-65	207	150	6	2.00	3.58	0.61	0.08	0.25	n.d	18
Col-66	208	150	6	1.66	3.56	0.67	0.07	0.18	n.d	10
Col-67	209	150	6	1.43	3.41	0.57	0.06	0.18	2.14	23
Col-68	213	550	3	1.42	3.41	0.58	0.06	0.19	n.d	22
Col-69	214	150	5	1.40	3.40	0.60	0.06	n.d	n.d	19
Col-70	215	150	3	1.60	3.57	0.72	0.06	n.d	2.70	3
Col-71	221	225	8	2.01	4.00	0.68	0.07	n.d	n.d	9
Col-72	227	190	12	1.77	3.49	0.65	0.06	n.d	n.d	12
Col-73	236	180	17	2.12	3.50	0.55	0.06	n.d	n.d	26
Col-74	242	225	16	1.69	3.57	0.67	0.08	n.d	n.d	10
Col-75	245	130	12	1.69	3.49	0.66	0.07	n.d	n.d	12
Col-76	250	150	12	1.66	3.50	0.63	0.11	n.d	n.d	15
Col-77	255	170	14	1.80	3.57	0.62	0.10	n.d	n.d	16
Col-78	259	150	14	1.72	3.60	0.64	0.12	n.d	n.d	14
Col-79	263	150	13	1.70	3.54	0.70	0.09	n.d	n.d	5
Col-80	269	225	14	1.70	3.48	0.72	0.12	n.d	n.d	3
Col-81	273	150	14	1.71	3.54	0.74	0.09	n.d	n.d	0
Col-82	278	190	15	1.79	3.51	0.65	0.08	n.d	n.d	13
Col-83	283	200	14	1.69	3.64	0.70	0.08	n.d	n.d	5
Col-84	290	250	17	1.71	3.59	0.74	0.08	n.d	n.d	1
Col-89	332	400	36	2.12	3.96	0.74	b.d.l	n.d	n.d	0

Table C.1.2: Results of chemical characterization for column experiment. (n.d.: not determined)

Sample	t (days)	K^+ (mM)	Na^+ (mM)	Ca^{2+} (mM)	Mg^{2+} (mM)	NH_4^+ (mM)	pH
First denitrification stage							
Initial	0	0.10	0.62	3.03	4.36	0.02	8.4
Ini-1	1	9.19	111.6	3.49	59.7	0.02	8.4
Ini -3	7	6.47	54.4	1.58	29.8	0.01	8.3
Ini -4	8	2.90	18.1	0.72	10.6	0.01	8.1
Ini -5	11	2.41	8.86	0.55	7.20	0.04	8.1
Ini -6	12	1.45	2.23	0.58	5.55	0.05	7.8
Col-1	13	n.d	n.d	n.d	n.d	0.02	8
Col-6	21	n.d	n.d	n.d	n.d	0.02	8
Second denitrification stage							
Col-7	22	n.d	n.d	n.d	n.d	n.d	8.1
Col-9	26	0.44	1.01	1.18	4.13	n.d	8
Col-14	36	n.d	n.d	n.d	n.d	n.d	8.1
Col-16	39	0.44	1.09	1.31	4.30	n.d	7.9
Col-21	46	n.d	n.d	n.d	n.d	n.d	7.9
Col-22	47	0.45	1.09	1.40	4.56	n.d	7.9
Col-23	48	n.d	n.d	n.d	n.d	0.01	7.9
Col-26	55	0.69	0.87	1.25	4.39	n.d	7.9
Col-27	57	n.d	n.d	n.d	n.d	0.02	7.9
Col-28	60	0.63	0.82	1.17	4.22	n.d	7.9
Col-29	62	n.d	n.d	n.d	n.d	0.02	7.9
Col-35	76	n.d	n.d	n.d	n.d	0.02	8.0
Col-38	85	0.73	0.86	1.25	4.52	n.d	7.9
Col-39	92	n.d	n.d	n.d	n.d	0.02	7.9
Col-40	96	n.d	n.d	n.d	n.d	0.02	7.9
Col-41	104	1.68	1.04	1.16	4.28	0.02	8.0
Col-42	115	n.d	n.d	n.d	n.d	n.d	8.0
Col-43	133	2.04	1.07	1.16	4.26	n.d	8.0
Col-44	145	n.d	n.d	n.d	n.d	0.02	8.0
Col-45	158	1.90	1.11	1.09	4.44	0.02	8.0
Col-46	160	n.d	n.d	n.d	n.d	0.02	8.0
Col-50	172	0.47	0.97	0.97	4.36	0.02	8.0
Col-52	176	0.47	0.95	0.96	4.45	n.d	8.0
Col-55	186	0.48	1.01	0.89	4.32	n.d	8.1
Col-56	189	n.d	n.d	n.d	n.d	0.02	8.1
Col-57	194	0.79	1.03	0.90	4.34	n.d	8.1
Col-58	195	n.d	n.d	n.d	n.d	n.d	8.1
Col-75	245	n.d	n.d	n.d	n.d	n.d	8.2
Col-89	332	n.d	n.d	n.d	n.d	n.d	8.2

Table C.1.3. Results of isotopic characterization for column experiment. (n.d.: not determined)

Sample	t (days)	$\delta^{13}C_{DIC}$ (‰)	$\delta^{34}S_{SO4}$ (‰)	$\delta^{18}O_{SO4}$ (‰)	$\delta^{15}N_{NO3}$ (‰)	$\delta^{18}O_{NO3}$ (‰)
First denitrification stage						
Initial	0	-10.1	-16.8	+5.3	+9.0	+4.8
Ini -1	1	n.d.	-21.6	+15.7	+27.7	+24.2
Ini -2	5	n.d.	-21.5	+15.3	+43.4	+40.6
Ini -3	7	-11.7	-21.4	+14.7	+40.7	+37.0
Ini -4	8	n.d.	-20.6	+13.2	+27.0	+22.2
Ini -5	11	-9.9	-19.2	+9.9	+19.2	+14.8
Ini -6	12	n.d.	-17.6	+5.8	+14.3	+9.9
Col-1	13	-8.9	n.d.	n.d.	n.d.	n.d.
Second denitrification stage						
Col-7	22	-13.4	-17.0	+5.0	+14.3	+9.8
Col-21	46	n.d.	n.d.	n.d.	+11.2	+4.9
Col-23	48	n.d.	n.d.	n.d.	+13.4	+4.9
Col-29	62	-14.2	-16.8	+5.0	+16.1	+11.7
Col-31	67	n.d.	-16.8	+5.3	n.d.	n.d.
Col-35	76	-19.7	-16.9	+5.7	+18.2	+13.4
Col-38	85	n.d.	-16.8	+5.2	n.d.	n.d.
Col-39	92	n.d.	-17.0	+5.5	+16.9	+12.4
Col-40	96	n.d.	-16.9	+5.4	n.d.	n.d.
Col-41	104	n.d.	-17.0	+5.5	n.d.	n.d.
Col-44	145	-21.2	-16.9	n.d.	n.d.	n.d.
Col-45	158	n.d.	-16.9	n.d.	+44.5	+35.5
Col-46	160	-21.2	n.d.	n.d.	+29.4	+23.0
Col-56	189	-21.5	-16.9	n.d.	n.d.	n.d.
Col-68	213	-23.2	n.d.	n.d.	n.d.	n.d.

Appendix C.2:

Chemical and Isotopic data from
the batch and flow-through
experiments of Appendix A-2

Table C.2.1. Results of chemical characterization of outflow water for column experiment. (b.d.l.: below detection limit. n.d.: not determined)

Sample	t (days)	Cl^- (mM)	SO_4^{2-} (mM)	NO_3^- (mM)	NO_2^- (mM)	NH_4^+ (mM)	DIC (mM)	DOC (mM)	Eh (mV)	Cond (mS/cm)
Input Water	0	1.41	4.00	0.91	0.00	0.02	n.d.	0.17	88	1.17
RC-03-00	1	1477.5	673.9	0.93	0.15	0.34	n.d.	17.5	88.0	88.3
RC-03-01	2	914.1	511.8	0.15	0.52	0.30	n.d.	16.3	-192.5	76.9
RC-03-02	3	628.2	378.3	0.02	0.24	0.65	n.d.	12.2	-169.6	58.2
RC-03-03	4	222.9	130.6	0.01	0.15	0.88	n.d.	8.15	-166.2	31.8
RC-03-04	7	56.6	63.9	0.00	0.21	0.61	3.46	2.81	-165.8	11.91
RC-03-05	8	28.7	37.6	0.02	0.22	0.39	n.d.	1.28	-174.3	7.78
RC-03-06	9	23.8	32.3	0.00	0.15	0.30	n.d.	1.34	-181.4	6.98
RC-03-07	10	24.3	33.8	0.05	0.16	0.27	n.d.	1.19	-165.7	6.99
RC-03-08	11	21.1	33.4	0.12	0.15	0.23	n.d.	0.96	-138.4	6.64
RC-03-09	13	20.1	36.7	0.01	0.17	0.18	2.27	0.91	-59.5	6.05
RC-03-10	15	16.7	35.6	0.01	0.09	n.d.	n.d.	n.d.	-25.0	5.66
RC-03-11	16	13.7	29.4	0.12	0.01	n.d.	n.d.	n.d.	-30.3	5.54
RC-03-12	17	12.5	28.8	0.01	b.d.l.	n.d.	n.d.	n.d.	-77.0	5.31
RC-03-13	19	10.4	28.2	0.02	b.d.l.	n.d.	2.63	n.d.	n.d.	4.97
RC-03-14	22	8.61	27.0	0.07	b.d.l.	n.d.	n.d.	n.d.	n.d.	4.66
RC-03-15	23	7.71	27.0	0.01	b.d.l.	0.11	n.d.	0.82	-161.5	4.31
RC-03-16	24	7.34	27.2	b.d.l.	b.d.l.	n.d.	n.d.	n.d.	-142.8	4.28
RC-03-17	25	6.83	26.3	b.d.l.	b.d.l.	n.d.	n.d.	n.d.	-160.9	4.19
RC-03-18	27	6.08	26.1	b.d.l.	b.d.l.	n.d.	3.08	n.d.	-183.3	4.08
RC-03-19	29	5.50	25.7	b.d.l.	b.d.l.	n.d.	n.d.	n.d.	-216.0	3.97
RC-03-20	30	5.97	30.7	b.d.l.	b.d.l.	n.d.	n.d.	0.66	-239.4	3.93
RC-03-21	31	4.92	25.4	b.d.l.	b.d.l.	n.d.	n.d.	n.d.	-252.8	3.84
RC-03-22	32	5.10	29.6	b.d.l.	b.d.l.	n.d.	3.18	n.d.	-261.3	3.79
RC-03-23	34	4.22	24.7	b.d.l.	b.d.l.	n.d.	n.d.	n.d.	-266.5	3.72
RC-03-24	36	4.25	28.4	b.d.l.	b.d.l.	n.d.	n.d.	n.d.	-267.5	3.62
RC-03-25	37	4.11	28.5	b.d.l.	b.d.l.	0.13	n.d.	0.57	-274.9	3.57
RC-03-26	38	3.55	23.8	b.d.l.	b.d.l.	n.d.	n.d.	n.d.	-277.7	3.53
RC-03-27	39	4.11	29.0	b.d.l.	b.d.l.	n.d.	n.d.	n.d.	-258.3	3.56
RC-03-28	41	3.58	27.8	b.d.l.	b.d.l.	n.d.	2.84	n.d.	-275.6	3.50
RC-03-29	43	3.39	28.3	b.d.l.	b.d.l.	n.d.	n.d.	n.d.	-285.4	3.42
RC-03-30	44	3.28	27.4	b.d.l.	b.d.l.	n.d.	n.d.	n.d.	-282.7	3.38
RC-03-31	45	3.15	27.4	b.d.l.	b.d.l.	n.d.	n.d.	n.d.	-261.9	3.34
RC-03-32	46	2.93	27.0	b.d.l.	b.d.l.	n.d.	n.d.	n.d.	-292.2	3.32
RC-03-33	49	2.91	26.7	b.d.l.	b.d.l.	n.d.	2.43	0.69	-280.8	3.26
RC-03-34	50	2.82	26.5	b.d.l.	b.d.l.	n.d.	n.d.	n.d.	-223.0	3.23
RC-03-35	51	2.78	26.9	b.d.l.	b.d.l.	0.09	n.d.	n.d.	-283.9	3.20
RC-03-36	52	2.69	25.9	b.d.l.	b.d.l.	n.d.	n.d.	0.67	-289.5	3.19
RC-03-37	53	2.66	25.8	b.d.l.	b.d.l.	n.d.	n.d.	n.d.	-248.0	3.12
RC-03-38	56	2.47	25.8	b.d.l.	b.d.l.	n.d.	2.24	n.d.	-275.0	3.15
RC-03-39	57	2.38	25.7	b.d.l.	b.d.l.	n.d.	n.d.	n.d.	-282.9	3.14
RC-03-40	58	2.02	23.0	b.d.l.	b.d.l.	n.d.	n.d.	0.37	-287.4	3.13
RC-03-41	59	1.97	22.9	b.d.l.	b.d.l.	n.d.	n.d.	n.d.	-287.7	3.12
RC-03-42	60	2.21	27.0	b.d.l.	b.d.l.	n.d.	n.d.	n.d.	-291.1	3.12
RC-03-43	63	1.90	22.8	b.d.l.	b.d.l.	n.d.	2.44	n.d.	-289.4	3.10
RC-03-44	64	1.85	22.5	b.d.l.	b.d.l.	n.d.	n.d.	n.d.	-290.9	3.09

Table C.2.1. (continued)

Sample	t (days)	Cl^- (mM)	SO_4^{2-} (mM)	NO_3^- (mM)	NO_2^- (mM)	NH_4^+ (mM)	DIC (mM)	DOC (mM)	Eh (mV)	Cond (mS/cm)
RC-03-45	65	1.83	22.8	b.d.l.	b.d.l.	0.08	n.d.	n.d.	-294.5	3.09
RC-03-46	66	1.80	22.5	0.01	b.d.l.	n.d.	n.d.	n.d.	-297.9	3.08
RC-03-47	67	1.77	22.6	b.d.l.	b.d.l.	0.08	n.d.	n.d.	-300.0	3.07
RC-03-48	71	1.62	21.9	b.d.l.	b.d.l.	n.d.	2.26	n.d.	-296.1	2.99
RC-03-49	72	1.90	25.3	b.d.l.	b.d.l.	n.d.	n.d.	n.d.	-301.0	2.97
RC-03-50	73	1.73	25.2	b.d.l.	b.d.l.	n.d.	n.d.	n.d.	-304.8	2.95
RC-03-51	74	1.71	25.2	b.d.l.	b.d.l.	n.d.	n.d.	n.d.	-303.7	2.93
RC-03-52	77	1.70	25.3	b.d.l.	b.d.l.	n.d.	2.41	n.d.	-280.3	2.92
RC-03-53	78	1.65	25.0	b.d.l.	b.d.l.	n.d.	n.d.	n.d.	-262.9	2.91
RC-03-54	79	1.82	25.2	b.d.l.	b.d.l.	n.d.	n.d.	n.d.	-292.6	2.91
RC-03-55	80	1.64	25.3	b.d.l.	b.d.l.	n.d.	n.d.	n.d.	-295.8	2.90
RC-03-56	81	1.65	25.3	b.d.l.	b.d.l.	n.d.	n.d.	n.d.	-293.6	2.90
RC-03-57	84	1.44	23.8	b.d.l.	b.d.l.	0.06	n.d.	0.72	-119.1	2.88
RC-03-58	85	1.40	23.4	b.d.l.	b.d.l.	n.d.	n.d.	n.d.	-130.1	2.88
RC-03-59	86	1.38	23.3	b.d.l.	b.d.l.	0.04	n.d.	n.d.	-225.4	2.88
RC-03-60	87	1.37	23.2	b.d.l.	b.d.l.	0.05	n.d.	n.d.	-260.2	2.86
RC-03-61	88	1.36	23.6	0.01	b.d.l.	0.05	n.d.	0.58	-270.4	2.85
RC-03-62	91	1.35	23.1	b.d.l.	b.d.l.	n.d.	n.d.	n.d.	-92.1	2.85
RC-03-63	92	1.40	20.1	0.02	b.d.l.	n.d.	n.d.	n.d.	-97.3	2.83
RC-03-64	93	1.27	17.3	0.01	b.d.l.	n.d.	n.d.	n.d.	-214.4	2.82
RC-03-65	94	1.40	20.3	0.01	b.d.l.	n.d.	n.d.	0.81	-247.6	2.82
RC-03-66	95	1.25	17.4	0.01	b.d.l.	n.d.	n.d.	n.d.	-267.8	2.82
RC-03-67	98	1.28	17.2	0.10	b.d.l.	n.d.	n.d.	n.d.	-219.4	2.82
RC-03-68	99	1.37	20.1	b.d.l.	b.d.l.	n.d.	n.d.	n.d.	-135.2	2.81
RC-03-69	100	1.25	17.3	b.d.l.	b.d.l.	n.d.	n.d.	n.d.	-208.8	2.82
RC-03-70	101	1.23	17.2	0.03	b.d.l.	0.03	n.d.	0.35	-91.9	2.81
RC-03-71	102	1.39	20.1	0.01	b.d.l.	n.d.	n.d.	n.d.	-134.7	2.82
RC-03-72	105	1.22	17.3	0.01	b.d.l.	n.d.	n.d.	n.d.	-184.0	2.81
RC-03-73	106	1.39	19.9	b.d.l.	b.d.l.	n.d.	n.d.	n.d.	-205.5	2.81
RC-03-74	107	1.37	20.2	b.d.l.	b.d.l.	n.d.	n.d.	n.d.	-241.5	2.83
RC-03-75	108	1.43	20.3	b.d.l.	b.d.l.	n.d.	n.d.	n.d.	-225.0	2.84
RC-03-76	109	1.41	20.1	b.d.l.	b.d.l.	n.d.	n.d.	n.d.	-202.9	2.82
RC-03-77	112	1.41	20.0	b.d.l.	b.d.l.	n.d.	n.d.	n.d.	-19.9	2.82
RC-03-78	114	1.38	20.7	b.d.l.	b.d.l.	n.d.	n.d.	n.d.	-98.2	2.82
RC-03-79	115	1.37	20.4	b.d.l.	b.d.l.	n.d.	n.d.	n.d.	-2.6	2.82
RC-03-80	116	1.39	20.4	b.d.l.	b.d.l.	0.03	n.d.	0.54	22.6	2.81
RC-03-81	119	1.39	17.7	b.d.l.	b.d.l.	n.d.	n.d.	n.d.	35.7	2.56
RC-03-82	120	1.42	10.5	b.d.l.	b.d.l.	n.d.	n.d.	n.d.	-18.3	1.81
RC-03-83	121	1.43	8.98	b.d.l.	b.d.l.	0.02	n.d.	0.49	-72.9	1.63
RC-03-84	123	1.45	7.40	b.d.l.	b.d.l.	n.d.	n.d.	n.d.	-204.7	1.44
RC-03-85	126	1.34	5.23	b.d.l.	0.09	n.d.	n.d.	n.d.	-30.5	1.22
RC-03-86	127	1.39	4.94	b.d.l.	0.13	n.d.	n.d.	0.34	95.3	1.17
RC-03-87	129	1.25	4.41	b.d.l.	0.08	n.d.	n.d.	n.d.	43.2	1.15
RC-03-88	130	1.40	4.75	b.d.l.	0.05	n.d.	n.d.	n.d.	16.4	1.13
RC-03-89	133	1.44	4.57	0.13	0.03	n.d.	n.d.	0.31	84.4	1.11
RC-03-90	134	1.44	4.37	0.21	0.03	0.02	n.d.	n.d.	82.5	1.11

Table C.2.1. (continued)

Sample	t (days)	Cl^- (mM)	SO_4^{2-} (mM)	NO_3^- (mM)	NO_2^- (mM)	NH_4^+ (mM)	DIC (mM)	DOC (mM)	Eh (mV)	Cond (mS/cm)
RC-03-91	135	1.43	4.37	0.22	0.02	n.d.	n.d.	n.d.	73.0	1.11
RC-03-92	137	1.48	4.52	0.03	0.02	n.d.	n.d.	n.d.	35.9	1.11
RC-03-93	140	1.47	4.53	b.d.l.	b.d.l.	n.d.	n.d.	n.d.	-56.7	1.10
RC-03-94	141	1.37	3.76	0.01	b.d.l.	n.d.	n.d.	n.d.	-30.8	1.09
RC-03-95	142	1.37	3.76	0.03	0.02	0.02	n.d.	n.d.	-21.3	1.09
RC-03-96	143	1.38	3.79	0.05	0.02	n.d.	n.d.	0.22	24.9	1.09
RC-03-97	144	1.27	3.28	0.04	0.01	n.d.	n.d.	n.d.	37.1	1.10
RC-03-98	149	1.44	3.81	0.06	0.01	n.d.	n.d.	n.d.	96.4	1.10
RC-03-99	151	1.54	3.92	0.10	0.02	n.d.	n.d.	0.23	74.3	1.10
RC-03-101	163	1.67	6.09	0.05	0.03	n.d.	n.d.	n.d.	-67.0	n.d.
RC-03-104	184	1.69	3.92	0.23	0.05	n.d.	n.d.	n.d.	69.8	n.d.
RC-03-105	192	1.72	5.49	0.27	0.06	n.d.	n.d.	n.d.	118.6	n.d.
RC-03-106	205	1.67	5.70	0.60	0.09	n.d.	n.d.	n.d.	138.5	n.d.
RC-03-107	211	2.42	3.97	0.67	0.05	n.d.	n.d.	n.d.	83.6	n.d.
RC-03-108	218	2.39	3.80	0.64	0.07	0.02	n.d.	n.d.	120.0	n.d.
RC-03-109	232	2.33	5.09	0.56	0.09	n.d.	n.d.	n.d.	125.0	n.d.
RC-03-110	243	4.10	5.23	0.49	0.11	n.d.	n.d.	n.d.	121.0	n.d.
RC-03-114	288	2.31	5.87	0.76	b.d.l.	n.d.	n.d.	0.18	104.9	n.d.
RC-03-115	296	2.44	6.10	0.94	b.d.l.	n.d.	n.d.	n.d.	85.5	n.d.

Table C.2. 2: Chemical characterization of the input water along experiment. (b.d.l.: below detection limit. n.d.: not determined)

t (day)	Input water Sample	Cl^- (mM)	SO_4^{2-} (mM)	NO_3^- (mM)	NO_2^- (mM)
0	RC-03-00-1	1.32	4.00	0.86	b.d.l.
4	RC-03-00-2	1.21	3.27	0.76	b.d.l.
8	RC-03-00-3	1.32	4.00	0.85	b.d.l.
11	RC-03-00-4	1.20	3.36	0.76	b.d.l.
15	RC-03-00-5	1.33	4.00	0.88	b.d.l.
18	RC-03-00-6	1.34	3.93	0.86	b.d.l.
21	RC-03-00-7	1.35	4.02	0.86	b.d.l.
24	RC-03-00-8	1.25	3.33	0.81	b.d.l.
27	RC-03-00-9	1.41	3.37	0.83	b.d.l.
28	RC-03-00-10	1.43	3.45	0.84	b.d.l.
31	RC-03-00-11	1.29	3.35	0.85	b.d.l.
35	RC-03-00-12	1.24	3.29	0.80	b.d.l.
37	RC-03-00-13	1.39	3.99	0.91	b.d.l.
42	RC-03-00-14	1.40	3.94	0.91	b.d.l.
46	RC-03-00-15	1.39	4.07	0.90	b.d.l.
48	RC-03-00-16	1.39	4.09	0.91	b.d.l.
53	RC-03-00-17	1.39	3.91	0.84	b.d.l.
55	RC-03-00-18	1.36	4.01	0.88	b.d.l.
59	RC-03-00-19	1.33	3.72	0.82	b.d.l.
62	RC-03-00-20	1.24	3.84	0.84	b.d.l.
66	RC-03-00-21	1.43	3.90	0.78	b.d.l.
72	RC-03-00-22	1.38	4.34	0.92	b.d.l.
76	RC-03-00-23	1.37	4.54	0.93	b.d.l.
87	RC-03-00-24	1.38	4.04	0.88	b.d.l.
100	RC-03-00-25	1.20	3.64	0.95	b.d.l.
116	RC-03-00-26	1.28	3.53	0.91	b.d.l.

Table C.2.3. Isotopic characterization of SO_4^{2-} for outflow water of column experiment.

Sample	$\delta^{34}S_{SO4}$ (‰)	$\delta^{18}O_{SO4}$ (‰)
Input water	-17.0	-+4.9
RC-03-00	-20.1	+4.3
RC-03-01	-20.3	+5.3
RC-03-02	-19.8	+6.8
RC-03-03	-19.9	+6.4
RC-03-04	-19.4	+4.9
RC-03-05	-19.1	+6.9
RC-03-07	-19.2	+6.4
RC-03-08	-19.3	n.d.
RC-03-09	-19.3	+6.7
RC-03-15	-19.8	+5.7
RC-03-25	-19.4	+4.0
RC-03-30	-19.4	+6.4
RC-03-35	-19.2	+5.0
RC-03-40	-19.3	+5.1

Table C.2. 4. Chemical results for column profiles

Profile day 39		Flow rate = 150 mL/day			
Sample	Height (cm)	Cl^- (mM)	SO_4^{2-} (mM)	NO_3^- (mM)	NO_2^- (mM)
Input water	24	1.40	3.94	0.91	b.d.l.
RC-PV-1-1	19	1.42	9.93	0.58	0.07
RC-PV-1-2	12	1.59	23.47	0.07	0.01
RC-PV-1-3	10	1.60	23.29	b.d.l.	0.01
RC-PV-1-4	7	1.89	23.85	b.d.l.	b.d.l.
RC-PV-1-7	0	3.58	27.77	b.d.l.	b.d.l.

Profile day 67		Flow rate = 150 mL/day			
Sample	Height (cm)	Cl^- (mM)	SO_4^{2-} (mM)	NO_3^- (mM)	NO_2^- (mM)
Input water	24	1.40	3.94	0.91	b.d.l.
RC-PV-2-1	19	1.44	4.25	0.80	0.05
RC-PV-2-2	12	1.38	21.09	0.03	b.d.l.
RC-PV-2-3	10	1.49	24.62	b.d.l.	b.d.l.
RC-PV-2-4	7	1.32	21.02	b.d.l.	b.d.l.
RC-PV-2-5	5	1.51	24.75	b.d.l.	b.d.l.
RC-PV-2-6	2	1.53	24.48	0.01	b.d.l.
RC-PV-2-7	0	1.80	22.50	0.01	b.d.l.

Profile day 74		Flow rate = 200 mL/day			
Sample	Height (cm)	Cl^- (mM)	SO_4^{2-} (mM)	NO_3^- (mM)	NO_2^- (mM)
Input water	24	1.40	3.94	0.92	b.d.l.
RC-PV-3-1	19	1.33	3.63	0.75	0.09
RC-PV-3-2	12	1.27	20.22	0.04	b.d.l.
RC-PV-3-3	10	1.45	24.18	0.03	b.d.l.
RC-PV-3-4	7	1.48	24.20	0.01	b.d.l.
RC-PV-3-5	5	1.45	24.40	b.d.l.	b.d.l.
RC-PV-3-6	2	1.32	20.49	b.d.l.	b.d.l.
RC-PV-3-7	0	1.71	25.16	b.d.l.	b.d.l.

Profile day 81		Flow rate = 200mL/day			
Sample	Height (cm)	Cl^- (mM)	SO_4^{2-} (mM)	NO_3^- (mM)	NO_2^- (mM)
Input water	24	1.40	3.94	0.93	b.d.l.
RC-PV-4-1	19	1.52	4.68	0.81	0.11
RC-PV-4-2	12	1.46	17.97	0.15	0.03
RC-PV-4-3	10	1.47	23.91	b.d.l.	b.d.l.
RC-PV-4-4	7	1.48	24.23	b.d.l.	b.d.l.
RC-PV-4-5	5	1.49	24.17	b.d.l.	b.d.l.
RC-PV-4-6	2	1.47	23.95	b.d.l.	b.d.l.
RC-PV-4-7	0	1.43	24.54	b.d.l.	b.d.l.

Table C.2. 4. (continued)

Profile day 88		Flow rate = 200 mL/day			
Sample	Height (cm)	Cl^- (mM)	SO_4^{2-} (mM)	NO_3^- (mM)	NO_2^- (mM)
Input water	24	1.40	3.94	0.88	b.d.l.
RC-PV-5-1	19	1.29	3.30	0.72	0.07
RC-PV-5-2	12	1.42	6.10	0.33	0.03
RC-PV-5-3	10	1.26	17.96	0.10	0.01
RC-PV-5-4	7	1.42	0.00	0.07	b.d.l.
RC-PV-5-5	5	1.29	22.48	0.01	b.d.l.
RC-PV-5-6	2	1.28	22.43	0.01	b.d.l.
RC-PV-5-7	0	1.36	23.58	0.01	b.d.l.

Profile day 112		Flow rate = 200 mL/day			
Sample	Height (cm)	Cl^- (mM)	SO_4^{2-} (mM)	NO_3^- (mM)	NO_2^- (mM)
Input water	24	1.20	3.64	0.95	b.d.l.
Supernatant	24	1.28	4.11	0.91	0.02
RC-PV-6-1	19	1.29	4.10	0.90	0.03
RC-PV-6-2	12	1.29	4.21	0.67	0.03
RC-PV-6-3	10	1.28	4.36	0.57	0.01
RC-PV-6-4	7	1.25	4.49	0.38	b.d.l.
RC-PV-6-5	5	1.25	6.85	0.12	b.d.l.
RC-PV-6-6	2	1.26	21.56	0.01	b.d.l.
RC-PV-6-7	0	1.26	22.53	b.d.l.	b.d.l.

Profile day 123		Flow rate = 290 mL/day			
Sample	Height (cm)	Cl^- (mM)	SO_4^{2-} (mM)	NO_3^- (mM)	NO_2^- (mM)
Input water	24	1.28	3.53	0.91	b.d.l.
RC-PV-7-1	19	1.52	3.16	0.81	0.02
RC-PV-7-2	12	1.40	3.22	0.67	0.02
RC-PV-7-3	10	1.66	3.80	0.65	0.02
RC-PV-7-4	7	1.71	3.97	0.51	0.01
RC-PV-7-5	5	1.75	4.44	0.23	b.d.l.
RC-PV-7-6	2	1.44	11.82	0.06	b.d.l.
RC-PV-7-7	0	1.37	15.72	0.05	b.d.l.

Profile day 135		Flow rate = 290 mL/day			
Sample	Height (cm)	Cl^- (mM)	SO_4^{2-} (mM)	NO_3^- (mM)	NO_2^- (mM)
Input water	24	1.28	3.53	0.91	b.d.l.
RC-PV-8-1	19	1.34	3.56	0.86	b.d.l.
RC-PV-8-2	12	1.41	3.95	0.69	0.03
RC-PV-8-3	10	1.44	3.98	0.62	0.03
RC-PV-8-4	7	1.41	3.98	0.59	0.02
RC-PV-8-5	5	1.43	4.11	0.52	b.d.l.
RC-PV-8-6	2	1.44	4.45	0.29	b.d.l.
RC-PV-8-7	0	1.39	4.50	0.22	b.d.l.

Table C.2. 4. (continued)

Profile day 243 Flow rate = 50 mL/day

Sample	Height (cm)	Cl^- (mM)	SO_4^{2-} (mM)	NO_3^- (mM)	NO_2^- (mM)
Input water	24	1.25	4.42	0.85	b.d.l.
RC-PV-9-1	19	1.49	5.54	0.77	0.03
RC-PV-9-3	10	1.55	5.47	0.72	0.03
RC-PV-9-4	7	1.45	5.42	0.64	0.01
RC-PV-9-5	5	1.80	5.54	0.55	0.01
RC-PV-9-6	2	1.47	5.54	0.55	b.d.l.
RC-PV-9-7	0	1.67	5.23	0.60	0.09

Table C.2.5. NO_3^- isotopic characterization for profile day 112

Sample	$\delta^{15}N_{NO3}$ (‰)	$\delta^{18}O_{NO3}$ (‰)
Input water	+9.5	+4.0
RC-PV-6-1	+9.5	+7.0
RC-PV-6-2	+16.5	+12.2
RC-PV-6-3	+21.0	+17.8
RC-PV-6-4	+25.6	+22.3
RC-PV-6-5	+27.2	+24.5

Table C.2. 6. Chemical results for batch experiment. (b.d.l.: below detection limit. n.d.: not determined)

Sample	Cl^- (mM)	SO_4^{2-} (mM)	NO_3^- (mM)	NO_2^- (mM)	NH_4^+ (mM)	DIC (mM)	DOC (mM)
Initial	1.288	3.58	0.89	0.00	0.02	6.23	0.2
RC-04-01	115.9	67.0	0.60	0.23	n.d.	n.d.	n.d.
RC-04-02	n.d.	n.d.	0.55	0.11	0.03	5.19	1.17
RC-04-03	114.6	70.3	0.55	0.34	n.d.	n.d.	n.d.
RC-04-04	n.d.	n.d.	0.47	0.38	0.07	5.59	0.77
RC-04-05	n.d.	n.d.	0.45	0.35	n.d.	n.d.	n.d.
RC-04-06	124.2	76.8	0.26	0.55	0.08	5.60	0.72
RC-04-07	115.7		0.13	0.66	0.01	5.64	0.65
RC-04-08	131.5	81.3	0.09	0.70	n.d.	n.d.	n.d.
RC-04-09	118.7	75.2	b.d.l.	0.63	n.d.	n.d.	0.68

Table C.2. 7. Nitrate and SO_4^{2-} isotopic characterization for batch experiments

Sample	$\delta^{34}S_{SO4}$ (‰)	$\delta^{18}O_{SO4}$ (‰)	$\delta^{15}N_{NO3}$ (‰)	$\delta^{18}O_{NO3}$ (‰)
Input water	-17.0	+4.9	+9.5	+4.0
RC-04-02	-21.6	+17.0	+20.1	+15.0
RC-04-04	-21.7	+16.3	+31.0	+23.0
RC-04-06	-21.0	+16.6	+31.0	+28.9
RC-04-07	-21.4	+16.5	n.d.	n.d.

Appendix C.3:

Chemical and Isotopic data of
Pétrola groundwater
Appendix A-3

Table C.3.1: Values of pH, Conductivity, Hardness and oxygen for Pétrola groundwater samples of Zone 1. (n.d.: not determined)

Sample ID	Sampling Date	pH	Conductivity (µS/cm)	Hardness (mg/L)	O_2 (mg/L)
Zone 1					
2560	Apr-2008	8.3	1137	574.8	n.d.
2564	Apr-2008	8	1383	759.9	n.d.
2579	Apr-2008	7.49	2180	1283.2	n.d.
2581	Apr-2008	7.31	1173	647.7	n.d.
2582	Apr-2008	7.19	1621	890.6	n.d.
2535	May-2008	7.5	1096	553.3	0.9
2537	May-2008	7.65	615	308.3	1.32
2560	May-2008	8.67	1064	633.5	3.09
2564	May-2008	8.11	1463	725.1	1.07
2579	May-2008	7.48	1237	633.5	0.82
2581	May-2008	7.48	1248	660.1	0.69
2582	May-2008	7.38	1757	932.3	0.73
2535	Jun-2008	7.85	899	474.3	0.94
2537	Jun-2008	7.54	561	312.2	1.03
2560	Jun-2008	8.92	761	371.5	3.51
2564	Jun-2008	7.48	1090	699.6	0.98
2579	Jun-2008	7.1	949	509.9	0.9
2581	Jun-2008	7.51	1106	616.6	0.73
2582	Jun-2008	7.58	1358	774.7	0.68
2535	Jul-2008	7.36	1044	529.4	4.73
2537	Jul-2008	7.36	619	309.8	1.62
2560	Jul-2008	8.15	971	454.9	2.67
2564	Jul-2008	7.76	1223	576.4	0.72
2579	Jul-2008	7.52	999	490	1.17
2581	Jul-2008	7.68	1144	615.6	0.76
2582	Jul-2008	7.53	1757	948	1.05
2535	Aug-2008	7.33	1029	513.8	1.32
2537	Aug-2008	7.21	543	284.6	1.36
2560	Aug-2008	7.41	1234	608.7	2.29
2564	Aug-2008	7.64	1329	628.4	1.5
2579	Aug-2008	7.65	964	474.3	0.92
2581	Aug-2008	7.49	1173	636.3	1.11
2582	Aug-2008	7.89	1730	893.2	1.24
2621	Aug-2008	7.33	878	438.7	1.04
2535	Sep-2008	7.27	986	520.5	0.99
2537	Sep-2008	7.37	541	310.8	1.94
2560	Sep-2008	8.02	967	470.5	1.9
2564	Sep-2008	8.04	1310	637.1	1.11
2581	Sep-2008	7.92	846	412.2	0.67
2582	Sep-2008	7.75	1688	928.6	0.91
2621	Sep-2008	7.59	903	487.2	0.78
2579	Sep-2008	7.57	964	479.6	0.89

Table C.3.1 (continued)

Sample ID	Sampling Date	pH	Conductivity (µS/cm)	Hardness (mg/L)	O_2 (mg/L)
2535	Oct-2008	8.45	842	454.2	1.68
2537	Oct-2008	7.21	507	266.9	1.11
2560	Oct-2008	7.95	984	525.9	2.23
2564	Oct-2008	7.6	1384	653.4	1.2
2579	Oct-2008	7.94	840	406.4	0.7
2581	Oct-2008	7.66	1124	577.7	0.87
2582	Oct-2008	7.52	1622	868.5	0.91
2621	Oct-2008	7.65	898	475.6	2.25
2535	Nov-2008	n.d.	n.d.	n.d.	n.d.
2537	Nov-2008	n.d.	n.d.	n.d.	n.d.
2560	Nov-2008	8.28	889	385.5	3.95
2564	Nov-2008	8	1520	710.8	1.18
2581	Nov-2008	7.53	1260	677.3	0.389
2582	Nov-2008	n.d.	n.d.	n.d.	n.d.
2621	Nov-2008	7.63	1012	525.9	1.39
2579	Nov-2008	8.11	1089	641.4	1.32
2535	Dec-2008	7.69	971	481.7	0.77
2537	Dec-2008	7.26	665	315.7	1.74
2560	Dec-2008	8.26	861	384.6	3.61
2564	Dec-2008	7.33	1425	672	1.66
2581	Dec-2008	7.78	1071	631.5	0.93
2582	Dec-2008	8.32	1548	797.5	0.81
2621	Dec-2008	7.73	995	457.4	1.91
2579	Dec-2008	7.36	1041	522.2	0.66
2535	Jan-2009	7.93	1100	565.1	n.d.
2537	Jan-2009	7.8	649	296.8	n.d.
2560	Jan-2009	8.33	943	430.9	n.d.
2564	Jan-2009	7.85	1223	625.5	n.d.
2579	Jan-2009	7.46	883	466.1	n.d.
2581	Jan-2009	7.65	1158	617.5	n.d.
2582	Jan-2009	7.7	1374	784.8	n.d.
2621	Jan-2009	7.71	902	443.1	n.d.
2535	Feb-2009	n.d.	n.d.	579	n.d.
2537	Feb-2009	n.d.	n.d.	345	n.d.
2560	Feb-2009	n.d.	n.d.	472	n.d.
2564	Feb-2009	n.d.	n.d.	591	n.d.
2579	Feb-2009	n.d.	n.d.	369	n.d.
2581	Feb-2009	n.d.	n.d.	651	n.d.
2581	Feb-2009	n.d.	n.d.	n.d.	n.d.
2621	Feb-2009	n.d.	n.d.	456	n.d.
2536	Feb-2009	n.d.	n.d.	660	n.d.
2535	Mar-2009	n.d.	n.d.	317	n.d.
2537	Mar-2009	n.d.	n.d.	496	n.d.
2560	Mar-2009	n.d.	n.d.	528	n.d.

Table C.3.1. (continued)

Sample ID	Sampling Date	pH	Conductivity (µS/cm)	Hardness (mg/L)	O_2 (mg/L)
2564	Mar-2009	n.d.	n.d.	583	n.d.
2581	Mar-2009	n.d.	n.d.	556	n.d.
2621	Mar-2009	n.d.	n.d.	444	n.d.
2535	Apr-2009	n.d.	n.d.	519.9	n.d.
2537	Apr-2009	n.d.	n.d.	341	n.d.
2560	Apr-2009	n.d.	n.d.	440.5	n.d.
2564	Apr-2009	n.d.	n.d.	564	n.d.
2579	Apr-2009	n.d.	n.d.	377	n.d.
2581	Apr-2009	n.d.	n.d.	517.8	n.d.
2621	Apr-2009	n.d.	n.d.	567	n.d.
2535	May-2009	n.d.	n.d.	544	n.d.
2564	May-2009	n.d.	n.d.	579	n.d.
2579	May-2009	n.d.	n.d.	452	n.d.
2621	May-2009	n.d.	n.d.	n.d.	n.d.
2581	May-2009	n.d.	n.d.	556	n.d.
2579	Jun-2009	n.d.	n.d.	n.d.	n.d.
2579	Jun-2009	n.d.	n.d.	587	n.d.
2564	Feb-2010	n.d.	n.d.	n.d.	n.d.
2579	Feb-2010	n.d.	n.d.	n.d.	n.d.
2581	Feb-2010	n.d.	n.d.	n.d.	n.d.
2564	Apr-2010	n.d.	n.d.	696	n.d.
2579	Apr-2010	n.d.	n.d.	455	n.d.
2581	Apr-2010	n.d.	n.d.	632	n.d.
2564	Jul-2010	n.d.	n.d.	719	n.d.
2579	Jul-2010	n.d.	n.d.	534	n.d.
2581	Jul-2010	n.d.	n.d.	668	n.d.
2564	Oct-2010	n.d.	n.d.	766	n.d.
2581	Oct-2010	n.d.	n.d.	721	n.d.
2564	Nov-2010	n.d.	n.d.	766	n.d.

Table C.3.2: Values of pH, Conductivity, Hardness and oxygen for Pétrola groundwater samples of Zone 2. (n.d. not determined)

Sample ID	Sampling Date	pH	Conductivity (µS/cm)	Hardness (mg/L)	O_2 (mg/L)
Zone 2					
2554	Apr-2008	7.97	1754	1036.3	1.00
2571	Apr-2008	7.90	1738	943.2	5.00
2554	May-2008	8.12	1861	1035.5	2.75
2571	May-2008	8.24	1725	897.2	6.87
2602	May-2008	8.70	2930	1454.5	4.77
2554	Jun-2008	8.06	762	968.3	2.78
2571	Jun-2008	7.46	1402	782.2	5.35
2602	Jun-2008	8.45	2880	1560.4	5.26
2554	Jul-2008	8.16	1692	908.5	1.29
2571	Jul-2008	7.59	1612	799.9	7.07
2602	Jul-2008	8.47	2600	1317	5.25
2554	Aug-2008	8.11	1747	956.5	2.07
2554	Sep-2008	8.55	1760	1028.5	2.93
2554	Oct-2008	8.03	1937	1099.3	2.80
2554	Nov-2008	n.d.	n.d.	n.d.	n.d.
2602	Nov-2008	8.18	3350	1677.3	6.47
2554	Dec-2008	7.73	1819	574.8	1.50
2571	Dec-2008	8.30	1693	846	7.92
2602	Dec-2008	8.06	3380	1740.6	n.d
2554	Jan-2009	7.93	1727	959.4	n.d.
2571	Jan-2009	7.45	1679	857.8	n.d.
2602	Jan-2009	8.16	3010	1528.5	n.d.
2554	Feb-2009	n.d.	n.d.	916	n.d.
2571	Feb-2009	n.d.	n.d.	754	n.d.
2602	Feb-2009	n.d.	n.d.	1556	n.d.
2554	Mar-2009	n.d.	n.d.	917	n.d.
2571	Mar-2009	n.d.	n.d.	790	n.d.
2602	Mar-2009	n.d.	n.d.	1344	n.d.
2554	Apr-2009	n.d.	n.d.	893	n.d.
2571	Apr-2009	n.d.	n.d.	806	n.d.
2602	Apr-2009	n.d.	n.d.	1416.7	n.d.
2554	May-2009	n.d.	n.d.	897	n.d.
2554	Feb-2010	n.d.	n.d.	n.d.	n.d.
2571	Feb-2010	n.d.	n.d.	n.d.	n.d.
2602	Feb-2010	n.d.	n.d.	n.d.	n.d.

Table C.3.2. (continued)

Sample ID	Sampling Date	pH	Conductivity (µS/cm)	Hardness (mg/L)	O_2 (mg/L)
2554	May-2010	n.d.	n.d.	72.6	n.d.
2571	May-2010	n.d.	n.d.	838	n.d.
2602	May-2010	n.d.	n.d.	1012	n.d.
2642	May-2010	8.05	2510	1530	n.d.
2640	Jun-2010	8.00	1046	n.d.	1.19
2554	Jul-2010	n.d.	n.d.	941	n.d.
2571	Jul-2010	n.d.	n.d.	968	n.d.
2602	Jul-2010	n.d.	n.d.	1431	n.d.
2554	Oct-2010	n.d.	n.d.	1008	n.d.
2571	Oct-2010	n.d.	n.d.	889	n.d.
2602	Oct-2010	n.d.	n.d.	1602	n.d.
2640	Oct-2010	n.d.	n.d.	1213	n.d.
2641	Oct-2010	n.d.	n.d.	635	n.d.
2642	Oct-2010	n.d.	n.d.	1549	n.d.
2554	Nov-2010	n.d.	n.d.	1000	n.d.
2571	Nov-2010	n.d.	n.d.	984	n.d.
2602	Nov-2010	n.d.	n.d.	1611	n.d.
2640	Nov-2010	n.d.	n.d.	1193	n.d.
2641	Nov-2010	n.d.	n.d.	627	n.d.
2642	Nov-2010	n.d.	n.d.	1607	n.d.

Table C.3.3: Values of pH, Conductivity, Hardness and oxygen for Pétrola groundwater samples of Zone 3 (n.d. not determined, s.w. surface water)

Sample ID	Depth m	Sampling Date	pH	Conductivity (µS/cm)	Hardness (mg/L)	O_2 (mg/L)
Zone 3						
2623	37.0	Sep-2008	7.86	2750	1380.4	1.24
2623	37.0	Oct-2008	7.31	3040	1669.8	1.28
2623	37.0	Nov-2008	7.26	3020	1618.4	1.39
2623	37.0	Dec-2008	7.66	2720	1457.3	1.22
2623	37.0	Jan-2009	7.49	2730	1490	n.d..
2623	37.0	Feb-2009	n.d.	n.d.	1068	n.d.
2623	37.0	Mar-2009	n.d.	n.d.	1419	n.d.
2623	37.0	Apr-2009	n.d.	n.d.	1408.8	n.d.
2623	37.0	May-2009	7.45	2410	1294.8	n.d.
2624	25.8	May-2009	7.14	51200	18724.8	n.d.
2626	12.1	May-2009	7.18	96000	54580.8	n.d.
2626	12.1	May-2009	n.d.	n.d.	n.d.	n.d.
2623	37.0	May-2009	n.d.	n.d.	1452	n.d.
2624	25.8	May-2009	n.d.	n.d.	10787	n.d.
2626	12.1	May-2009	n.d.	n.d.	52556	n.d.
2623	37.0	May-2009	n.d.	n.d.	n.d.	n.d.
2625	34.1	May-2009	n.d.	n.d.	n.d.	n.d.
2626	12.1	Jan-2009	n.d.	n.d.	n.d.	n.d.
2623	37.0	Feb-2010	7.25	2660	1570	n.d.
2624	25.8	Feb-2010	7.05	63500	31900	n.d.
2625	34.1	Feb-2010	7.55	22600	9800	n.d.
2626	12.1	Feb-2010	7.2	93900	59800	n.d.
2635	s.w.	Feb-2010	9.18	72500	n.d.	0.23
2623	37.0	Apr-2010	7.5	2650	1570	n.d.
2624	25.8	Apr-2010	7	68100	36400	n.d.
2625	34.0	Apr-2010	7.6	8390	3850	n.d.
2626	12.1	Apr-2010	7	92700	63200	n.d.
2635	s.w.	Apr-2010	8.48	59300	n.d.	0.05
2623	37.0	May-2010	7.3	2750	n.d.	0.26
2623	37.0	Jun-2010	7.38	2730	n.d.	0.18
2623	37.0	Jul-2010	7.5	2670	1580	n.d.
2624	25.8	Jul-2010	7	58700	29400	n.d.
2625	34.1	Jul-2010	7.55	5940	2650	n.d.
2626	12.1	Jul-2010	7	86700	59400	n.d.

Table C.3.3. (continued)

Sample ID	Depth m	Sampling Date	pH	Conductivity (µS/cm)	Hardness (mg/L)	O_2 (mg/L)
2635	s.w.	Jul-2010	8.28	62500	n.d.	0.09
2623	37.0	Oct-2010	37.0	37.0	37.0	37.0
2624	25.8	Oct-2010	25.8	25.8	25.8	25.8
2625	34.1	Oct-2010	34.1	34.1	34.1	34.1
2626	12.1	Oct-2010	12.1	12.1	12.1	12.1
2635	s.w.	Oct-2010	7.6	116800	n.d.	0.13
2623	37.0	Nov-2010	8.15	2540	1500	n.d.
2624	25.8	Nov-2010	7.7	40200	17800	n.d.
2625	34.1	Nov-2010	7.9	15060	6700	n.d.
2626	12.1	Nov-2010	7.1	86900	58800	n.d.
2635	s.w.	Nov-2010	7.63	123000	n.d.	0.12

Table C.3.4. Chemical data for Pétrola groundwater samples of Zone 1. (n.d. not determined; b.d.l. below detection limit)

Sample-ID	Sampling Date	NH_4^+	HCO_3^-	Cl^-	SO_4^{2-}	NO_3^-	NO_2^-	Na^+	K^+	Ca^{2+}	Mg^{2+}	Fe_{tot}	Mn^{2+}
Zone 1							mg/L						
2560	Apr-2008	0.18	326.3	91.0	240.3	7.3	0.3	40.9	3.9	62.4	99.8	64.7	2.2
2564	Apr-2008	0.04	331.0	85.9	227.6	38.7	b.d.l.	43.1	3.4	123.2	106.2	10.8	0.6
2579	Apr-2008	0.04	316.3	87.0	803.6	60.5	b.d.l.	41.9	8.1	193.6	192.2	13.3	0.6
2581	Apr-2008	0.01	296.5	58.1	370.4	45.3	b.d.l.	19.0	3.5	107.2	90.3	16.2	1.4
2582	Apr-2008	0.01	343.9	74.7	501.5	15.7	b.d.l.	37.9	6.2	136.0	131.8	6.4	8.1
2535	May-2008	0.07	293.8	81.8	341.0	1.0	b.d.l.	23.0	9.4	82.5	84.3	36.0	25.0
2537	May-2008	1.04	199.5	12.7	62.7	77.6	0.7	3.9	1.8	54.0	42.1	7.8	1.4
2560	May-2008	0.09	238.3	117.2	286.1	22.4	0.5	37.0	21.6	65.1	114.4	50.2	0.8
2564	May-2008	0.08	280.8	164.2	438.4	74.1	b.d.l.	45.3	3.4	120.6	102.9	13.4	0.7
2579	May-2008	0.08	336.9	89.8	347.2	2.4	b.d.l.	28.2	5.0	104.8	90.3	52.2	8.1
2581	May-2008	0.07	280.8	62.9	418.5	73.6	b.d.l.	19.7	3.4	106.3	95.8	18.6	2.3
2582	May-2008	0.06	334.4	129.3	724.4	10.6	b.d.l.	45.8	6.4	125.4	150.4	49.5	11.7
2535	Jun-2008	0.01	203.3	53.4	221.5	0.5	b.d.l.	24.9	3.2	44.1	88.5	5.0	3.8
2537	Jun-2008	0.15	177.9	10.9	45.5	80.2	0.1	4.7	1.4	47.2	47.2	5.4	2.5
2560	Jun-2008	0.04	121.6	60.4	164.4	1.7	b.d.l.	34.4	3.8	29.9	72.1	12.2	2.5
2564	Jun-2008	0.01	168.8	85.0	284.9	35.5	b.d.l.	34.4	2.4	72.4	126.0	10.8	2.5
2579	Jun-2008	0.02	236.0	58.7	192.6	1.8	b.d.l.	27.9	5.3	66.1	83.7	5.0	2.5
2581	Jun-2008	0.01	236.0	46.2	351.5	57.5	b.d.l.	18.7	3.2	91.3	94.3	5.0	2.5
2582	Jun-2008	0.01	265.0	77.1	562.1	3.9	b.d.l.	30.8	4.1	122.8	113.6	8.6	5.3
2535	Jul-2008	0.06	202.8	58.2	274.2	1.6	b.d.l.	26.2	3.0	60.6	91.8	265.9	13.9
2537	Jul-2008	0.03	139.5	12.8	61.0	127.1	0.4	7.2	1.3	49.4	45.3	24.3	3.0
2560	Jul-2008	0.05	187.9	48.8	156.1	16.3	1.1	26.5	3.0	43.0	84.4	128.6	5.9
2564	Jul-2008	0.03	228.8	89.4	254.8	40.9	b.d.l.	36.0	2.5	87.6	85.9	28.9	2.5
2579	Jul-2008	0.03	253.0	61.5	208.7	1.4	b.d.l.	22.8	4.3	78.1	71.7	151.0	5.0
2581	Jul-2008	0.03	240.0	45.1	312.2	56.4	b.d.l.	19.6	3.2	84.5	97.3	169.5	2.5
2582	Jul-2008	0.03	303.2	96.1	601.3	7.0	b.d.l.	50.8	6.6	143.4	143.5	191.0	8.4
2535	Aug-2008	0.03	262.3	54.8	240.1	1.1	b.d.l.	22.6	2.9	62.2	87.1	22.5	6.1
2537	Aug-2008	0.03	167.4	10.0	48.9	83.7	b.d.l.	4.4	1.1	41.4	44.0	6.4	2.5
2560	Aug-2008	0.11	212.1	70.9	380.3	18.8	1.6	36.1	4.2	82.9	97.6	56.8	3.0
2564	Aug-2008	0.03	212.1	114.4	305.1	51.4	b.d.l.	42.0	3.1	81.3	103.3	23.7	2.5
2579	Aug-2008	0.12	260.5	63.8	182.8	2.7	b.d.l.	20.7	4.5	70.1	72.7	7.0	2.5
2581	Aug-2008	0.22	254.9	36.0	263.4	42.0	b.d.l.	13.2	2.5	94.0	97.5	19.2	2.5
2582	Aug-2008	0.03	273.5	91.1	563.5	5.7	b.d.l.	38.9	6.4	124.3	141.5	70.0	7.3
2621	Aug-2008	0.12	215.2	39.4	191.3	1.1	b.d.l.	12.9	6.1	62.2	68.9	834.5	15.8
2535	Sep-2008	0.03	223.8	58.4	281.9	1.4	b.d.l.	25.1	3.0	76.8	77.9	59.9	36.3
2537	Sep-2008	0.04	158.5	9.0	44.6	80.5	b.d.l.	4.1	1.0	42.7	47.7	5.9	2.5
2560	Sep-2008	0.12	214.5	66.8	195.2	16.9	0.5	32.3	4.0	42.3	88.8	26.3	6.4
2564	Sep-2008	0.03	169.7	99.7	272.8	44.3	b.d.l.	41.0	2.8	76.8	108.1	7.5	2.5
2581	Sep-2008	0.03	158.5	34.1	209.1	42.3	b.d.l.	23.3	3.8	61.2	61.0	13.7	2.5
2582	Sep-2008	0.03	298.4	93.4	559.8	5.3	b.d.l.	47.1	6.6	128.6	147.5	14.6	7.5

Table C.3.4. (continued)

Sample-ID	Sampling Date	NH_4^+	HCO_3^-	Cl^-	SO_4^{2-}	NO_3^-	NO_2^-	Na^+	K^+	Ca^{2+}	Mg^{2+}	Fe_{tot}	Mn^{2+}
Zone 1							mg/L						
2621	Sep-2008	0.03	255.5	38.1	187.5	0.5	b.d.l.	12.3	5.9	72.1	74.6	173.6	5.9
2579	Sep-2008	0.03	274.7	44.1	99.7	1.6	b.d.l.	23.4	3.8	80.0	66.0	46.6	9.4
2535	Oct-2008	0.07	201.4	50.6	202.5	1.1	b.d.l.	21.6	2.8	41.1	85.4	54.0	11.6
2537	Oct-2008	0.03	152.9	9.0	45.7	77.7	b.d.l.	3.9	0.7	37.9	40.9	21.5	2.5
2560	Oct-2008	0.2	216.3	66.6	197.5	10.0	b.d.l.	33.5	3.6	47.4	98.0	26.8	2.5
2564	Oct-2008	0.03	229.4	115.9	309.5	51.9	b.d.l.	45.2	3.2	85.4	105.9	7.9	2.5
2579	Oct-2008	0.03	190.2	58.7	156.6	0.5	b.d.l.	20.7	4.1	64.8	58.4	28.2	3.3
2581	Oct-2008	0.03	197.7	44.2	304.4	54.4	b.d.l.	18.7	3.2	75.9	93.3	8.6	2.5
2582	Oct-2008	0.031	292.8	93.5	531.8	4.6	b.d.l.	43.2	6.1	128.0	132.3	11.4	5.9
2621	Oct-2008	0.2	222.7	37.8	186.6	0.5	b.d.l.	12.8	5.6	75.1	68.0	134.3	13.0
2535	Nov-2008	n.d.	n.d.	44.0	141.4	1.5	n.d.	23.1	2.7	n.d.	n.d.	18.3	7.5
2537	Nov-2008	n.d.	n.d.	9.7	33.4	71.8	n.d.	7.7	0.4	n.d.	n.d.	5.0	2.5
2560	Nov-2008	0.06	136.5	69.1	203.9	3.2	b.d.l.	29.6	3.5	43.4	66.4	39.4	3.6
2564	Nov-2008	0.03	273.0	113.9	306.2	51.8	b.d.l.	45.1	3.2	120.5	98.6	12.9	2.5
2581	Nov-2008	0.03	261.6	44.4	313.4	51.7	b.d.l.	18.7	3.3	105.9	99.3	18.7	5.7
2582	Nov-2008	n.d.	n.d.	126.1	619.5	6.7	n.d.	49.8	5.1	n.d.	n.d.	11.5	7.3
2621	Nov-2008	0.24	278.7	38.3	185.9	0.5	b.d.l.	12.9	6.5	101.2	65.4	10.6	85.2
2579	Nov-2008	0.05	266.0	69.5	322.8	6.7	0.1	44.7	5.5	103.6	93.9	62.8	9.7
2535	Dec-2008	0.03	243.6	55.5	210.7	0.8	b.d.l.	19.0	2.5	52.0	81.6	280.3	23.6
2537	Dec-2008	0.03	163.6	13.2	54.7	115.0	b.d.l.	6.0	1.5	44.1	46.1	135.0	2.6
2560	Dec-2008	0.03	174.5	61.4	190.5	4.8	b.d.l.	26.4	3.5	48.8	59.9	575.9	3.8
2564	Dec-2008	0.03	216.4	115.9	321.8	54.4	b.d.l.	43.2	3.1	85.0	109.7	37.1	10.4
2581	Dec-2008	0.03	223.6	55.5	348.4	47.9	b.d.l.	17.8	3.1	86.6	98.9	81.5	8.2
2582	Dec-2008	0.03	194.5	95.0	512.3	8.1	b.d.l.	36.5	5.5	103.9	128.7	428.8	6.6
2621	Dec-2008	0.48	203.6	49.0	230.9	1.4	b.d.l.	12.9	9.8	67.7	68.1	571.4	3.2
2579	Dec-2008	0.03	276.4	54.9	141.3	0.5	b.d.l.	25.9	4.9	81.0	70.9	16.2	3.0
2535	Jan-2009	0.05	193.2	24.0	115.7	0.5	b.d.l.	34.2	2.5	61.3	98.1	n.d.	4.6
2537	Jan-2009	0.6	115.9	10.8	44.1	90.0	b.d.l.	11.6	1.9	43.5	43.7	n.d.	2.5
2560	Jan-2009	0.05	141.1	35.0	119.1	3.0	0.0	23.9	3.4	40.3	78.2	n.d.	2.5
2564	Jan-2009	0.06	196.6	48.7	151.8	22.4	b.d.l.	56.1	4.2	76.2	103.8	n.d.	2.5
2579	Jan-2009	0.05	264.1	38.9	103.0	0.5	b.d.l.	25.4	4.4	69.8	68.9	n.d.	6.6
2581	Jan-2009	b.d.l.	235.5	27.6	189.3	31.8	b.d.l.	24.2	3.2	90.5	92.2	14.2	2.5
2582	Jan-2009	0.03	267.9	93.0	491.5	2.4	b.d.l.	38.5	6.0	125.4	112.6	n.d.	6.2
2621	Jan-2009	0.5	183.6	21.1	106.2	0.5	b.d.l.	11.3	6.8	56.5	71.4	n.d.	2.5
2535	Feb-2009	0.07	241.1	26.7	102.1	0.5	b.d.l.	31.0	3.8	76.0	93.0	n.d.	20.2
2537	Feb-2009	0.03	117.5	10.8	39.1	60.7	b.d.l.	12.5	2.1	44.0	56.0	n.d.	2.5
2560	Feb-2009	0.06	202.6	32.4	97.4	6.3	0.1	35.0	4.2	55.0	80.0	n.d.	2.5
2564	Feb-2009	0.03	202.6	57.6	144.0	26.5	b.d.l.	48.4	3.3	102.0	80.0	n.d.	2.5
2579	Feb-2009	0.03	119.5	37.7	92.3	0.5	b.d.l.	24.0	5.0	34.0	69.0	n.d.	8.0
2581	Feb-2009	0.03	250.0	22.2	114.4	23.8	b.d.l.	24.4	3.8	103.0	94.0	n.d.	2.5

Table C.3.4. (continued)

Sample-ID	Sampling Date	NH_4^+	HCO_3^-	Cl^-	SO_4^{2-}	NO_3^-	NO_2^-	Na^+	K^+	Ca^{2+}	Mg^{2+}	Fe_{tot}	Mn^{2+}
Zone 1							mg/L						
2581	Feb-2009	n.d.	n.d.	n.d.	n.d.	55.8	n.d.	n.d.	n.d.	n.d.	n.d.	n.d.	n.d.
2621	Feb-2009	0.26	192.5	19.2	66.5	1.6	b.d.l.	17.7	7.2	53.0	77.0	n.d.	12.9
2536	Feb-2009	0.09	228.9	24.3	205.8	32.9	b.d.l.	37.1	6.0	96.0	101.0	n.d.	2.5
2535	Mar-2009	0.03	83.1	63.9	307.3	0.5	b.d.l.	26.9	1.9	37.0	51.0	n.d.	184.6
2537	Mar-2009	0.22	208.7	19.6	97.2	149.2	b.d.l.	12.1	1.2	61.0	79.0	n.d.	6.0
2560	Mar-2009	0.031	222.9	64.8	232.0	16.0	0.2	32.3	2.7	73.0	80.0	n.d.	7.9
2564	Mar-2009	0.03	156.3	122.3	326.4	57.2	b.d.l.	45.5	2.1	69.0	96.0	n.d.	2.5
2581	Mar-2009	0.03	188.4	45.4	324.5	56.8	b.d.l.	18.8	1.9	77.0	84.0	n.d.	3.2
2621	Mar-2009	0.14	218.8	42.4	201.5	0.8	b.d.l.	13.2	4.6	61.0	67.0	n.d.	82.4
2535	Apr-2009	2.62	106.4	13.8	57.2	79.4	b.d.l.	20.6	2.9	45.2	95.0	n.d.	2.5
2537	Apr-2009	0.03	104.4	39.7	114.9	31.6	b.d.l.	34.1	4.9	65.0	41.0	n.d.	2.5
2560	Apr-2009	0.42	130.0	42.5	155.3	1.3	0.2	20.2	3.6	37.1	82.6	n.d.	12.0
2564	Apr-2009	0.03	122.2	99.3	268.2	43.3	b.d.l.	48.7	3.1	56.0	100.0	n.d.	2.5
2579	Apr-2009	0.03	143.8	55.3	144.8	1.0	b.d.l.	24.2	4.4	40.0	64.0	n.d.	5.0
2581	Apr-2009	0.24	128.1	40.4	233.5	52.5	b.d.l.	25.8	3.7	58.1	91.1	n.d.	2.5
2621	Apr-2009	0.09	137.9	42.6	204.1	6.7	b.d.l.	25.3	6.4	68.0	94.0	n.d.	3.6
2535	May-2009	0.23	234.5	38.0	170.0	0.5	b.d.l.	28.2	3.8	61.0	92.0	n.d.	24.2
2564	May-2009	0.03	116.3	83.5	202.3	38.4	b.d.l.	63.8	4.3	58.0	103.0	n.d.	2.5
2579	May-2009	0.06	230.5	49.3	123.7	0.8	b.d.l.	27.0	5.4	63.0	69.0	n.d.	2.5
2621	May-2009	n.d.	n.d.	65.4	429.6	20.3	n.d.	25.7	6.5	n.d.	n.d.	n.d.	22.8
2581	May-2009	0.09	149.8	36.7	235.8	54.0	b.d.l.	24.1	3.7	69.0	90.0	n.d.	2.5
2579	Jun-2009	n.d.	n.d.	58.8	155.3	0.5	b.d.l.	22.2	4.5	n.d.	n.d.	n.d.	8.7
2579	Jun-2009	0.03	272.7	59.5	147.1	0.1	b.d.l.	24.0	4.8	84.0	89.0	n.d.	9.3
2564	Feb-2010	n.d.	270.0	n.d.	n.d.	66.5	n.d.	n.d.	n.d.	n.d.	n.d.	n.d.	n.d.
2579	Feb-2010	n.d.	340.0	n.d.	n.d.	0.5	n.d.	n.d.	n.d.	n.d.	n.d.	n.d.	n.d.
2581	Feb-2010	n.d.	300.0	n.d.	n.d.	69.1	n.d.	n.d.	n.d.	n.d.	n.d.	n.d.	n.d.
2564	Apr-2010	0.17	221.7	99.94	281.5	54.2	b.d.l.	52.7	3.4	104.0	95.0	n.d.	n.d.
2579	Apr-2010	0.17	135.8	63.88	179.3	5.6	b.d.l.	21.5	4.4	69.0	57.0	n.d.	n.d.
2581	Apr-2010	0.15	177.3	45.41	296.6	68.0	b.d.l.	20.0	3.6	80.0	94.0	n.d.	n.d.
2564	Jul-2010	0.04	296.2	103.73	301.3	51.7	b.d.l.	47.5	3.4	125.0	95.0	n.d.	1.0
2579	Jul-2010	b.d.l.	310.3	55.78	159.2	5.6	b.d.l.	19.2	3.8	101.0	64.0	n.d.	n.d.
2581	Jul-2010	b.d.l.	270.0	47.01	309.1	70.2	b.d.l.	21.6	3.8	116.0	88.0	n.d.	n.d.
2564	Oct-2010	0.08	299.0	111	310.6	54.9	b.d.l.	58.1	6.9	134.0	103.0	n.d.	n.d.
2581	Oct-2010	0.05	276.7	45.77	310.6	56.9	b.d.l.	21.8	0.0	127.0	96.0	n.d.	1.0
2564	Nov-2010	0.08	303.0	115.97	323.3	57.3	b.d.l.	57.4	0.1	132.0	104.0	n.d.	1.0

Table C.3.5. Chemical data for Pétrola groundwater samples of Zone 2. (n.d. not determined; b.d.l. below detection limit)

Sample-ID	Sampling Date	NH_4^+	HCO_3-	Cl^-	SO_4^{2-}	NO_3^-	NO_2^-	Na^+	K^+	Ca^{2+}	Mg^{2+}	Fe_{tot}	Mn^{2+}
Zone 2							mg/L						
2554	Apr-2008	0.04	305.8	127.39	687.78	9.6	b.d.l.	43.07	5.01	131.2	170.1	22.7	1.74
2571	Apr-2008	0.05	572.5	153.92	367.26	66.1	0.3	40.99	12.56	116.8	156.3	44.9	1.66
2554	May-2008	0.17	288.2	149.54	917.87	11.8	0.2	46.68	5.48	127	172.6	29.2	1.08
2571	May-2008	0.1	376.9	204.48	492.86	64.5	0.2	40.84	24.89	111.1	150.5	19.3	0.66
2602	May-2008	2.13	386.1	309.3	902.36	77.3	0.2	115.18	4.13	130.2	274.4	19.5	1
2554	Jun-2008	0.05	206.9	100.3	557.45	5.6	b.d.l.	54.51	5.82	99.2	175	13.2	2.5
2571	Jun-2008	0.08	314	124.38	348.15	36.5	b.d.l.	31.49	10.26	82.2	140.1	5.0	4.06
2602	Jun-2008	0.04	326.7	522.27	2009.03	96.1	0.1	117.68	4.68	120.2	306.2	44.0	2.5
2554	Jul-2008	0.03	212.1	93.21	601.6	21.0	0.2	40.22	4.62	106.8	155	135.0	3.41
2571	Jul-2008	0.22	333	6.57	365.3	31.2	b.d.l.	44	11.28	71.7	150.8	1172.5	29.46
2602	Jul-2008	0.33	293.9	277.36	803.51	64.6	0.3	111.37	5.00	106.8	255.3	243.8	9.1
2554	Aug-2008	0.03	223.2	105.92	657.84	20.4	0.2	42.12	5.06	105.2	168.5	135.9	3.54
2554	Sep-2008	0.03	177.2	216.99	1176.34	25.1	b.d.l.	39.24	5.19	94.1	192.8	17.8	2.5
2554	Oct-2008	0.27	283.4	110.41	688.91	9.4	0.1	48.96	5.32	122.3	192.8	52.7	2.5
2554	Nov-2008	n.d.	n.d.	86.81	399.81	20.7	n.d.	51.11	5.56	n.d.	n.d.	6.4	2.5
2602	Nov-2008	0.03	377.3	354.18	966.37	74.3	b.d.l.	138.32	5.58	137.5	323.1	33.9	3.36
2554	Dec-2008	0.03	241.8	99.09	631.77	33.8	b.d.l.	36.44	4.43	110.2	68.8	141.6	2.97
2571	Dec-2008	0.03	236.4	142.5	354.24	65.6	b.d.l.	35.32	16.54	102.4	140.5	318.7	12.09
2602	Dec-2008	0.24	285.5	405.68	1252.64	60.6	b.d.l.	150.71	0.54	129.1	341.7	147.3	2.76
2554	Ene-2009	0.13	201	34.11	239.32	9.7	b.d.l.	56.23	6.32	112.9	164.5	n.d.	2.5
2571	Ene-2009	0.11	280.2	80.95	205.63	44.4	b.d.l.	63.41	11.13	96.8	149.6	n.d.	2.5
2602	Ene-2009	0.06	287.9	132.44	393.1	29.6	b.d.l.	218.61	6.04	100.0	308.7	n.d.	2.5
2554	Feb-2009	0.06	170.1	69.82	366.46	18.1	b.d.l.	70	4.65	100	161.8	n.d.	2.5
2571	Feb-2009	0.03	233	89.61	214.86	50.2	b.d.l.	66.47	14.03	61	146	n.d.	2.5
2602	Feb-2009	0.03	301.9	141.35	349.24	32.8	b.d.l.	193.45	6.47	89	324	n.d.	3.26
2554	Mar-2009	0.09	180.3	103.51	674.09	29.3	b.d.l.	43.31	4.71	108	156	n.d.	2.5
2571	Mar-2009	0.03	226.9	153.02	386.58	73.5	0.1	41.13	13.23	116	117	n.d.	2.57
2602	Mar-2009	0.26	231	363.79	1056.17	79.4	b.d.l.	157.7	4.72	104	262	n.d.	3.37
2554	May-2009	0.03	179.3	57.6	325.1	20.6	b.d.l.	48.1	5.06	103	151	n.d.	2.5
2571	May-2009	0.04	165.5	106.45	313.85	50.8	b.d.l.	2.12	15.89	89	139	n.d.	5.2
2602	May-2009	0.31	216.7	341.96	921.44	86.8	b.d.l.	134.9	4.32	106.5	277.7	n.d.	1.21
2554	May-2009	0.05	203	59.25	383.44	22.8	b.d.l.	158	0.1	94	158	n.d.	5.19
2554	Feb-2010	n.d.	320	n.d.	n.d.	34.6	n.d.	n.d.	n.d.	n.d.	n.d.	n.d.	n.d.
2571	Feb-2010	n.d.	440	n.d.	n.d.	57.2	n.d.	n.d.	n.d.	n.d.	n.d.	n.d.	n.d.
2602	Feb-2010	n.d.	520	n.d.	n.d.	44.7	n.d.	n.d.	n.d.	n.d.	n.d.	n.d.	n.d.
2554	May-2010	0.18	118.9	85.45	533.24	43.1	b.d.l.	36.8	4.71	89	135	n.d.	n.d.

Table C.3.5. (continued)

Sample-ID	Sampling Date	NH_4^+	HCO_3-	Cl^-	SO_4^{2-}	NO_3^-	NO_2^-	Na^+	K^+	Ca^{2+}	Mg^{2+}	Fe_{tot}	Mn^{2+}
Zone 2							mg/L						
2571	May-2010	0.13	124.9	137.53	399.58	61.0	b.d.l.	44.15	12.13	97	133	n.d.	n.d.
2602	May-2010	0.15	173.3	293.32	772.61	48.5	b.d.l.	123.07	5.33	115	165	n.d.	n.d.
2642	May-2010	0.85	395.3	187.9	1152.7	20.7	b.d.l.	122	12.3	212.4	243.2	n.d.	0.05
2640	Jun-2010	n.d.	n.d.	n.d.	n.d.	20.8	n.d.	n.d.	n.d.	n.d.	n.d.	n.d.	n.d.
2554	Jul-2010	0.08	270	84.37	524.31	32.0	0.20	35.46	4.65	151	133	n.d.	n.d.
2571	Jul-2010	0.21	384.9	133.1	371.6	49.9	b.d.l.	43.72	11.4	135	150	n.d.	n.d.
2602	Jul-2010	0.29	409	252.9	650.17	46.8	0.20	92.01	4.4	144	256	n.d.	n.d.
2554	Oct-2010	0.17	272.7	94.83	595.65	29.2	0.12	43.85	10.3	131	164	n.d.	n.d.
2571	Oct-2010	0.30	333.3	115.04	313	65.5	b.d.l.	44.25	12.53	132	134	n.d.	n.d.
2602	Oct-2010	0.22	389.9	303.9	865.51	50.4	b.d.l.	139.63	23.1	165	287	n.d.	n.d.
2640	Oct-2010	0.45	296.9	142.06	746.38	55.3	b.d.l.	62.45	0.19	202	170	n.d.	n.d.
2641	Oct-2010	0.07	343.4	161.61	177.84	47.9	b.d.l.	99.94	0.05	95	95	n.d.	n.d.
2642	Oct-2010	0.14	337.3	169.28	1061.25	23.2	0.13	88.13	0.04	206	249	n.d.	n.d.
2554	Nov-2010	0.11	278.8	96.08	601.72	32.2	0.11	43.25	0.1	129	163	n.d.	n.d.
2571	Nov-2010	0.30	414.1	133.11	396.88	61.7	b.d.l.	46.54	16.33	145	149	n.d.	n.d.
2602	Nov-2010	b.d.l.	440.4	309.61	884.22	48.4	b.d.l.	129.26	6.14	183	278	n.d.	n.d.
2640	Nov-2010	0.61	321.2	131.44	699.61	53.4	b.d.l.	55.5	6.3	175	182	n.d.	n.d.
2641	Nov-2010	0.08	369.7	161.48	175.62	49.6	b.d.l.	91.45	6.58	85	99	n.d.	n.d.
2642	Nov-2010	0.25	377.7	176.93	1120.29	26.0	0.37	88.74	14.31	224	253	n.d.	1.5

Table C.3.6. Chemical data for Pétrola surface and groundwater of Zone 3. (n.d.: not determined; b.d.l.: below detection limit)

Sample - ID	Depth (m)	Sampling date	NH_4^+	HCO_3^-	Cl^-	SO_4^{2-}	NO_3^-	NO_2^-	Na^+	K^+	Ca^{2+}	Mg^{2+}	Fe_{tot}	Fe^{2+}	Mn^{2+}	DOC
Year 2008								mg/L								
2623	37	Sep.	0.04	278.2	254.6	1077	b.d.l.	b.d.l.	108.3	11.5	157.4	239.8	212.7	n.d.	15	n.d.
2623	37	Oct.	0.8	371.1	268.1	1161	b.d.l.	b.d.l.	117.7	12.6	144.3	318.1	147.4	n.d.	19	n.d.
2623	37	Nov.	0.03	341.3	245.8	1181	2.11	b.d.l.	109.3	11.7	155.8	297.6	18.9	n.d.	7	n.d.
2623	37	Dec.	0.03	332.7	221.9	1200	b.d.l.	b.d.l.	94.2	11.2	157.5	256.5	314.5	n.d.	8	n.d.
Year 2009																
2623	37	Jan.	0.03	316.1	82.2	510.2	b.d.l.	b.d.l.	100.8	12.3	130.2	280.1	124.9	n.d.	12	n.d.
2623	37	Feb.	0.09	255.1	264.6	1176	2.3	b.d.l.	144.6	16.8	129	181.1	n.d.	58	6	n.d.
2623	37	Mar.	0.08	305.9	217.2	1146	2.2	b.d.l.	97.2	11.1	140	259	n.d.	266	14	n.d.
2623	37	Apr.	0.33	232.5	193.0	959.9	2.6	b.d.l.	16.1	11.6	137.1	257.1	n.d.	109	5	n.d.
2626	6	May	0.71	2876	39885	36273	b.d.l.	b.d.l.	1906	1079	790.5	12780	1529.0	2	0	n.d.
2624	21	May	0.86	1623	17061	11319	12	b.d.l.	7737	406.5	869.9	4018	761.7	n.d.	109	n.d.
2623	37	May	0.03	221.9	162.7	829.6	7.6	b.d.l.	124.2	11.2	134.9	229.8	67.5	n.d.	3	n.d.
2626	6	May	0.58	360.9	24440	26529	n.d.	b.d.l.	11453	881.0	430	12505	n.d.	128	73	n.d.
2626	6	May	0.06	206.9	7812	4587	b.d.l.	b.d.l.	3748	214.6	287	2444	n.d.	41	22	n.d.
2623	37	May	0.03	325.1	134.4	740.5	b.d.l.	b.d.l.	76.2	9.6	144	263	n.d.	47	8	n.d.

Table C.3.6. (continued)

Sample - ID	Depth (m)	Sampling date	NH_4^+	HCO_3^-	Cl^-	SO_4^{2-}	NO_3^-	NO_2^-	Na^+	K^+	Ca^{2+}	Mg^{2+}	Fe^{2+}	Mn^{2+}	DOC
Year 2010									mg/L						
2635	lake water	Feb.	0.03	326.9	21768	43200	b.d.l.	b.d.l.	11150	1336	497	11811	n.d.	n.d.	140
2626	6	Feb.	0.93	478.2	41834.5	38424	b.d.l.	b.d.l.	16800	3060	481	14251.5	4.6	0.17	23.5
2624	21	Feb.	0.82	439.2	23257.2	17867.2	b.d.l.	b.d.l.	8720	980	761.5	7296	9.3	0.14	8
2625	31	Feb.	0.96	488	6523.4	6090.2	b.d.l.	b.d.l.	2710	292	304.6	2198.5	0.05	0.16	3.9
2623	37	Feb.	0.45	449	219.8	1056.7	b.d.l.	b.d.l.	97	10.1	160.3	284.5	0.05	0.05	2
2635	lake water	Apr.	0.43	473.2	25810	45696	b.d.l.	b.d.l.	12599	1169	481	13182	n.d.	n.d.	163
2626	6	Apr.	1.16	473.4	42011.8	38616.1	b.d.l.	b.d.l.	15800	2560	432.9	15107.6	4.2	0.19	22.3
2624	21	Apr.	1.75	453.8	26731.6	21037.1	1.4	b.d.l.	10450	1145	581.2	8499.8	2.48	0.12	10.8
2625	31	Apr.	1.68	449	1967.6	2439.9	b.d.l.	b.d.l.	824	67.5	280.6	766.1	0.05	0.15	2.5
2623	37	Apr.	1.22	449	216.3	1123.9	0.8	b.d.l.	120.5	12.1	156.3	287	0.05	0.05	4.1
2635	lake water	Jul.	0.04	926.9	45664	75840	b.d.l.	b.d.l.	24999	3166	521	20503	n.d.	n.d.	304
2626	6	Jul.	0.75	468.5	39352.8	34581.6	b.d.l.	b.d.l.	13800	2410	408.8	14198	0.05	0.05	22.5
2624	21	Jul.	1.33	444.1	22548.1	23342.6	b.d.l.	b.d.l.	11800	1310	601.2	6785.3	0.05	0.05	7.2
2625	31	Jul.	0.96	499	1162.9	1940.4	b.d.l.	b.d.l.	620	43.5	256.5	488.8	0.05	0.05	2
2623	37	Jul.	1.15	453.8	219.8	1143.1	b.d.l.	b.d.l.	131	13.8	168.3	282.1	0.05	0.05	2
2635	lake water	Oct.	0.06	2134.3	102814	122880	b.d.l.	b.d.l.	115995	14239	20	165	n.d.	n.d.	646
2626	6	Oct.	1.06	473.4	37367.5	38808.2	b.d.l.	b.d.l.	14800	2680	400.8	13959.7	0.05	0.05	22.2
2624	21	Oct.	0.96	419.7	15953.9	17098.7	b.d.l.	b.d.l.	9600	1075	641.3	4134.4	0.125	0.05	7.74
2625	31	Oct.	1.44	434.3	1432.3	2190.2	b.d.l.	b.d.l.	648	49.6	280.6	608	0.05	0.05	4.05
2623	37	Oct.	1.54	458.7	390	1421.7	b.d.l.	b.d.l.	231	24.7	184.4	345.3	0.05	0.05	7.8
2635	lake water	Nov.	0.04	2048.9	94837	108000	b.d.l.	b.d.l.	37798	4009	701	38490	n.d.	n.d.	500
2626	6	Nov.	0.95	478.2	39423.7	38039.8	b.d.l.	b.d.l.	15600	2680	464.9	14018	0.05	0.05	18.1
2624	21	Nov.	1.48	409.9	14890.3	13448.4	b.d.l.	b.d.l.	7640	828	621.2	3952	0.66	0.09	7.05
2625	31	Nov.	1.65	453.8	4077.1	4380.3	b.d.l.	b.d.l.	1760	164	320.6	1434.9	0.05	0.05	3.45
2623	37	Nov.	1.36	414.8	212.7	999	b.d.l.	b.d.l.	79.5	7.9	160.3	267.5	0.05	0.05	2.31

Table C.3. 7. Isotopic characterization of Pétrola basin. (n.d. not determined)

Data Point	Data of Sampling	$\delta^{15}N_{NO3}$ (‰)	$\delta^{18}O_{NO3}$ (‰)	$\delta^{13}C_{DIC}$ (‰)	$\delta^{18}O_{water}$ (‰)
Year 2010					
2564	Apr.	+7.1	+2.4	-11.1	-7.2
2581	Apr.	+7.3	+2.6	-12.3	-7
2602	May	+12.2	+7.9	-12.7	-5.9
2554	May	+6.6	+5.3	-11.6	-6.2
2571	May	+14.3	+7.5	-12.7	-6.4
2602	Jul.	+14.2	+9.2	n.d.	-6.1
2554	Jul.	+8.3	+5.9	n.d.	-6.8
2571	Jul.	+17.0	+10.0	n.d.	-6
2564	Jul.	+7.0	+2.1	n.d.	-7.6
2581	Jul.	+7.4	+2.3	n.d.	-7
2642	Oct.	+18.5	+15.7	n.d.	-5.7
2602	Oct.	+13.7	+14.4	-11.8	-6.1
2554	Oct.	+9.5	+9.8	-8.6	-5.4
2571	Oct.	+9.5	+10.0	-10	-5.9
2641	Oct.	+9.8	+8.8	n.d.	-6
2640	Oct.	+9.2	+11.5	n.d.	-6.2
2564	Oct.	+6.1	+3.6	-8.9	-6.7
2581	Oct.	+7.6	+4.7	-11.1	-7.1
2642	Nov.	+19.9	+16.2	n.d.	-7
2602	Nov.	+12.0	+10.7	-10.1	-6.3
2554	Nov.	+9.0	+10.2	-8	-6.4
2571	Nov.	+10.5	+8.7	-11.9	-7.2
2641	Nov.	+12.2	+8.8	n.d.	-7.1
2640	Nov.	+8.7	+8.5	n.d.	-6.8

Table. C.3.8. SO_4^{2-} Isotopic characterization of Pétrola basin

Data point	Sampling date	$\delta^{34}S_{SO4}$ (‰)	$\delta^{18}O_{SO4}$ (‰)
2554	Jun-2003	-21.2	+12.3
2564	Sep-2008	-16.3	+2.3
2581	Sep- 2008	-17.4	+4.8
2554	Sep-2008	-22.5	+7.7
2602	Sep-2008	-15.5	+7.9
2564	Feb-2010	-13.2	+3.2
2581	Feb-2010	-12.9	+4.5
2554	Feb-2010	-19.4	+7.6
2602	Feb-2010	-14.3	+5.2
2571	Feb-2010	-17.2	+2.9

Table C.3.9. Isotopic characterization of S-sediments from Utrillas Facies in Pétrola basin.

Sample material	$\delta^{34}S_{so4}$ (‰)	$\delta^{18}O_{SO4}$ (‰)
Gypsum	-15.7	-1.8
Gypsum	-23.1	-2.8
Gypsum	-23.5	+5.1
Gypsum	-21.7	+1.1
Gypsum	-28.1	+9.0
Gypsum	-21.4	-1.1
Gypsum	-20.9	+2.3
Gypsum	-1.8	-3.2
Gypsum	-20.3	+11.5
Gypsum	-20.5	+6.7
Gypsum	-27.4	+5.5
Gypsum	+3.0	+14.0
Gypsum	-30.3	+5.1
Gypsum	-20.8	+12.1
Sulphide	-35.5	-
Sulphide	-38.1	-
Sulphide	-40.5	-
Sulphide	-35.0	-
Sulphide	-19.2	-
Sulphide	-34.2	-
Sulphide	-33.9	-
Sulphide	-34.6	-
Sulphide	-12.2	-
Sulphide	-11.7	-
Sulphide	-34.0	-
Sulphide	-35.8	-

Appendix C.4:

Chemical and Isotopic data from
flow-through experiment of
Appendix A-4

Table C.4.1. Results of chemical characterization for column experiment. (b.d.l.: below detection limit. n.d.: not determined)

Sample	t (hours)	Cl^- (mM)	SO_4^{2-} (mM)	NO_3^- (mM)	NO_2^- (mM)	NH_4^+ (mM)	$C_6H_{12}O_6$ (mM)	Eh (mV)	pH
C/N 1.6									
RC-02-00	0	2.45	3.33	0.84	0.02	0.10	b.d.l.	+180.0	8.5
RC-02-01	12	4.03	3.35	0.81	0.08	0.11	b.d.l.	+167.4	8.5
RC-02-02	24	4.46	3.44	0.67	0.24	0.09	0.06	+183.9	8.5
RC-02-03	36	4.11	3.50	0.08	0.64	0.07	0.17	+135.9	8.5
RC-02-04	48	4.04	3.34	0.01	0.15	0.06	0.13	+54.4	8.6
RC-02-05	60	3.97	3.45	0.01	b.d.l.	0.05	0.07	-68.8	8.5
RC-02-06	72	4.67	3.58	0.04	0.26	0.05	0.01	-82.5	8.4
RC-02-07	84	4.37	3.56	0.18	0.26	0.05	n.d.	-7.0	8.5
RC-02-08	96	4.55	3.48	0.28	0.23	0.04	n.d.	+60.8	8.4
RC-02-09	108	4.03	3.33	0.17	0.34	0.05	n.d.	+79.2	8.5
RC-02-10	120	4.03	3.48	0.02	0.29	0.05	n.d.	+27.2	8.6
RC-02-11	132	4.38	3.40	0.00	0.17	0.05	n.d.	-17.1	8.7
RC-02-12	144	4.58	3.54	0.05	0.35	0.05	n.d.	-7.4	8.7
RC-02-13	156	4.36	3.46	0.28	0.26	0.06	n.d.	+71.0	8.6
RC-02-14	168	4.40	3.41	0.32	0.17	0.06	n.d.	+104.9	8.5
RC-02-15	180	4.63	3.52	0.34	0.23	0.06	n.d.	+112.1	8.5
RC-02-16	192	4.34	3.41	0.06	0.29	0.06	n.d.	+109.5	8.5
RC-02-17	204	4.32	3.34	0.00	0.12	0.06	n.d.	+62.1	8.7
RC-02-18	216	4.38	3.42	0.07	0.20	0.06	n.d.	+91.3	8.7
RC-02-19	228	4.43	3.47	0.30	0.16	0.07	n.d.	+123.2	8.7
RC-02-20	240	4.07	3.40	0.18	0.23	0.06	n.d.	+130.2	8.5
RC-02-21	252	4.50	3.46	0.00	0.34	0.04	n.d.	+54.0	8.7
RC-02-22	264	4.69	3.54	b.d.l.	b.d.l.	0.04	n.d.	-84.9	8.5
RC-02-23	276	4.84	3.40	b.d.l.	b.d.l.	0.03	n.d.	-136.2	8.4
RC-02-24	288	4.46	3.42	b.d.l.	0.02	0.03	n.d.	-134.7	8.4
RC-02-25	300	4.61	3.37	0.05	0.17	0.03	n.d.	-79.1	8.5
RC-02-26	312	4.74	3.54	b.d.l.	0.24	0.02	n.d.	+132.4	8.6
RC-02-27	324	4.57	3.34	0.01	0.10	n.d.	n.d.	+20.5	8.7
RC-02-28	336	4.62	3.62	b.d.l.	0.01	n.d.	n.d.	-64.0	8.6
RC-02-29	348	4.24	3.38	0.01	0.00	n.d.	n.d.	-88.0	8.5
RC-02-30	360	4.17	3.39	b.d.l.	0.01	n.d.	n.d.	-84.5	8.5
RC-02-31	372	4.37	3.31	0.05	0.17	n.d.	n.d.	-36.6	8.5
RC-02-32	384	4.46	3.30	0.03	0.24	0.02	n.d.	+130.3	8.6
RC-02-33	396	4.05	3.36	b.d.l.	0.09	n.d.	n.d.	-7.5	8.6
RC-02-34	408	4.10	3.34	b.d.l.	b.d.l.	n.d.	n.d.	-92.8	8.5
RC-02-35	432	4.27	3.42	b.d.l.	b.d.l.	n.d.	n.d.	-129.0	8.4
RC-02-36	444	4.71	3.53	b.d.l.	0.01	n.d.	0.02	-128.0	8.4
RC-02-37	456	4.22	3.38	b.d.l.	0.07	n.d.	0.09	+26.2	8.5
RC-02-38	468	3.99	3.33	b.d.l.	b.d.l.	0.02	0.05	-106.9	8.4
RC-02-39	480	4.08	3.35	b.d.l.	b.d.l.	n.d.	0.14	-127.2	8.3
RC-02-40	504	3.61	3.23	b.d.l.	b.d.l.	n.d.	0.07	-123.5	8.2
RC-02-41	516	4.45	3.35	b.d.l.	b.d.l.	n.d.	n.d.	-140.4	8.3
RC-02-42	540	4.02	3.31	b.d.l.	b.d.l.	n.d.	n.d.	-105.4	8.3
RC-02-43	564	4.20	3.34	b.d.l.	b.d.l.	n.d.	n.d.	-132.2	8.2

Table C.4.1. (continued)

Sample	t (hours)	Cl (mM)	SO_4^{2-} (mM)	NO_3 (mM)	NO_2 (mM)	NH_4^+ (mM)	$C_6H_{12}O_6$ (mM)	Eh (mV)	pH
RC-02-45	588	4.33	3.51	b.d.l.	0.11	0.02	n.d.	-98.5	8.3
RC-02-46	600	4.23	3.48	b.d.l.	0.16	0.02	n.d.	-39.0	8.5
RC-02-47	612	4.24	3.54	b.d.l.	0.06	n.d.	n.d.	-23.1	8.5
RC-02-48	624	4.02	3.56	b.d.l.	b.d.l.	0.02	n.d.	-103.3	8.3
RC-02-49	648	4.21	3.27	b.d.l.	b.d.l.	n.d.	0.06	-131.4	8.1
RC-02-50	660	4.10	3.33	b.d.l.	b.d.l.	n.d.	0.01	-159.4	8.2
RC-02-51	672	4.24	3.33	b.d.l.	b.d.l.	n.d.	0.05	-173.4	8.2
RC-02-52	684	4.50	3.48	b.d.l.	b.d.l.	n.d.	0.14	-174.1	8.1
RC-02-53	696	3.95	3.28	b.d.l.	b.d.l.	n.d.	0.17	-184.6	8.0
RC-02-54	720	4.31	3.33	b.d.l.	b.d.l.	n.d.	0.06	-204.9	8.0
RC-02-55	732	4.28	3.28	b.d.l.	b.d.l.	n.d.	n.d.	-228.7	8.1
RC-02-56	744	4.12	3.33	b.d.l.	b.d.l.	0.02	n.d.	-150.3	8.2
RC-02-57	756	3.50	3.39	b.d.l.	b.d.l.	n.d.	n.d.	-221.7	8.1
RC-02-58	768	4.42	3.41	b.d.l.	b.d.l.	0.02	n.d.	-267.5	8.0
RC-02-59	792	3.92	3.46	b.d.l.	b.d.l.	0.02	n.d.	-272.2	8.1
RC-02-60	804	4.52	3.30	0.01	0.01	n.d.	n.d.	-211.8	8.2
RC-02-61	816	3.59	3.44	b.d.l.	0.04	n.d.	n.d.	-80.5	8.3
RC-02-62	828	3.30	3.36	0.01	b.d.l.	0.02	n.d.	-187.6	8.2
RC-02-63	840	4.47	3.31	b.d.l.	b.d.l.	n.d.	n.d.	-249.1	8.0
RC-02-64	864	4.14	3.39	b.d.l.	0.01	n.d.	n.d.	-258.7	8.0
RC-02-65	876	3.67	3.41	0.01	b.d.l.	0.02	n.d.	-250.3	8.2
RC-02-66	888	4.10	3.24	b.d.l.	0.02	n.d.	n.d.	-140.4	8.4
RC-02-67	912	0.00	0.00	b.d.l.	b.d.l.	n.d.	n.d.	-202.0	8.2
RC-02-68	936	3.48	3.26	b.d.l.	b.d.l.	n.d.	0.08	-237.1	8.1
C/N 1.25									
RC-02-69	948	3.95	3.33	b.d.l.	b.d.l.	0.02	b.d.l.	-239.9	8.2
RC-02-70	960	3.51	3.27	b.d.l.	b.d.l.	n.d.	0.02	-165.1	8.3
RC-02-71	984	0.00	3.26	b.d.l.	b.d.l.	n.d.	0.12	-217.9	8.2
RC-02-72	1008	3.96	3.19	0.01	b.d.l.	n.d.	0.06	-247.7	8.1
RC-02-73	1023	4.52	3.19	b.d.l.	b.d.l.	n.d.	n.d.	-246.6	8.2
RC-02-74	1045	4.05	3.15	0.01	b.d.l.	n.d.	n.d.	-205.4	8.2
RC-02-75	1080	3.65	3.22	b.d.l.	b.d.l.	n.d.	n.d.	-217.3	8.1
RC-02-76	1118	4.35	3.31	0.01	b.d.l.	0.02	n.d.	-141.1	8.2
RC-02-77	1152	3.48	3.28	0.01	b.d.l.	n.d.	n.d.	-206.6	8.0
RC-02-78	1172	4.56	3.36	0.01	b.d.l.	n.d.	0.00	-210.7	8.2
RC-02-79	1196	4.29	3.50	0.02	b.d.l.	n.d.	0.09	-117.3	8.3
RC-02-80	1224	4.21	3.51	b.d.l.	b.d.l.	n.d.	0.08	-202.9	8.1
RC-02-81	1341	3.97	3.55	0.01	b.d.l.	n.d.	n.d.	-209.2	8.3
RC-02-82	1368	3.79	3.39	0.01	b.d.l.	n.d.	0.05	-248.2	n.d.
RC-02-83	1392	4.05	3.35	b.d.l.	b.d.l.	n.d.	0.03	-238.6	n.d.
RC-02-84	1440	3.61	3.28	0.01	b.d.l.	0.02	0.07	-213.9	n.d.
RC-02-85	1459	3.46	3.22	b.d.l.	b.d.l.	n.d.	n.d.	-204.5	n.d.
RC-02-86	1483	3.40	3.30	b.d.l.	b.d.l.	n.d.	n.d.	-194.3	n.d.
RC-02-87	1512	3.88	3.25	b.d.l.	b.d.l.	n.d.	n.d.	-205.6	8.2
RC-02-88	1533	3.93	3.25	0.01	b.d.l.	n.d.	n.d.	-194.8	8.3
RC-02-89	1557	3.80	3.39	b.d.l.	b.d.l.	n.d.	n.d.	-211.0	8.3

Table C.4.1. (continued)

Sample	t (hours)	Cl^- (mM)	SO_4^{2-} (mM)	NO_3^- (mM)	NO_2^- (mM)	NH_4^+ (mM)	$C_6H_{12}O_6$ (mM)	Eh (mV)	pH
RC-02-90	1582	3.58	3.58	b.d.l.	b.d.l.	0.02	n.d.	-222.3	8.2
RC-02-91	1630	3.76	3.49	b.d.l.	b.d.l.	n.d.	n.d.	-238.4	8.2
RC-02-92	1654	3.69	3.32	b.d.l.	b.d.l.	n.d.	n.d.	-238.5	8.1
RC-02-93	1678	3.71	3.30	0.01	b.d.l.	n.d.	n.d.	-237.5	8.1
RC-02-94	1726	3.68	3.21	b.d.l.	b.d.l.	n.d.	n.d.	-242.4	8.1
RC-02-95	1798	3.75	3.30	b.d.l.	b.d.l.	n.d.	n.d.	-184.9	8.0
RC-02-96	1840	0.00	0.00	b.d.l.	b.d.l.	n.d.	n.d.	-192.0	8.1
RC-02-97	1870	3.65	3.30	0.01	b.d.l.	n.d.	n.d.	-204.5	8.2
RC-02-98	1911	3.91	3.29	b.d.l.	b.d.l.	n.d.	n.d.	-251.6	8.1
RC-02-99	1942	3.77	3.33	b.d.l.	b.d.l.	0.02	n.d.	-238.1	8.2
RC-02-100	1986	3.73	3.32	0.01	b.d.l.	n.d.	n.d.	-242.0	8.1
RC-02-101	2015	4.21	3.41	b.d.l.	b.d.l.	n.d.	n.d.	-226.7	8.1
RC-02-102	2033	3.71	3.44	b.d.l.	b.d.l.	n.d.	n.d.	-259.3	8.0
RC-02-103	2061	3.87	3.43	0.01	b.d.l.	n.d.	n.d.	-261.0	8.0
RC-02-104	2087	4.18	3.38	b.d.l.	b.d.l.	0.02	n.d.	-262.5	8.1
C/N 1.12									
RC-02-105	2104	3.81	3.51	b.d.l.	b.d.l.	n.d.	n.d.	-270.7	8.0
RC-02-106	2129	3.72	3.42	b.d.l.	b.d.l.	n.d.	n.d.	-265.4	8.0
RC-02-107	2159	3.26	3.42	0.01	b.d.l.	n.d.	n.d.	-258.8	8.1
RC-02-108	2183	3.65	3.39	0.01	0.01	n.d.	n.d.	-276.9	8.0
RC-02-109	2207	4.34	3.28	b.d.l.	b.d.l.	n.d.	0.29	-264.5	8.1
RC-02-110	2231	3.75	3.34	0.01	b.d.l.	0.02	0.29	-268.4	8.2
RC-02-111	2272	3.72	3.37	b.d.l.	b.d.l.	n.d.	0.30	-224.0	8.1
RC-02-112	2303	4.05	3.39	b.d.l.	b.d.l.	0.02	0.29	-186.6	8.2
RC-02-113	2327	3.71	3.53	b.d.l.	b.d.l.	n.d.	n.d.	-258.7	8.1
RC-02-114	2351	4.04	3.38	b.d.l.	b.d.l.	n.d.	n.d.	-258.4	8.1
RC-02-115	2377	4.45	3.43	0.01	b.d.l.	n.d.	n.d.	-270.5	8.1
RC-02-116	2396	3.56	3.37	b.d.l.	b.d.l.	n.d.	n.d.	-265.9	8.0
RC-02-117	2419	2.85	3.38	b.d.l.	b.d.l.	n.d.	n.d.	n.d.	8.1
RC-02-118	2449	3.13	3.31	b.d.l.	0.03	n.d.	n.d.	n.d.	8.0
RC-02-119	2471	3.41	3.43	b.d.l.	b.d.l.	n.d.	n.d.	n.d.	8.1
RC-02-120	2496	3.26	3.40	b.d.l.	b.d.l.	n.d.	n.d.	n.d.	8.2
RC-02-121	2521	3.33	3.34	b.d.l.	b.d.l.	0.02	n.d.	-260.7	8.1
RC-02-122	2563	3.27	3.25	b.d.l.	b.d.l.	n.d.	n.d.	-248.2	8.3
RC-02-123	2593	3.16	3.28	b.d.l.	b.d.l.	n.d.	n.d.	-315.7	8.3
RC-02-124	2633	3.24	3.29	b.d.l.	b.d.l.	n.d.	n.d.	-283.7	8.4
RC-02-125	2664	3.17	3.34	b.d.l.	b.d.l.	n.d.	n.d.	-355.0	8.3
RC-02-126	2736	3.49	3.47	b.d.l.	b.d.l.	n.d.	n.d.	-286.0	8.2
RC-02-127	2760	3.30	3.41	b.d.l.	b.d.l.	n.d.	n.d.	-353.8	8.2
RC-02-128	2800	3.49	3.27	b.d.l.	b.d.l.	n.d.	n.d.	-312.4	8.2
RC-02-129	2825	3.54	3.42	b.d.l.	b.d.l.	n.d.	n.d.	-340.7	8.2
RC-02-130	2849	3.62	3.34	0.01	b.d.l.	n.d.	n.d.	-231.3	8.2
RC-02-131	2873	3.09	3.41	b.d.l.	b.d.l.	0.02	n.d.	-337.3	8.2
RC-02-132	2904	3.30	3.37	b.d.l.	b.d.l.	n.d.	n.d.	-345.4	8.3
RC-02-133	2976	3.81	3.35	b.d.l.	b.d.l.	0.02	n.d.	n.d.	8.3

Table C.4.2. NO_3^- isotopic characterization for induced experiment

Sample	$\delta^{15}N_{NO3}$ (‰)	SD ^{15}N	$\delta^{18}O_{NO3}$ (‰)	SD ^{18}O
RC-02-00	+9.6	0.2	+3.3	0.8
RC-02-01	+12.6	0.4	+11.4	0.7
RC-02-02	+17.5	0.4	+18.5	1.9
RC-02-07	+34.3	1.0	+31.6	2.0
RC-02-08	+25.1	1.0	+30.1	2.0
RC-02-09	+32.3	0.1	+29.1	1.0
RC-02-12	+39.3	0.4	+39.9	2.0
RC-02-13	+22.0	0.3	+21.3	1.1
RC-02-14	+19.6	1.0	+20.5	2.0
RC-02-15	+22.7	0.2	+21.8	2.0
RC-02-16	+34.2	1.2	+32.3	2.0
RC-02-18	+33.8	0.2	+27.6	1.4
RC-02-19	+21.0	0.2	+20.3	2.0
RC-02-20	+29.5	0.5	+22.4	1.4
RC-02-25	+39.5	0.6	+33.7	0.3
RC-02-31	+35.6	1.0	+31.9	2.0

Table C.4. 3. SO_4^{2-} isotopic characterization for induced experiment

Sample	$\delta^{18}O_{SO4}$ (‰)	$\delta^{34}S_{SO4}$ (‰)
Input water	+4.9	-17.0
RC-02-40	+5.6	-17.2
RC-02-49	+5.4	-17.2
RC-02-68	+5.4	-17.2
RC-02-74	+5.2	-17.2
RC-02-75	+5.3	-17.1
RC-02-87	+5.4	-17.2
RC-02-94	+5.4	-17.2
RC-02-113	+5.8	-17.1
RC-02-126	+5.5	-17.1